Effect of INPP4B loss on DNA repair and treatment strategies in ovarian cancer

Laura Ren Huey Ip

A thesis submitted to the University College London for the degree of Doctor of Philosophy

2016

Declaration

I, Laura Ren Huey Ip, confirm that the work presented in this thesis is my own. Where information has been derived from other sources, I confirm that this has been indicated in the thesis.

Abstract

Treatment options for ovarian cancer patients remain limited and overall survival is less than 50 percent despite recent clinical advances. The lipid phosphatase inositol polyphosphate 4-phosphatase type II (INPP4B) has been described as a tumour suppressor in the PI3K/Akt pathway with loss of expression found most pronounced in breast, ovarian cancer and melanoma. Using microarray technology a DNA repair defect was identified in INPP4B-deficient MCF-10A cells. After validation of the microarray data, I further characterised the DNA repair defect by comet assays and quantification of γH2AX, RAD51 and 53BP1 foci formation through immunofluorescence studies. Mechanistically, with collaborative efforts I discovered that INPP4B forms a protein complex with the key players of DNA repair, ATR and BRCA1, in GST pulldown and 293T overexpression assays. Finally, I assessed whether or not INPP4B loss resulted in synthetically lethal interaction with PARP inhibition, as evidenced with tumours harbouring *BRCA1/2* mutations. INPP4B loss resulted in significantly increased sensitivity towards PARP inhibition, *in vitro* and *in vivo*. Given that INPP4B loss has been found in 40% of ovarian cancer patients, this study provides the rationale for establishing INPP4B as a biomarker of PARP inhibitor response, and consequently offers novel therapeutic options for a significant subset of patients.

Table of Contents

Acknowledgements

I would like to thank my PhD supervisors Christina Gewinner, Daniel Hochhauser and John Hartley for their support and guidance over the last four years. In particular, I am extremely thankful for my primary supervisor Christina for her unwavering efforts to teach me, challenge my weaknesses and always encourage me, and for being an excellent supervisor, life mentor and friend. My thanks also go to Felipe Cia Viciano, Victoria Spanswick and Su-kit Chew for their assistance with experimental procedures and to Julie Olszewski for her support throughout my programme. I am beyond grateful for the support of my family who have been cheering me on so patiently and for funding this degree. Finally, words cannot express my gratitude to God for providing me with strength and perseverance, as well as a revelation of His love and goodness over the last four years.

Abbreviations

53BP1	p53-binding protein 1
AP	apurinic/apyrimidinic
APE1	apurinic/apyrimidinic endonuclease 1
APLF	aprataxin and PNKP like factor
APS	ammonium persulphate
AT	ataxia telangiectasia
ATM	ataxia telangiectasia mutated
ATR	ATM and Rad3-Related
ATRIP	ATR-interacting protein
BAD	Bcl-2 associated death promoter
BER	base excision repair
BH	BCR homology
BH3	Bcl-2 homology 3
BL	BRCA-like
BRAF	homologv-raf murine sarcoma viral oncogene homolog B
BRCA1	breast cancer 1, early onset
BRCA2	breast cancer 2, early onset
BSA	bovine serum albumin
CA125	cancer antigen 125
cAMP	cyclic adenosine monophosphate
CDC25	cell division cycle 25
CDK	cyclin-dependent kinase
Chk1	checkpoint kinase 1
Chk2	checkpoint kinase 2

CT	computed tomographic
CtIP	CtBP-interacting protein
DBB	DNA binding complex
DDR	DNA damage response
dHJ	double Holliday junction
DNA-PK	DNA-dependent protein kinase
DNA-PKcs	catalytic subunit of DNA dependent protein kinase
dNTP	deoxyribonucleotide triphosphate
DSB	double-strand break
dsDNA	double stranded DNA
DTT	dithiothreitol
E. coli	escherichia coli
EDGR	epidermal growth factor receptor
EDTA	ethylenediaminetetraacetic acid
EOC	epithelial ovarian cancer
ER	oestrogen receptor
ERCC1-XPF	excision repair cross complementation group 1/xeroderma pigmentosum group F complex
ERK	extracellular signal-regulated kinase
EXO1	exonuclease 1
FANC	Fanconi Anemia, complementation
FCS	foetal calf serum
FHA	forkhead-associated
FOXO	forkhead box O
Glut	glucose transporter

GPCR	G-protein coupled receptor
GSEA	gene set enrichment analysis
GSK3	glycogen synthase kinase 3
GST	glutathione S-transferase
H2AX	histone family H2A, member X
HER2	human epidermal growth factor receptor 2
HGEC	high grade endometrioid carcinoma
HGSC	high grade serous carcinoma
HIF1α	hypoxia-inducible factor-1 α
hMSH2	human mutS homolog 2
HR	homologous recombination
ICL	interstrand crosslinks
INPP4A	inositol polyphosphate 4-phosphatase type I
INPP4B	inositol polyphosphate 4-phosphatase type II
Ins(1,3,4)P_3	inositol 1,3,4-trisphosphate
Ins(3,4)P_2	inositol 3,4-bisphosphate
IPTG	isopropyl β – D – 1 – thiogalactopyranoside
IR	ionising radiation
KEGG	Kyoto encyclopedia of genes and genomes
KRAS	Kirsten rat sarcoma viral oncogene and mutations.
LB	Luria-Bertani
LGEC	low grade endometrioid carcinoma
LGSC	low grade serous carcinoma
LIG	ligase
LOH	loss of heterozygosity

MAPK	mitogen-activated protein kinase
MDC1	mediator of DNA-damage checkpoint 1
MDM2	mouse double minute 2
MGMT	O^6 methylguanine DNA methyltransferase
MMR	mismatch repair
MRN	MRE11-Rad50-NBS1
MSI	microsatellite instability
mTOR	mammalian target of rapamycin
mTORC1	mammalian target of rapamycin complex 1
mTORC2	mammalian target of rapamycin complex 2
NBL	non-BRCA-like
NBS1	nibrin
NER	nucleotide excision repair
NHEJ	non-homologous end joining
NO	nitric oxide
OS	overall survival
PALB2	partner and localiser of BRCA2
PAR	poly(ADP-ribose)
PARP	poly(ADP-ribose) polymerase
PBS	phosphate buffered saline
PBST	1 X PBS containing 0.1% Tween20
PCNA	proliferating cell nuclear antigen
PCR	polymerase chain reaction
PDGF	plate derived growth factor
PDK1	phosphoinositide-dependent kinase-

PEI	polyethylenimine
PH	pleckstrin homology
PI	phosphoinositide
PI4K	phosphoinositol-4-kinase
PIK	phosphatidylinositol kinase homology
PIK3CA	phosphatidylinositol-4,5-bisphosphate 3-kinase, catalytic subunit alpha
PIKK	phosphatidylinositol 3-kinase related kinases
PIP5K	phosphatidylinositol-4-phosphate 5-kinase
PNK	polynucleotide kinases
pol	DNA polymerase
PRAS40	proline-rich Akt substrate of 40 kDa
PtdIns	phosphatidylinositols
PTEN	phosphatase and tensin homolog
qPCR	real-time polymerase chain reaction
RAD51AP1	RAD51 associated protein 1
RB1	Retinoblastoma 1
Rheb	ras homolog enriched in brain
RNF	ring finger protein
ROS	reactive oxygen species
RPA	replication protein A
RTK	receptor tyrosine kinase
SDS	sodium dodecyl sulphate
SDS-PAGE	sodium dodecyl sulphate polyacrylamide gel
SDSA	ynthesis dependent strand annealing

SH2	Src homology 2
SH3	Src homology 3
SHIP1/2	SH2 domain-containing inositol-5'-phosphatase 1/2
SSB	single-strand break
ssDNA	single-stranded DNA
TAE	tris acetate EDTA
TBS	tris-buffered saline
TBST	1 X TBS containing 0.1% Tween20
TE	tris-EDTA
TEMED	tetramethylethylenediamine
TMZ	temozolomide
TOP	tomoisomerase
TOPBP1	topoisomerase (DNA) II binding protein 1
TSC	tuberous sclerosis complex
UV	ultraviolet
VEGF	vascular endothelial growth factor
Vsp34	vacuolar protein-sorting defective-34
XP	xeroderma pigmentosum
XRCC	x-ray repair cross-complementing protein

CHAPTER 1. Literature Review

1.1 Ovarian cancer

1.1.1 The biology of ovarian cancer

1.1.1.1 The female reproductive system

The human female reproductive system consists of network of organs that co-ordinate together and gives rise the ability to produce and bear offspring. The principal organs that make up the female reproductive system are the ovaries, fallopian tubes, uterus, vagina, and components of the external genitalia, as shown in figure 1.1. The ovaries are paired female pelvic reproductive organs, which house the female egg cells (also known as ovum/ova) and are responsible for the production of sex hormones oestrogen and progesterone. The paired organs are located on either side of the uterus relative to the lateral wall of the pelvis and attached to the back of the broad ligament of the uterus. The ovary consists of four types of cells: the surface epithelium, the stroma, germ cells and granulosa cells. The surface epithelium of the ovary is composed of a single layer of cells and lines the external surface of the ovaries. The bulk of the internal substance consists of the stroma, a dense, fibrous tissue. Germ cells, or oocytes, are located near the periphery of the stroma. Granulosa cells are specialised cells that surround the germ cells to form ovarian follicles, essential cellular structures released during ovulation. The fallopian tubes extend from the left and right of the uterus to the edge of the ovaries, ending in a funnel shaped structure covered with small finger-like projections called fimbriae. The function of the fimbriae is to sweep over the outside of the ovaries to pick up the released ova and carry them for transport into the uterus. The internal lining of the fallopian tubes is covered in cilia which work with the smooth muscle of the tube to move the ovum to the uterus. The uterus is a hollow, muscular organ which

is connected to the two fallopian tubes on its superior end, and to the vagina, via the cervix, on its inferior end. The uterus houses the developing foetus during pregnancy and the inner lining of the uterus, known as the endometrium, provides support to the embryo during early development. The vagina is an elastic, muscular tube that connects the cervix of the uterus to the exterior of the body, and is located inferior of the uterus. The vagina functions as a receptacle of the penis during sexual intercourse and carries sperm to the uterus and fallopian tubes. It also serves as the birth canal to allow delivery of the foetus during childbirth. During menstruation the menstrual flow exits the body via the vagina.

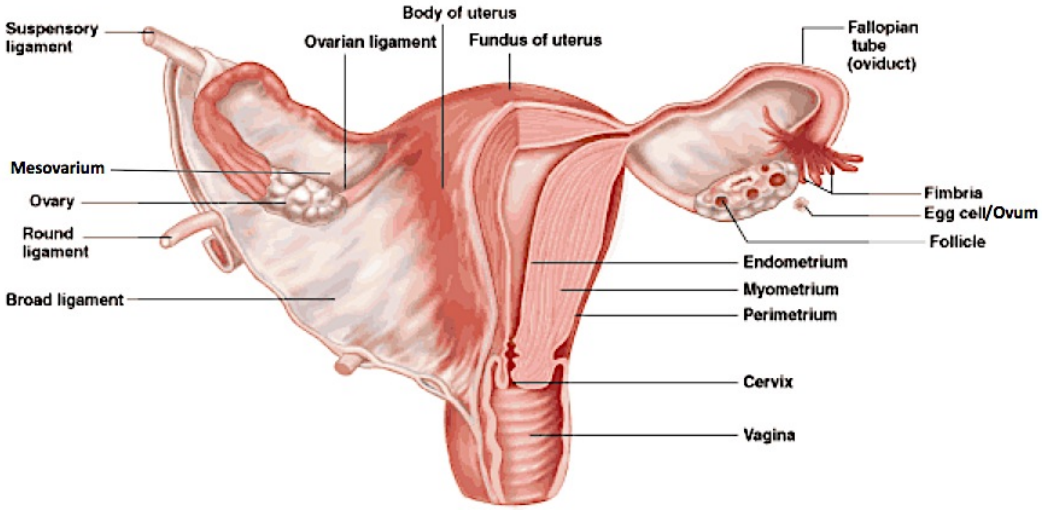

Figure 1.1 Anatomy of the female reproductive system. The principal organs of the female reproductive system are the ovaries, uterine tubes, uterus, vagina, and components of the external genitalia. The ovaries, uterine tubes, and uterus are enclosed within an extensive mesentery known as the broad ligament. The uterine tubes run along the superior border of the broad ligament and open into the pelvic cavity lateral to the ovaries. A segment of the broad ligament, known as the mesovarium, supports and stabilises the position of each ovary. Image source: http://healthcare.utah.edu/healthlibrary/related/doc.php?type=34&id=17114-1

1.1.1.2 Incidence, epidemiology and risk factors of ovarian cancer

Ovarian cancer is the leading cause of death from gynaecological cancers and the fourth most common cause of death in women in the UK (Jemal et al., 2007; Zhang et al., 2009c). In 2011, there were 225,000 new cases of ovarian cancer and 140,000 deaths due to ovarian cancer worldwide, accounting for approximately 4% of all cancers diagnosed in women (Jemal et al., 2011). Incidence rates vary considerably across the globe, with more developed countries possessing an incidence rate of almost twice that of less developed countries. The highest ovarian cancer incidence rates are found in northern, central and eastern Europe and the lowest rates in Africa and parts of Asia (Ferlay J, 2010). The 5-year survival rate of ovarian cancer ranges from 94% for localised disease, 73% for regional disease, and 28% for distant disease with an overall survival of 46% across all stages (Jemal et al., 2010). While the 5-year survival has increased over the last three decades, the overall cure rate has not improved and remains at less than 40%. The cure rate for the most common and most aggressive form of ovarian cancer, high grade serous ovarian carcinoma, is even worse. Furthermore, approximately 80% of patients present with disease spread beyond the ovaries, giving rise to poor prognosis and poor overall survival (Jemal et al., 2010).

Risk factors for developing ovarian cancer include increasing age, positive family history of ovarian, breast, uterine, or colon cancer, and high numbers of ovulatory cycles. Ovarian cancer is predominantly a disease of older, post-menopausal women with over 80% of cases being diagnosed in women over 50 years (ONS, 2010). The life-time risk of developing ovarian cancer is 1 in 54 for women in the UK (Sasieni et al., 2011), and this risk increases by three to four fold in women who have a first-degree relative diagnosed with ovarian cancer compared with women with no family cancer

history. Consequently, positive family cancer history plays a significant role in developing ovarian cancer, and approximately 13 – 15% of ovarian cancers are associated with germline mutations in members of the *BRCA* breast and ovarian cancer susceptibility family of genes, *BRCA1* and *BRCA2 (*breast cancer 1, early onset; breast cancer 2, early onset). Other non-inherited risk factors that increase the likelihood of developing ovarian cancer include high ovulatory cycle numbers, infertility as well exposure to talc in the genital areas. Conversely, factors that decrease the number of ovulatory cycles reduce this risk; these include multiple pregnancies, the use of oral contraceptives, and prolonged lactation. Tubal ligation and hysterectomy have also been found to reduce the risk of developing ovarian cancer.

1.1.1.3 Types of ovarian cancer

One of the problems in understanding the pathogenesis of ovarian cancer is the diverse histological, clinicopathological and behavioural nature of the disease. Ovarian cancer is a heterogeneous disease that is composed of a collection of molecularly and aetiologically distinct tumours that share a common anatomical location. Both benign and malignant tumours can arise from three cell types: germ cell tumours, sex cord-stromal tumours and surface epithelial tumours. (Romero and Bast, 2012).

Surface epithelial ovarian tumours usually develop after the age of 40 and account for approximately 90% of malignant ovarian tumours (Chen et al., 2003). Due to the majority of malignant ovarian tumours being epithelial in origin, the focus of this study will be on this particular subtype. Epithelial ovarian cancer (EOC) was initially thought to originate from the ovarian epithelium. In recent years, it has become apparent that some ovarian cancers and primary peritoneal carcinomas can also arise from

endometriosis, epithelial rests in the normal peritoneum, or the fimbriae of fallopian tubes (Romero and Bast, 2012). EOCs are now believed to be derived from flattened nondescript epithelial cells that resemble the epithelium of the fallopian tube and/or ovaries, endometrium, mucin-secreting endocervical glands, glycogen-filled vaginal rests and internal lining of the urinary bladder. These sites of origins define the five EOC subtypes, serous, endometrioid, mucinous, clear cell and transitional cell carcinomas, respectively, as depicted in figure 1.2. In agreement, a recent finding from Perets et al. demonstrated in animal models that some EOC serous carcinomas can originate from fallopian tubal secretory epithelial cells (Perets et al., 2013). Carcinomas are malignancies that have an epithelial origin. Serous and endometrioid carcinomas can further be subdivided into low and high aggressive states, termed low grade and high grade cancers respectively. Epithelial tumours that lack any specific differentiation are classified as undifferentiated. The distribution of histological subtypes is as follows: 60% serous, 10 – 20% endometrioid, <10% clear cell, 6% transitional, <5% mucinous and <1% undifferentiated tumours. High grade serous carcinomas (HGSCs) are by far the most common subtype and account for 90% of all serous tumours, representing over 50% of all ovarian carcinomas.

Identification of the spread of ovarian cancer involves the use of the International Federation of Obstetricians and Gynaecologists staging system, also known as the FIGO system. In brief, ovarian cancer staging is stratified into four stages: I, II, III and IV. Stage I tumours are confined to the ovaries and stage II tumours involve the ovaries and an extension into the pelvis. Once the tumour has spread to the peritoneum the cancer is classified as stage III, with stage IV tumours involving metastasis beyond the peritoneum. Grading of ovarian cancer indicates how active or aggressive the cancer is.

There are three grades, grade I, II and III, which represent low, moderate and high grade tumours, respectively. Low grade tumours are typically well differentiated, and are less likely to spread than high grade cancers. High grade tumours are usually represented by poorly differentiated cells with a higher likelihood of invasion. Moderate grade carcinomas represent an intermediate state between low and high grade.

A two-tier system has been derived to recognise this complexity and stratify tumours into two designated types, type I and type II, based on histological grade, molecular phenotype and genotype (Shih Ie and Kurman, 2004). Type I cancers include low grade serous carcinomas (LGSCs), mucinous carcinomas, low grade endometrioid carcinoma (LGECs), and clear cell carcinoma, and these tumours are often large and diagnosed at an early stage. They are slow growing, and are less sensitive to standard chemotherapy but may be responsive towards hormonal treatment. The more prevalent type II subtype includes HGSCs, high grade endometrioid carcinomas (HGECs) and undifferentiated carcinoma, all of which typically present at late stage. They evolve rapidly, undergo metastasis early in their course, and are clinically aggressive. Type II cancers are responsive towards conventional chemotherapy but do not respond as well towards hormonal strategies.

The other two less prevalent ovarian cancer subtypes are the germ cell tumours and sex cord stromal tumours. Germ cell tumours are ovarian tumours formed by cells that are presumably derived from primordial germ cells. Germ cell tumours arise most frequently in women in their twenties and thirties and account for 3% of ovarian cancers (Smith et al., 2006). Sex cord stromal tumours are believed to be derived from theca cells, stromal cells, granulosa cells and their testicular sex cord counterparts, Sertoli and

Leydig cells. Sex cord stromal tumours can occur in women of all ages, comprising approximately 7% of all ovarian malignancies.

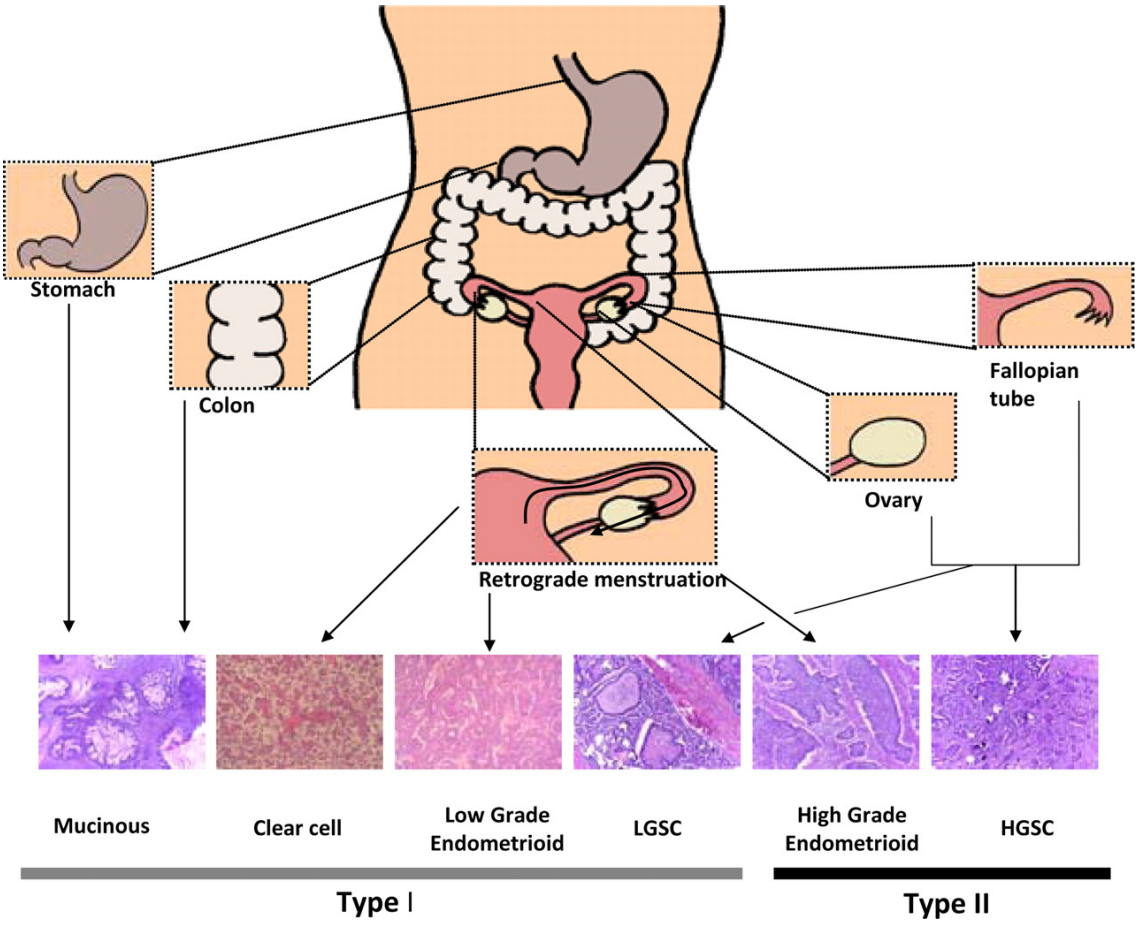

Figure 1.2 Origin and histological epithelial ovarian cancer subtypes associated with type I and type II molecular classification. LGSC – low grade serous carcinoma; HGSC – high grade serious carcinoma. Image source: (Romero and Bast, 2012)

1.1.1.4 Molecular alterations in epithelial ovarian cancer

The different subtypes of EOC can be also distinguished by their molecular alterations. Type I epithelial carcinomas are characterised by Kirsten rat sarcoma viral oncogene homolog (*KRAS),* v-raf murine sarcoma viral oncogene homolog B *(BRAF),* phosphatase and tensin homolog *(PTEN)* and phosphatidylinositol-4,5-bisphosphate 3-kinase, catalytic subunit alpha (*PIK3CA)* mutations. *KRAS* and *BRAF* encode for upstream components of the mitogen-activated protein kinase (MAPK) pathway, which coordinate diverse cellular activities like gene expression, cell cycle control, cellular metabolism, motility, survival, apoptosis, and differentiation (Krishna and Narang, 2008). *PTEN* and *PIK3CA* encode for components of the phosphatidylinositol-3-kinase (PI3K)/Akt signalling pathway, which promote cell proliferation, invasion/migration and survival. Approximately one third of low grade serous tumours have a mutation in one of these genes (Singer et al., 2003a; Singer et al., 2003b). Similarly, *KRAS* and *BRAF* are found frequently mutated (50 – 75%) in mucinous and endometrioid tumours (Garrett et al., 2001; Gemignani et al., 2003). Endometrioid, mucinous and LGSCs exhibit frequent inactivating mutations and epigenetic silencing of *PTEN*, as well as activating mutations of *PI3KCA* (Campbell et al., 2004; Landen et al., 2008; Nakayama et al., 2006; Willner et al., 2007). LGSCs tend to have normal karyotype and wild-type *TP53* and *BRCA1/2* (Press et al., 2008).

Of the type II cancers, *TP53* mutations has been found in over 90% of HGSCs and display high levels of genomic instability (Bell D, 2011; Landen et al., 2008). Approximately 13 – 15% of HGSCs are associated with germline mutations of *BRCA1* and *BRCA2* (Alsop et al., 2012; Pal et al., 2005; Zhang et al., 2011). 18% of HGSCs have gene amplification of *AKT2,* a component of the PI3K/Akt pathway (Nakayama et

al., 2006). Additionally, genomic analysis of HGSCs revealed a deregulation of the retinoblastoma 1 (RB1) pathway, a pathway involved in cell cycle suppression, and PI3K/RAS pathways in 67% and 45% of cases, respectively. However, somatic mutations were rare and gene amplifications were more commonly found (CGARN, 2011). In table 1.1 the frequency of somatic gene mutations in EOCs is summarised.

Table 1.1 Frequency of somatic gene mutations in epithelial ovarian cancer

	Type I				Type II
Gene Mutation	Low Grade Serous	Clear Cell	Endometrioid	Mucinous	High Grade Serous
BRAF	24 – 33%[1,2]	1%[3]	24%[2]	50 – 75%[4]	<1%[5]
KRAS	33%[1,2]	<1 – 7%[2,3]	<1%[2]	50 – 75%[4]	<1%[5]
PIK3CA	5%[1]	20 – 33%[3,6]	20%[6]	rare	<1%[5]
PTEN	20%[7]	<1 – 5%[3,8]	20 – 31%[8,9]	rare	<1%[5]

[1]Nakayama et al., 2006; [2]Singer et al., 2003a; [3]Kuo et al.,. 2009; [4]Gemignani et al., 2003; [5]CGARN, 2001; [6]Campbell et al., 2004; [7]Landen et al., 2008; [8]Winner et al., 2007; [9]Kurman and Shih Ie, 2011

1.1.2 Diagnosis, staging, and clinical management

Ovarian cancer remains the leading gynaecological cancer killer in part due to non-specific symptoms and lack of reliable biomarkers. The symptoms of early ovarian cancer are minimal, and progression of the disease leads to development of gastrointestinal symptoms such as abdominal pain, swelling and bloating. Patients and their health care providers often attribute these changes to menopause, aging, dietary indiscretions, stress, depression, or functional bowel problems. Frequently, women are medically managed without having a pelvic examination. As a result, early detection of ovarian cancer fails.

When abnormal ovarian pathology is suspected an ultrasound is conducted followed by cancer antigen 125 (CA125) tumour marker assessment. CA125 is a high molecular weight glycoprotein discovered in 1981 by Bast et al. and is important for adhesion, motility, and invasion of ovarian cancer (Bast et al., 1981; Bast and Spriggs, 2011). Elevated CA125 levels are observed in the majority of ovarian cancer sub-types, as well as 50% of stage I, 90% of stage II and over 90% of stages III/IV ovarian cancer patients (Carlson et al., 1994). However, CA125 is also found increased in several other cancers such as endometrial, pancreatic and lung cancer and consequently has limited specificity for detecting ovarian cancer. A study conducted in 2010 revealed that treatment of patients with recurrent ovarian cancer based on elevated CA125 did not increase overall survival (OS) compared to patients with delayed treatment. On the contrary, early treatment was associated with an early deterioration of quality of life (Rustin et al., 2010). While there have been numerous novel biomarkers discovered for ovarian cancer, an evaluation conducted by Cramer et al. concluded that CA125 remains the single best biomarker amongst the ovarian cancer specimens tested (Cramer

et al., 2011). Despite the limitations of the biomarker, assessing CA125 levels is currently considered standard of care for ovarian cancer screening, as well as for monitoring response to treatment and detecting disease recurrence (Lutz et al., 2011).

To detect any disease spread beyond the ovaries, a computed tomographic (CT) scan of the pelvis, abdomen and chest is conducted. Ovarian cancer is one of the few malignancies where surgeons will undertake cytoreductive operations, even if all macroscopic tumours cannot be removed. If the disease is limited to the ovary, the ovary is removed surgically. For women who wish to retain their fertility, the contralateral ovary and uterus is preserved upon normal imaging presentation and at surgery. If the cancer is found to have spread beyond the ovaries, debulking surgery is conducted in late-stage disease to achieve no residual visible disease, which has been found to improve prognosis (Schorge et al., 2010). Residual tumour size of over 2 cm is associated with reduced survival of 12 – 16 months, compared to a survival of 40 – 45 months if the tumour is less than 2 cm (Mutch, 2002).

1.1.2.1 Conventional chemotherapy and drug resistance

Administration of a combination of carboplatin and paclitaxel is currently considered the standard of care for ovarian cancer. Chemotherapy treatment and numerous randomised clinical trials have yielded a total of over 80% response rates, of which 40 – 60% were complete responses (du Bois et al., 2003; Neijt et al., 2000; Ozols et al., 2003; Sandercock et al., 2002). Carboplatin interacts with DNA to interfere with DNA repair and paclitaxel stabilises microtubules to inhibit cell division. Despite the high response rate, the majority of patients eventually relapse with a median progression-free survival of 18 months (Greenlee et al., 2001). The addition of other chemotherapeutic

agents, such as gemcitabine, liposomal doxorubicin and topotecan, to standard treatment has not resulted in any survival advantage (Bookman et al., 2009). Gemcitabine interferes with DNA replication, liposomal doxorubicin intercalates with DNA and topotecan/etoposide administration results in irreversible DNA damage. At relapse, if the patients are treated with the same drugs, their response rates reflect the treatment-free interval (Gore et al., 1990). This treatment response can be categorised into platinum-sensitive, platinum-resistant and platinum-refractory disease which indicates recurrence of disease after more than six months, less than six months, during or on completion of platinum chemotherapy, respectively. While the response rate of platinum-sensitive disease to carboplatin is greater than 50%, the response rate of platinum-resistant disease is 10 – 20% and even less for platinum-refractory disease. If the patient displays poor response towards carboplatin, alternative treatments such as liposomal doxorubicin, gemcitabine, topotecan, etoposide and hormonal therapies are implemented. However, with each subsequent relapse follows a decrease in response rate due to the development of drug resistance. Efforts to circumvent this resistance have been made by the use of different chemotherapy agents in varying combinations, doses and schedules, but have only led to marginal improvements in survival of patients with recurrent disease compared to mono-therapy (Bolis et al., 1999; Bookman et al., 2003; Buda et al., 2004; De Placido et al., 2004; Gonzalez-Martin, 2013; Monk et al., 2010; Sehouli et al., 2008).

1.2 PI3K/Akt pathway

The activation of the PI3K/Akt pathway has been found in several human cancers and is crucial for tumour progression and resistance development against chemotherapy and targeted therapies. This pathway regulates cell metabolism, growth, proliferation, migration and survival via regulation of a multitude of components in a signalling cascade driven manner, as depicted in figure 1.3. The next sections will discuss in depth the various components of PI3K signalling responsible for the activation and termination of this pathway, as well as the mutations of these components that exist in human cancers.

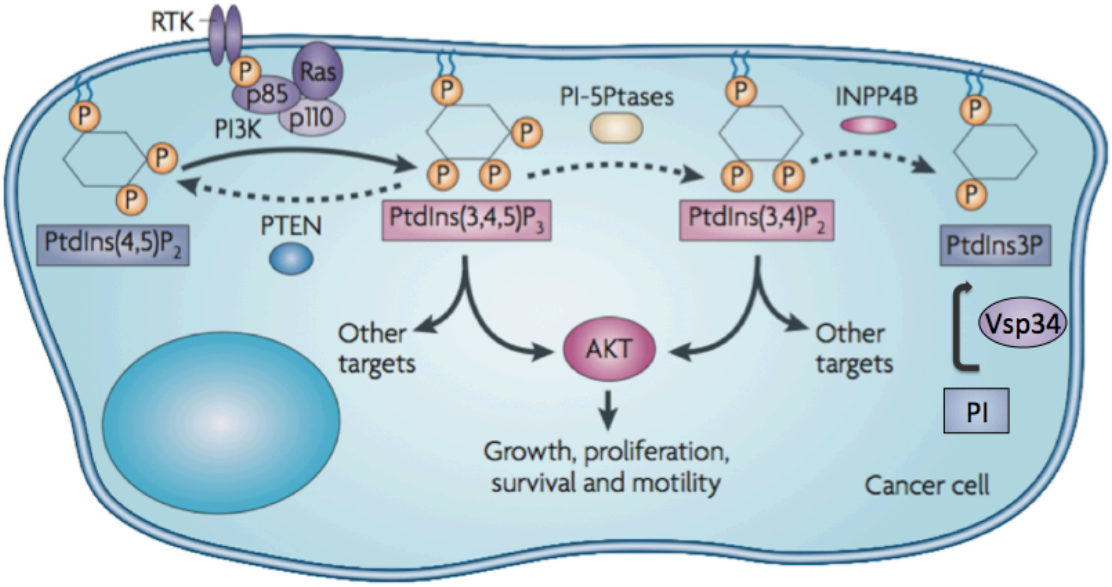

Figure 1.3 PI3K/Akt signalling. Growth factors and hormones activate receptor tyrosine kinases (RTKs) and G-protein coupled receptors (GPCRs), which in turn activate PI3K. Activated Ras protein can also activate PI3K directly. Upon activation, class I PI3K gives rise to phosphatidylinositol-3,4,5-trisphosphate (PIP_3). Akt, along with other proteins carrying a phosphoinositide binding domain, is recruited to the plasma membrane with binding affinity for both PIP_3 and $PI(3,4)P_2$ where it is activated

and subsequently initiates responses that regulate cell growth, proliferation, survival and motility. The pathway can be terminated by three phosphatases: phosphatase and tensin homologue (PTEN), SH2 domain-containing inositol-5'-phosphatase 1/2 (SHIP1/2) and inositol polyphosphate 4-phosphatase type II (INPP4B). PTEN hydrolyses PIP_3 to phosphatidylinositol-4,5-bisphosphate ($PI(4,5)P_2$), SHIP1/2 dephosphorylates PIP_3 to $PI(3,4)P_2$ and INPP4B fully terminates the signalling pathway by the hydrolysis of $PI(3,4)P_2$ to phosphatidylinositol-3-phosphate (PI(3)P). PI(3)P can also be produced from phosphatidylinositol (PtdIns) by class III PI3K, Vsp34. Image source: (Engelman et al., 2006)

1.2.1 Phosphoinositides

Phosphatidylinositol (PtdIns) and its phosphorylated derivatives are lipid molecules which reside in cellular membranes. Once phosphorylated, the phosphorylated PtdIns, otherwise known as phosphoinositides (PIs), attract specific proteins with a binding domain for PIs. PIs initiate various responses that result in cellular growth, cell cycle entry, cell migration and cell survival.

PtdIns consists of a myo-inositol ring that contains six hydroxyl groups configured with five of its six hydroxyl groups being equatorial and one at position D2 being axial, as shown in figure 1.4. PtdIns has a glycerol backbone esterified to two fatty acid chains and a phosphate, and attached to a polar myo-inositol head group that extends into the cytoplasm. The inositol head group has free hydroxyl groups at positions D2 through D6, and those at positions D3, D4 and D5 are readily phosphorylated by cytoplasmic lipid kinases. The combination of phosphorylated products gives rise to seven known PIs (figure 1.4): PI(3)P, PI(4)P, PI(5)P, PI(3,4)P_2, PI(4,5)P_2, PI(3,5)P_2, PIP_3. The amounts of PIs within cells have been estimated in different cells and tissues, and significant variance has been found in human tissue type distribution, as well as between yeast and plants (Nasuhoglu et al., 2002; Wenk et al., 2003).

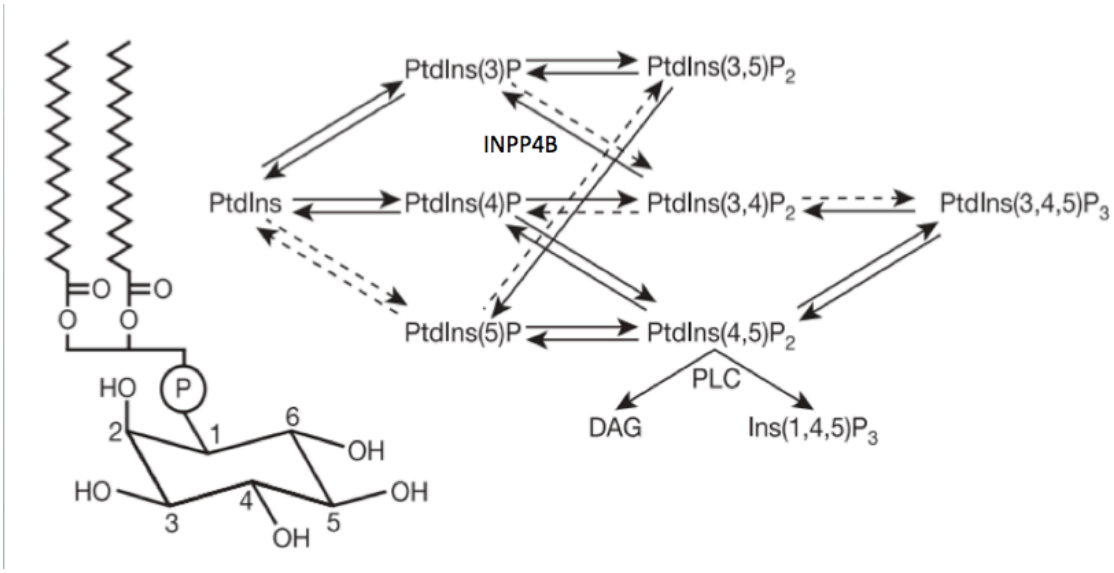

Figure 1.4. Phosphatidylinositol structure and metabolic reactions generating phosphoinositides. Here, INPP4B dephosphorylates PI(3,4)P_2 to PI(3)P. Image source: (Di Paolo and De Camilli, 2006)

PtdIns is synthesised in the endoplasmic reticulum from cytidine diphosphate diacylglycerol and myo-inositol by PtdIns synthase (Agranoff et al., 1958) and distributed throughout the cell via several PtdIns transfer proteins (Cockcroft and Carvou, 2007; Ile et al., 2006). PIs affect cellular functions by interacting with molecules that either reside in the membrane or are recruited to the membrane through interaction with PIs via inositide binding protein domains, such as the pleckstrin homology (PH) domain that has lipid binding selectivity for PI(3)P, PI(4)P, $PI(3,4)P_2$, $PI(4,5)P_2$, PIP_3. Table 1.2 lists the PI-binding modules, their binding preferences and examples of proteins that contain them. PI metabolism is strictly controlled in cells by the action of specific lipid kinases and lipid phosphatases. In general, phosphorylation occurs in two sites within the cell. Mono-phosphorylations of most PIs by Class II phosphoinositol-4-kinase (PI4K) and Class III PI3K occur in endomembranes, such as the endosomes and the Golgi network. Phosphorylation of PI(4)P to $PI(4,5)P_2$ by phosphatidylinositol-4-phosphate 5-kinase (PIP5K) and further phosphorylation to PIP_3 by class I PI3Ks occurs primarily at the plasma membrane. PIs have also been found in the nucleus and their functions encompass many aspects of transcription, chromatin remodeling, and mRNA maturation; however, defined mechanisms have yet to be established (Shah et al., 2013). The phosphorylation status of PIs can be changed by phosphoinositide phosphatases and hydrolysis by phosphoinositide-specific phospholipase C enzymes (PLCs). While some of the phosphoinositide phosphatases remove phosphate groups located in a specific position on the inositol ring, others, mainly the ones that dephosphorylate mono-phosphorylated PIs, possess functional specificity related to PI localisation. The localisation and site of phosphorylation and dephosphorylation of PIs is depicted in figure 1.5.

Table 1.2. Phosphoinositide binding modules, binding preferences and examples of proteins that contain them. Image source: (Di Paolo and De Camilli, 2006)

Module	Specificity	Examples of proteins
A/ENTH	PtdIns(4)P	EpsinR
	PtdIns(3,5)P_2	Ent3p, Ent5p
	PtdIns(4,5)P_2	AP180, CALM, epsin, HIP
C2	PtdIns(4,5)P_2	Synaptotagmin
FERM	PtdIns(4,5)P_2	Ezrin, moesin, radixin, talin
FYVE	PtdIns(3)P	EEA1, Hrs, SARA, PIKfyve
GRAM	PtdIns(3,5)P_2	Myotubularin
PDZ	PtdIns(4,5)P_2	Syntenin
PH	PtdIns(4)P	FAPP1/2, OSBP
	PtdIns(3,4)P_2	AKT/PKB, TAPP1,2
	PtdIns(4,5)P_2	PLCδ1, dynamin
	PtdIns(3,4,5)P_3	BTK, AKT/PKB, ARNO, GRP1
PHD	PtdIns(5)P	ING2
PTB	PtdIns(4,5)P_2	Dab1, ARH, SHC
	PtdIns(3,4,5)P_3	SHC
PX	PtdIns(3)P	SNX2,3,7,13
	PtdIns(5)P	SNX13
	PtdIns(3,4)P_2	p47PHOX
	PtdIns(4,5)P_2	Class II PI(3)kinase
	PtdIns(3,4,5)P_3	CISK

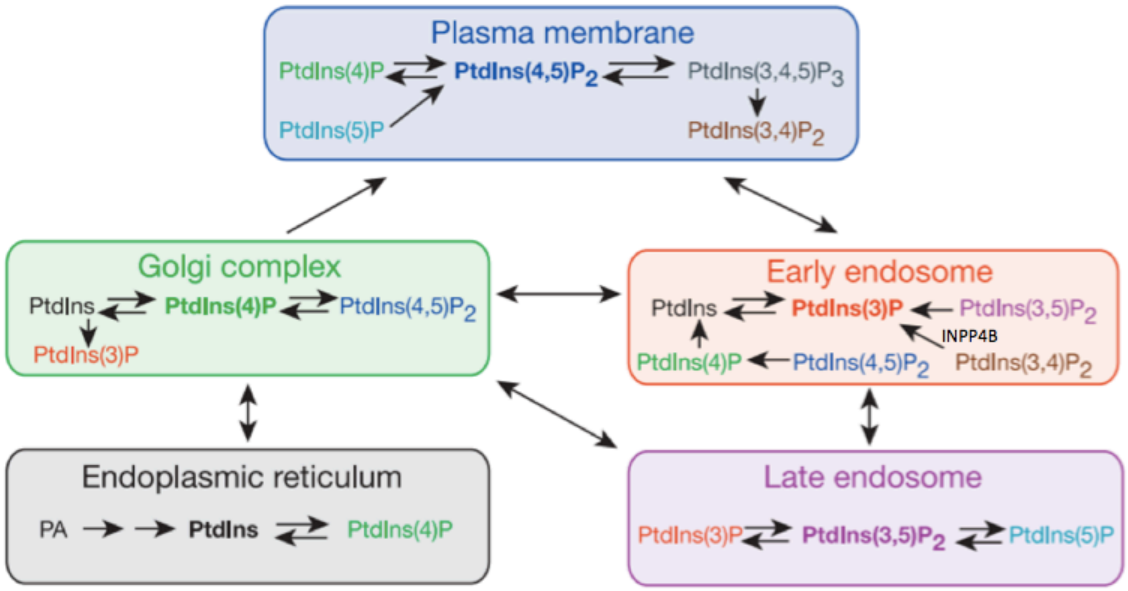

Figure 1.5 Predominant subcellular localisation of phosphoinositides and locations of phosphorylation/dephosphorylation events. $PI(4,5)P_2$ and PIP_3 are primarily located at the plasma membrane. $PI(3,4)P_2$ is predominantly found in the plasma membrane and early endosome. PI(4)P is found concentrated at the Golgi complex, but also found in the plasma membrane as well. PI(3)P is mostly found in the early endosomes and $PI(3,5)P_2$ on the late compartments of the endosomal pathway. Image source: (Di Paolo and De Camilli, 2006)

1.2.2 Activation of the PI3K pathway

1.2.2.1 Phosphatidylinositol-3-kinases

PI3Ks are a family of intracellular signalling enzymes that phosphorylate the 3'-hydroxyl group of the inositol ring of lipid second messenger phosphoinositides (Toker and Cantley, 1997). PI3Ks can be divided into three classes, based on lipid substrate preference and sequence homology: class I, class II, and class III (Domin and Waterfield, 1997; Vanhaesebroeck et al., 1997). The domain structures of the PI3K isoforms are shown in figure 1.6. All PI3K isoforms are widely expressed across tissue types, with the exception of class IA p55γ and p110δ subunits, which are predominately expressed in the brain/testes, and in lymphocytes, respectively. Several growth factors and signalling compounds can initiate activation of PI3K, including fibroblast growth factor, vascular endothelial growth factor (VEGF), angiopoietin I, and insulin. All of these molecules activate RTKs and lead to autophosphorylation of the receptors, which subsequently provide a docking site for PI3K. Other receptors and proteins such as GPCRs and the GTPase Ras are also able to activate PI3K.

1.2.2.1.1 Class I PI3Ks

Class I PI3Ks can utilise PtdIns, PI(4)P, and $PI(4,5)P_2$ as a substrate *in vitro*, whereas *in vivo*, Class I PI3Ks primarily generate PIP_3 from $PI(4,5)P_2$. Class I PI3Ks can further be subdivided into class IA and class IB.

Class IA PI3Ks are the most widely implicated class in human cancer and consist of a regulatory subunit (p85α, p85β, p50α p55α and p55γ) and a catalytic subunit (p110α, p110β and p110δ). *PIK3R1, PIK3R2* and *PIK3R3* encode p85α, p85β and p55γ, respectively. Through alternative transcription initiation sites, the *PIK3R1* gene also

gives rise to two shorter isoforms, p50α and p55α. A common core structure is shared between the p85 isoforms consisting of a p110-binding domain flanked by two Src-homology 2 (SH2) domains, as depicted in figure 1.6. The p85 regulatory subunit plays an essential role in maintaining the p110 catalytic subunit in a low activity state in quiescent cells and mediating activation through binding of the SH2 domains of p85 to phospho-tyrosine residues containing the motif pYxxM located on RTKs or adaptor molecules, where x represents any amino acid (Songyang et al., 1993). The p110 subunit is only stable in complex with a p85 subunit and no evidence for free p85 or p110 subunits has been obtained (Geering et al., 2007). Class IA PI3K catalytic subunits p110α, p110β and p110δ are expressed by genes *PIK3CA*, *PIK3CB*, and *PIK3CD*, respectively (Fruman et al., 1998). The p110 isoforms contain an N-terminal p85-binding domain, a Ras-binding domain, a phosphatidylinositol kinase homology (PIK) domain, and a C-terminal catalytic domain. Mutations in the *PIK3CA* genes encoding the catalytic subunit p110α are found frequently across a variety of cancer tissue types. *PIK3CA* mutations occur most commonly in hepatocellular (36%), breast (26%), colon (26%), ovarian (10%), glioma (8%), and gastric (7%) cancers (Bunney and Katan, 2010). Over 80% of the mutations have been observed around two hotspots: E545 in the helical phosphatidylinositol kinase homology domain, and H1047 near the end of the catalytic domain. The resulting effect of the mutations promotes constitutive PI3K signalling. Recent data have suggested that glioblastomas, ovarian cancers and colon carcinomas also harbour activating mutations in *PIK3R1*, which encodes p85α, however the mechanism and the broader implications of these mutations have yet to be defined (CGARN, 2008; Philp et al., 2001).

Class IB PI3Ks have a p110γ catalytic subunit and a two part regulatory subunit, consisting of p101 and p87. Class IB PI3Ks do not have a p85 regulatory subunit and are therefore not regulated by RTKs. Instead, class IB PI3Ks are activated by GPCRs via interaction with the Gβγ subunit of trimeric G proteins (Stephens et al., 1997). Other p110 regulatory subunit homologues include p84 and p87PIKAP which also mediate activation of p110γ (Suire et al., 2005; Voigt et al., 2006).

1.2.2.1.2 Class II PI3Ks

Class II PI3Ks consist of a p110-like catalytic subunit only, with no regulatory subunit. The three isoforms of class II PI3Ks, PIK3C2α, PIK3C2β and PIK3C2γ are encoded by three distinct genes. The structure of class II PI3Ks includes a divergent N-terminus, a PI binding PX domain and an additional C2 domain at the C-terminus. These enzymes preferentially phosphorylate PI, as well as PI(4)P, although to a lesser extent (Engelman et al., 2006). Class II PI3Ks play a role in regulating membrane trafficking and receptor internalisation by binding to clathrin, a protein involved in formation of coated vesicles (Gaidarov et al., 2001). Activation of class II PI3Ks can be mediated by RTKs, cytokine receptors and integrins; however, downstream functions in response to activation are less well defined (Katso et al., 2001).

1.2.2.1.3 Class III PI3Ks

Class III PI3Ks consist of the catalytic subunit vacuolar protein-sorting defective-34 (Vsp34). Originally identified in budding yeast as the gene product required for trafficking vesicles from the Golgi apparatus to the vacuole (Odorizzi et al., 2000), Vps34 has also been found to have mammalian functions. Vps34 has been implicated in

controlling cell growth through regulation of mammalian target of rapamycin (mTOR) activity in response to amino acid availability (Byfield et al., 2005; Nobukuni et al., 2005), as well as in autophagy, a cellular response to nutrient starvation (Kihara et al., 2001; Wurmser and Emr, 2002).

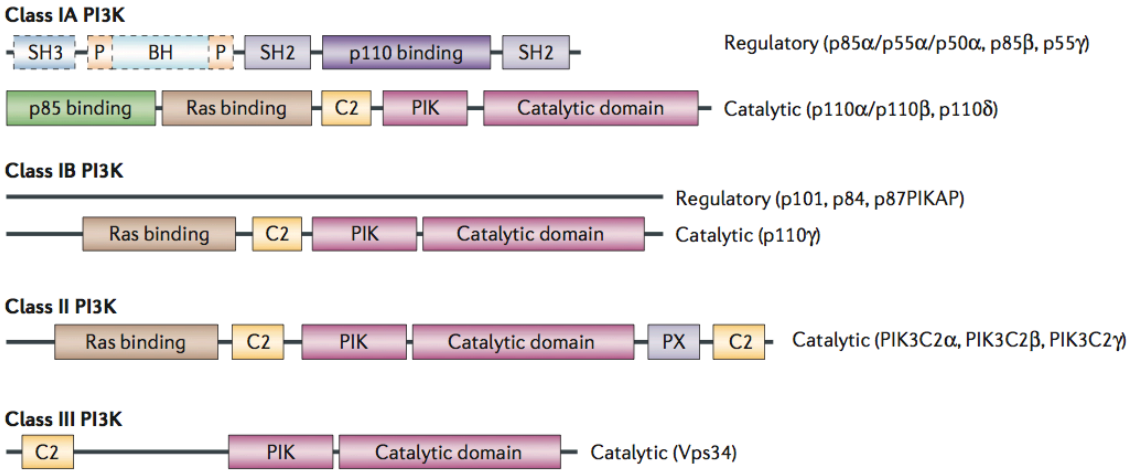

Figure 1.6 The domain structures of PI3K isoforms. PI3Ks can be divided into three classes based on lipid substrate preference and sequence homology. Class IA PI3K is a heterodimer that consists of a regulatory subunit (p85α/p55α/p50α/p85β/p55γ) and a catalytic subunit (p110α/p110β/p110∂). The p85 regulatory subunit consists of a p110-binding domain flanked by two Src-homology 2 (SH2) domains. The longer isoforms p85α and p85β also have an extended N-terminal region containing an Src-homology 3 (SH3) domain, and a BCR homology (BH) domain flanked by two proline-rich (P) regions as indicated by the dotted lines (Fruman et al., 1998). Class IA catalytic subunits, as with the rest of the PI3K isoforms, contain a C2 domain, phosphatidylinositol kinase homology (PIK) domain, as well as a C-terminal catalytic domain. The class IA p110 subunit also shares a Ras binding domain with class IB, and Class II PI3K. A p85 binding domain at the N-terminus of class IA p110 interacts with

the p85 regulatory subunit. Class IB PI3Ks are heterodimers consisting of regulatory subunits (p101, p84, p87PIKAP) and the p110γ catalytic subunit. Although P110γ share extensive homology with class IA p110 proteins, class IB p110 regulatory subunit is distinct from p85 proteins. Class II PI3Ks contain only a p110-like catalytic subunit (PIK3C2α, PIK3C2β, PIK3C2γ), which contain an extended divergent N-terminus and a PX domain at the C-terminus. Class III PI3K consists of a single member, Vsp34. As described above, class IB, class II and class III catalytic subunits shares significant sequence homology with class IA p110 subunits. Image source: (Engelman et al., 2006)

1.2.2.2 Akt

Akt, also known as protein kinase B, is a serine-threonine kinase that is activated downstream of PI3K. There are three mammalian isoforms of Akt: Akt1, Akt2 and Akt3 (Brodbeck et al., 1999; Cheng et al., 1992; Jones et al., 1991). The isoforms share approximately 80% amino acid homology and are thought to have similar primary substrate specificity (Vanhaesebroeck and Alessi, 2000). In addition, a splice variant of the Akt3 isoform has been found which contains a truncated C-terminus hydrophobic domain (Brodbeck et al., 2001). Akt is widely expressed across various tissue types. Akt1 is primarily expressed in the brain, heart and lung (Coffer and Woodgett, 1991); Akt2 is mainly expressed in skeletal muscles and embryonic brown fats (Altomare et al., 1995; Altomare et al., 1998); Akt3 is predominantly expressed in the lung, brain and kidney (Brodbeck et al., 1999). The three Akt isoforms share a conserved N-terminal PH domain, a central kinase domain and a C-terminal regulatory domain, which contains a hydrophobic motif, characteristic of the cyclic adenosine monophosphate (cAMP) dependent protein kinase A/protein kinase G/protein kinase C super family of protein kinases, as depicted in figure 1.7 (Song et al., 2005). The N-terminal PH domain of Akt interacts with PIP_3 and $PI(3,4)P_2$ (Franke et al., 1997).

In vivo, knockout of the different Akt isoforms in mice has revealed distinct biological roles: *Akt1* knockout mice were found to be smaller than the control mice and showed increased rates of apoptosis in some tissues, reflecting the role of *Akt1* in cell survival (Chen et al., 2001; Cho et al., 2001b). *Akt2* null mice developed type II diabetes and had impaired glucose utilisation revealing a role of *Akt2* in the insulin receptor signalling pathway (Cho et al., 2001a; Garofalo et al., 2003). In a separate study, point mutations in the kinase domain of *Akt2* were identified in a familial form of severe insulin

resistance, supporting the role of *Akt2* in glucose metabolism (George et al., 2004). *Akt3* knockout mice display impairments in brain development, however the exact functional role of *Akt3* has been less well defined (Yang et al., 2004).

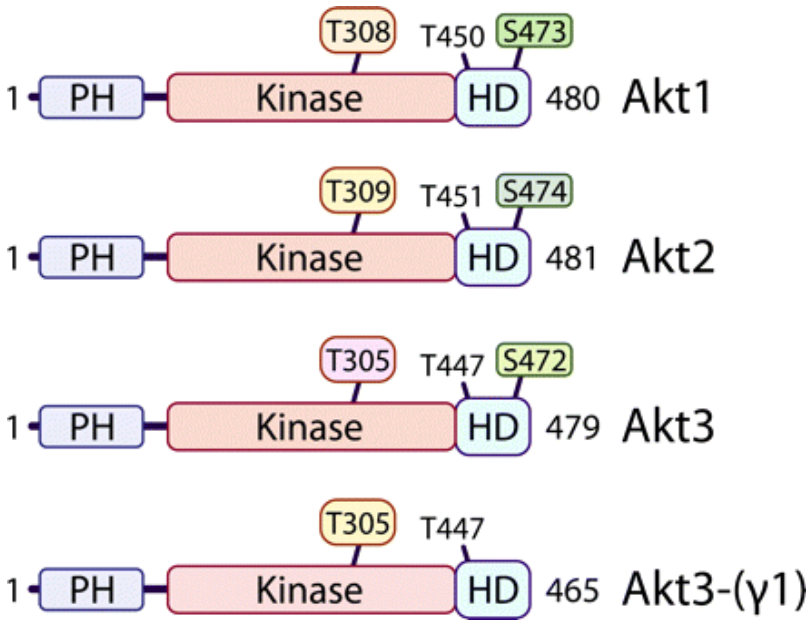

Figure 1.7 Domain structures of the Akt isoforms. Three human isoforms of Akt have been identified that share approximately 80% amino acid sequence homology. In addition, a splice variant of Akt3 has been found with a truncated hydrophobic domain. PH – pleckstrin homology domain; HD – hydrophobic domain. Image source: (Matheny and Adamo, 2009)

1.2.2.2.1 Akt regulation

The coordinated activation of Class I PI3K and SHIP1/2 gives rise to PIP_3 and $PI(3,4)P_2$ accumulation at the plasma membrane to which Akt can bind via its PH domain. Akt is activated by site-specific phosphorylation at residues Thr308 and Ser473, by phosphoinositide-dependent kinase-1 (PDK1) and mTOR complex 2 (mTORC2)/DNA-dependent protein kinase (DNA-PK), respectively (Alessi et al., 1996; Feng et al., 2004; Sarbassov et al., 2005). Other molecules, including integrin-linked kinase and mitogen-activated protein kinase-activated protein kinase-2 have also been reported to phosphorylate the Ser473 residue of Akt (Balendran et al., 1999; Delcommenne et al., 1998). Activation of Akt can also be PI3K-independent: cAMP elevating agents have been shown to activate Akt through protein kinase A (Filippa et al., 1999; Sable et al., 1997) and non-kinase interactors such as heat shock protein 90, heat shock protein 27, T cell leukaemia/lymphoma 1, and fucosyltransferase 1 have also been found to positively regulate Akt catalytic activity (Song et al., 2005).

Genetic alterations of all three Akt isoforms have been found in various cancer types. A somatic mutation in the PH-domain of *Akt1* was discovered in breast (8%), colorectal (6%) and ovarian (1%) cancers (Carpten et al., 2007). The PH domain mutation allows promiscuous binding to the plasma membrane in the absence of 3' PIs. In the absence of serum, constitutive phosphorylation of S473 was observed in these mutants. However, T308 phosphorylation required serum, suggesting that cancers harbouring this mutation may still require some PI3K activity for full activation of Akt. Mutations in *Akt2* and *Akt3* were identified in melanoma samples as well as colorectal cancer, albeit infrequently occurring (Davies et al., 2008; Parsons et al., 2005).

1.2.2.2.2 Akt and cell survival

The substrates of Akt are involved in crucial processes that promote cell survival, metabolism, cell proliferation, cell growth, angiogenesis and glucose uptake; these are all important functions in the development and maintenance of cancer cells.

Akt enhances cell survival by blocking the function of the Bcl-2 homology domain 3 (BH3)-only proapoptotic proteins, which exert their effects by binding and sequestering pro-survival Bcl-2 family members. Akt directly phosphorylates BH3-only protein Bcl-2 associated death promoter (BAD) on S136, which creates a binding site for 14-3-3 regulatory proteins and triggers the release of BAD from their target proteins (Datta et al., 1997; Datta et al., 2000; del Peso et al., 1997). Akt also inhibits expression of BH3-only proteins by phosphorylation of forkhead box O (FOXO) proteins in the nucleus, which results in FOXO transcription factors being displaced from target genes that promote apoptosis, cell-cycle arrest and metabolic processes, as well as being exported out of the nucleus (Tran et al., 2003). Other targets of Akt involved in cell survival include the multi-site phosphorylation of E3 ubiquitin ligase mouse double minute 2 (MDM2) homolog by Akt, which in turn inhibits p53 function and transcription of the BH3-only proapoptotic proteins Puma and Noxa. Akt also phosphorylates glycogen synthase kinase (GSK) family member 3 (GSK3) isoforms, which inhibit anti-apoptotic family member MCL-1. However, it is unclear what importance these targets play in cell survival. Finally, Akt indirectly promotes cell survival through its roles in nutrient uptake, metabolism, and maintenance of mitochondrial membrane potential.

1.2.2.2.3 Akt and cell growth

In addition to cell survival, Akt also plays a role in a well conserved function of cell growth through activation of mTOR complex 1 (mTORC1), a critical regulator of translation initiation and ribosome biogenesis (Wullschleger et al., 2006). mTORC1, a complex composed of the protein kinase mTOR, Raptor and mammalian lethal with SEC13 protein 8, promotes cell growth in response to nutrients and growth factors. Upon activation, mTORC1 alters metabolism from catabolic metabolism to growth-promoting anabolic metabolism, stimulating the synthesis of proteins, lipids, and nucleotides (Howell et al., 2013). Due to the resource demanding cellular processes downstream of mTORC1, cells have evolved mechanisms whereby the activation state of mTORC1 is influenced by the intracellular availability of nutrients and energy (Dibble and Manning, 2013). mTORC1 is regulated by a variety of secreted factors including growth factors, cytokines, and hormones, such as insulin and insulin-like growth factor 1. Insulin activates mTORC1, which inhibits the TSC1-TSC2-TBC1D7 complex (the tuberous sclerosis complex (TSC) complex) to turn on Ras homolog enriched in brain (Rheb), an essential activator of mTORC1 (Menon et al., 2014). Loss of the PTEN tumour suppressor results in constitutive activation of mTORC1 (Menon et al., 2014). While the mechanism of mTORC1 activation of downstream substrates by Akt is unclear, it has been suggested that Akt directly phosphorylates mTORC1 at S2448 and activates it, but the effects of this stimulation has failed to demonstrate functional significance (Scott et al., 1998; Sekulic et al., 2000) and S6K1 rather than Akt has been shown to be responsible for phosphorylation of the S2448 site (Chiang and Abraham, 2005; Holz and Blenis, 2005). A second Akt substrate that regulates mTORC1 is proline-rich Akt substrate of 40 kDa (PRAS40). Overexpression of the mutant homologue of PRAS40 blocked Akt activation of S6K1, suggesting that Akt-

mediated phosphorylation of PRAS40 stimulates mTORC1 signalling (Sancak et al., 2007; Vander Haar et al., 2007).

1.2.2.2.4 Akt and cell proliferation

Cell proliferation is another key process that Akt promotes through regulation of downstream targets involved in cell cycle progression. In brief, progression of the cell cycle can be divided into four stages: S phase, M phase, G1 phase, and G2 phase (discussed in detail in section 1.3.6.4). After mitosis occurs in the M phase, the cells undergo cell growth in the G1 phase. DNA replication follows in the S phase, and the cell prepares for entry into mitosis in the G2 phase. The phosphorylation of the $p27^{Kip1}$ cyclin-dependent kinase inhibitor by Akt (Liang et al., 2002; Shin et al., 2002; Viglietto et al., 2002) results in cytosolic sequestering of $p27^{Kip1}$ through 14-3-3 protein binding (Sekimoto et al., 2004). Preventing nuclear localisation of $p27^{Kip1}$ results G1 cell cycle progression through cyclin E and cyclin A. Akt also regulates p27 by phosphorylating FOXO transcription factors, thus inhibiting p27 transcription. Akt dependent phosphorylation of targets such as GSK3, tuberous sclerosis 2, and PRAS40, is also likely to drive cell proliferation by regulating the stability and synthesis of proteins involved in G1 cell cycle progression. GSK3 mediates phosphorylation of the G1 cyclins, cyclin D and cyclin E, and the transcription factors c-jun and c-myc, which all play a central role in the G1/S phase cell cycle transition. Phosphorylation of these molecules targets them for proteasomal degradation (Diehl et al., 1998; Wei et al., 2005; Welcker et al., 2003; Yeh et al., 2004). The importance of Akt in the transition through other phases of the cell cycle remains unclear. Elevated Akt activity has been shown during the G2/M phase of the cell cycle, and Akt activation promotes mitosis

progression even upon DNA damage (Kandel et al., 2002; Shtivelman et al., 2002). Constitutively active Akt has been found to directly phosphorylate the DNA damage checkpoint kinase Chk1 on S280 (King et al., 2004), stimulating Chk1 translocation to the cytosol, where it is sequestered by DNA damage sensors ataxia telangiectasia mutated (ATM) and ATM and Rad3-Related (ATR) (Puc et al., 2005).

1.2.2.2.5 Akt and angiogenesis

PI3K/Akt pathway activation by VEGF and phosphorylation of Akt substrates is likely to contribute to angiogenesis though endothelial cell survival, growth and proliferation. Furthermore, Akt directly phosphorylates and activates endothelial nitric oxide (NO) synthase, which stimulates vasodilation, vascular remodelling and angiogenesis (Morbidelli et al., 2003). The Akt1 isoform exerts an essential role in blood flow control, cellular migration, and NO synthesis during postnatal angiogenesis (Ackah et al., 2005). Through PI3K/Akt signalling, mTORC1 mediated translation of hypoxia-inducible factor-1/2 α (HIF1α and HIF2α) leads to expression and secretion of VEGF and other angiogenic factors, stimulating angiogenesis in a dual autocrine and paracrine fashion (Gordan and Simon, 2007; Semenza, 2003).

1.2.2.2.6 Akt and cell metabolism

Akt signalling also regulates nutrient uptake and cell metabolism through a variety of downstream targets, the more prominent function of Akt being its ability to stimulate glucose uptake in response to insulin (figure 1.8). Akt2 associates with glucose transporter (Glut) family member 4 (Glut4)-containing vesicles upon insulin stimulation

of adipocytes (Calera et al., 1998) and Akt activation results in the translocation of Glut4 to the plasma membrane. Activation of mTORC1 promotes the transcription of Glut1, the main glucose transporter in most cell types, in a HIF1α dependent manner (Taha et al., 1999; Zelzer et al., 1998). Akt has also been found to regulate amino acid uptake, through mTORC1 driven signalling (Edinger and Thompson, 2002), however, the mechanism of this effect remains unclear. Glucose and lipid metabolism is regulated by Akt activation through stimulation of hexokinases, which aid in converting glucose to its glucose 6-phosphate active form, but the direct target involved in this regulation is currently unknown (Robey and Hay, 2006). Glucose 6-phosphate can be processed for storage by conversion to glycogen or catabolised to produce cellular energy through glycolysis and Akt can regulate both of these mechanisms. As a result, Akt activation significantly contributes to the highly glycolytic nature of tumour cells by increasing the rate of glycolysis (Elstrom et al., 2004). Akt-mediated inhibition of GSK3 by phosphorylation inhibits phosphorylation and inhibition of glycogen synthase, thereby stimulating glycogen synthesis. Expression of glycolytic enzymes is promoted through the activity of HIF1α and FOXO1 inhibition contributes to glucose homeostasis (Accili and Arden, 2004). Lipid metabolism is regulated by Akt through phosphorylation and inhibition of GSK3, which targets promoting transcription factors involved the biosynthesis of cholesterol and fatty acids (Sundqvist et al., 2005).

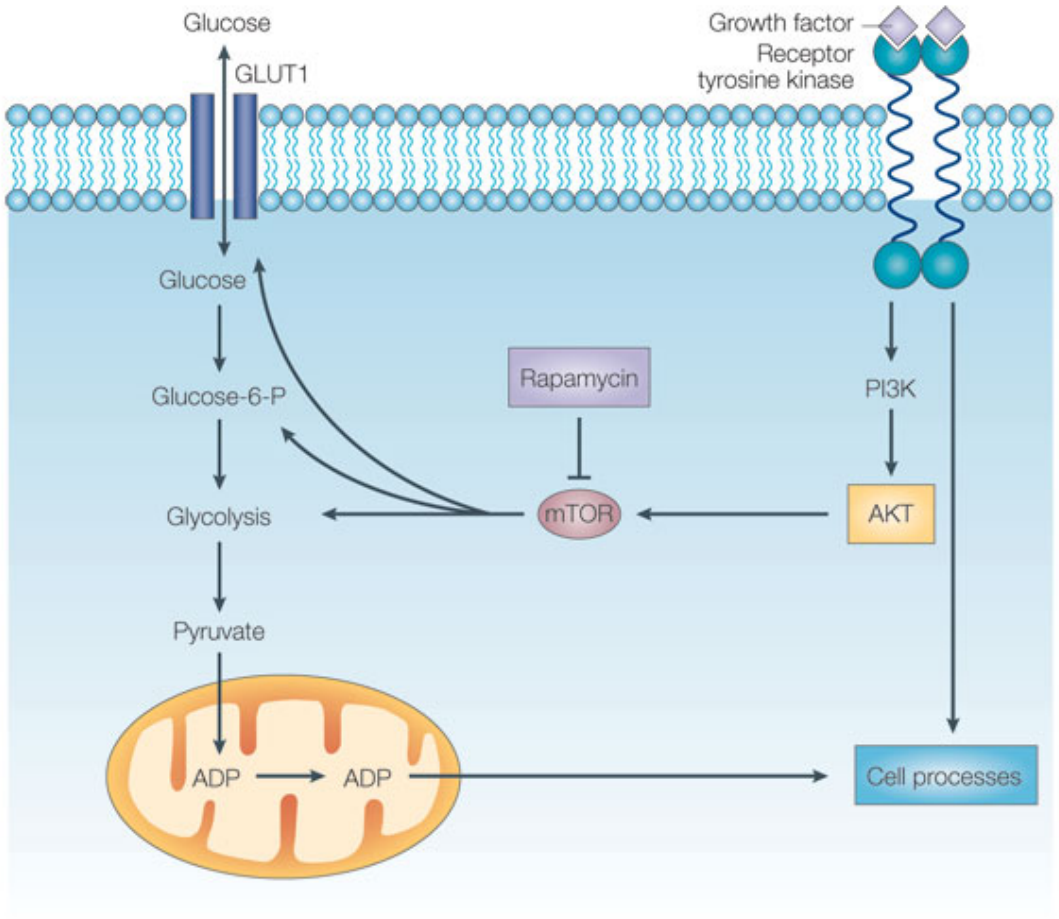

Figure 1.8. Signalling pathway of Akt in cell metabolism. Activation of RTK activates Akt and mTOR, which stimulate glycolysis in part by Akt-induced localisation of glucose transporters to the cell surface. Image source: (Hennessy et al., 2005)

1.2.2.2.7 Akt and cellular migration and invasion

Over the last few years, the role of Akt in cellular migration and invasion has been better defined. Activation of Akt1 decreases mammary epithelial cell migration, and promotes an epithelial to mesenchymal transition that resembles events required for metastasis (Irie et al., 2005; Yoeli-Lerner et al., 2005). Akt1 has an inhibitory effect on the *in vitro* migration and leads to the degradation of nuclear factor of activated T cells transcription factors (Yoeli-Lerner et al., 2005). Small interfering RNA knockdown of Akt1, but not Akt2, led to an increase in the migration of mammary epithelial cells, and also increases activation of extracellular signal-regulated kinases (ERK) family members 1 and 2 (ERK1 and ERK2), a signalling event required for the enhanced migration. The mechanism for these two effects remains unknown. Studies of Akt isoforms in mouse tumour models have the same effect, with one study suggesting Akt1 inhibits metastases, whereas Akt2 promotes it, and vice versa in another study (Arboleda et al., 2003; Hutchinson et al., 2004; Zhou et al., 2006). These studies demonstrate that Akt has significant cross talk with other signalling pathways and also emphasises the differing roles of Akt isoforms.

1.2.2.3 Akt and autophagy

Class I PI3K can regulate autophagy indirectly via Akt and mTORC1. Once activated, Akt phosphorylates and inhibits TSC2, which allows GTP-bound Rheb to activate the mTORC1 complex. This results in inhibition of autophagy by phosphorylation and regulation of proteins involved in autophagosome formation. When there is an abundance of nutrients, active mTORC1 inhibits autophagosome formation by associating with the ULK1-ATG13-FIP200 complex and phosphorylating ULK1 (the

mammalian homologue of the autophagy yeast protein Atg1) and Atg13. (Hosokawa et al., 2009; Jung et al., 2009). The activity of downstream target of mTORC1, S6 kinase, has also been associated with autophagy suppression, however other studies suggest that S6 kinase promote autophagy instead (Armour et al., 2009; Blommaart et al., 1995; Zeng and Kinsella, 2008). A study of another downstream target of mTORC1, death-associated protein-1 (DAP1), revealed that under amino acid deprivation, decrease in DAP1 phosphorylation restores the anti-autophagic function of DAP1 (Koren et al., 2010). mTORC2 can negatively regulate autophagy indirectly through Akt. Akt activation results in the inactivation of FoxO3, which prevents expression of its target genes, such as autophagy-related genes, such as LC3 and Bnip3 (Brunet et al., 1999).

1.2.3 Termination of the PI3K/Akt pathway

Negative regulation of the PI3K/Akt pathway can be initiated by several components, namely by the phosphatase activity of PTEN, SH2-containing inositol 5'-phosphatase 1/2 (SHIP 1/2) and inositol polyphosphate 4-phosphatase type I and II (INPP4A/INPP4B).

1.2.3.1 PTEN

Negative regulation of the PI3K/Akt signalling pathway is conducted in part by the catalytic function of tumour suppressor PTEN, which dephosphorylates PIP_3 to $PI(4,5)P_2$. This prevents PIP_3-dependent recruitment of Akt and PDK1 to the plasma membrane and activation of AKT. The domain structure of PTEN is a 403 amino acid protein that is composed of five functional domains: a $P(4,5)P_2$ binding domain , a phosphatase domain, a C2 domain, a carboxyl-terminal tail and a post synaptic density

protein (PSD95), Drosophila disc large tumor suppressor (Dlg1), and zonula occludens-1 protein (zo-1) (PDZ) binding domain.

Cytogenetic and molecular studies in the 1980s were the first to reveal partial or complete loss of chromosome 10 in brain, bladder and prostate cancer (Bigner et al., 1984). It was not until 1997 that the tumour suppressor gene *PTEN* was identified at the 10q23 locus and found to be disrupted in multiple sporadic tumour types (Li et al., 1997; Steck et al., 1997). Germline mutations of *PTEN* were also linked with Cowden syndrome (Liaw et al., 1997), a rare disorder characterised by multiple tumour-like growths as well as a predisposition to develop certain forms of cancer.

Inactivation of *PTEN* leads to loss of its lipid phosphatase activity, resulting in an accumulation of PIP_3 and consequently increased PIP_3-dependent activation of Akt and activation of its downstream targets. The majority of somatic mutations in *PTEN* result in protein truncation. Missense mutations have also been found in central nervous system (20%), endometrial (39%), colorectal (9%), skin (17%), prostate (14%), breast (6%) and ovarian (4%) cancers, as documented by the Sanger Institute Catalogue of Somatic Mutations in Cancer (COSMIC) website (http://www.sanger.ac.uk/perl/genetics/CGP/cosmic?action=gene&ln=PTEN). *PTEN* inactivation has also been found to be due to epigenetic silencing, through promoter hypermethylation in a variety of cancers (Alvarez-Nunez et al., 2006; Garcia et al., 2004; Goel et al., 2004; Ho et al., 2009; Salvesen et al., 2001). PTEN protein levels correlate with disease severity, suggesting that PTEN is functionally haploinsufficient (Alimonti et al., 2010; Salmena et al., 2008). A graphical representation of the

correlation between gradual PTEN loss, Akt signalling and disease phenotype in mice is depicted in figure 1.9.

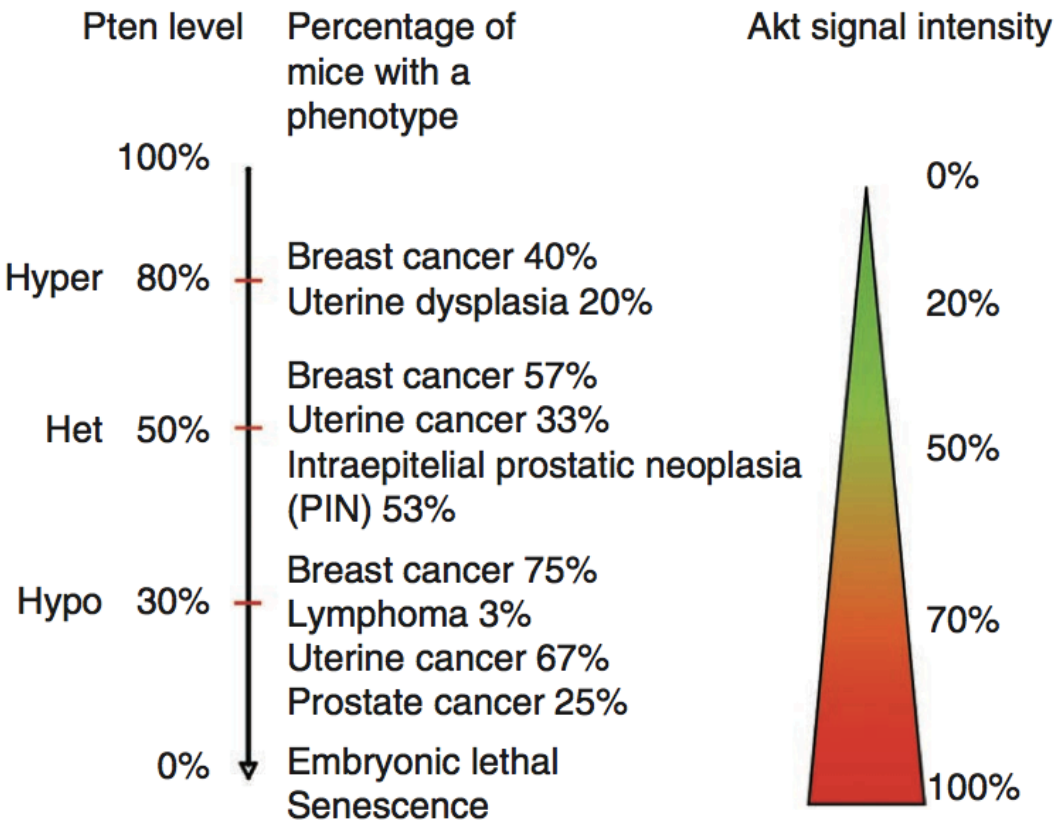

Figure 1.9. Correlation between PTEN loss, Akt signal intensity and incidence of the indicated phenotypes. Through the generation and characterisation of a $PTEN^{hy/+}$ mouse model, even a negligible decrease in PTEN expression is sufficient to promote cancer susceptibility in mice. Image and method source: (Alimonti et al., 2010)

Heterozygous loss of *PTEN* in mice results in neoplasia of multiple epithelia, including the intestine, prostate, endometrium and mammary glands (Podsypanina et al., 1999) and homozygous deletion of *PTEN* leads to aggressive prostate carcinoma (Trotman et al., 2003; Wang et al., 2003). Furthermore, loss of PTEN expression in primary tumours is associated with higher Gleason scores, a measure of prognosis evaluation in men with prostate cancer, and an accumulation of *PTEN* mutations have been found in metastatic disease as well (Sansal and Sellers, 2004). Interestingly, while loss of PTEN is tumorigenic, it has not been clearly established if PTEN loss alone is sufficient to activate Akt. Studies have shown that RTK inhibitors can downregulate Akt, even when PTEN expression is lost, suggesting that loss of PTEN might not preclude the capacity of RTK inhibitors to shut down PI3K signalling (Stommel et al., 2007). However, it seems to reduce to likelihood of cancers responding to these inhibitors as single agent therapies (Berns et al., 2007; Bianco et al., 2003; Mellinghoff et al., 2005; Nagata et al., 2004). Lastly, PTEN also possesses protein phosphatase activity and plays a key role in autodephosphorylation-mediated regulation of its lipid phosphatase activity (Tibarewal et al., 2012).

1.2.3.2 SHIP1/2

SRC homology 2 (SH2)-containing inositol 5'-phosphatase 1 (SHIP1) and SHIP2 proteins are negative regulators of the PI3K/Akt pathway. SHIP1/2 consists of an N-terminal SH2 domain which binds to specific phosphotyrosine-containing sequences found in proteins such as SRC homology 2 domain-containing protein, a central catalytic phosphatase domain and a C-terminal proline-rich domain which is recognised by SH3-domain containing proteins. SHIP2 contain an additional C-terminal sterile α-domain. The haematopoietic-restricted SHIP1 hydrolyses PIP_3 to $PI(3,4)P_2$. The SHIP1

homologue, SHIP2, is found more widely expressed in tissues, such as the heart, liver, skeletal muscles, and brain (Hamilton et al., 2011), and like SHIP1, dephosphorylates PIP_3 to $PI(3,4)P_2$ *in vitro* and *in vivo* (Kagawa et al., 2008; Pesesse et al., 1997; Wada et al., 2001). While $PI(3,4)P_2$ can still act as a second messenger through affinity of Akt for $PI(3,4)P_2$ (Klippel et al., 1997), SHIP1 dampens the PIP_3 – mediated Akt signalling, and thus acts as a negative regulator of the PI3K pathway. SHIP1 is mutated or markedly reduced in many leukemias and lymphomas; cells from acute myeloid leukemia patients display down regulation of SHIP1 expression (Luo et al., 2003) and SHIP1 is also found truncated, or totally absent in T cells from patients with T acute lymphoblastic leukemia (Lo et al., 2009). Considering that SHIP1 inhibition promotes cancer cell growth, it has been described that oncogenic proteins, such as leukemia associated oncogene breakpoint cluster region-C-Abl oncogene, induce SHIP1 down-regulation (Ruschmann et al., 2010; Sattler et al., 1999). The role of SHIP2 in tumour initiation is more ambiguous and laboratories have failed to identify SHIP2 as a tumour suppressor; however, the phosphatase may play a role in tumour progression (Prasad et al., 2008; Yamanaka et al., 2009).

Knockout mouse models have revealed greater insight into the functional role of SHIP1/2. SHIP1 knockout mice remained viable and fertile, but with reduced lifespan due to myeloid infiltration (Liu et al., 1999), suggesting that modulation of PIP_3 levels by SHIP1 negatively regulates cytokine-induced myeloid cells proliferation. SHIP1 knockout also affected a variety of lymphocytes, including impaired B cell development and function (Helgason et al., 1998), defective natural killer cells (Wang et al., 2002) and reduced T-cells, along with their precursors (Collazo et al., 2009; Kashiwada et al., 2006). While SHIP1 knockout results in impaired haematopoietic development, SHIP2

transgenic mice display markedly differing phenotypes due to different tissue-specific expression levels. Overexpression of SHIP2 in mice resulted in a reduction of Akt phosphorylation in liver, adipose tissue and skeletal muscles and as a consequence the mice developed insulin sensitivity and impaired glucose homeostasis (Kagawa et al., 2008). By reducing the pool of PIP_3, SHIP2 decreased Akt activation, glycogen synthesis (Sasaoka et al., 2001) and glucose uptake (Wada et al., 2001). SHIP2 is therefore considered a crucial negative regulator of glucose homeostasis. On the other hand, SHIP2 knockout mice generated in several studies have resulted in contradicting characteristics (Clement et al., 2001; Sleeman et al., 2005). Further studies will need to be conducted to clarify the role of SHIP2 in glucose homeostasis.

1.2.3.3 Inositol polyphosphate 4-phosphatases

Inositol polyphosphate 4-phosphatases are the only known $PI(3,4)P_2$ phosphatases in mammalian cells and consists of two types: type I (INPP4A) and type II (INPP4B). Apart from $PI(3,4)P_2$, INPP4A and INPP4B also hydrolyse the soluble inositol phosphates, inositol 1,3,4-trisphosphate ($Ins(1,3,4)P_3$) and inositol 3,4-bisphosphate ($Ins(3,4)P_2$), however the rate of hydrolysis is over 100-fold slower than hydrolysis of PIs (Norris and Majerus, 1994). Mammalian INPP4A and INPP4B share 37% amino acid sequence homology, as well as a core domain structure consisting of an N-terminal C2 lipid-binding domain, a largely uncharacterised central domain and a C-terminal dual phosphatase domain. The C2 lipid-binding domains of the 4-phosphatases are calcium-independent and interact with the membrane through electrostatic and PI interactions (Murray and Honig, 2002; Norris et al., 1997a; Norris and Majerus, 1994). While not much is known about the central domains of the 4-phosphatases, it has been proposed that these domains contain predicted PEST sequences, polypeptide sequences

enriched in amino acids proline (P), glutamic acid (E), serine (S), and threonine (T) which target proteins for rapid intracellular proteolysis (Norris et al., 1997b; Rechsteiner and Rogers, 1996). The greatest sequence similarity between the INPP4A and INPP4B is exhibited within their lipid phosphatase domain. This region contains the $C(X)_5R$ catalytic region, where X represents any amino acid. This domain is also found in PTEN, as well as other dual specificity protein phosphatases, which are capable of dephosphorylating both lipids and proteins. Splice variants of INPP4A and INPP4B have been identified consisting of an α and β form. INPP4Aα and INPP4Bα consist of a hydrophilic C-terminal region, whereas INPP4Aβ and INPP4Bβ consist of a hydrophobic C-terminal region (Norris et al., 1997a; Norris et al., 1995a); however, their individual functions remain unknown.

INPP4A is predominantly expressed in brain, whereas INPP4B is found highly expressed in skeletal muscle, heart, brain, and pancreas, epithelial cells of the breast, and prostate glands. INPP4A is critical for neuronal function, and its loss results in neurodegeneration and early postnatal mortality (Nystuen et al., 2001; Sasaki et al., 2010). However, limited evidence points to INPP4A and its role as a tumour suppressor. INPP4B, on the other hand, has been found to play a role in cancer development in a variety of different tissues and is the protein of interest for this study.

INPP4B was initially isolated from rat brain and shown to be an enzyme that accounts for 4-phosphate activity present in rat tissue (Norris et al., 1997a; Norris et al., 1995b). The murine *INPP4B* locus was mapped on chromosome 8 in a synthetic synthesised region of the human 4q27-31 interval between the cytokine interleukin 15 gene and the ubiquitin specific peptidase 38 gene. The two murine isoforms of INPP4B, INPP4Bα

and INPP4Bβ, are encoded by this locus and are highly conserved; consensus phosphatase catalytic sites and conserved C2 domains share vast similarity with human and rat homologues with INPP4B C2 lipid-binding domains sharing more that 91% sequence homology (Ferron and Vacher, 2006). A novel shorter isoform of INPP4Bα has also been characterised resulting from an alternative translation initiation site and exon 5 skipping (Ferron and Vacher, 2006). The two isoforms have different expression patterns and cell localisations; INPP4Bα exhibits relatively ubiquitous expression with a wide tissue distribution and mainly a cytosolic subcellular localisation. In contrast, INPP4Bβ is mainly expressed in brain, heart, intestine, skeletal muscles and spleen tissue and is associated with the Golgi apparatus (Ferron and Vacher, 2006).

1.2.3.3.1 INPP4B substrates

The main substrate of INPP4B is PI(3,4)P_2, which it dephosphorylates on the D4 position generating PI(3)P. The murine C2 domain of INPP4B preferentially binds to phosphatidic acid and PIP_3; however, INPP4B has been found to be able to dephosphorylate PIP_3 in the context of bone morphogenesis (Ferron and Vacher, 2006). Gewinner e*t al.* reported that INPP4B is solely able to dephosphorylate PI(3,4)P_2 *in vitro* in mammary epithelial cells and overexpression of INPP4B depletes this phospholipid pool (Gewinner et al., 2009). The substrates of INPP4B also include the soluble inositol phosphates, Ins(1,3,4)P_3 and inositol 3,4-bisphosphate; however, the rate of hydrolysis is over 120-fold and 900-fold slower than for the PI(3,4)P_2, respectively (Norris et al., 1997a; Norris and Majerus, 1994). In osteoclasts, INPP4B was found to also dephosphorylate PI(4,5)P_2 and the rate of hydrolysis for Ins(1,3,4)P_3 was approximately five times higher than for the PIs (Mathieu Ferron, 2011).

1.2.3.3.2 INPP4B in human diseases

Studies conducted over the last few years have provided evidence linking INPP4B as a tumour suppressor gene in several epithelial cancers, including breast cancer, prostate cancer and melanoma (Agoulnik et al., 2011; Fedele et al., 2010; Gewinner et al., 2009; Hodgson et al., 2011; Kim et al., 2012; Perez-Lorenzo et al., 2013a). INPP4B has also been implicated as a tumour biomarker for radioresistance in laryngeal cancer (Kim et al., 2012) and loss of INPP4B is associated with squamous cell lung carcinoma (Magnussen A., 2011). Table 1.3 summarises INPP4B loss across several epithelial human cancers.

The role of INPP4B in breast cancer is the most well established study amongst all the cancer sub-types. INPP4B expression in normal breast tissue correlates with oestrogen receptor (ER) expression. The protein is mostly located in the ducts and lobule epithelium, and primarily in ER positive and mostly non-proliferative cells (Fedele et al., 2010). INPP4B is frequently lost in the more aggressive subtypes of breast cancer, such as triple negative (ER negative, progesterone receptor negative and epidermal growth factor receptor ErbB/HER negative) and basal-like breast cancer (Fedele et al., 2010). Genomic studies of INPP4B in breast cancer cell lines revealed over half of basal-like breast cancers exhibit loss of heterozygosity (LOH) of INPP4B, whilst only a small fraction of non-basal like cancers carry the same allelic loss. Furthermore, INPP4B LOH is detected in the 60% of BRCA1 mutant breast cancers (Gewinner et al., 2009). Expression of INPP4B may therefore represent a breast cancer prognostic marker, since it is expressed in the luminal A ER-positive and low grade carcinomas, and correlates to better patient survival, while loss of expression is frequently found in the more aggressive breast cancer subtypes (Fedele et al., 2010; Gewinner et al., 2009).

Evidence for the role of ER in the regulation of INPP4B, however, remain rudimentary and contradictory; Transcription levels of INPP4B are not altered in response to oestradiol stimulation, nor does INPP4B expression affect ER levels in ER-positive and INPP4B-positive MCF-7 breast cancer cells (Fedele et al., 2010). In contrast, a gene array study of breast tumour xenografts has shown INPP4B transcription is enhanced following oestrogen receptor stimulation (Harvell et al., 2006). Further investigation will be required to clearly define the role of ER in INPP4B regulation. Loss of INPP4B in conjunction with loss of PTEN has also been observed in breast cancer; Gewinner *et al.* reported that loss of both INPP4B and PTEN resulted in cellular senescence in human mammary epithelial cells (HMECs) and Fedele *et al.* observed that INPP4B loss occurred more in PTEN-null breast cancers (Fedele et al., 2010; Gewinner et al., 2009).

INPP4B has also been discovered as a tumour suppressor in prostate cancer. Analysis of the genome and transcriptome of 218 prostate cancer tumours revealed that 42% of primary prostate cancers and all metastatic prostate cancers exhibit aberrations in the PI3K/Akt pathway (Taylor et al., 2010). Interestingly, in the metastatic prostate cancer samples almost half of the samples had reduced INPP4B expression, to a similar extent as reduced of PTEN expression (Taylor et al., 2010). Hodgson *et al.* found that *INPP4B* is an androgen responsive gene, and androgen receptor (AR) activation results in an increase in INPP4B transcription in the LNCaP prostate cancer cell line (Hodgson et al., 2011). In addition, PTEN did not demonstrate androgen-regulated expression. Androgen ablation therapies in the treatment of advanced prostate cancers are associated with increased Akt signalling (Wang et al., 2007). Since INPP4B is an androgen regulated tumour suppressor gene in prostate epithelium, INPP4B expression

levels should be assessed when considering androgen ablation therapies for advanced prostate cancer patients.

INPP4B has also been implicated in other diseases. Kim *et al.* identified INPP4B as a novel tumour resistance biomarker in the Hep-2 human laryngeal cancer cell line. INPP4B was highly expressed in radioresistant Hep-2 cells and induced by treatment with radiation or other anti-cancer drugs in lung, colon and breast cancer cell lines (Kim et al., 2012). Furthermore, INPP4B induced expression by radiation was blocked by ERK inhibition, suggesting that ERK-dependent induction of INPP4B expression triggers development of a tumour-resistance phenotype via Akt signalling (Kim et al., 2012). Thus, INPP4B is an important target molecule for the resolution of radio-resistance in cancer cells. INPP4B has also been associated with lung squamous cell carcinoma, with one-fifth of 180 samples analysed showing a LOH of INPP4B, as well as almost half showing reduced levels or INPP4B protein expression (Magnussen A., 2011; Stjernstrom et al., 2014). In addition, a decrease in INPP4B expression has been found to correlate with tumour progression in melanocytic neoplasm (Perez-Lorenzo et al., 2013b). Ferron *et al.* identified INPP4B as a major modulator of osteoclast differentiation and as a gene linked to variability of bone mineral density in mice and humans, providing evidence for INPP4B as a potential therapeutic target and biomarker for osteoclast defects and osteoporosis (Ferron et al., 2011). Finally, INPP4B aberrations have also been identified in ovarian cancer. High rates of copy number loss at the 4q31.1-3 locus was found in 39.8% of ovarian cancers (Etemadmoghadam et al., 2009). Gewinner *et al.* observed that loss of INPP4B expression in ovarian cancer tissues correlated with decreased patient survival as well as increased lymph node metastasis (Figure 1.10). It is clear that loss of INPP4B plays an important role in

cancer through its association with tumourigenesis, poor survival, therapeutic resistance and aggressive sub-types across a broad spectrum of tissue types. Further investigation is warranted to address using INPP4B as a marker for designation of therapeutic strategies.

Table 1.3. INPP4B loss in different tumour types

Tumour Type	INPP4B Loss
Breast, total (Richardson et al., 2006)	32.6% - loss of heterozygosity
Breast, BRCA1 mutant (Gewinner et al., 2009)	60.0% - loss of heterozygosity
Breast, basal-like (Fedele et al., 2010)	8.0% - loss of expression
Breast, basal-like (Weigman et al., 2011)	40% - copy number variation
Ovarian (Etemadmoghadam et al., 2009)	39.8% - copy number variation
Melanoma (Lin et al., 2008)	21.6% - loss of heterozygosity
Prostate, primary (Agoulnik et al., 2011; Taylor et al., 2010)	8.0% - loss of expression or mutation
Prostate, metastatic (Taylor et al., 2010)	47.0% - loss of expression or mutation
Nasopharyngeal carcinoma (Yuen et al., 2014)	49.2% - loss of expression

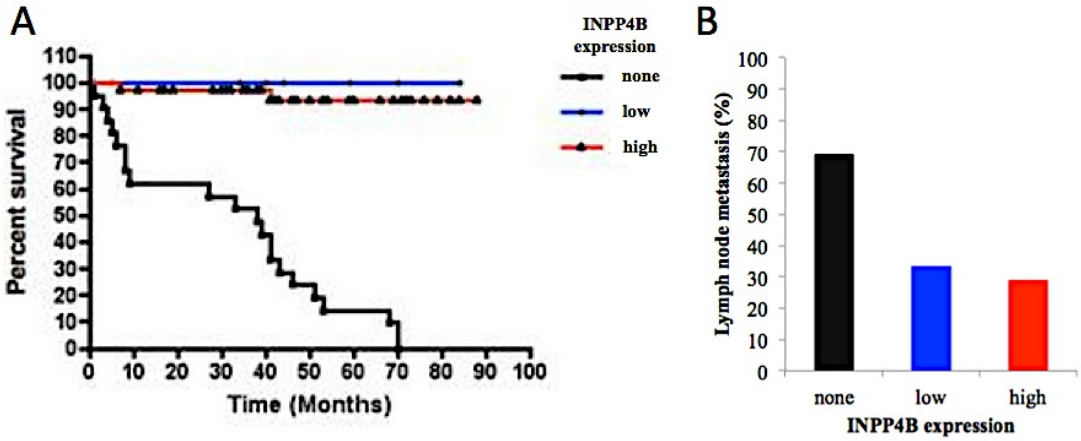

Figure 1.10. INPP4B expression levels correlate with patient survival and metastasis in ovarian cancer. (A) Survival graph over time (in months) for ovarian cancer tissue stained for INPP4B expression. Black, blue and red lines indicate no, low and high INPP4B expression, respectively. Ovarian cancer patients with no INPP4B expression had poor overall survival compared to patients with low or high INPP4B expression ($p<0.00001$). (B) INPP4B expression levels were investigated to assess correlation of lymph node metastasis in ovarian cancer tissues. Tissues that had no INPP4B expression exhibited more lymph node metastasis (9 samples, n=13), compared to tissues exhibiting low or high INPP4B expression (2 samples, n=6; 9 samples, n=31). Image source: (Gewinner et al., 2009)

1.3 DNA damage response

Recently, more research on the PI3K/Akt pathway components and their relevance to genomic stability has been conducted. Hyperactivation of Akt was found to lead to cell cycle checkpoint progression aberrations and overexpression of Akt1 was found to promote genome instability through repression of HR (Plo et al., 2008b; Puc et al., 2005). Genomic instability is recognised as a characteristic of most solid tumours and adult onset leukaemias, and ranges from obvious chromosomal changes of DNA copy number and structure alterations, to the more conspicuous DNA structure aberrations, such as nucleotide substitutions, insertions and deletions. These genetic mutations have a resulting effect on tumourigenesis, tumour development and cellular behaviour. Importantly, these mutations also influence how the tumour will respond to therapy.

Genomic integrity maintenance is controlled by the DNA damage response (DDR) network, an elaborate signal transduction system which senses DNA damage and recruits the appropriate repair factors. With the integrity of DNA being continually challenged both endogenously and exogenously, this extensive signalling network has evolved to sense different types of damage and co-ordinate a response that includes activation of transcription, cell cycle control, apoptosis, senescence, and DNA repair processes (Figure 1.11). 'Sensor proteins' respond to genotoxic stress and activate a collection of protein kinases, which co-ordinate a signalling cascade by targeting several substrates that regulate the function of downstream effectors. At the core of the DDR pathway abide the related protein kinases, ATM and ATR, which act as DNA damage sensors and are activated by DNA damage. ATM and its regulator, the MRE11-Rad50-NBS1 (MRN) complex, sense double-strand breaks (DSBs). ATR and its regulator ATR-interacting protein (ATRIP) sense single-strand breaks (SSBs), which

can be generated by the processing of DSBs, as well as SSBs present at stalled replication forks. Both kinases then phosphorylate a plethora of downstream proteins to initiate a signalling cascade that includes many common substrates and further amplify the signal. Two key proteins involved in the downstream signalling cascade are checkpoint kinase 1 and 2 (Chk1 and Chk2), two important kinases which when activated, delay cell cycle progression to facilitate DNA repair or eliminate hazardous damaged cells depending on the extent of the DNA damage. The next sections will discuss sources of DNA damage and the variety of DNA mechanisms established to counter genetic insults.

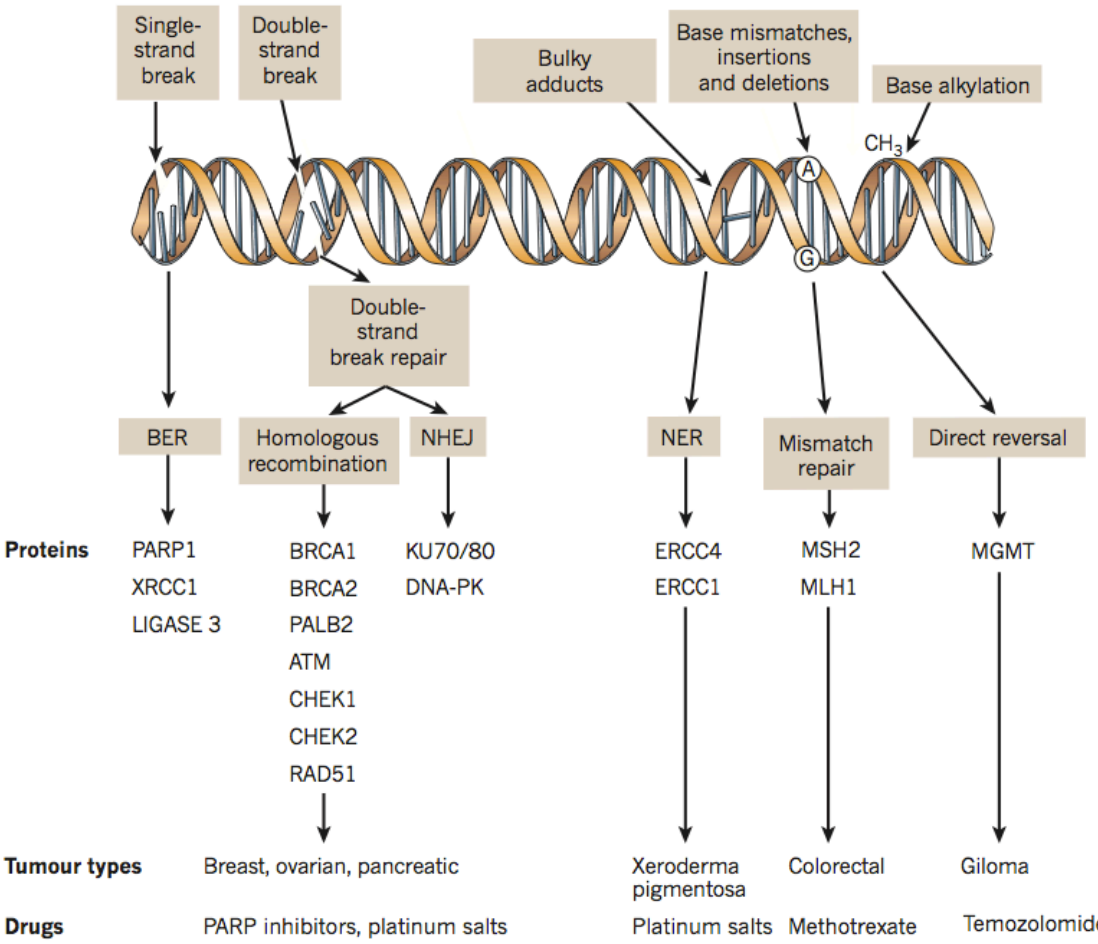

Figure 1.11. Forms of DNA damage and associated DNA damage response (DDR) pathways. Through both endogenous and exogenous sources, DNA is constantly being damaged resulting in a variety of lesions being formed, including SSBs, DSBs, bulky adducts, base mismatches/insertions/deletions and base alkylation. Upon DNA damage, various DNA repair mechanisms are implemented according to the particular insult encountered. The cell cycle stage also determines what type of DNA repair mechanism is used. Key proteins involved in each DDR mechanism are shown above, as well as the tumour types associated with DDR defects and the drugs that target these defects. BER – base excision repair; NER – nucleotide excision repair; NHEJ – non homologous end joining. Image source: (Lord and Ashworth, 2012).

1.3.1 Sources of DNA damage

In order to maintain genomic integrity, DNA must be protected from DNA damage induced by environmental agents or spontaneously generated. Spontaneous DNA alterations can occur due to deoxyribonucleotide triphosphates (dNTP) misincorporation during DNA replication, interconversion between DNA bases caused by deamination, loss of DNA bases following DNA depurination and modification of DNA bases by alkylation. In addition, oxidation of DNA bases and DNA breaks by reactive oxygen species (ROS) can be generated by normal cellular metabolism. In total, it has been estimated that a cell may experience up to 10^5 spontaneous DNA lesions per day (Hoeijmakers, 2009). DNA damage can also be generated by environmental agents and can be produced by physical or chemical sources. Ionising radiation (IR) and ultraviolet (UV) light from sunlight can induce up to 10^5 DNA lesions per cell per day. IR from cosmic radiation or medical equipment generating X-ray or radiotherapy can induce oxidation of DNA bases and DNA breaks.

1.3.2 Base excision repair

Subtle base changes to DNA through oxidative lesions, alkylation products, and deamination are repaired by base excision repair (BER). The essence of core base excision repair requires the function of four proteins: a DNA glycosylase, an AP endonuclease, a DNA polymerase, and a DNA ligase. All of these proteins co-operate together to remove a damaged DNA base and replace it with the correct base. Two forms of BER have been found, short-patch BER and long-patch BER, and varying combinations of enzymes work in concert to repair DNA damage, depending on the type of BER implemented. The decision to proceed via the long-patch or short-patch BER mechanism, however, is poorly understood. Usually, the damaged base is

recognised by a DNA glycosylase. After recognition this glycosylase catalyses the cleavage of an N-glycosidic bond, effectively removing the damaged base and creating an apurinic or apyrimidinic site (AP site). The AP endonuclease creates a single-stranded DNA nick 5' to the AP site. In short-patch BER, X-ray repair cross-complementing protein (XRCC) family member 1 (XRCC1) is recruited to the nick generated by the action of a glycosylase and/or AP endonuclease, functioning as a scaffolding protein. The AP endonuclease further processes the nick, creating a single-nucleotide gap in the DNA and DNA polymerase fills in the gap with the correct nucleotide. Finally, a DNA ligase seals the nick and completes the repair process. BER is depicted in figure 1.12.

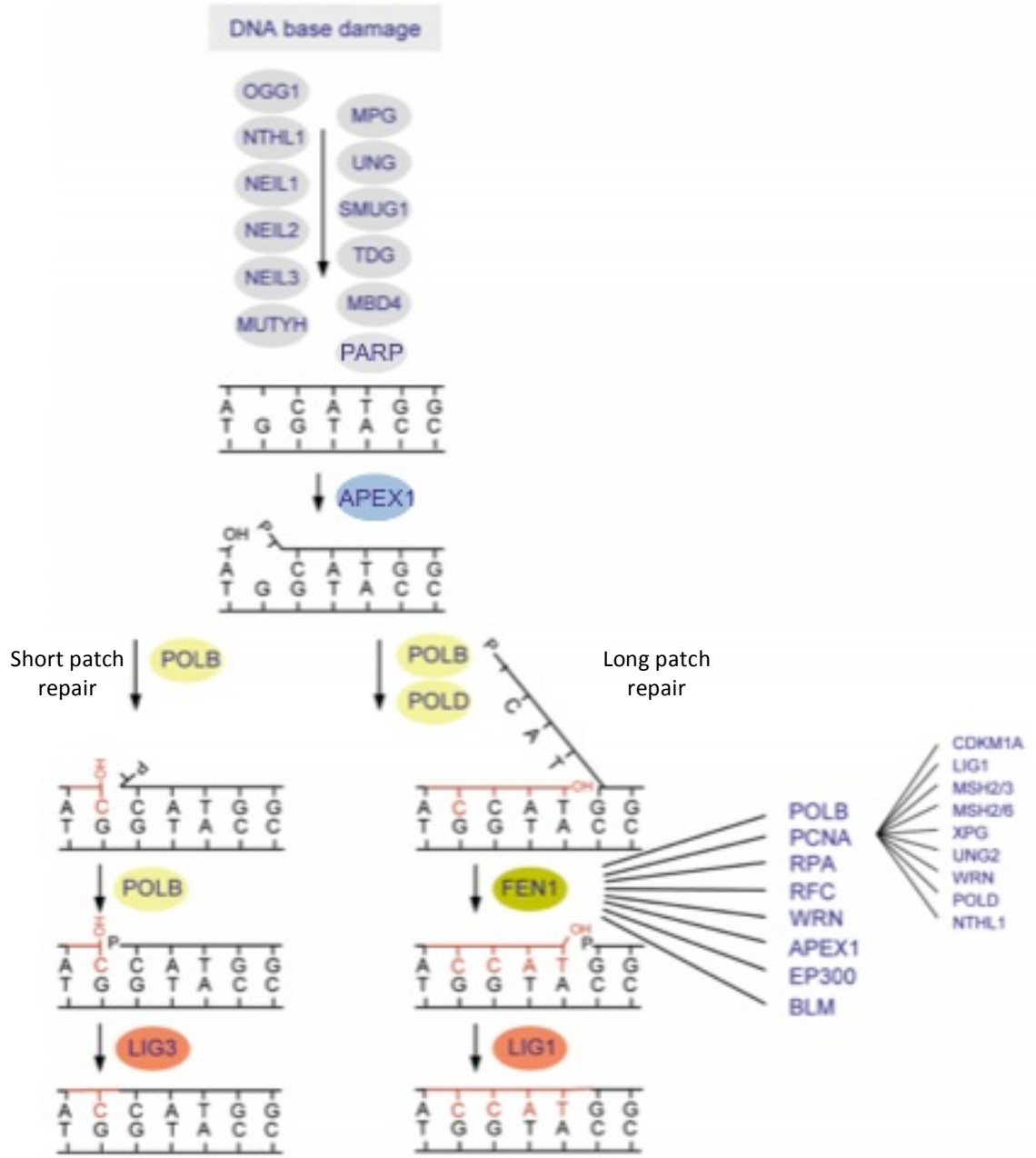

Figure 1.12. Base excision repair. DNA damage results in several proteins being recruited for base excision repair. The grey, blue, yellow and pink proteins represent DNA glycosylases, endonucleases, DNA polymerases and DNA ligases, respectively. Proteins indicated in purple font represent protein interactions involved in long patch BER. Image source: (Robertson et al., 2009)

1.3.3 Nucleotide excision repair

Nucleotide excision repair (NER) recognises and repairs DNA lesions that are caused by chemicals, which covalently bind to a DNA base and form a bulky adduct and distort the DNA helix. Compounds which produce such lesions include chemicals typically present in the environment in a relatively harmless form, such as nitrosamine found in latex and food and benzopyrenes from cigarette smoke (Wogan et al., 2004) and cross-linking agents, which have the ability to form two distinct covalent bonds with DNA, by intrastrand or interstrand crosslinks (Trimmer and Essigmann, 1999). The latter crosslink tends to be the more toxic lesion due to both strands being damaged. Detection of the structure distortion of DNA caused by the bulky adducts is conducted by sensor complex xeroderma pigmentosum (XP) group C (XPC) protein complex (XPC-HR23B-Cen2). Smaller distortions are recognised by the damaged DNA binding complex (DBB). Transcription factor II human opens a denaturation bubble of approximately thirty nucleotides around the lesion. The resulting exposed single strand DNA is then bound by replication protein A (RPA). XPG incises the damaged strand 3' of the lesion and the excision repair cross complementation group 1/xeroderma pigmentosum group F complex (ERCC1-XPF) incises the damaged strand at the 5' end. The resulting gap is filled by DNA polymerase delta/epsilon (pol δ/ε). Finally, the nick is sealed by ligase (LIG) family member 3 (LIG3), with the minority of nicks sealed by LIG1 in replicating cells (Nouspikel, 2009). Since NER requires an intact strand to serve as a template to repair the other, interstrand crosslinks repair requires a combination of NER with other DNA repair mechanisms, such as HR. NER is depicted in figure 1.13.

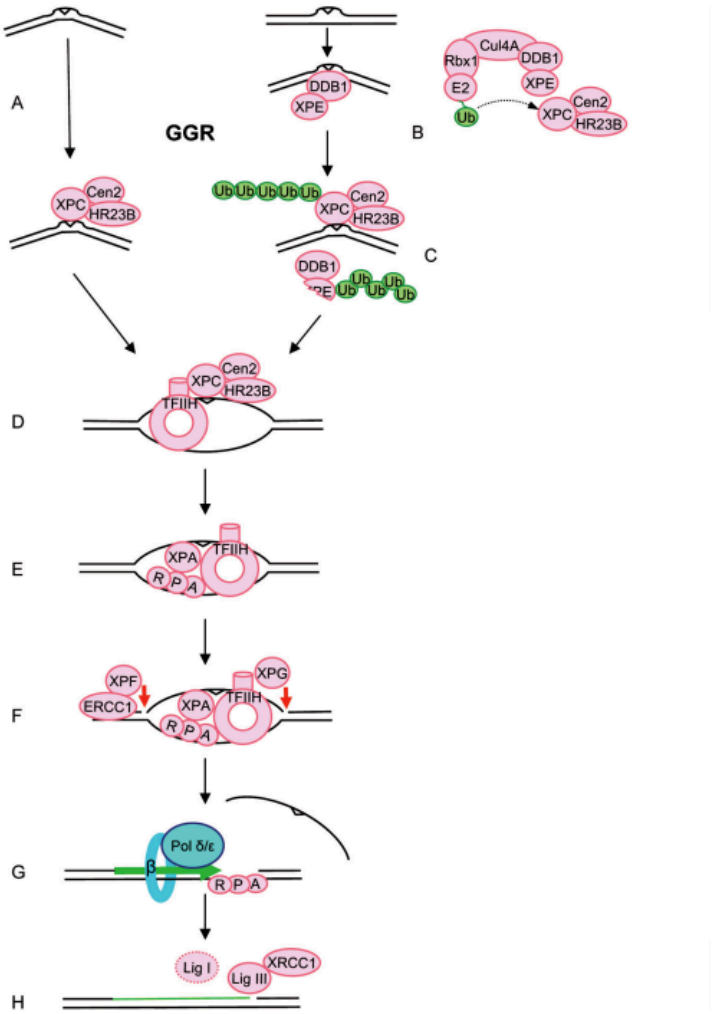

Figure 1.13. Nucleotide excision repair. (A) DNA distortion is detected by protein sensor complex XPC-HR23B-Cen2. (B) DNA lesions with small distortions are detected by the DDB complex, which results in ubiquitination of XPC and XPE. (C) Ubiquitation of XPC leads to increased affinity for DNA, whereas ubiquitation of XPE results in its degradation. (D) Transcription factor II human (TFIIH) opens up a nucleotide bubble of approximately 30 nucleotides around the lesion. (E) The XPA-RPA complex displaces the XPC complex and RPA binds to the single stranded DNA. (F) XPG removes the damaged strand 3' of the lesion; ERCC1-XPF removes the damaged strand 5' of the lesion. (G) The resulting gap is replaced by DNA polymerase ∂ or ε. (H) The nick is sealed by LIG3 or LIG1 in replicating cells. Image source: (Nouspikel, 2009)

1.3.4 Mismatch repair

Mismatch repair (MMR) substitutes bases that are incorrectly incorporated during DNA replication, thereby preventing mutations from becoming permanent in dividing cells. Defects in MMR result in a higher spontaneous mutation rate and inactivation of MMR is associated with hereditary and spontaneous cancers (Modrich and Lahue, 1996). Initially studied in *Escherichia coli* (E. coli), understanding of MMR in eukaryotes has been built upon the framework derived from prokaryotic observations. Key to the process of MMR are proteins encoded by the human homologues of E. coli proteins, mutS and mutL. Human mutS homolog 2 (hMSH2) heterodimerises with hMSH6 or hMSH3 to form hMutSα or hMutSβ, respectively, and initiates repair. hMutSα preferentially recognises mismatches of 1 or 2 nucleotides, while hMutSβ preferentially recognises larger insertion/deletion mispairs. Proliferating cell nuclear antigen (PCNA) and exonuclease 1 (EXO1) remove a patch of nascent DNA, including the misincorporated nucleotide, in a bi-directional manner. The excision gap is filled by high-fidelity DNA synthesis by pol δ and PCNA and LIG1 subsequently restores strand continuity. Defects in MMR have been associated with resistance to many DNA damaging anticancer therapeutic agents, such as cisplatin and the antimetabolite 6-thioguanine (Karran and Marinus, 1982). MMR is depicted in figure 1.14.

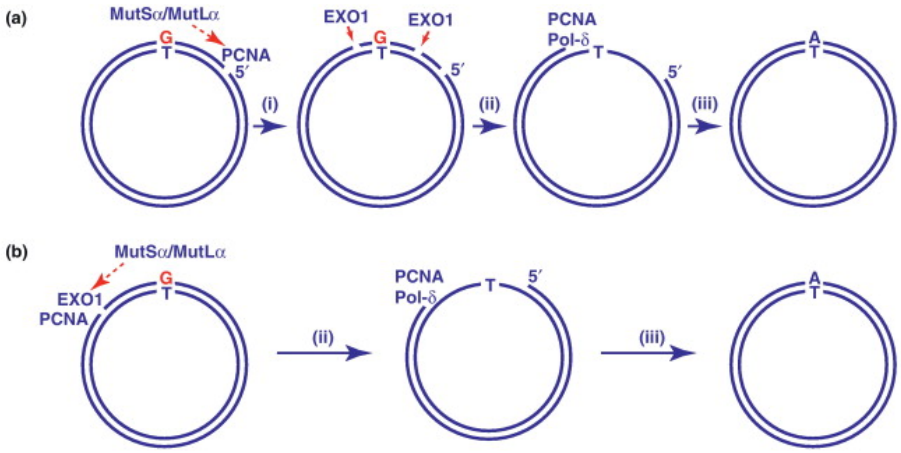

Figure 1.14. Mismatch repair. Depending on where a nick is made relative to the mismatch determines what kind of repair is conducted. A nick introduced at the outer strand either the 3' (A) or 5' (B) end of the mismatch results in a G/T to A/T repair. An inner strand nick, however, results in the repair of G/T to G/C. (A) A nick in the 3' end of the mismatch on the outer ring results in the MutSα/MutLα heterodimer complex binding to the mismatch and translocating along the DNA strand until it encounters PCNA bound at the 3' end of the nick. Additional nicks are introduced by the ternary structure, where EXO1 is loaded, generating a long single stranded gap. The gap is filled by the PCNA/pol δ complex and the nick is sealed by a DNA ligase. (B) A 5' nick relative to the mismatch allows the MutSα/MulLα complex to load EXO1 directly at the nick. The strand is degraded and the gap filled by the PCNA/pol δ complex. Image source: (Pena-Diaz and Jiricny, 2012)

1.3.5 Double strand break repair

DSBs are the most dangerous and life-threatening lesions whose repair is initiated by several DNA repair pathway mechanisms. Two main pathways are used for DSB repair: homologous recombination (HR) and non-homologous end joining (NHEJ). HR is primarily induced in the S and G2 phases of the cell cycle, when sister chromatids can be used as a template for HR (You and Bailis, 2010) resulting in error-free repair. On the other hand, NHEJ does not require the presence of a homologous DNA strand and is therefore more error prone. Failure to repair DSBs can result in chromosome loss, chromosomal rearrangements, apoptosis, or carcinogenesis (Hoeijmakers, 2001).

1.3.5.1 Classical Non homologous end joining

NHEJ repairs DSBs by rejoining the DNA ends without requiring sequence homologies, and thus is recognized as having a high potential for error. The repair mechanism proceeds by three steps: recognition of the break, DNA processing to remove non-ligatable ends and damaged DNA ends, and ligation of the DNA ends. DSBs are rapidly bound by the Ku heterodimer Ku70/Ku80, which loads onto the DSB ends by its toroidal structure (Mahaney et al., 2009). The Ku heterodimer acts as a scaffold for the association of the catalytic subunit of DNA dependent protein kinase (DNA-PKcs), recruiting the kinase to the DNA ends and activating it (Meek et al., 2008). While DNA-PKcs has several targets, the most extensively studied target is DNA-PKcs itself. There are currently 16 amino acid residues identified within the DNA-PKcs protein that can be autophosphorylated, and mutations of several of these autophosphorylation sites have resulted in diminished DNA repair and sensitivity of cells to IR (Chan et al., 2002a; Ding et al., 2003). Once bound to the DSB, autophosphorylation of DNA-PKcs on the six residue ABCDE cluster results in the destabilisation of the DNA-PKcs

interaction with the DNA ends, providing access for processing enzymes. ATM can also induce ABCDE DNA-PKcs autophosphorylation, which has been shown to facilitate access of DNA ends to DSB resecting enzymes in order to promote HR when NHEJ fails (Shrivastav et al., 2008). Excessive processing is prevented by DNA-PKcs autophosphorylation, on the five-residue PQR cluster, which helps protect DNA ends (Meek et al., 2008). After DNA-PKcs is loaded, the XRCC4/LIG4 DNA repair complex is recruited and promotes the religation of the broken ends with the help of stimulatory factor XRCC4-like factor (XLF) (Mahaney et al., 2009). Nucleases ARTEMIS and aprataxin and PNKP like factor (APLF), as well as polynucleotide kinases (PNK), process DNA termini that contain non-ligatable end groups prior to DNA ligation (Mahaney et al., 2009). ARTEMIS and APLF are phosphorylated in an ATM-dependent manner (Macrae et al., 2008; Zhang et al., 2004). NHEJ is depicted in figure 1.15.

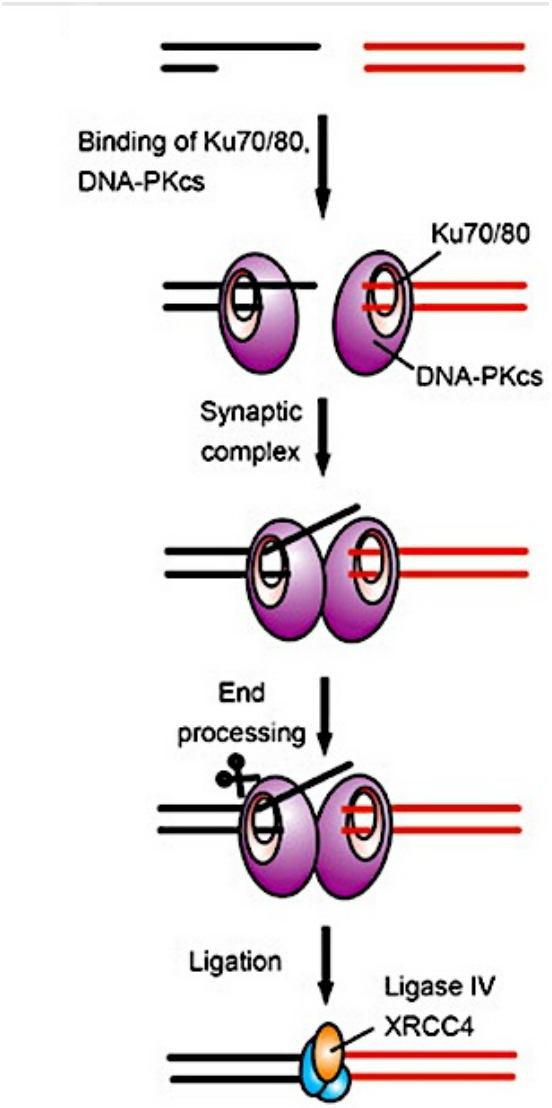

Figure 1.15. Non homologous end joining repair. The Ku 70/80 heterodimer rapidly binds to the DSB and recruits DNA-PKcs to the site of damage, where it provides access for enzymes to process DNA ends. The XRCC4/LIG4 complex ligates the DNA ends. Image source: (Weterings and Chen, 2008)

1.3.5.2 Homologous Recombination

HR comprises a series of events that use DNA strand invasion and template-directed DNA repair synthesis, culminating in high fidelity, error-free repair. Due to HR requiring a sister chromatid, this mechanism of repair is restricted to the S and G2 phases of the cell cycle, where chromatids exist in duplicate. Recognition of the DSBs by the MRN complex promotes activation of ATM and preparation of DNA for HR, through a process known as DNA resection. Resection is mediated in part by direct phosphorylation of CtBP-interacting protein (CtIP), which promotes resection in collaboration with the MRN complex (Yun and Hiom, 2009). Nucleolytic degradation of the 5' strand leaves a long 3' single-stranded DNA (ssDNA) overhang. The ssDNA is initially bound by RPA, which displays higher affinity and specificity for ssDNA than Rad51 (Wold, 1997). RAD51, the key protein in HR which catalyses homology search and DNA strand exchange, displaces RPA to yield the presynaptic filament. Recombination mediators such as BRCA2, human homologue of RAD52 XRCC2, and XRCC3 interact with RAD51 to aid in this process. Purification of full-length BRCA2 by Jensen et al. shows that BRCA2 both binds RAD51 and potentiates recombinational DNA repair by promoting assembly of RAD51 onto ssDNA (Jensen et al., 2010). RAD51 associated protein 1 (RAD51AP1) and partner and localiser of BRCA2 (PALB2) promotes the invasion of the presynaptic filament to pair with the homologous double stranded DNA (dsDNA), forming the D-loop. DNA synthesis extends the D-loop. BRCA1 is an important protein involved in DNA repair and a large body of evidence supports a direct role of BRCA1 in HR. In mouse embryonic stem cell lines, BRCA1 has been found to associate and co-localise with RAD51 in nuclear foci, and, accordingly, BRCA1 is required for their formation (Bhattacharyya et al., 2000; Scully et al., 1997). Furthermore, recruitment of BRCA1 has been found at sites of DNA

damage induced by IR, and is required for efficient generation of ssDNA (Schlegel et al., 2006). BRCA1 has also been shown to be required for the activation of cell cycle arrest after DNA damage (Xu et al., 2001). It has been suggested that part of the function of BRCA1 is recruitment of BRCA2 and the HR machinery through its interaction with PALB2 (Zhang et al., 2009a; Zhang et al., 2009b). From here HR can be split into 3 distinct sub-pathways: Synthesis dependent strand annealing (SDSA), double-strand break repair (DSBR), and double Holliday junction (dHJ) dissolution. In SDSA, the structure can be dismantled by Fanconi Anemia, Complementation (FANC) Group M (FANCM), leading to a non-crossover repair outcome. Alternatively, a second event of invasion occurs by engaging the second end of the DSB to the template strand, forming a dHJ. DSBR resolves the dHJ by specialised nucleases termed resolvases, yielding crossover and non-crossover products. In dHJ dissolution, these junctions are dissolved by the helicase-topoisomerase complex BLM-Topo IIIα-RMI1-RMI2 to yield non-crossover products. The pathway is depicted in figure 1.16.

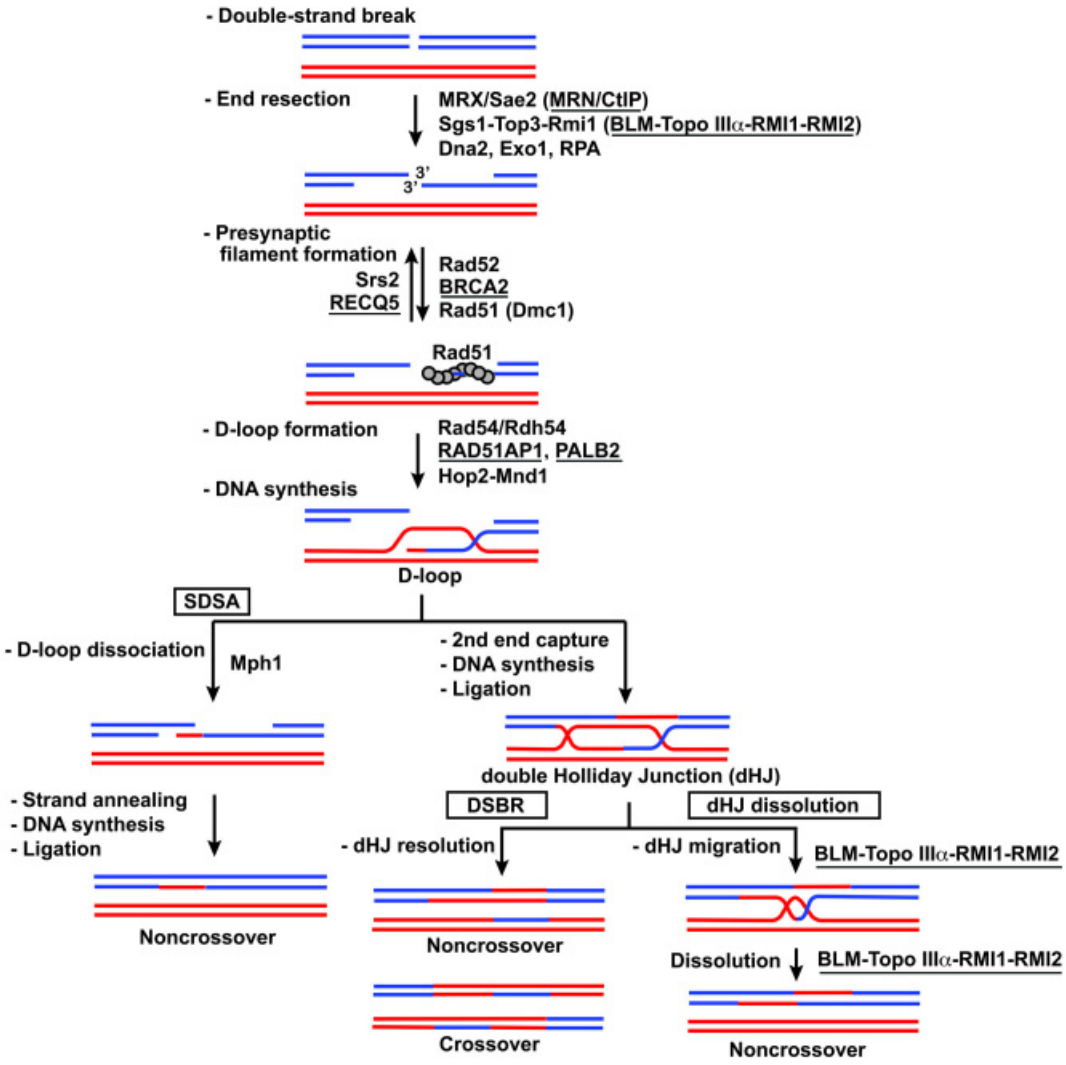

Figure 1.16. Homologous recombination pathways. Three distinct HR pathways are depicted: Synthesis dependent strand annealing (SDSA), double-strand break repair (DSBR), and double Holliday junction (dHJ) dissolution. *Saccharomyces cerevisiae* and human proteins (underlined) involved are indicated above. Source: (Daley et al., 2013; Wold, 1997)

1.3.6 DNA damage sensing

The DDR pathway consists of a complex interwoven signalling network, and at the core of DDR are the ATM and ATR kinases. Signal sensors recognise aberrant DNA structures associated with DNA damage as well as replication stress and activate transducers which include ATM, ATR and their downstream kinases. The effectors of these kinases then regulate a number of cellular processes required to maintain genomic integrity. This DDR framework is depicted in figure 1.17. ATM and ATR, as well as DNA-PKcs, belong to a family of phosphatidylinositol 3-kinase related kinases (PIKKs). While ATM and ATR phosphorylate hundreds of proteins in response to DNA damage, DNA-PKcs regulate a smaller number of targets and chiefly plays a role in NHEJ. Studies have shown that ATM and ATR responses have distinct functions. ATM, in conjunction with the MRN sensor complex, primarily responds to DSBs generated by radiation and genotoxins, but only weakly by agents that block DNA replication without inducing damage (Matsuoka et al., 2000). ATR, on the other hand, is activated when DNA replication is impeded, such as through replication fork stalling or damage through UV and other replication-associated genotoxins. In addition, ATR is activated through processing of DSBs, as well as in NER.

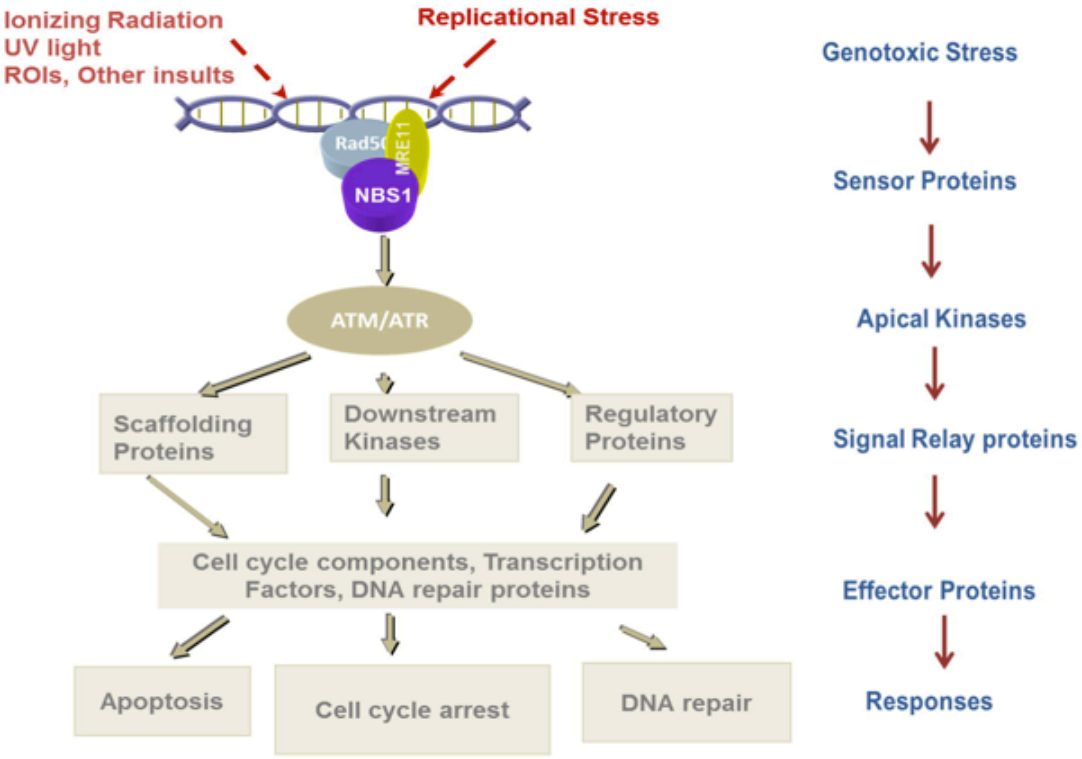

Figure 1.17. The DNA damage response network. Upon DNA damage, kinases ATM and ATR are recruited to the site of damage via sensor proteins, where they phosphorylate downstream kinases, scaffolding proteins and regulatory proteins. This leads to further activation of effector proteins which regulate cell cycle components, transcription factors and DNA repair proteins, resulting in a response of cellular apoptosis, cell cycle arrest, of DNA repair, depending on the extent of DNA damage. Image source: (Furgason and Bahassi el, 2013)

1.3.6.1 ATM and DNA damage sensing

In undamaged cells, ATM is thought to exist as an inactive homodimer. Upon DNA damage, inactive ATM homodimers are induced to autophosphorylate *in trans*, and result in the dissociation of the dimers to partially active monomers (Bakkenist and Kastan, 2003). While the primary signal that induces autophosphorylation of ATM is unknown, it does not appear to be linked to the vicinity of the damage and may be linked to long range alterations in the chromatin structure (Bakkenist and Kastan, 2003). Autophosphorylation sites S1981, S367 and S1893 have been linked with the activation of ATM, as well as the acetylation by TIP60 acetyl-transferase (Lavin and Kozlov, 2007). Upon DNA damage, the MRN complex is recruited to sites of damage and binds to the DSB ends. While the mechanism of the MRN complex in ATM activation in a DSB – dependent manner is not fully understood, MRN is required for localisation and activation of ATM to DSBs and MRN is therefore suggested to play the role as a sensor protein for ATM activation (Lee and Paull, 2005; Uziel et al., 2003). Once activated, ATM regulates a number of events on the chromatin flanking the DSB, the key event being phosphorylation of histone family H2A, member X (H2AX). Phosphorylation of H2AX (known as γH2AX) takes place minutes after DNA damage and spans chromatin domains larger than 500 kb which flank the site of damage. This allows for an accumulation of DNA repair proteins and chromatin-remodeling complexes to form around the DSBs. ATM also aids in the propagation of the H2AX phosphorylation via its interaction with mediator of DNA-damage checkpoint 1 (MDC1). MDC1 binds to γH2AX via its BRCA1 C-terminus domain, as this binding is required for full-sized γH2AX foci formation (Stewart et al., 2003). MDC1 can also directly bind to ATM via its forkhead-associated (FHA) domain, and indirectly through binding to nibrin (NBS1), which is part of the MRN complex, and this binding enables MDC1 to recruit ATM to

the nucleosomes containing γH2AX and propagate H2AX phosphorylation along chromatin. Interestingly, whereas MDC1 is important for the spreading of ATM on chromatin near DSBs, studies with mouse cells suggest that ATM is also able to phosphorylate H2AX on chromatin distal to DSBs in the absence of MDC1 (Savic et al., 2009). How ATM reaches and acts on chromatin distal from DSBs remains to be elucidated. Recruitment of ATM to γH2AX has also been associated with Tip60 acetyltransferase, although in depth studies have yet to be conducted (Sun et al., 2009). Phosphorylation of H2AX by ATM results in a series of ubiquitination and SUMOylation reactions which promote the recruitment of BRCA1 and p53-binding protein 1 (53BP1). ATM activation is depicted in figure 1.18.

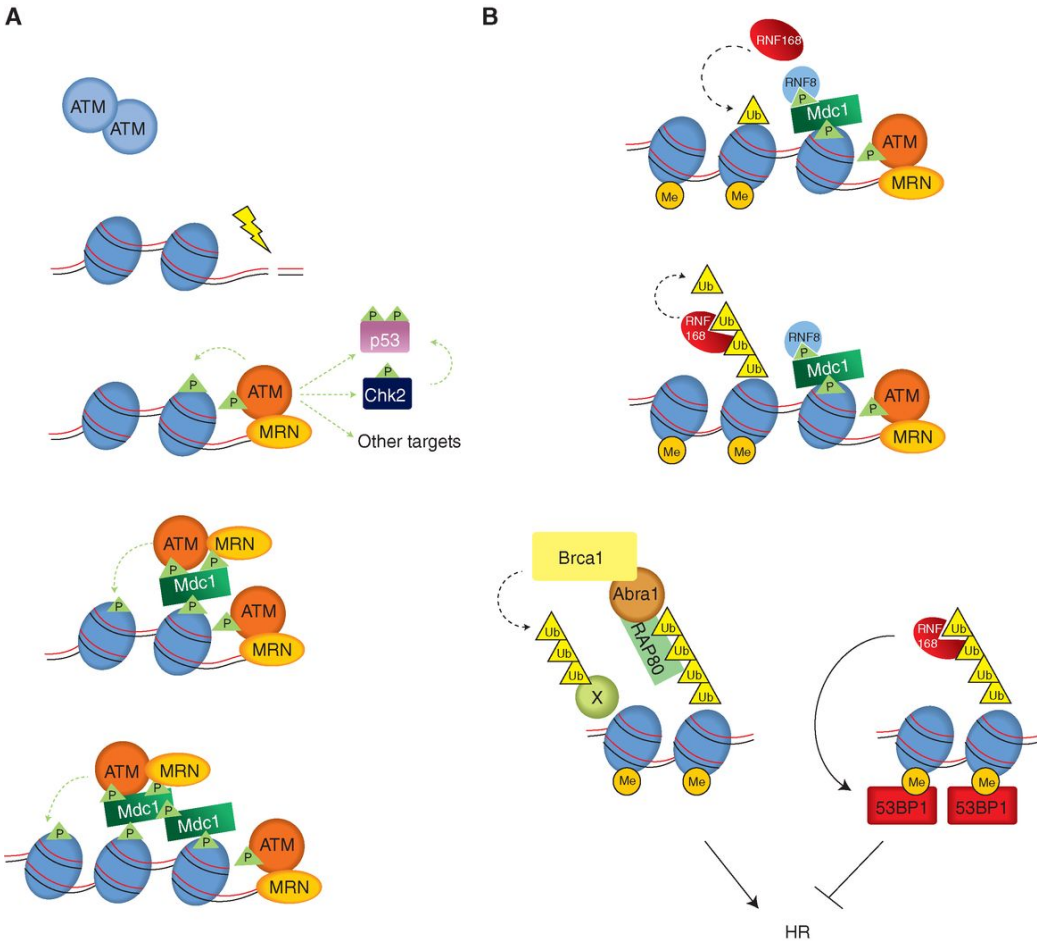

Figure 1.18. Activation of ATM by DSBs. (A) ATM recognises DNA ends, and is recruited to the site of damage. MRN functions as a sensor of strand breaks and activated ATM via phosphorylation. ATM in turn activates substrates such as H2AX in flanking nucleosomes, as well as p53 and Chk2. MDC1 recognises γH2AX and further activates ATM, propagating H2AX phosphorylation along large chromatin domains. (B) Phosphorylated MDC1 also recruits E3 ligase ring finger protein (RNF) family member 8 (RNF8) to the DSB, which in turn promotes another E3 ligate RNF168 to ubiquitinate substrates including H2A and H2AX. RNF168 extends the ubiquitin chains on the substrate and RAP80 recognises the ubiquitin chains, and forms a complex with BRCA1 through Abraxas. RNF168 also promotes the recruitment of 53BP1, which bind to the dimethylated lysine 20 of histone H4 exposed around the DSBs. The co-ordination of the recruitment of BRCA1 and 53BP1, which act to promote and

antagonise HR respectively, remains unknown. Dashed green and black lines represent phosphorylation and ubiquitination events, respectively. Image source: (Marechal and Zou, 2013)

1.3.6.2 ATM to ATR switch at DNA breaks

A study conducted by Shiotani and Zou found that ATR activation results in an attenuation of ATM activation and subsequently revealed an ATM-ATR switch in response to DSB (Shiotani and Zou, 2009). Processing of DSBs in HR results in the generation of RPA-coated ssDNA strands by DNA resection, to which ATRIP binds to in a complex containing ATR and ATRIP, leading to a series of processes that activate ATR fully (figure 1.19). As ssDNA lengthens, the DDR response to DSB ends changes from an ATM-driven response to ATR activation. This suggests the ssDNA is the key structure that recruits ATR and elicits a response upon DNA damage. The RPA and ssDNA binding also promotes the recruitment of the Rad17-Rfc2-5 complex which act as clamp loaders in the junction between ssDNA and dsDNA, and the loading of the 9-1-1 checkpoint clamps onto the dsDNA. Topoisomerase (DNA) II binding protein 1 (TOPBP1) is recruited to the dsDNA by way of the association of phosphorylated Rad9 and Rhino with the 9-1-1 complex, and stimulates ATR-ATRIP to its full capacity, leading to phosphorylation of other targets by ATR (Delacroix et al., 2007). CtIP has also been implicated in this process by promoting DNA end resection, and the ensuing ATR activation (Sartori et al., 2007).

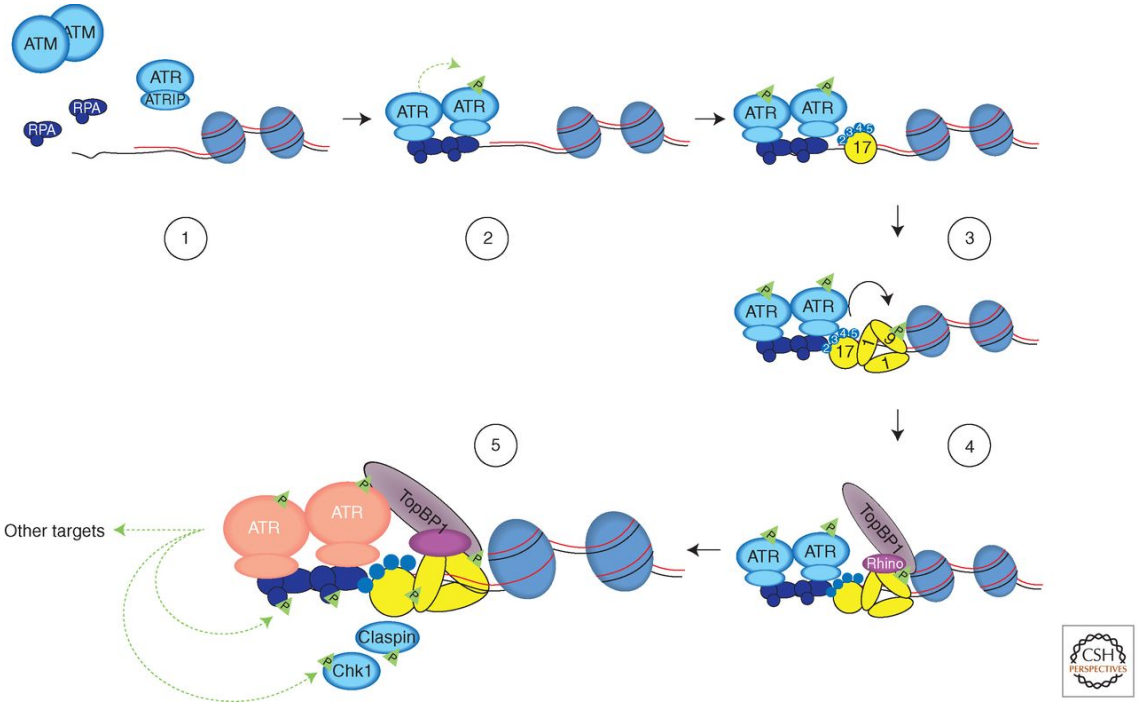

Figure 1.19. ATR activation via DSB resection. (1) RPA binding to ssDNA promotes ATR-ATRIP binding to RPA. (2) ATR is auto-transphosphorylated. (3) The rad17-rfc2-5 complex binds as a clamp loader to junctions between ssDNA and dsDNA. The 9-1-1 complex acts as a clamp and binds onto the dsDNA. (4) TOPBP1 interacts with phosphorylated rad9 and rhino, which binds to the 9-1-1 complex. (5) TOPBP1 engages with the ATR-ATRIP complex via autophosphorylation of ATR and enables TOPBP1 to stimulate ATR-ATRIP to its full capacity, resulting in the phosphorylation of targets downstream of ATR. Image source: (Marechal and Zou, 2013)

1.3.6.3 Activation of the ATM-Chk2 and ATR-Chk1 DNA pathways

One of the key substrates of ATM and ATR are the serine-threonine checkpoint kinases, Chk1 and Chk2, which are selectively phosphorylated and activated to trigger a wide range of downstream responses to DNA damage (figure 1.20.). ATM phosphorylates Chk2, whereas ATR phosphorylates Chk1. ATM phosphorylates Chk2 on T68 located within an N-terminal serine/threonine-glutamine (SQ/TQ) rich motif (Ahn et al., 2000). The SQ/TQ motif of Chk2 is then recognised by the FHA domain of another Chk2 molecule and transient homodimerisation occurs followed by intermolecular activation loop autophosphorylation and full activation of Chk2 (Ahn et al., 2002; Oliver et al., 2006). Chk2 is then thought to dissociate from sites of DNA damage and disperse throughout the nucleus to act on substrates involved in cell cycle progression, apoptosis and gene transcription (Lukas et al., 2003). Substrates of Chk2 include p53, double minute 4 protein, cell division cycle 25 (CDC25) family phosphatases, BRCA1 and transcription factors forkhead box M1 and E2F1 (Smith et al., 2010).

The phosphorylation of Chk1 by ATR is dependent on the claspin mediator protein. Claspin is subjected to ATR-dependent phosphorylation, and once modified, binds Chk1 (Kumagai and Dunphy, 2003). Two additional mediators, timeless and timeless-interacting protein have been associated with normal replication as well as ATR-Chk1 activation in response to replication stress (Kondratov and Antoch, 2007). Phosphorylated claspin recruits Chk1 to ssDNA bringing it into close proximity with ATR, thus enabling ATR to phosphorylate Chk1 directly at multiple SQ/TQ sites within the C-regulatory domain, such as S317 and S345 (Kumagai and Dunphy, 2003). Phosphorylation of these sites plays an essential role in Chk1 activity, although the mechanisms for this regulation remain poorly understood (Niida et al., 2007; Walker et

al., 2009). Chk1 has been reported to also undergo autophosphorylation during activation, however the significance of this modification has yet to be clearly established (Kumagai et al., 2004). Once activated, Chk1 is thought to dissociate from claspin to act on nuclear and cytoplasmic substrates (Lukas et al., 2003). Chk1-mediated regulation includes degradation of CDC25A and CDC25C phosphatases, stimulation of wee1 kinase activity, modulation of RAD51 and BRCA2, and repression of gene transcription through phosphorylation of histone H3 (Bahassi et al., 2008; Blasina et al., 1999; Falck et al., 2002; Lee et al., 2001; Shimada et al., 2008; Sorensen et al., 2005).

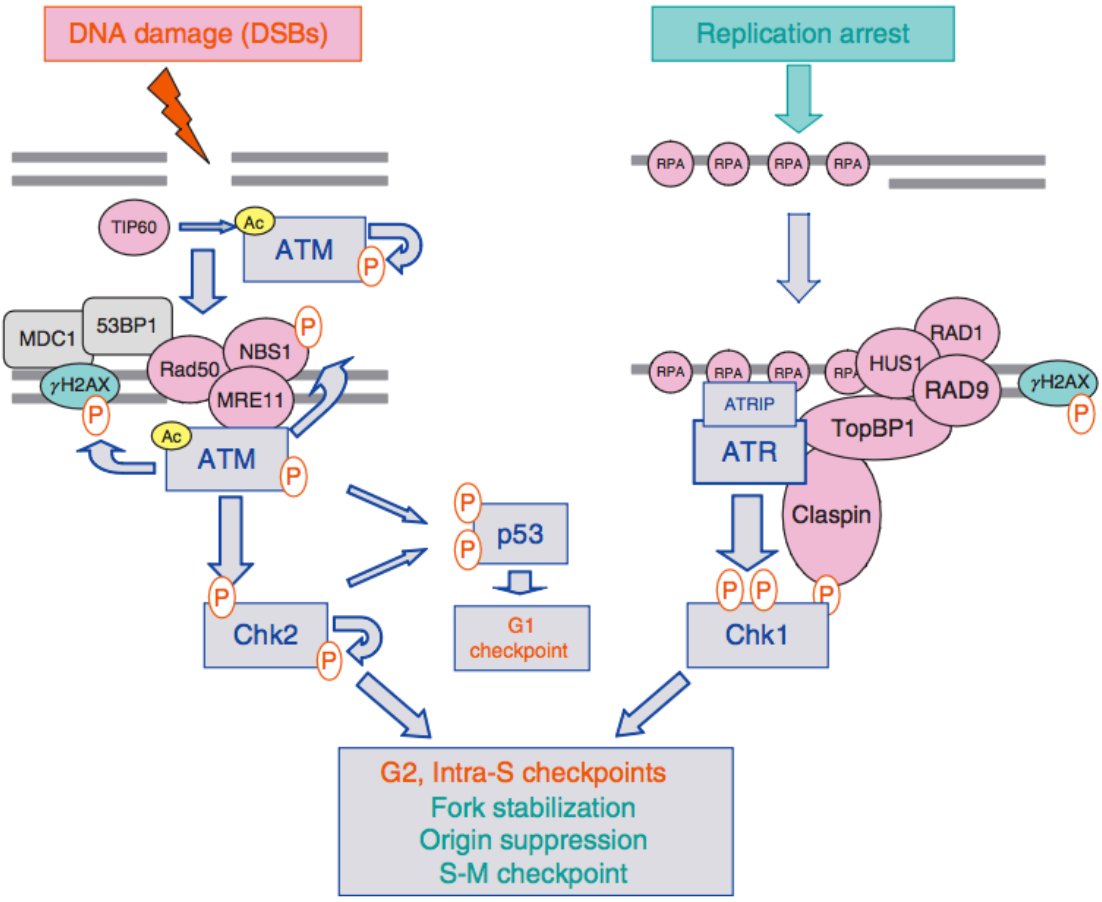

Figure 1.20. Activation of ATM-Chk2 and ATR-Chk1 pathways. ATM and ATR are activated by DSBs and RPA bound ssDNA, respectively. ATM, along with the MRN sensor complex, activates numerous proteins in response to DSBs, including Chk2. Activation of ATR results in the phosphorylation of Chk1, among other substrates. The two checkpoint kinases then activate multiple DNA damage and replication checkpoint responses. Phosphorylation events are depicted by 'P' in orange and acetylation events by 'Ac' in yellow. Image source: (Smith et al., 2010)

1.3.6.4 ATM/ATR activation and the cell cycle

One of the downstream signalling events that occur upon ATM/ATR activation due to DNA damage is the inhibition of cell cycle progression, to permit time for DNA repair or eliminate damaged cells through apoptosis. Deregulation of signals that regulate cell cycle progression can lead to constitutive mitogenic signalling as well as a resistance towards anti-mitogenic signalling, and consequently cells acquire sustained proliferative signalling, a hallmark of cancer (Hanahan and Weinberg, 2011). Furthermore, most tumour cells possess genomic instability, which further contributes to the accumulation of mutations and development of more aggressive phenotypes.

The cell cycle can be divided into four stages (figure 1.21). The S phase is where DNA replication occurs and the M phase is where the cell divides into two daughter cells in a process known as mitosis. Separating these two important phases are the G1 and G2 phases. The G1 phase occurs after the M phase and is a stage where the cell is sensitive to positive and negative regulatory growth signals. The G2 phase occurs after the S phase and is a time where the cell prepares for entry into mitosis. A fifth state exists called the G0 phase, where the cell has reversibly withdrawn from the cell cycle due to mitogen deprivation or high cell density (Zetterberg and Larsson, 1985). Progression through the cell cycle is controlled by the cyclin-dependent kinase (CDK) family of serine/threonine kinases, and their cyclin regulatory subunits and is marked by sensor mechanisms, called checkpoints, which maintain the correct order of events. CDK activity requires binding of cyclins, which are synthesised and destroyed at specific times during the cell cycle, thus regulating kinase activity temporally. Only a certain subset of CDK – cyclin complexes is directly involved in regulation of the cell cycle. They include three interphase CDKs (CDK2, CDK4 and CDK6), a mitotic CDK

(CDK1) and ten cyclins that belong to four different classes (the A-, B-, D- and E-type cyclins). Cyclin D-CDK4, cyclin D-CDK6 and cyclin E-CDK2 drive G1 progression through the restriction point, which is the point at which the cell is committed to complete the cycle (Planas-Silva and Weinberg, 1997). S phase is initiated by cyclin A-CDK2, and cyclin B-CDK1 regulates progression through G2 and entry into mitosis (Nigg, 2001). Tumour associated mutations frequently deregulate CDK-cyclin complexes, resulting in either sustained proliferation or unscheduled re-entry into the cell cycle, two properties characteristic of cancer (Hanahan and Weinberg, 2011).

If the sensor mechanisms detect aberrant cell cycle progression, such as detection of DNA damage, checkpoint pathways carry the signal to effectors that can trigger cell cycle arrest until the problem is resolved through modulation of CDK activity. CDK activity is regulated by two families of inhibitors: INK4 proteins, including INK4A, INK4B, INK4C and INK4D, and the Cip and Kip family, composed of p21, p27 and p57. Cell cycle arrest allows for the repair of defects or elimination of the defective cell, thus preventing transmission of mutations to the daughter cells. Accumulation of DNA mutations may promote genomic instability and lead to cellular transformation and oncogenesis. For example, G1 arrest can be induced through the action of the INK4, which inhibit CDK4 and CDK6, or, alternatively, via the Cip/Kip family of inhibitors, which suppress CDK2 activity.

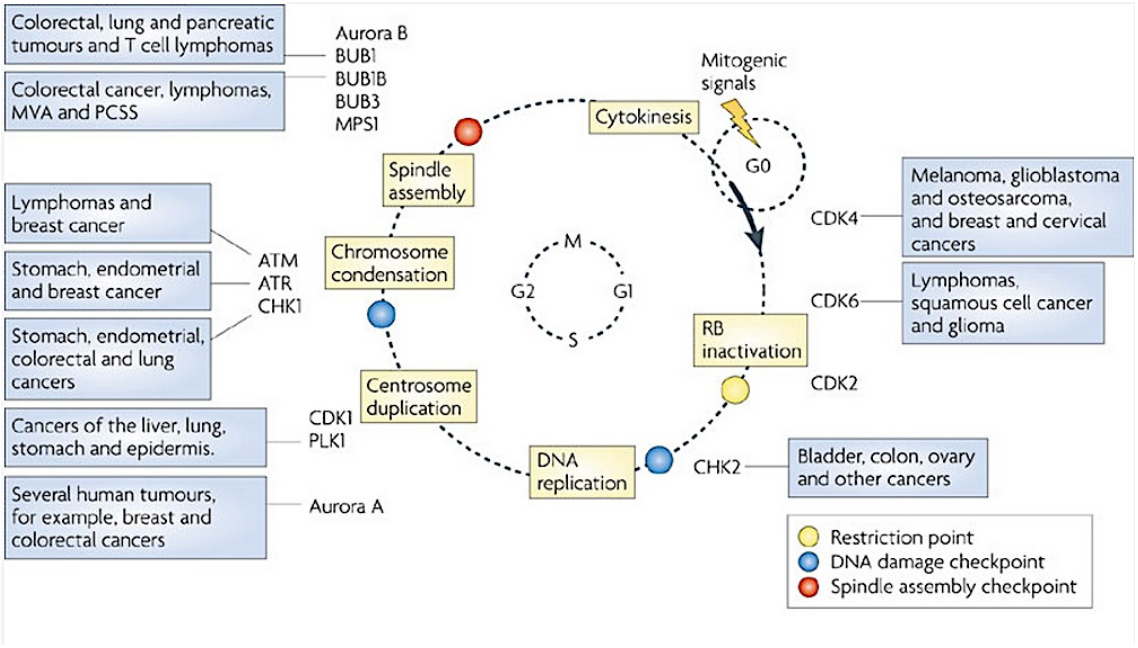

Figure 1.21. Cell cycle regulation. The cell cycle depicted here in the middle can be divided into four phases: G1, S, G2 and M. A fifth phase known as G0 represents cells in quiescence. CDKs drive the cell out of quiescence (G0), resulting in the cell being irreversibly committed to S phase transition. Various cyclin-dependent kinases (CDKs) act in concert to regulate cell cycle progression, as well as modulate the activities of other cell-cycle-related kinases. The DNA-damage checkpoint kinases Chk1 and Chk2 can induce cell cycle arrest upon DNA damage in the transition between G1/S and G2/M, respectively. Cancers associated with genetic alteration of specific kinases are indicated in blue boxes. BUB1, budding uninhibited by benzimidazoles 1; BUB1B, BUB1 homologue beta (also known as BUBR1); MPS1, monopolar spindle 1; MVA, mosaic variegated aneuploidy; PCSS, premature chromatid separation syndrome; RB, retinoblastoma protein family members. Image source: (Lapenna and Giordano, 2009)

Multiple checkpoints exist to evoke multiple responses upon DNA damage (figure 1.22). DNA damage induces cell cycle delays at the G1/S and G2/M transitions (known as the G1 and G2 checkpoints), as well as a reduction in the rate of DNA synthesis (known as the intra-S checkpoint). The G1 checkpoint is predominantly regulated by the tumour suppressor p53 through its activation of the cyclin-dependent kinase inhibitor p21CIP1 (Kastan and Bartek, 2004). The G2 checkpoint, on the other hand, is regulated by blocking the activation of the mitotic CDK1-cyclin B complex (O'Connell et al., 2000). Inhibition of the CDC25 family phosphatases results in the prevention of the removal of inhibitory threonine 14/tyrosine 15 phosphorylation of CDK1 (Boutros et al., 2007). The intra-S checkpoint involves active replication fork slowing and suppression of replication origin firing; however, the molecular mechanism for these responses is less clearly defined (Grallert and Boye, 2008; Seiler et al., 2007). Aberrations in DNA synthesis result in a replication checkpoint response that stabilise stalled replication forks and prevents formation of new forks by the suppression of late replication origin firing (Branzei and Foiani, 2009). In addition, the S-M checkpoint is implemented which delays mitosis until replication is complete, most likely through maintenance of inhibitory phosphorylation of CDK1 (O'Connell et al., 2000).

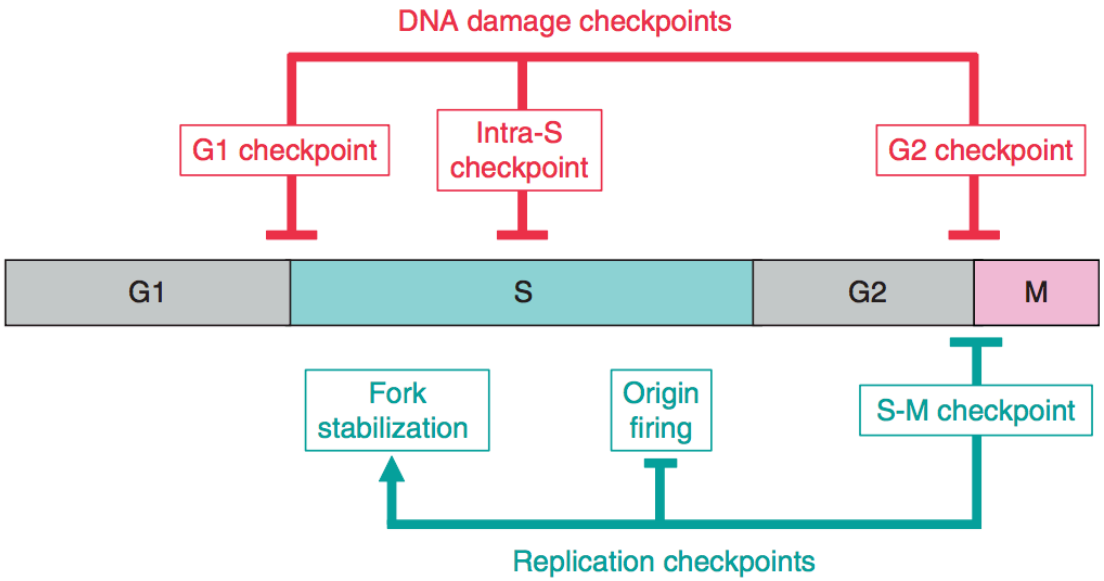

Figure 1.22. DNA damage and replication checkpoints induced upon DNA damage and DNA synthesis inhibition. In response to DNA damage the entry to S-phase is delayed, DNA replication is slowed, and entry to mitosis is prevented through implementation of the G1, intra-S and G2 checkpoints, respectively. Inhibition of DNA synthesis results in the activation of replication checkpoints, which stabilise stalled replication forks, suppress the late replication origin firing and enable mitotic delay until DNA replication is complete. Image source: (Smith et al., 2010)

1.3.6.5 ATM-Chk2 and ATM-Chk1 pathways and cancer

Alterations of DDR pathway components result in inherited human cancer predispositions syndromes as well as genomic instability through sporadic mutations. Homozygous inherited loss-of-function mutations of ATM result in ataxia telangiectasia (AT) syndrome, which is characterised by radiation hypersensitivity, immunodeficiency, neurodegeneration, and spontaneous predisposition to lymphoma (Abadir and Hakami, 1983; Morrell et al., 1986; Taylor et al., 1975). Similarly, knockdown of ATM in mice results in radiosensitivity, as well as a predisposition to lymphoma (Xu and Baltimore, 1996). Individuals who harbour heterozygous mutations of ATM have an increased incidence of breast cancer, and some other cancers, possibly due to environmental exposure to radiation (Briani et al., 2006; Thompson et al., 2005), and sensitivity to radiation *in vitro* in heterozygous cells from individuals result in a intermediate sensitivity between AT patients and normal individuals (Swift et al., 1991). Sporadic mutations of ATM have been found in lung and lymphoid malignancies, albeit in relatively low incidences (Ding et al., 2008; Gumy-Pause et al., 2004). ATM can therefore be viewed as a cancer susceptibility gene that interacts with certain environmental factors resulting in a heightened predisposition to cancer. Mutations in genes encoding the MRE11 and NBS1 proteins result in ataxia-like disorder, as well as Nijmegen breakage syndrome (NBS), of which both disorders share clinical similarities with AT (Stewart et al., 1999; Varon et al., 1998). Hypomorphic mutations of NBS1 or RAD50 also result in a cancer predisposition in mice (Bender et al., 2002; Kang et al., 2002). Homozygous mutations of ATR result in the development of Seckel syndrome, which is associated with growth retardation and microcephaly. However, unlike AT patients, individuals with Seckel syndrome do not suffer from an increased incidence of cancer. Studies in mouse models revealed degenerative and premature aging-like

phenotypes in ATR knockout mice, pointing to a role of ATR in normal development, stem cell survival and tissue homeostasis (Ruzankina et al., 2007). Loss of function of ATR, however, does not result in genomic instability that promotes tumourigenesis, and somatic mutations of ATR have not been frequently found in human cancers, with the exception of stomach and endometrial tumours with microsatellite instability (MSI) (Heikkinen et al., 2005; Menoyo et al., 2001; Vassileva et al., 2002).

Mutations further downstream of the sensor proteins also result in cancer predispositions. Li Fraumeni syndrome is a cancer predisposition syndrome that is linked to germline mutations of *TP53* (Birch, 1994). Heterozygous germline mutations of Chk2 confer increased incidences of breast, prostate and other cancers; however, tumours of individuals that harbour heterozygous mutations of Chk2 do not consistently exhibit LOH in the remaining functional allele unlike typical tumour suppressor genes (Antoni et al., 2007). Germline mutations in Chk1 have not been associated with any human disease, and somatic mutations in Chk1 are infrequently found in cancers, with the exception of tumours with MSI (Vassileva et al., 2002). ATR knockout in mice results in chromosomal fragmentation and early embryonic lethality, and Chk1 heterozygous mice developed tumours more rapidly upon oncogenic tumour induction compared to the wildtype mice (Brown and Baltimore, 2000; Liu et al., 2000). Loss of the remaining functional allele of Chk1 was not observed, suggestive of an important role of Chk1 in maintaining cell proliferation and survival (Liu et al., 2000). Heterozygous carriers of BRCA1/2 mutations are developmentally normal but possess a greater incidence of breast and ovarian cancer (King et al., 2003). Somatic loss of function mutations of BRCA1 and BRCA2 have been found in numerous cancer types, most notably the most prevalent form of ovarian cancer, high grade serous carcinoma.

As previously mentioned, BRCA1/2 largely play a role in HR-mediated repair of DSBs and heterozygous loss of BRCA1/2 in cells through LOH results in HR deficiency and genomic instability. In the absence of HR, the cells use alternative error-prone DNA repair mechanisms which lead to an accumulation of mutations, which likely promotes tumourigenesis (Tutt et al., 2002). While the presence of these mutations results in an environment that fosters carcinogenesis, the absence of efficient DNA repair mechanisms provides an exploitable therapeutic strategy that enables targeting of tumour cells defective in DNA repair. A comprehensive list of DDR aberrations and associated DNA repair pathways are shown in figure 1.23.

Pathway	Proteins	Importance in cancer
Direct repair	MGMT	Higher levels in tumours than in normal tissue confers resistance to DNA-alkylating agents. Methylation of the *MGMT* promoter is associated with better response to BCNU and TMZ in brain tumours
BER	OGG1	Truncating mutations and R46Q variant (which has reduced activity) observed in renal cancers. *OGG1* methylation is seen in various cancers and loss of expression is associated with poor prognosis in breast cancer. The polymorphism OGG1-S326C is associated with reduced activity and increased risk of developing lung cancer
	APE1	High APE1 expression in several tumour types is associated with drug and radiotherapy resistance
	XRCC1	The polymorphism XRCC1-R194W increased the efficiency of BER and is protective against cancer. The polymorphism XRCC1-R399Q reduced the efficiency of BER and predisposes to cancer
	PARP1	Higher levels of expression occur in tumours. The polymorphism PARP1-V762A confers reduced activity and predisposes to various cancers
	Pol β	30% of tumours have Pol β mutations that are not found in normal tissue, including frameshifts, del208-236, and K289M and I260M dominant-negative, transforming mutations
Global NER	XP proteins	XP (which is caused by defective global NER) is characterized by UV radiation sensitivity and skin cancer. *XPC* methylation occurs in bladder cancer. SNPs in XPA and XPC have been associated with lung and bladder cancer, and SNPs in XPG have been associated with sensitivity to chemotherapy
	ERCC1	ERCC1 polymorphisms are associated with skin and lung cancer. *ERCC1* methylation occurs in glioma
TLS	Pol H and Pol Q	Aberrant expression observed in several tumour types
MMR	MSH2 and MLH1	MMR defects cause Lynch syndrome and HNPCC, which are associated with colorectal, stomach, ovarian and endometrial cancers. *MLH1* promoter methylation is associated with spontaneous tumours in these tissues. MMR defects confer resistance to the DNA-methylating agents 6-thioguanine and cisplatin
DSB repair	NBS1	Nijmegen breakage syndrome (which is caused by defective NBS1) is characterized by chromosome instability, immunodeficiency, ionizing radiation sensitivity and cancer predisposition, especially lymphoma; heterozygous mutants are also cancer prone
	MRE11	Point mutations are observed in ovarian cancers and shortening of the T(11) repeat microsatellite occurs in 93% of primary colorectal cancer probably as a result of MMR-induced microsatellite instability
NHEJ	KU70	SNPs associated with breast cancer, and epigenetic silencing is associated with breast, colorectal and lung cancer
	KU80	Epigenetic silencing is associated with lung cancer
	DNA-PKcs, ligase 4 and XRCC4	SNPs associated with glioma. SNPs may protect against breast and lung cancer. MiR-101 (which is induced by NMYC) targets DNA-PKcs and thus reduces its expression
HRR	BRCA1 and BRCA2	BRCA1 and BRCA2 mutation carriers have increased risk of breast, ovarian, prostate, pancreatic, melanoma and other gastrointestinal, gynaecological and haematological malignancies. Methylation of the *BRCA1* promoter is common in spontaneous breast, ovarian and lung cancers
	XRCC2	XRCC2 is a RAD51 paralogue, frameshift mutation owing to microsatellite slippage that in MSI tumours confers sensitivity to crosslinking agents
	RAD50	Frameshift mutations in the *RAD50*-associated microsatellite, which results in a truncated protein, occur in 31% of gastrointestinal cancers
	FANC proteins	Fanconi's anaemia is associated with haematological malignancies, especially MDS and AML, HNSCC, and oesophageal and gynaecological cancer. Most mutations occur in FANCA (65%), FANCC (15%) or FANCG (10%). *FANCD1* (*BRCA2*), *FANCN* (*PALB2*) and *FANCJ* (*BACH1*; also known as *BRIP1*) are breast cancer susceptibility genes. Methylation of FANC genes is common in sporadic cancers; for example, *FANCF* is methylated in lung, ovarian and cervical cancer
Cell cycle checkpoints	ATM and CHK2	Ataxia telangiectasia (which is caused by defects in ATM) is associated with radiosensitivity and 100-fold increased cancer predisposition. Heterozygous germline mutations in *ATM* are associated with leukaemia and breast and pancreatic cancer. Epigenetic silencing of *ATM* and *ATM* polymorphisms are associated with breast, lung and colorectal cancer. MiR-421 and miR-101, which are induced by NMYC, both target ATM. CHK2 is a candidate tumour suppressor gene, inactivation is observed in multiple human tumours
	ATR	Frameshift mutations caused by deletions in the A(10) microsatellite as a consequence of MMR defects are associated with leukaemia, lymphoma and stomach and endometrial cancer

Figure 1.23. DDR aberrations in cancer. Abbreviations: AML, acute myeloid leukaemia; APE1, AP endonuclease 1; ATM, ataxia-telangiectasia mutated; ATR, ataxia-telangiectasia and Rad3-related; BACH1, BRCA1-associated C-terminal helicase 1; BER, base excision repair; BRIP1, BRCA1-interacting protein C-terminal helicase 1; DDR, DNA damage response; DNA-PKcs, DNA-dependent protein kinase catalytic subunit; DSB, DNA double-strand break; FANC, Fanconi anaemia group protein;

HNPCC, hereditary nonpolyposis colorectal cancer; HNSCC, head and neck squamous cell carcinoma; HRR, homologous recombination repair; MGMT, O6-methylgyuanine DNA methyltransferase; MDS, myelodysplastic syndrome; miR, microRNA; MMR, mismatch repair; MSI, microsatellite instability; NBS1, Nijmegen breakage syndrome protein 1; NER, nucleotide excision repair; NHEJ, non-homologous end joining; OGG1, 8-oxoguanine DNA glycosylase; PARP1, poly(ADP-ribose) polymerase 1; Pol, DNA polymerase; SNP, single nucleotide polymorphism; TLS, translesion synthesis; TMZ, temozolomide; UV, ultraviolet; XP, Xeroderma pigmentosum. Image source: (Curtin, 2012)

1.3.7 Cancer therapy

Anti-cancer therapies involve using methods to kill cancer cells more efficiently than normal cells. Since most cancer cells exhibit enhanced cell proliferation compared to their normal counterparts, several cancer drugs target the cell cycle to exploit this trait; targeted therapies using inhibitors of the mitotic spindle, hormonal manipulation, immunotherapy and drugs that inhibit growth signalling pathways can be used to target the cell cycle. However, the most common method of targeting the cell cycle is by the use of DNA damaging drugs, which result in cell cycle arrest and cell death, either directly or following DNA replication.

1.3.7.1 DNA damaging agents in cancer therapy

DNA damaging agents used in the clinic result in high levels of DNA damage, cell cycle arrest and either immediate death through apoptosis, or following DNA replication, thus making these drugs highly effective in killing proliferating cells. The agents used in cancer treatment that induce a variety of toxic DNA lesions can be divided into six categories of delivery mechanisms: Radiotherapy and radiomimetics, alkylating agents, antimetabolites, topoisomerase inhibitors and replication inhibitors.

Alkylating agents result in chemical modifications of DNA bases, resulting in the formation of adducts through the attachment of an alkyl group to the guanine base of DNA. These agents can be divided into two groups, mono-functional alkylating agents and bi-functional alkylating agents, which have the ability to modify one and two bases, respectively. Bi-functional agents form two covalent adducts with DNA bases, either within the same DNA strand (intrastrand crosslinks) or between opposite DNA strands (interstrand crosslinks) (ICLs). Interstrand crosslinks are considered the more potent

lesion, and result usually in irreversible block to replication forks, and severe toxicity in cells. Examples of mono-functional alkylators include alkylsulphonates, nitrosourea compounds and temozolomide (TMZ). Nitrogen mustard, motomycin C and cisplatin are examples of bi-functional alkylating agents. DNA replication inhibitors target DNA synthesis directly, resulting in replication fork progression impairment and DNA lesion formation. Aphildocolin inhibits DNA polymerases, and hydroxyurea inhibits ribonucleotide reductase, an enzyme required for the production of dNTP molecules necessary for DNA replication. Antimetabolites, such as 5-fluorouracil and thiopurines, are also used in cancer therapy to induce DNA damage, by way of inhibiting the nucleotide metabolism pathway through depletion of dNTPs. These drugs can also incorporate themselves into the DNA, resulting in replication fork progression impairment. Topoisomerases (TOP) are critical enzymes involved in DNA replication which relieve torsional stress imposed by the introduction of transient strand breaks. Inhibitors of this enzyme prevent the re-ligation of these breaks, resulting in the retention of strand breaks. TOP1 is associated with controlled rotations of DNA supercoiling and subsequent DNA relaxation; TOP1 inhibitors, such as camptothecins, bind at the interface of the TOP1-DNA complex and cause replication associated DSBs. On the other hand, TOP2 inhibitors, such as etoposide and doxorubicin, change DNA topology by a “two gate” mechanism (Nitiss, 2009). IR and radiomimetics agents, such as bleomycin, can target non-replicating cells and therefore also target replication-independent DSBs. The therapeutic strategy and associated DNA repair target is shown in figure 1.24.

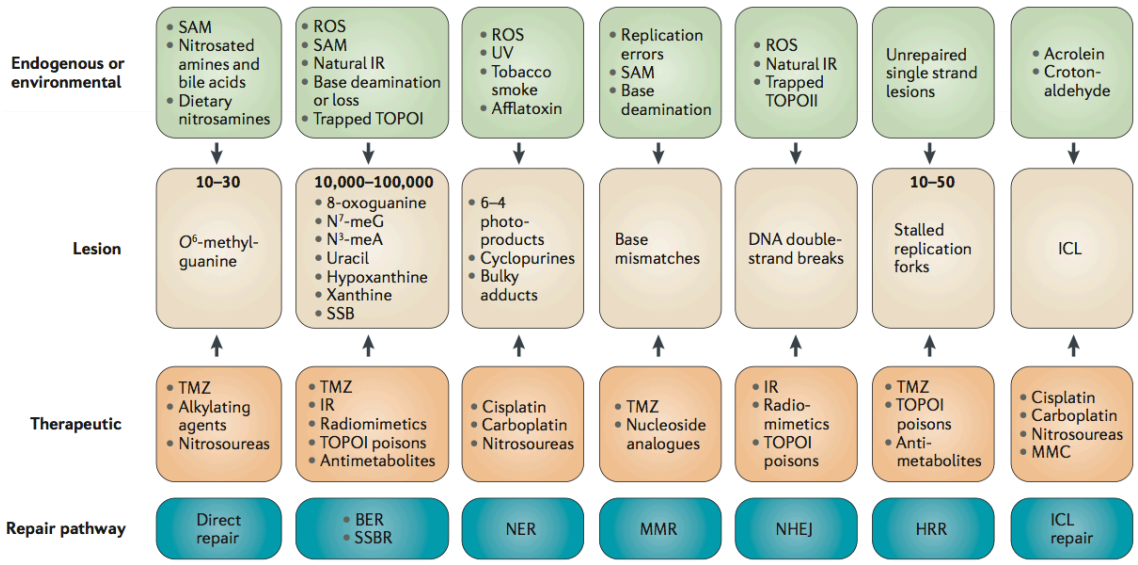

Figure 1.24. Overview of DNA damage and the associated DNA repair pathways. Approximate number of the indicated type of lesion that occurs naturally in a cell each day is shown in parentheses in the beige box. Therapeutic DNA damaging agents that cause the corresponding DNA lesion are shown in orange boxes. BER, base excision repair; HRR, homologous recombination repair; ICL, interstrand crosslink; IR, ionising radiation; MMC, mitomycin C; MMR, mismatch repair; NER, nucleotide excision repair; NHEJ, non-homologous end joining; ROS, reactive oxygen species; SAM, S-adenosyl methionine; SSB, single-strand break; SSBR, SSB repair; TMZ, temozolomide; TOPO, topoisomerase; UV, ultraviolet. Image source: (Curtin, 2012)

1.3.7.2 DNA repair pathways as targets for cancer therapy

Despite the potency of DNA damaging treatment, the effects of the drugs can be attenuated by intact DNA repair mechanisms that remove the lesions imposed, resulting in cell survival. DNA repair mechanisms thus modulate the efficiency of DNA damage based cancer therapy.

Direct reversal of a DNA lesion marks the simplest form of DNA repair. O^6 methylguanine DNA methyltransferase (MGMT) gene encodes a DNA repair protein that removes alkyl groups from the O^6 position of guanine, an important site of DNA alkylation. Agents that induce alkylations at this position, such as TMZ, decarbazine and nitrosoureas, inhibit this repair resulting in distorted base pairing. MGMT is ubiquitously expressed, and high MGMT expression levels in tumour cells are associated with resistance to the nitrosoureas carmustine, and TMZ (Lijinsky et al., 1994; Zaidi et al., 1996), suggesting that depletion of MGMT via pseudo-substrates may sensitise tumour cells to O^6 alkylating agents. However, trials using O^6-benzylguanine as a pseudo-substrate in tumour tissues, including gliomas, resulted in marginal clinical benefit due to increased toxicities in both normal and tumour tissues (Rabik et al., 2006). Consequently, the drug has not entered phase III trials. Trials using other pseudo-substrates, such as lomeguatrib, have shown promising preclinical activity, but phase II trials failed to show any clinical benefit in patients with melanoma or colon cancer (Ranson et al., 2006; Watson et al., 2010). Epigenetic silencing of *MGMT* by promoter methylation has been associated with longer overall survival in patients with glioblastoma who received carmustine or TMZ, and therefore *MGMT* silencing status in patients may be useful for stratifying patients for treatment with alkylating agents (Hegi et al., 2005).

BER repairs DNA damage that is therapeutically induced by IR, DNA methylating agents, TOP1 poisons, and some antimetabolites. The BER pathway consists of four major components: glycosylates, endonucleases, DNA polymerases and DNA ligases. Inhibitors of DNA polymerase-β (pol β), FEN1, LIG1 and LIG3 increased sensitivity towards IR, TMZ and methyl methanesulphonate, respectively (Chen et al., 2008; Gao et al., 2008; Kumamoto-Yonezawa et al., 2010; Panda et al., 2009). AP endonuclease 1 (APE1) inhibitors, such as methoxyamine, also target this pathway by binding to the AP site in DNA, as well as inhibitors of APE1 endonuclease activity. In a Phase I trial of methoxyamine, responses were seen in combination with pemetrexed (Eli Lilly, USA), and there is a study currently ongoing with TMZ. Novel and more specific APE1 endonuclease inhibitors increased the persistence of AP sites *in vitro* and increased the cytotoxicity of alkylating agents, but they have not yet moved into advanced preclinical or clinical evaluation (Mohammed et al., 2011).

Enzymes poly(ADP-ribose) polymerase (PARP) 1 and PARP2 also greatly facilitate repair by BER. Furthermore, PARP1 also has an important role in DSB repair. PARP1 is an abundant nuclear protein and is the founding member of the PARP family. PARP1 has several structural and regulatory roles across the genome, including roles in DNA repair, DNA methylation, transcription, chromatin structure and histone modification (Krishnakumar and Kraus, 2010). PARP1 is comprised of three functional domains: an amino-terminal DNA-binding domain containing three zinc fingers, an auto-modification domain and carboxyl-terminal catalytic domain. Zinc finger 2 has the strongest affinity for DNA breaks whereas zinc finger 1 is responsible for DNA-dependent PARP1 activation, in which zinc finger 3 also takes part (Langelier et al., 2011). With respect to DNA repair, PARP1 detects DNA strand breaks through its

DNA-binding domain, binds to the DNA strand break and activates PARP1 to cleave nicotinamide adenine dinucleotide (NAD^+) generating nicotinamide and ADP ribose. The ADP ribose units form long chains of poly (ADP)ribose (PAR), which, through PARylation, covalently binds to histones and several DNA repair proteins, such as XRCC1 (Schreiber et al., 2006). Like other nuclear proteins that play key roles in regulatory processes, PARP1 is subject to a variety of covalent post - translational modifications as endpoints of cellular signalling pathways. These include PARylation, acetylation, phosphorylation, ubiquitylation, and SUMOylation. PARP1 PARylation results in an inhibition of DNA-binding and catalytic activity (D'Amours et al., 1999). PAR chains are rapidly disassembled by the PAR hydrolysing enzyme PARG minutes after synthesis, thus providing a quick response to DNA damage lasting mere minutes (Schreiber et al., 2006). Therefore, inhibitors of PARP1 result in inefficient BER. Preclinical studies revealed that PARP inhibition through small molecule compounds or genetic inactivation of *PARP1* enhanced the cytotoxicity and anti-tumour activity of TMZ, TOP1 poisons and IR (Rouleau et al., 2010). The first clinical trial of PARP inhibitor rucaparib in 2003 with TMZ demonstrated modest clinical response in patient samples, and phase II trials were accompanied by myelosuppression (Plummer et al., 2008; R. Plummer, 2006). Eight more PARP inhibitors have undergone or are currently undergoing clinical evaluation in combination with alkylating agents dacarbazine and TMZ, as well as TOP1 inhibitors (see figure 1.24 for an extensive list of PARP inhibitors). Some of these combination studies have revealed no increase in anti-tumour activity, such as PARP inhibition in conjunction with paclitaxel treatment. PARP inhibitor treatment with DNA-damaging chemotherapy has generally been disappointing due to toxicities encountered, possibly due to using the same dose established for single-agent studies, in combination studies. Radiosensitisation by

PARP inhibition has been shown in preclinical studies, and phase I trials have revealed that PARP inhibitor veliparib was well tolerated with whole-brain radiotherapy in patients with brain metastases (Minesh P. Mehta, 2012).

NER contributes to repair of ICLs and XP and ERCC1 proteins play a crucial role in this repair. In testis tumour cells, NER deficiency results in sensitivity to platinum-based therapy, and a reduced capacity to repair ICL lesions (Koberle et al., 1997; Usanova et al., 2010). Hereditary defects of NER result in increased UV sensitivity and skin cancer development (Andressoo et al., 2005). Currently there are no small-molecule inhibitors of NER. Findings of *in vitro* studies revealed that the immunosuppressant cyclosporine and epidermal growth factor receptor (EGFR) inhibitor cetuximab may downregulate XPG and ERCC1-XPF, respectively (Kuschal et al., 2011; Prewett et al., 2007).

Whereas most DNA repair pathways mediate resistance to DNA damage, MMR is required for the toxicity of some anticancer drugs. The futile repair cycle model proposes that drug-induced DNA lesions in the daughter strands result in MMR processing without removing damage from the parental strands, which is thought to lead to repetitive strand breaks that may be a signal for G2-M arrest (Karran and Bignami, 1994; Karran and Marinus, 1982). Further, the MMR system is required for cell cycle arrest and apoptosis (Li, 1999), which might mediate increase cytotoxicity. Defective MMR increased mutation rates up to 1,000-fold and the resulting MSI is associated with cancer development (Umar et al., 2004). Thus, MMR plays a role in the DDR pathway as well as prevention of short-term mutagenesis and long-term tumourigenesis. Inhibitors of MMR have not been developed due to evidence showing that defective

MMR results in tolerance to TMZ, platinum-based compounds and some nucleoside analogues, conferring to drug resistance (Fordham et al., 2011; Karran and Bignami, 1994). While preclinical data have revealed chemo-sensitivity, clinical trials conducted using drugs to reactivate epigenetically silenced components of MMR in conjunction with chemotherapy resulted in adverse reactions (NCT00748527, 2008; Plumb et al., 2000).

DNA-PKcs is a critical DNA repair protein involved in NHEJ DSB repair, and inhibitors of this enzyme in preclinical studies have shown to slow DSB repair and increase cytotoxicity of IR, radiomimetics and TOP2 agents *in vitro* and *in vivo* (Munck et al., 2012; Zhao et al., 2006). In B cell chronic lymphocytic leukaemia cells, increased DNA-PKcs levels were associated with poor prognosis in patient derived samples, and DNA-PKcs inhibitors NU7026 and NU7441 potentiated the cytotoxicity of poor prognosis cells to TOP2 poisons (Willmore et al., 2004). Dual mTOR and DNA-PKcs inhibitor CC-115 is currently undergoing clinical evaluation in patients with advanced solid tumours and haematological malignancies (NCT01353625, 2011).

HR is a high fidelity repair mechanism that resolves stalled and collapsed replication forks, as well as the processing of ICLs in cooperation with NER (Deans and West, 2011). Tumours that harbour HR defects are more sensitive towards crosslinking agents, as well as antimetabolites that induce base lesions and/or replication fork stalling. (Evers et al., 2010). There are few HR inhibitors in clinical evaluation; one such inhibitor is mirin, which inhibits MRE11, although its effects are non-specific and target inhibition of both HR and NHEJ repair (Dupre et al., 2008). *In vitro* studies of imatinib, which inhibits RAD51 phosphorylation, resulted in the drug sensitising cells

to IR, as well as crosslinking agents (Choudhury et al., 2009). However, the most common way to target HR repair is by inhibition of the ATM-Chk2 and ATM-Chk1 pathways. The first selective ATM inhibitor, KU55933, demonstrated inhibition of IR-induced ATM-dependent phosphorylation events and sensitised cancer cells to IR and TOP poisons (Hickson et al., 2004). Treatment of cells with novel ATR inhibitors VE-821 and NU6027 resulted in sensitisation of the cells towards DNA-damaging agents, however, the response was dependent on p53 status (Peasland et al., 2011; Reaper et al., 2011). Targeting checkpoints is an attractive strategy for cancer therapy, mainly due to the loss of G1 checkpoint control found in cancer cells (Massague, 2004). WEE1 and CDC25 inhibitors have been developed, which inhibit the entry into mitosis, although clinical data remains limited (J. H. M. Schellens, 2011; Lavecchia et al., 2010). The majority of research has focused on the development of Chk1 inhibitors. While preclinical studies revealed a modest impact on viability, the drugs enhanced cytotoxicity induced by DNA-damaging agents in xenograft studies (Blasina et al., 2008; Matthews et al., 2007; Zabludoff et al., 2008). The non-specific staurosporine analogue, UNC-01, was the first Chk1 inhibitor to enter clinical trials, but was discontinued due to poor specificity and pharmacokinetics. Phase I trials with newer Chk1 inhibitors, in conjunction with gemcitabine, resulted in major toxicity due to myelosuppression and ultimately a termination of the trial (Chen et al., 2012; Garrett and Collins, 2011). An extensive list of pharmacological drugs that inhibit DNA repair components for cancer treatment is listed in figure 1.25.

Pathway	Target	Inhibitor	Current stage
Direct repair	MGMT	O^6-benzylguanine and lomeguatrib	The first clinical trial of O^6-benzylguanine in combination with BCNU was reported in 1998 (REF. 10). Currently in Phase II clinical trials with toxicity issues and marginal benefit. Lomeguatrib plus TMZ combinations are in Phase II trials but no positive data have been reported (dose and tumour type issues?)[12]
BER	FEN1	NSC-281680	*In vitro* TMZ sensitization[173]
	Pol β	Pamoic acid, oleanolic acid and eicosapentaenoic acid	*In vitro* sensitization to IR and bleomycin[174,175]
	Ligase 1 and ligase 3	L67 and L189	*In vitro* sensitization to MMS and IR[176]
	APE1	Methoxyamine	Responses in combination with pemetrexed seen in Phase I trial. Phase II combinations with pemetrexed and with TMZ are underway[177]
		Lucanthone	Phase I trial of combination with TMZ induced radiosensitization (also undergoing testing with a topoisomerase II poison)[30]
		CRT0044876	Preclinical evidence of TMZ sensitization[31,178]
	PARP	AG014688 (also known as CO-338 and rucaparib)	The first PARPi in clinical trial. Phase I and II trials with TMZ in patients with melanoma showed profound PARP inhibition and some clinical responses but increased myelosuppression in Phase II trials, single agent Phase II trials in patients with breast and ovarian cancer with BRCA mutations[35,36]. Phase I trials with various cytotoxic combinations are underway
		AZD2281 (also known as olaparib)	Good single agent activity (40% response rate) demonstrated in BRCA mutation-associated ovarian cancer and 41% in breast cancer and 24% in patients with ovarian cancer without BRCA mutations at the MTD[103]. Phase II single agent trial in selected patients[104,179]. Several Phase I and II trials with a variety of drug combinations; however, there have been toxicity issues with topotecan combination and little benefit was observed with dacarbazine combination[180,181]
		ABT-888 (also known as veliparib)	Phase 0 trial to determine active dose, Phase I/II single agent and combination trials are ongoing in various solid and lymphoid tumours. Combinations with topotecan and cyclophosphamide were tolerated and evidence of inhibition of PARP and DNA repair was obtained[142,143]
		INO-1001	Phase II trial of TMZ combinations in melanoma and glioblastoma
		MK4827	Phase I trial of single agent in BRCA mutation-associated ovarian cancer
		CEP-9722	Phase I trial of TMZ combination in solid tumours
		GPI-21016 (also known as E7016)	Phase I/II TMZ combination in solid tumours and melanoma
		BMN673	Phase I trial single agent in solid and haematological malignancies
		BSI-201 (also known as iniparib	Phase II/III trial of combination with gemcitabine and carboplatin. This is no longer considered a PARP inhibitor[182]
NER	XPG	Cyclosporine	Preliminary *in vitro* studies[183]
	ERCC1–XPF	Cetuximab	Preliminary *in vitro* studies[184]
TLS	Pol	3-*O*-methylfunicone, aurintricarboxylic acid and ellagic acid	Preliminary *in vitro* studies, aurintricarboxylic acid and ellagic acid displayed potent nanomolar activity[46,47]
MMR	MLH1	DAC (reactivation)	Preclinical sensitization to cisplatin, TMZ and epirubicin[53]. Phase II trial was terminated because of adverse reaction. Clinical trials are ongoing in combination with carboplatin and with TMZ
NHEJ	DNA-PKcs	NU7026, NU7441, IC86621 and IC87361	Preclinical *in vitro* and *in vivo* enhancement of responses to IR and etoposide, *ex vivo* sensitization of patient-derived CLL cells to mitoxantrone[61–65]
		OK-135	Preclinical inhibition of DNA repair in radioresistant L5178Y cells[185]
		SU11752	Preclinical *in vitro* inhibition of DSB repair and radiosensitization[186]
		CC-115	Dual DNA-PK and mTOR inhibitor in Phase I clinical trial
HRR	MRE11	Mirin	*In vitro* radiosensitization[70,71]
	RAD51	B02, A03, A10 and imatinib	*In vitro* identification of RAD51 inhibition by a high-throughput screen of NIH compound library and inhibition of plasmid rejoining by HRR[187]. Imatinib inhibits RAD51 phosphorylation, DNA damage-induced RAD51 focus formation and sensitized cells to chlorambucil, MMC and IR[72,73]
	BRCA1	AG024322 and SCH727965 (CDK1 inhibitors)	CDK1 activates BRCA1. Preclinical *in vitro* and *in vivo* studies showed that AG024322 is synthetically lethal with PARP inhibition[115]. A clinical trial has been initiated with SCH727965 and ABT-888

Figure 1.25. Inhibitors of the DDR pathway. Figure continued on the next page.

Pathway	Target	Inhibitor	Current stage
Checkpoints	ATM	KU55933, KU60019 and CP466722	Preclinical *in vitro* sensitization to IR, etoposide and camptothecin[81,188,189]
	ATR	Caffeine, shisandrin B, NU6027 and VE821	Preclinical *in vitro* chemosensitization and radiosensitization[92–95]
	WEE1	MK-1775	Preclinical *in vitro* and *in vivo* chemosensitization and radiosensitization[190,191] and patient-derived sarcoma explants *ex vivo* and as a single agent[192]. Evidence of activity in clinical trials[193]
	CDC25	Several, including IRC-083864 (Debio 0931)	IRC-083864 has activity in pancreatic and prostate cancer xenografts[194] and has entered clinical trial under the name of Debio 0931 (REF. 195) but no data are available
	CHK1 and CHK2	UCN-01	CHK1 and CHK2 (UCN-01 is a pan-kinase inhibitor): Phase I/II trials as a single agent and in combinations, trials were stopped owing to toxicities[91]
		AZD7762	CHK1 and CHK2: Phase I combinations with gemcitabine and with irinotecan
		PF00477736	CHK1: Phase I combination with gemcitabine
		SCH900776	CHK1: Phase I various drug combinations in leukaemia and lymphoma
		XL9844	CHK1 and CHK2: Phase I in combination with gemcitabine
		LY2606368	CHK1: Phase I single agent trial
		PV1019	CHK2: *in vitro* sensitization of topoisomerase I poisons and IR[196]

Figure 1.25. Inhibitors of the DDR pathway. References are indicated in the body of the text. Abbreviations: APE1, AP endonuclease 1; ATM, ataxia-telangiectasia mutated; ATR, ataxia-telangiectasia and Rad3-related; BER, base excision repair; CDC25, cell division cycle 25; CDK1, cyclin-dependent kinase 1; CLL, chronic lymphocytic leukaemia; DAC, decitabine; DDR, DNA damage response; DNA-PKcs, DNA-dependent protein kinase catalytic subunit; DSB, DNA double-strand break; FEN1, flap endonuclease 1; HRR, homologous recombination repair; IR, ionising radiation; MGMT, *O*6-methylguanine DNA methyltransferase; MMC, mitomycin C; MMR, mismatch repair; MMS, methyl methanesulphonate; MTD, maximum tolerated dose; NER, nucleotide excision repair; NHEJ, non-homologous end joining; NIH, US National Institutes of Health; PARP, poly(ADP-ribose) polymerase; PARPi, PARP inhibitor; Pol, DNA polymerase; TLS, translesion synthesis; TMZ, temozolomide; XP, Xeroderma pigmentosum. Image source: (Curtin, 2012)

1.3.7.3 Synthetic lethality

Since several cancers harbour DNA repair deficits, DNA repair mechanisms can be exploited for cancer treatment by specifically targeting cancer cells that possess genetic mutations that are not present in normal cells, a process known as synthetic lethality. The principle of synthetic lethality is based on the interaction between two genes that contribute to an essential process or processes, often nonlinearly (Guarente, 1993; Hartman et al., 2001). When either gene is mutated alone, the cell is viable; however, a combination of mutations in both results in cellular lethality as depicted in figure 1.26.

In the case of *BRCA1/2* mutant carriers, when cancer develops in these patients, there is almost always genetic or functional loss, leading to inefficient HR repair (Osorio et al., 2002). Cells and mouse models that possess HR defects by way of BRCA1/2 mutations are profoundly sensitised to PARP inhibitor treatment, resulting in chromosomal instability, cell cycle arrest and apoptosis (Bryant et al., 2005; Farmer et al., 2005). Furthermore, knockdown of other genes involved in HR have also rendered the cells sensitive to PARP inhibition (McCabe et al., 2006). Numerous clinical trials with PARP inhibitors in breast and ovarian cancers have resulted in encouraging data (discussed in section 1.3.7.4.6). However, resistance to PARP inhibitors can be developed through restoration of BRCA1/2 function (Sakai et al., 2008; Swisher et al., 2008). In addition, PARP inhibitor resistance can be restored through inactivation of 53BP1 and DNA-PKcs, crucial proteins involved in NHEJ (Bouwman et al., 2010; Patel et al., 2011). Therefore care must be taken to treat tumours which harbour deficits in NHEJ repair, such as in BRCA-1 mutant and triple negative breast cancers and lung cancers, where 53BP1 is a commonly lost (Bartkova et al., 2007).

Other examples of synthetic lethality encompassing HR defects and PARP inhibition have been found. Loss of ATM in haematological malignancies or mutation of MRE11 results in sensitivity to PARP inhibition in lymphoma and colorectal cancer cells (Vilar et al., 2011; Weston et al., 2010; Williamson et al., 2010). Compromised CDK1 activity sensitised BRCA-proficient cancers to PARP inhibition, and clinical trials for this combination have already commenced (Johnson et al., 2011). In short, the development of inhibitors of PARP has led to an increase in cytotoxicity of tumour cells in numerous models. Identification of suitable biomarkers paves the next step to effectively stratify patients that would benefit from the appropriate inhibitors, either for use as a single agent treatment, or in combination with other targeted therapies.

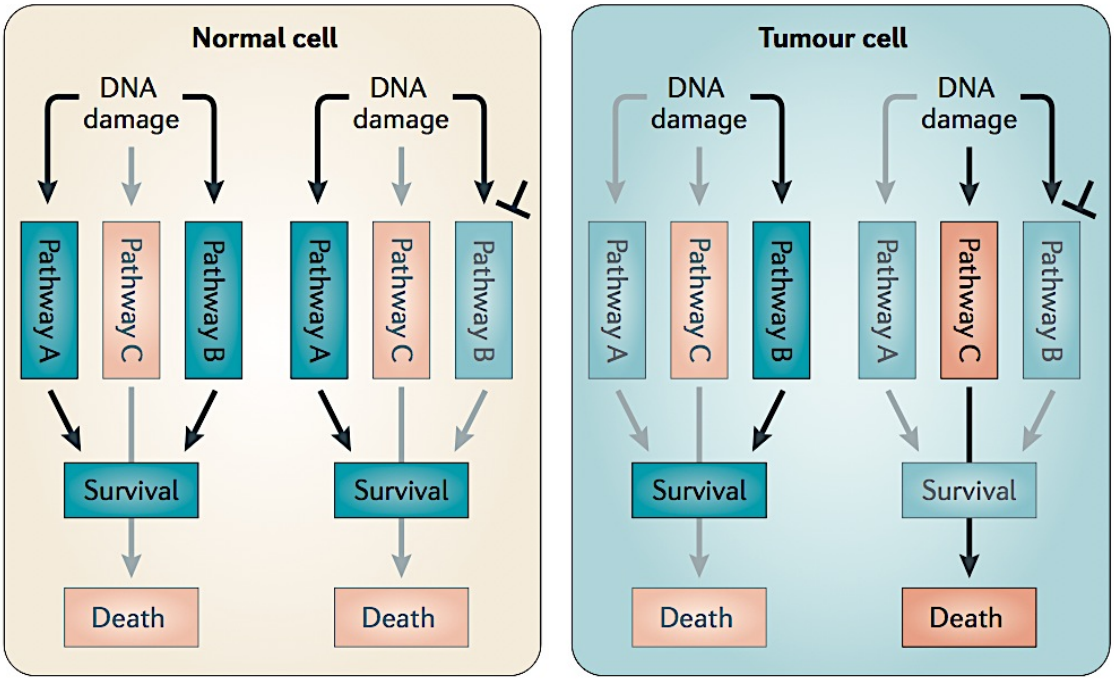

Figure 1.26. Principles of synthetic lethality. Pathways A and B represent repair pathways which respond to DNA damage. When pathway B is inhibited, normal cells can rely on functioning pathway A to repair the damage, resulting in cell survival as depicted in the image on the left. In tumour cells with defective repair mechanisms (represented by pathway A), inhibition of pathway B can result in the erroneous activation of repair pathway C, which is unable to repair the damage appropriately, resulting in cell death. Image source: (Curtin, 2012)

1.3.7.4 Targeted therapies in ovarian cancer

Improved understanding of the underlying biology of ovarian cancer has led to the development of molecular targeted therapies that target several hallmarks of cancer, including angiogenesis, survival, cell growth and metastases (Hanahan and Weinberg, 2011; Yap et al., 2009). The majority of current research in advanced and recurrent ovarian cancer focuses on the inhibition of signal transduction pathways and targeting DNA repair mechanisms. The most successful strategies so far are employing anti-angiogenesis and PARP inhibitors. Other approaches target aberrant pathways frequently upregulated in ovarian cancers such as the PI3K/Akt/mTOR network, the epidermal growth factor receptor, the WEE1 tyrosine kinase and the folate receptor alpha.

Table 1.4. Ovarian cancer targeted therapies and agents used in clinical trials

Targeted therapy	Agents in clinical trials
Anti-angiogenic agents	Bevacizumab is currently used in phase II and phase III trials as single agent therapy, as well as in combination with chemotherapy and other targeted therapies. Tyrosine kinase inhibitors that inhibit activity against tyrosine kinases inhibitors involved in angiogenesis are currently in phase III trials.
Epidermal growth factor receptor inhibitors	Gefitinib and erlotinib used with chemotherapy resulted in high overall response rates compared to single agent treatment. Monoclonal antibody pertuzumab which targets HER2 have reported increased response rates with gemcitabine versus gemcitabine monotherapy in ongoing phase III trials.
Oestrogen receptor antagonists and aromatise inhibitors	While anti-proliferative effects have been seen in *in vitro* and *in vivo*, oestrogen inhibitor tamoxifen and aromatase inhibitors have had modest response rates in clinical trials.
PI3K/Akt/mTOR pathway inhibitors	Second generation PI3K inhibitor XL147 is in phase I trial in combination with paclitaxel and carboplatin. mTOR inhibitor everolimus and temsirolimus are currently being explored in phase I/II in combination with other agents with promising results. Akt inhibit MK02206 are in phase II trial in a biomarker assessed trial.
WEE1 tyrosine kinases inhibitors	Wee-1 inhibitor MK-1775 is in phase II trial in p53 mutated refractory and resistant ovarian cancers.

PARP inhibitors	Phase II trials of PARP inhibitor olaparib revealed favourable response in ovarian cancers with *BRCA1/2* mutations. Phase III trials have begun in BRCA mutant ovarian cancer patients. Other PARP inhibitors include BMN-673 (phase II), MK04827 (niraparib), rucaparib and ABT-14699.

1.3.7.4.1 Anti-angiogenic therapy

Ovarian malignancies are characterised by increasing levels of numerous pro-angiogenic factors, including members of the VEGFs (Olson et al., 1994), and platelet derived growth factors (PDGFs) (Henriksen et al., 1993) family of proteins. Anti-angiogenic agents are being evaluated in the treatment of EOCs, the most promising of these being bevacizumab (Genentech-Roche), a human monoclonal antibody that inhibits VEGF family member A, which is currently being used in phase II and phase III clinical trials as single agent therapy, as well in combination with chemotherapy and other targeted therapies (Azad et al., 2008; Burger et al., 2007; Cannistra et al., 2007; Garcia et al., 2008; Micha et al., 2007). Results of the trials have revealed increased progression-free survival in single-agent studies in recurrent ovarian cancers, as well as maintenance therapy with concomitant standard carboplatin-paclitaxel treatment in first line therapy (Burger et al., 2011; Perren et al., 2011). In another randomised phase III trial evaluating bevacizumab plus chemotherapy for platinum resistant recurrent ovarian cancer patients, combination treatment resulted in improved progression free survival and overall response rate compared to chemotherapy alone (Eric Pujade-Lauraine, 2012). Other anti-angiogenic compounds under investigation are the tyrosine kinase inhibitors that possess potent inhibitory activity against multiple tyrosine kinases involved in angiogenesis. Phase III trials of tyrosine kinase inhibitors show promising results with good response rates alone or in conjunction with other treatments (du Bois et al., 2014; GlaxoSmithKline, 2010; JA Ledermann, 2013). However, since tyrosine kinase inhibitors are relatively new drugs, and as with most novel targeted therapies, the long-term side effects have yet to be clearly defined.

1.3.7.4.2 Epidermal growth factor receptor inhibitors

Another targeted therapy being exploited involves EGFR, which is overexpressed in 70% of ovarian cancers and is associated with advance disease upon diagnosis, as well as poor prognosis and chemo-resistance (Bartlett et al., 1996; Fischer-Colbrie et al., 1997). While preclinical data have suggested inhibition of EGFR may have anti-tumour activity and reverse chemo-resistance (Ciardiello et al., 2000; Sirotnak, 2003; Sirotnak et al., 2000), single agent studies of EGFR inhibitors, have resulted in little or no success with respect to clinical response (Gordon et al., 2005; Posadas et al., 2007; Schilder et al., 2005; Seiden et al., 2007). However, phase II trials of EGFR inhibitor gefitinib and erlotinib combined with chemotherapeutic agents have resulted in higher overall response rates of 61.9% and 60.0% in platinum-sensitive tumours compared to 19.2% and 7.0% in platinum-resistant tumours, respectively (Hirte et al., 2010; Pautier et al., 2010). Monoclonal antibody pertuzumab (Roche, Switzerland) is targeted against human epidermal growth factor receptor 2 (HER2) and ongoing phase III trials have revealed increased response rates in combination therapy with gemcitabine versus gemcitabine monotherapy (NCT01684878, 2012).

1.3.7.4.3 Oestrogen receptor antagonists and aromatase inhibitors

There is evidence that suggests oestrogen influences proliferation in a subset of ovarian cancers (Simpkins et al., 2013). Furthermore, anti-oestrogen compounds have been shown to inhibit proliferation of ER positive ovarian cancer cells *in vitro* and *in vivo* (Simpkins et al., 2012). Clinical trials have been conducted to evaluate ER antagonists such as tamoxifen and aromatase inhibitors, however treatment with tamoxifen and aromatase inhibitors for recurrent ovarian cancer resulted in a modest 13% and 8% overall response rate, respectively (Simpkins et al., 2013). Limitations of these studies

include a lack of preselecting patients based on hormone receptor or aromatase expression.

1.3.7.4.4 PI3K/Akt/mTOR Pathway inhibitors

Deregulation of the PI3K/Akt pathway is commonly found in ovarian cancer and inhibitors have been developed to target components of this pathway, as well as inhibitors against components of the downstream mTOR pathway, to deactivate aberrant signalling. mTOR is a critical target of AKT that targets proteins, such as S6 kinases, thus regulating protein translation of different effectors in cell growth and cell cycle progression. First generation PI3K inhibitors, such as Wortmannin and LY294002, were largely unsuccessful because of high toxicity, most likely due to the absence of selectivity (Gharbi et al., 2007; Wipf and Halter, 2005). Second generation inhibitors are currently under exploration, although few have reached the phase II stage due to insignificant response rates. XL147 (Exelixis, USA) is a reversible, highly selective PI3K inhibitor which is currently in phase I trials.

Single agent PI3K/Akt/mTOR inhibitors have also been largely unsuccessful, in part due to resistance mechanisms initiated by feedback regulation. Inhibition of mTORC1 leads to activation of PI3K signalling through loss of a feedback loop (O'Reilly et al., 2006), as well as activation of the growth and differentiation MAPK signalling pathway (Carracedo et al., 2008). Given the extensive cross-talk and feedback loops found in this pathway, combination treatment of several PI3K/Akt/mTOR component inhibitors with chemotherapy and other tumour targeted therapies have resulted in enhanced anti-tumour activity *in vitro* as well as *in vivo.* mTOR inhibitors such as everolimus (Novartis, USA) and temsirolimus (Pfizer, USA) are currently being explored in phase I

and phase II trials in combination with other treatments with promising results (NCT00886691, 2009; NCT01031381, 2009; NCT01281514, 2011; R. Morgan, 2011; Temkin et al., 2010). The Akt inhibitor MK-2206 (Merck & Co, USA) is in phase II investigation for platinum resistant ovarian, fallopian tube or primary peritoneal cancer in a biomarker-assessed trial (NCT01283035, 2011).

1.3.7.4.5 WEE1 tyrosine kinase inhibitors

Another DNA damage agent being used in a synthetically lethal manner is the WEE1 tyrosine kinase inhibitor. WEE1 kinase is a crucial enzyme involved in maintaining G2-cell cycle checkpoint arrest. Cells possessing a mutation in components involved in G1 regulation, such as those harbouring a p53 mutation, often rely on G2 checkpoint arrest for DNA repair, and therefore WEE1 inhibitors are candidates for enhancing anti-tumour activity through synthetic lethality. A phase 2 trial is currently studying whether p53 mutated refractory and resistance ovarian cancer patients will benefit from treatment with Wee-1 inhibitor MK-1775 (Merck, USA) and carboplatin (NCT01164995, 2010).

1.3.7.4.6 PARP inhibitors

Approximately 10% of EOCs have a germ line mutation in cancer susceptibility genes *BRCA1* and *BRCA2*, rendering them deficient in HR DNA repair. The presence of a *BRCA1* mutation in women is associated with a lifetime risk of ovarian cancer of 20-45% (Antoniou et al., 2003). *BRCA2* mutations are associated with a lifetime risk of 10-20% for ovarian cancer. 'BRCAness' is a term that describes cancers that do not possess mutations of *BRCA1/2*, but phenotypically behave like these tumours due to genetic and epigenetic events. Some of these aberrations may result in tumours

harbouring HR deficiency and with respect to ovarian cancer, up to 50% of EOCs harbour HR deficiency. While the progress of tumour-targeted therapies, as described in previous sections, has been slow in advancing in clinical trials phases, the development of PARP inhibitors have resulted in encouraging data. While several PARP inhibitors are currently being explored in clinical trials, the most advanced to date is olaparib (AZD2281, Astrazeneca, USA). Phase II trials with olaparib have produced response rates of 33% in ovarian cancers with *BRCA1/2* mutations (Audeh et al., 2010), and other studies in recurrent serous ovarian cancer have confirmed favourable responses as well (Gelmon et al., 2011; J. Ang, 2010). Phase II trials evaluating the benefit of olaparib treatment as maintenance therapy in platinum-sensitive ovarian cancer patients with or without *BRCA1*/2 mutations have revealed clear improvements in progression free survival (Ledermann et al., 2012). A phase II trial is currently evaluating olaparib treatment in conjunction with paclitaxel and carboplatin in patients with platinum sensitive advanced serous ovarian cancer versus paclitaxel and carboplatin treatment alone (NCT01081951, 2010). Lastly, there are two phase III trials underway (NCT01844986 and NCT1874353) which are evaluating a new tablet formulation of olaparib for maintenance treatment for BRCA mutant ovarian cancers.

Other PARP inhibitors are also being evaluated in clinical trials. Phase II trials of iniparib (BSI-201, BiPar Sciences, USA) in combination with carboplatin and gemcitabine in platinum sensitive and platinum resistance ovarian cancer yielded initially improved response rates (M. J. Birrer, 2011; R. T. Penson, 2011). Recent publications, however, have reported that the anti-tumour activity of iniparib is not consistent with PARP inhibition, and further preclinical assessment of the drug is required (Liu et al., 2012; Patel et al., 2012). Other PARP inhibitors currently in early

phase trials include MK-4827, Merck&Co, USA), ABT-14699 Pfizer, USA), and BMN-673 (Biomarin, USA).

1.3.7.5 Ovarian cancer models

Ovarian cancer is the seventh most common cancer diagnosed in women, and account for 4% of all cancers in women worldwide (Ferlay J, 2010). The majority of ovarian cancers are epithelial in origin; however, recent pathological and genomic findings have challenged the traditionally held viewpoint that EOC derives from ovarian tissues. Up until the early 2000s, EOC origins were believed to stem from the ovarian surface epithelium (Auersperg et al., 2001). However, histological and molecular analyses of EOCs led to the findings that suggest metastatic mucinous EOCs originate from the colon, and endometrioid and clear cell EOC may be derived from atypical endometriosis (Kelemen and Kobel, 2011; Qiu et al., 2013). The origin of HGSC, the most prevalent subtype of EOC, has also recently been further probed. The latest findings conducted by Perets et al. using de novo mouse models of HGSC suggests that high grade serous tumours can originate in fallopian tubal secretory epithelial cells (Perets et al., 2013). The study also identified the development of serous tubal intraepithelial carcinoma lesions as a precursor to HGSC, and advanced disease. Interestingly, mouse models carrying *TP53* deletion and mutations, one of the genetic hallmarks of HGSC, did not result in a drive in tumour progression, unlike loss of *BRCA1* or *BRCA2*, which resulted in widespread peritoneal disease. Therefore, *BRCA* status seems to play an important role in progression to metastatic disease, despite it being less frequently altered compared to *TP53* (Perets et al., 2013). Since approximately half of HGSC cases harbour defective HR repair, further work will need to be carried out to investigate the driving ability of components of HR in

tumourigenesis and progression to metastatic disease. Doing so will enable improved screening methods and therapeutic approaches for EOC patients, as well as provide a greater understanding of the pathogenesis of epithelial derived ovarian tumours.

1.4 Aims and objectives

Hyperactivation of the PI3K/Akt pathway has been identified in numerous cancers, and approximately 45% of high grade serous ovarian tumours exhibit altered components in this pathway. Therefore, further investigation of components of this pathway in ovarian cancer may reveal a greater understanding of the tumour biology of this disease. The establishment of INPP4B as an important component of tumourigenesis and cancer progression has solidified over the last few years due to accumulating evidence being found across a range of cancer tissue types. In addition, LOH of *INPP4B* was identified in 40% of ovarian cancer patients. Thus, further exploration of the function of INPP4B and its biomarker potential may benefit a large patient population in the stratification of effective treatment regimes. The discovery of defective HR repair in approximately half of high grade serous tumours has introduced a myriad of therapeutic strategies that specifically target this repair deficiency in the clinical setting. The aim of this investigation is to therefore understand the role of INPP4B in DNA repair and examine whether loss of INPP4B expression can be therapeutically exploited with already established clinical treatments in the context of ovarian cancer. I will investigate the bioinformatics analysis of the identification of a 'BRCAness' signature identified in INPP4B-deficient MCF-10A human mammary epithelial cells. Furthermore, I will endeavour to establish and explore the biological function of INPP4B in the context of DNA repair in ovarian cancer cells using INPP4B knockdown cell pools. Finally, I will investigate the effect of INPP4B loss in conjunction with DNA repair inhibitor treatment, both *in vitro* and *in vivo*.

CHAPTER 2. Materials and methods

2.1 General materials and methods

The methods in this subsection represent standard tissue culture, infections, microbiology and molecular biology procedures.

2.1.1 Tissue culture

2.1.1.1 Cell line, maintenance, storage and retrieval

The cell lines used for experiments were human mammary epithelial cells, MCF-10A, human epithelial ovarian cancer cell lines Ovca429 and Ovca433, and human embryonic kidney (HEK) 293T cells. MCF-10A cells were maintained in DMEM/F12 media (Invitrogen, UK) with 5% horse serum (Invitrogen, UK), 20 ng/ml epidermal growth factor (EGF, Peprotech, UK), 0.5 μg/ml hydrocortisone (Sigma-Aldrich, UK), 100 ng/ml cholera toxin (Sigma-Aldrich, UK), 10 μg/ml insulin (Sigma-Aldrich, UK) and 2 mM L-glutamine (Sigma-Aldrich, UK). Ovca429 and Ovca433 cell lines were maintained in RPMI1640 media (Sigma-Aldrich, UK) with 10% foetal calf serum (FCS, Sigma-Aldrich, UK) and 2 mM L-glutamine. HEK 293T cells were maintained in DMEM media supplemented with sodium pyruvate (Lonza, UK) with 10% FCS and 2 mM L-glutamine. INPP4B$^{fl/fl}$ MEFs were cultured in DMEM with 10% FCS, 5 mg/ml glutamine, 5 mg/ml penicillin streptomycin (Sigma-Aldrich, UK) and 1:1000 beta-mercaptoethanol (Sigma-Aldrich, UK). Knockdown derived cell lines were selected for in appropriate media containing 2 μg/ml puromycin (Invivogen, UK).

Cells were grown in either 100 mm^2 or 150 mm^2 tissue culture plates (BD Falcon, UK), depending on the number of cells required. Cells were incubated in a humidity-saturated

(95%) incubators (Forma Scientific, UK) at 37°C with 5% CO_2. On average cells were passaged three times a week, at a confluency of 80 – 90%. The cell media was aspirated from the plates and the cells washed with 10 ml sterile 1 X phosphate buffered saline (PBS, 80 g NaCl, 2.2 g KCl, 9.9 g $Na_2HPO_4.2H_2O$. 2.0 g K_2HPO_4 were added to 2 L of distilled water to make a 10 X stock and the pH adjusted to pH 7.4). The PBS was aspirated and the cells detached by the addition of 2 ml 0.05% Trypsin-Ethylenediaminetetraacetic acid (Trypsin-EDTA, Invitrogen, UK) and incubated at 37°C. 6 ml of growth media were added to the plate to deactivate the trypsin and the cells were transferred to a Falcon tube where they were thoroughly resuspended to get a single cell suspension. The cells were centrifuged at 300 g at room temperature for 5 min (Eppendorf, UK), and the supernatant was aspirated. The cell pellet was resuspended in growth media and transferred to a new plate at a maintenance ratio of 1:6 for 293T cells and 1:8 for the Ovca429, Ovca433 and MCF-10A cell lines.

Cells to be frozen were grown to a confluency of 90% before being trypsinised, pelleted by centrifugation and resuspended in 1 ml Bambanker serum-free freezing medium (Lymphotec Inc., Japan) per 100 mm^2 plate of cells. Cells were transferred into a cryovial and slowly frozen in a Nalgene freezing container (Sigma-Aldrich, UK) at -80°C. Cells were retrieved by thawing the cells briefly in a 37°C waterbath, adding 6 ml growth medium to the cells, and pelleting the cells by centrifugation. The supernatant was aspirated and cells resuspended in regular growth media, seeded in plates and left to attach overnight in the incubator at 37°C. The next morning growth media in plates was exchanged to remove dead cells.

2.1.1.2 Cell counting

Cells were counted using the Vi-CELL cell viability analyser (Beckman Coulter, UK). 1 ml of cell suspension was placed in holding vessels designed specifically for the machine. Cells were counted by the trypan blue dye exclusion method and the cell count and cell viability was noted.

2.1.1.3 Plasmids

Knockdown cell pools were generated by using pSM2 shRNA hairpins against Renilla luciferase, INPP4B, PTEN and BRCA1 (figure 2.1, OpenBiosystems, UK). shRNA hairpin-expressing retroviral vector Renilla luciferase (MSCV-U6miR30-PIGdeltaRI-FF2), and PTEN (MSCV-U6miR30-PIGdeltaRI) were generous gifts from Dr. Steven Elledge (Harvard University, Boston, MA). Specific shRNA-hairpins directed against human INPP4B (RHS1764-9399376, sequence: TGCTGTTGACAGTGAGCG ACGTTGGCATTTCCGATTTAAATAGTGAAGCCACAGATGTATTTAAATCGGA AATGCCAACGGTGCCTACTGCCTCGGA) and human BRCA1 (RHS4430-98708636, sequence: TGCTGTTGACAGTGAGCGCGGCATGAATATTTCATATCTATAGTGAAGCCAC AGATGTATAGATATGAAATATTCATGCCATGCCTACTGCCTCGGA) were obtained from Open Biosystems. pEAK FLAG-INPP4B, pcDNA3.1(+) FLAG-ATR, and pMT123 HA-Ubiquitin plasmids were used for protein overexpression studies and pcDNA3.1+ FLAG-EMPTY plasmids were used as the vector control . pEAK FLAG-INPP4B and pcDNA3.1+ FLAG-EMPTY were generous gifts from Dr. Robin Ketteler (MRC Laboratory for Molecular Cell Biology, UK) (figure 2.2). pMT123 HA-Ubiquitin, pENTR1A and pGEX-KG were generous gifts from Dr Pablo Rodriguez-

Viciano (UCL, UK) (figure 2.3). Finally, pcDNA3.1+ FLAG-ATR was kindly given by Dr Steve Jackson (Gurdon Institute, UK).

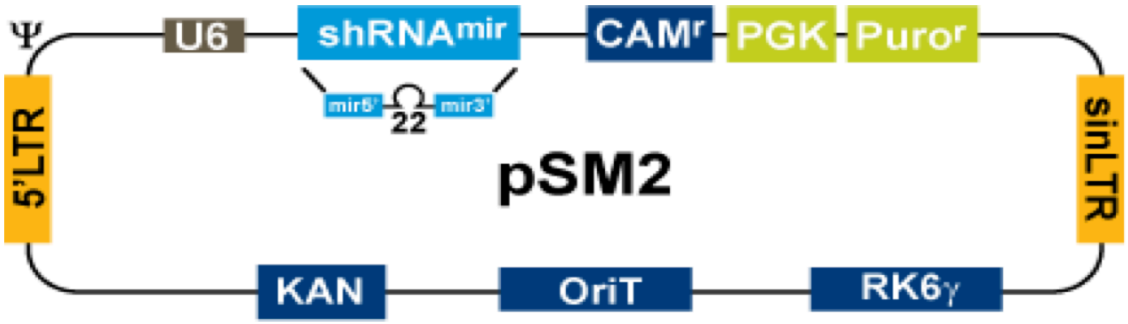

Figure 2.1. Plasmid for knockdown studies: pSM2 plasmid map. The pSM2 vector backbone was used for the expressing Renilla luciferase, INPP4B, PTEN and BRCA1 shRNA constructs**.** The plasmid contains an ampicillin bacterial selection element and a puromycin and zeomycin mammalian selection elements. Image source: Thermo Scientific Open Biosystems Expression Arrest GIPZ Lentiviral shRNAmi technical manual (http://www.thermo.com/eThermo/CMA/PDFs/Various/File_8305.pdf)

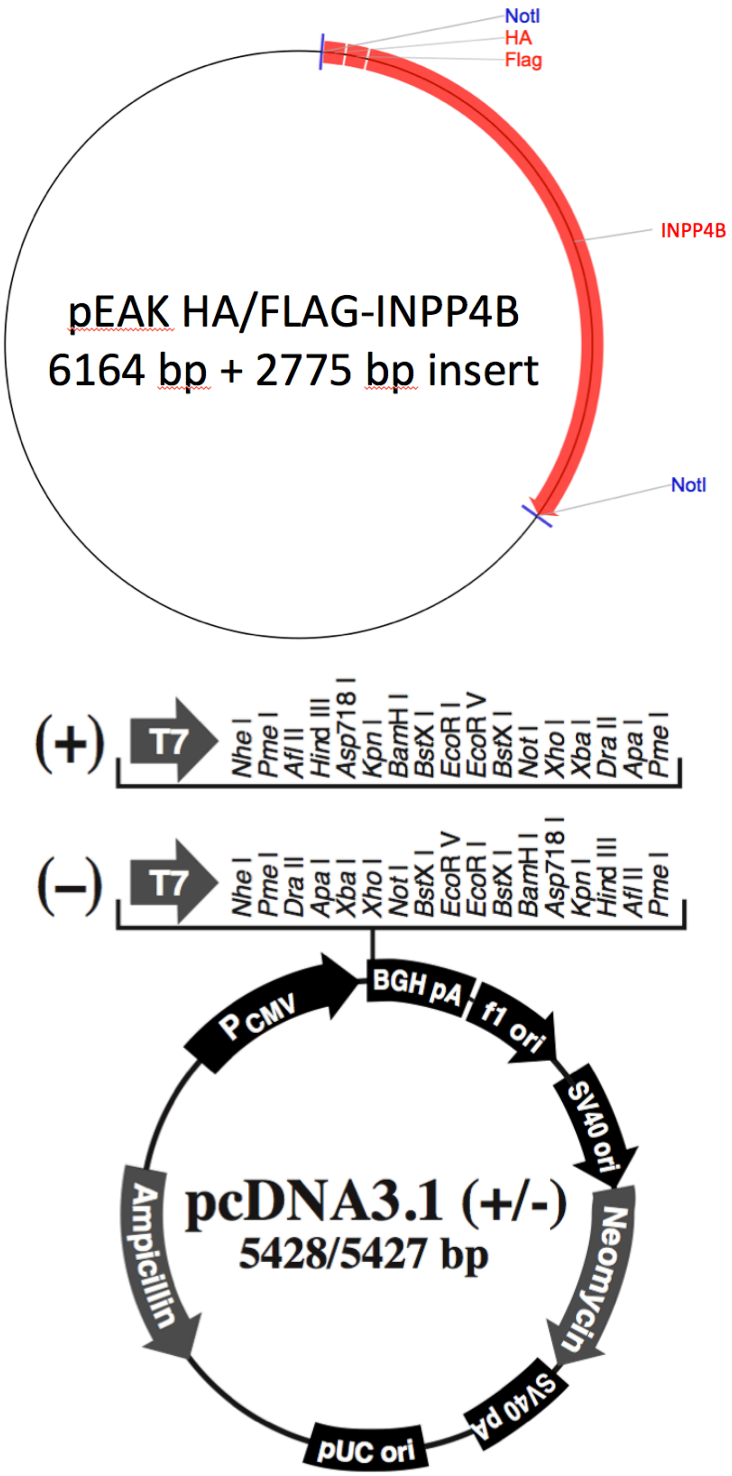

Figure 2.2. Plasmid for overexpression studies: pEAK and pcDNA3.1(+) plasmid maps. pEAK vector backbone containing a FLAG and INPP4B insert and pcDNA3.1(+) plasmid map. These vectors were used for protein overexpression studies. The plasmids contain an ampicillin bacterial selection element. Image source: (pEAK, http://www.addgene.org/24324/; pcDNA3.1(+), http://www.invitrogen.com)

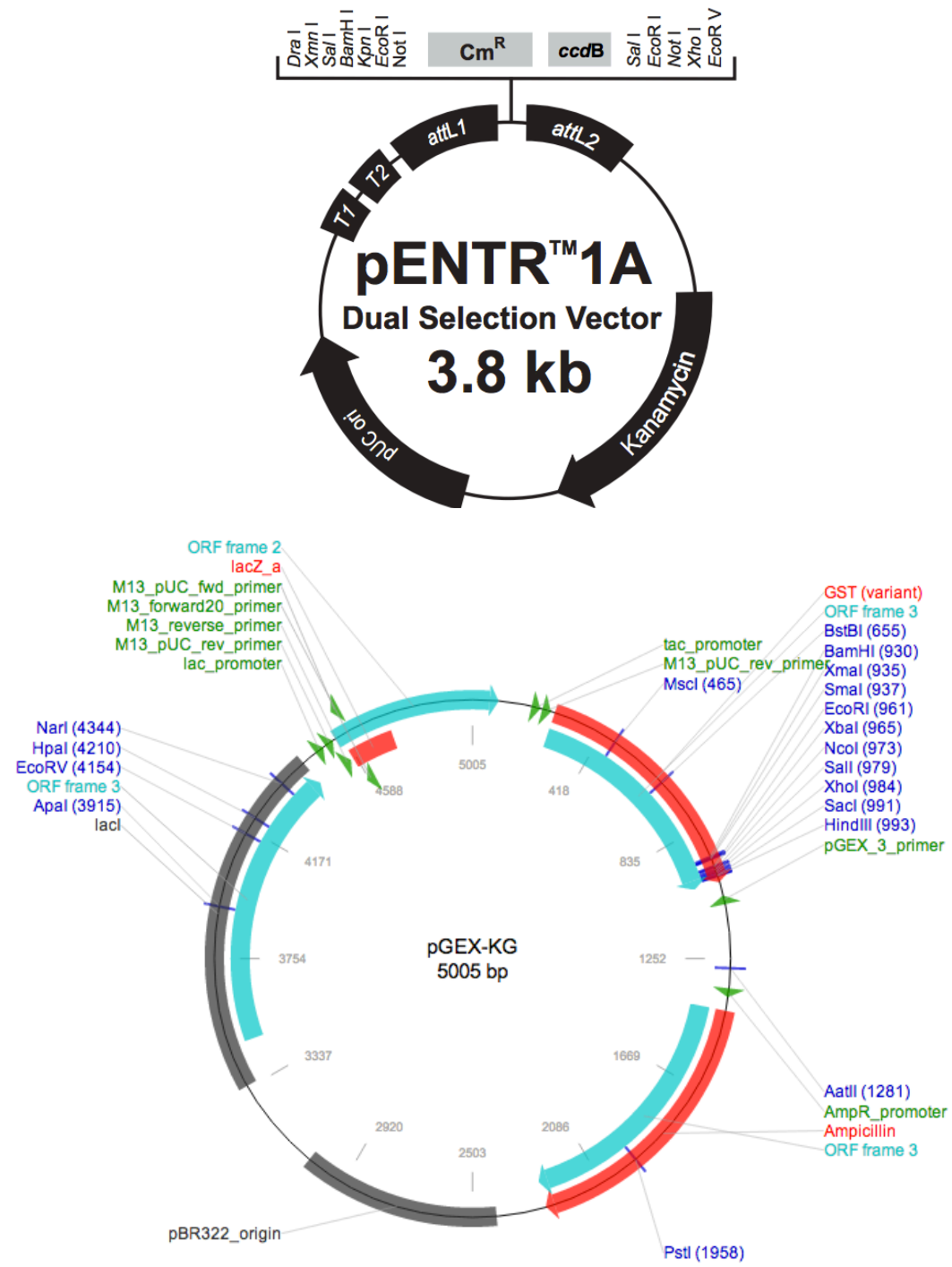

Figure 2.3. Plasmid for GST studies: pENTR1A and pGEX-KG plasmid maps. pENTR1A entry vector containing a *ccdB* gene and carrying a kanamycin bacterial selection element; pGEX-KG vector containing a Glutathione S-transferase (GST) tag and an ampicillin bacterial selection marker used as a destination vector for bacterial protein amplification and isolation. Image source: (pENTR1A,

http://www.invitrogen.com; pGEX-KG, http://www.addgene.org/vector-database/2890/)

2.1.1.4 Cell transfections for virus production

Viral stocks were generated using 293T cells and linear polyethylenimine (PEI, Polysciences Inc., UK) as a transfection agent. PEI granules were dissolved in distilled water to make a 1 mg/ml working stock, neutralised to pH 7.0, sterile filtered using a 0.22 μm filter (Corning Incorporated, UK) and 10 ml aliquots stored at -80°C. 2 x10^6 293T cells were seeded in a 100 mm plate and incubated at 37°C overnight. The plasmid DNA components were combined in a 1.5 ml microcentrifuge tube with the appropriate shRNA hairpin, viral gag-pol, and viral env plasmid DNA at a ratio of 4:3:1, totalling 15 μg DNA per 100 mm plate. 300 μl of DMEM serum-free media was added to the DNA and PEI was added at a DNA:PEI ratio of 1:6 (60 μg per 100 mm^2 plate). The microcentrifuge tube was immediately vortexed for 10 s and the solution incubated at room temperature for 15 mins to allow for DNA-PEI complexes to form. After the 15 mins incubation, the DNA-PEI complex solution was pipetted drop by drop onto the plate of 293T cells containing freshly replenished growth media. The cells were incubated at 37°C overnight and 24 hrs later, and the media was aspirated and replaced with 5 ml of growth media to concentrate the virus. 24 hrs later, the viral supernatant was collected, filtered using a 0.45 μm filter (Corning Incorporated, UK) and stored at -80°C until further use or used fresh to transduce cells. The cells were replenished with 5 ml of growth media and the viral supernatant collected as explained above 48 and 72 hrs after transduction.

2.1.1.5 Infection of cells with virus

Infection of the cell lines used from this study was based on the protocol defined by Debnath et al. (Debnath et al., 2003). Stable cell lines were generated by incubation of

40% confluent attached cells in 4.5 ml viral supernatant containing 10 μg/ml polybrene for 4 hrs. 10 ml of the appropriate cell line growth media was added to the virus supernatant and allowed to incubate overnight at 37°C. The next day, the virus and media mixture was aspirated and replaced with 10 ml of regular growth media. The following day the cells were subjected to selection by the addition of growth media containing 2 μg/ml puromycin (Invivogen, UK). The selection media was changed on a daily basis until only selected cells remained, which took approximately 3 days. The stable knockdown cell line was then maintained as described in section 2.1.1.1.

2.1.1.6 Transient transfections

6 x10^6 293T cells were seeded in 150 mm plates and grown overnight at 37°C. The 293T cells were replenished with fresh growth media, then cells were transfected with the 25 μg of the desired DNA plasmid and 100 μg of PEI. The DNA and PEI were added in DMEM serum free media, allowed to incubate for 15 min before being added onto the 293T cells. The cells were left to incubate for 48 hrs at 37°C. Cells were trypsinised, pelleted, and washed in ice-cold, sterile 1 X PBS before being lysed in 1 X cell signalling lysis buffer (20 mM Tris-HCl (pH 7.5), 150 mM NaCl, 1 mM Na_2EDTA, 1 mM EGTA, 1% Triton, 2.5 mM sodium pyrophosphate, 1 mM beta-glycerophosphate, 1 mM sodium orthovanadate, 1 μg/ml leupeptin) containing 1 X protease inhibitor (Roche, UK) and 1μM dithiothreitol (DTT, Sigma-Aldrich, UK). From this point forward, all experiments were carried out on ice or at 4°C. Cells were incubated on ice for 10 min, vortexed frequently, and centrifuged at 16,000 g at 4°C for 20 min. The protein lysate supernatant was extracted and placed in a new 2 ml microcentrifuge tube. The input lysates were quantified and stored as described in section 2.1.3.2.

2.1.2 Cloning

2.1.2.1 Preparation of Luria-Bertani (LB) broth and agar plates

20 g of Luria-Bertani (LB) broth powder (Sigma-Aldrich, UK) was resuspended in 1 L distilled water and autoclaved at 121°C for 15 min to sterilise. The LB broth was sealed and stored at room temperature until further use. Preparation of agar plates was conducted by autoclaving 8 g of agar (Fisher Scientific, UK) in 400 ml of LB broth, as described above. The agar was left to cool, antibiotics ampicillin or kanamycin added to the broth and mixed thoroughly in 100 mg/ml and 50 mg/ml concentrations, respectively, and poured into petri dishes (BD Falcon, UK), adhering to typical microbiology aseptic techniques. Once the agar solidified, the agar plates were inverted and stored in a sealed bag at 4°C until further use.

2.1.2.2 Plasmid transformation, inoculation, plasmid DNA isolation and DNA quantification

250 µl of DH5α competent cells at a efficiency of ~1 X 10^6 cfu/µg were thawed on ice for 15 min. 1 µg of the DNA required to be subcloned was added to the competent cells, thoroughly mixed by pipetting, and incubated on ice for 30 min. The tube was placed in a 42°C water bath for 30 s and then placed on ice for further 2 min. The transformation reaction was diluted by the addition of 1 ml of LB broth and incubated at 37°C in a shaker rotating at 220 rpm for 60 min. 200 µl of the cell transformation mixture was plated and spread on LB agar plates containing the appropriate antibiotic, and incubated inverted overnight at 37°C. Single colonies were picked using a sterile pipette tip and placed in flask of 200 ml LB broth with antibiotics. The culture was incubated at 37°C

in a shaker rotating at 220 rpm for 12 – 16 hrs. Plasmid DNA was isolated and purified using the NucleoBond® Xtra Midi kit (Macherey-Nagel, Germany) according to the protocol supplemented by the NucleoBond® Xtra Midi kit. Plasmid DNA was resuspended in distilled water, quantified with the Nanodrop 1000 spectrophotometer (Thermo Scientific, UK) and stored at -20°C until further use.

2.1.2.3 Sequencing

DNA sequencing was performed by the UCL sequencing technology facility. Plasmid DNA was resuspended in deionised water and 10µl of either 100 ng/µl plasmid DNA or 1 ng/µl per 100 bp PCR product was submitted for sequencing. 6 µl of sequence primers were provided at a concentration of 5pmol/µl.

2.1.3 Western blot

2.1.3.1 Total protein extraction

Cells were trypsinised, pelleted, and washed in ice-cold 1 X PBS before being lysed in 1 X cell signalling lysis buffer (see section 2.1.1.6. for recipe). Cells were incubated on ice for 10 min, vortexed frequently, and centrifuged at 16,000 g at 4°C for 20 min. The protein lysate supernatant was extracted and placed in a new microcentrifuge tube, and stored at -80°C.

2.1.3.2 Protein quantification

Protein concentration was quantified by adding 2 µl of protein lysate to 1 ml of Bradford reagent (Biorad, UK). The solution was vortexed briefly and the absorbance was measured using a spectrophotometer at 595 nm. A cuvette containing 1 ml

Bradford reagent and 2 μl of lysis buffer was used as a blank. Varying concentrations of bovine serum albumin (BSA, Sigma-Aldrich, UK) was used to calculate absolute protein concentrations. 25 μg of protein was mixed with 6 X laemmli sample buffer (12% sodium dodecyl sulphate (SDS, Sigma-Aldrich, UK), 6% bromophenol blue (Sigma-Aldrich, UK), 47% glycerol (Sigma-Aldrich, UK), 60 mM Tris pH 6.8, 600 mM DTT, 2.1 ml deionised water), denatured at 100°C for 5 min in the Accublock Digital Drybath (Labnet International Inc., USA) and stored at -80°C until ready for immunoblotting.

2.1.3.3 Casting gels

Sodium dodecyl sulphate polyacrylamide gels (SDS-PAGE) were cast using the Mini-PROTEAN® Tetra Handcast Systems (Biorad, UK). 1.0 mm and 1.5 mm glass plates along with 10 well combs (Biorad, UK) were used to form the gels were used containing 30% acrylamide (National Diagnostics, UK), 1.0 M Tris pH 6.8, 1.5 M Tris pH 8.8, 10% SDS, 10% ammonium persulphate (APS, Sigma-Aldrich, UK), and Tetramethylethylenediamine (TEMED, Sigma-Aldrich, UK). The detailed composition of the stacking and resolving gel is listed in Table 2.1. 6% gels were used to detect ATM, ATR and BRCA1. 8% gels were used to detect INPP4B, PTEN, AKT 1/2, and ERK 1/2.

Table 2.1 SDS-PAGE gel composition

Stacking SDS-PAGE (ml)		Resolving SDS-PAGE (ml)		
	5%		**6%**	**8%**
Deionised water	3.400	Deionised water	10.600	9.300
30% Acrylamide	0.840	30% Acrylamide	4.000	5.300
1.0M Tris pH 6.8	0.630	1.5M Tris pH 8.8	5.000	5.000
10% SDS	0.050	10% SDS	0.200	0.200
10% APS	0.050	10% APS	0.200	0.200
TEMED	0.005	TEMED	0.016	0.012

2.1.3.4 Gel Electrophoresis and Transfer

Protein lysates were thawed and pipetted into the wells of casted SDS-PAGE contained in a Mini-PROTEAN Tetra cell (Biorad, UK) filled with 1 X running buffer (250 mM Tris base, 1.9 M glycine, 0.1% SDS, deionised water up to 2 L were used to make a 10 X stock and stored at room temperature). The gel composition varied between 5% and 8% acrylamide, depending on the size of protein detected. Prosieve quadcolour protein marker (Lonza, UK) was used to determine protein size. The SDS-PAGE was electrophoresed at 4°C with an initial voltage of 45V, then 90V once the protein had entered the resolving gel. The gel was transferred onto a nitrocellulose membrane (Pall Corporation, USA) and transferred in 1 X transfer buffer (250 mM Tris base, 1.9M glycine, 0.05% SDS, 20% methanol (Sigma-Aldrich, UK) deionised water up to 2 L were used to make a 10 X stock and stored at room temperature) at 65V for 120 min at 4°C.

2.1.3.5 Protein detection

The proteins contained in the nitrocellulose membrane was stained with Ponceau S solution (Sigma-Aldrich, UK), then blocked with 5% skimmed milk (Sigma-Aldrich, UK) in 1 X Tris-buffered saline (TBS) (made from a 10 X stock containing 200 mM Tris base, 1.4 M sodium chloride and deionised water, pH 7.6) containing 0.1% Tween-20 (Sigma-Aldrich, UK) (TBST) for 30 min. The blots were then incubated with the appropriate primary antibodies (Table 2.2) overnight at 4°C in 1 X TBS containing 0.05% sodium azide (Sigma-Aldrich, UK) and 5% BSA. The BRCA1 primary antibody was diluted in 1 X TBS containing 0.05% sodium azide and 5% skimmed milk powder (Sigma-Aldrich, UK). The next day, the blots were washed three times in 1 X TBS containing 0.1% Tween20 (TBST, Sigma-Aldrich, UK) for 10 min per wash and probed

with the appropriate secondary antibody listed in Table 2.2. (α-rabbit-HRP, α-mouse-HRP: Cell Signaling, UK; α-goat-HRP, Santa Cruz Biotechnology Inc.,UK) at a dilution of 1:10000 for 1 hr at room temperature. The blots were washed a further three times in 1 X TBST for 10 min per wash. Protein expression levels were detected by incubation of the blots in Lumminata Forte western HRP substrate (Millipore, UK) for 5 min, followed by detection by film.

Table 2.2. Immunoblotting primary antibody dilutions and secondary antibody species specification

Primary Antibody	Primary antibody dilution	Primary antibody Supplier	Secondary antibody species	Predicted Molecular Weight (kDa)
ATM	1:5000	07-1286, Millipore, UK	rabbit	350
ATR	1:10,000	A300-138A, Bethyl Laboratories, UK	rabbit	300
BRCA1	1:500	sc-642, Santa Cruz, UK	rabbit	220
INPP4B	1:1000	#8450, Cell Signaling, UK	rabbit	110
PTEN	1:1000	sc-6817-R, Santa Cruz, UK	rabbit	55
Akt, 1/2	1:1000	sc-1619, Santa Cruz, UK	goat	55
Erk 1/2	1:1000	#4695, Cell Signaling, UK	rabbit	42, 44

2.2 Chapter 3 materials and methods

The methods below represent all the methods used in chapter 3 ('Establishment of a DNA repair defect in ovarian cancer cells').

2.2.1 Microarray

The microarray and bioinformatics analyses were conducted by Dr. George Pouligiannis (Harvard University, USA) and the methods used are described here for completeness of study. The MCF-10A human mammary epithelial cell line was infected with a retroviral shRNA against either *INPP4B* or *Renilla luciferase* vector control and each microarray experiment was performed in triplicate. Total RNA samples were isolated using the RNeasy mini kit (Qiagen, UK) and hybridised according to the standard protocol for Affymetrix U133 Plus 2.0 arrays at the Beth Israel Deaconess Medical Centre Genomics and Proteomics Core (USA). Data pre-processing and quality control were performed in R (http://www.r-project.org/) and Bioconductor. Prior to any statistical computation, data were normalised using the gc-Robust Multi-array Average algorithm. The differentially expressed genes were computed by an empirical Bayes shrinkage of the standard errors toward a common value approach embedded within the Limma package (Smyth, 2004). P – values were adjusted for multiple comparison using the false discovery rate approach implemented by Benjamini & Hochberg (Klipper-Aurbach et al., 1995).

2.2.2 RT-PCR

2.2.2.1 RNA extraction

Purification and isolation of RNA from cells was performed with the RNeasy Mini kit (Qiagen, UK) using the supplemented protocol.

2.2.2.2 DNase I digestion

Extracted RNA was digested with DNase I (Thermo Scientific, UK). 20 µg RNA, 20 µl 10 X reaction buffer, 20 U RNase-free DNase I and deionised water was added into a microcentrifuge tube and incubated at 37°C for 30 min. 20 µl of 50 mM EDTA was added to the solution and further incubated at 65°C in a heatblock for 10 min. The final concentration of the RNA was diluted to 100 ng/µl and the RNA was stored at -20°C. The resulting digested RNA was used as a template for reverse transcription.

2.2.2.3 cDNA reverse transcription

Single-stranded cDNA was obtained from the DNase I digested RNA by reverse transcription using the High Capacity cDNA Reverse Transcription Kit (Applied Biosystems, UK), adhering the supplemented protocol. The cDNA was stored at -20°C until further use.

2.2.2.4 qPCR

Real-time polymerase chain reaction (qPCR) was conducted using the Maxima SYBT Green/ROX qPCR Master Mix (2X) (Thermo Scientific, UK) according to the supplemented protocol. 1 µl of cDNA template and 200 ng of primer were used for the qPCR reaction mix composition. The reaction was run according to the following

conditions: 1 cycle of 10 min initial denaturation at 95°C; 40 cycles of 15 sec denaturation at 95°C and 30 sec annealing/extension at 60°C. Primers used are listed in table 2.3.

Table 2.3. Primers used for qPCR

	Amplicon Size	Sequence (Forward/Reverse)	Tm°	Location
ANKRD35	150	GCAGGCGTGCGATCTATCAT	62.5	1429-1448
		GCTGTCGTTGTCTGAGATGTTC	61.2	1578-1557
CA2	92	ATCACTGGGGGTACGGCAA	58.8	19 - 41
		TGTATGAGTGTCGATGTCAACAG	58.9	111 - 89
MPDZ	108	TGTCCAGCTAGTTATTGCCAGA	58.5	645 - 666
		GTGAACCGGATTAGAGTGAGC	59.8	753 - 755
TFPI	110	AGCCTTTTTGAATTTCACGGTCC	58.9	619 - 641
		GCGGCATTTCCCAATGACT	56.7	729 - 711
C5ORF13	118	GTCTGGGTCAGTCAAGAACCA	61.3	127-147
		AGGCAGCGTTTGTCTCATCG	62.8	244-225
β-actin	250	CATGTACGTTGCTATCCAGGC	60.8	393-413
		CTCCTTAATGTCACGCACGAT	60.2	642-622
CA12	100	ATCTTAAAGGAACAGCCTTCCAG	58.9	46 - 68
		GACGGGTACTTCTTGGACCA	59.4	146 - 127
SPARC	104	AGCACCCCATTGACGGGTA	58.8	719 - 737
		GGTCACAGGTCTCGAAAAAGC	59.8	823 - 803
GALNT7	137	GGTTCATCTTACGCAGTTTGCT	58.4	17 - 39
		GCATGGGGTCATTGACATCTC	59.8	154 - 134
NTN4	119	GAGTAGCTGGAGTGAGTTCCC	61.3	65-85
		GTACAGTTCGGTAGCATTCTGAC	60.7	183-161
GPC1	118	CCCTGCCCTGACTATTGCC	62.1	799-817
		CCCAGAACTTGTCGGTGATGA	61.7	916-896
CAMK2N1	67	GAGCAAGCGGGTTGTTATTGA	60.9	156-176
		TGCCTTGTCGGTCATATTTTTCA	60.5	222-200
TMEM98	151	GAAGACTGGATCGAAGATGCC	60.2	241-261
		CCACAATGATGTCGCTGACAC	61.6	391-371
INPP4B	156	CCCTGACATTTGTGCTCCTT	64.0	1802-1821
		GGAAGCCTGGGTCATACAGA	64.0	1957-1938

2.2.3 Comet assay

2.2.3.1 Preparation of samples for dose response curves and DNA repair curves

175,000 cells per well were seeded in a 6-well plate (BD Falcon, UK) and allowed to adhere overnight at 37°C. The cells were trypisised and resuspended with growth media to a final volume of $2.5x10^4$ cells per ml. For dose response experiments, the cells were irradiated with 15, 25 and 30 Gy X-ray using the A.G.O. HS 321 kV X-ray system. For the establishment of DNA repair curves, the cells were irradiated with 30 Gy X-ray. Untreated samples were kept on ice. The cells were allowed to recover 0, 15, 30, 45, 60 and 90 mins after irradiation at 37°C. At the specified time points, the cells were centrifuged at 300 g for 5 mins, media aspirated and cells thoroughly resuspended in freezing media containing FBS with 10% DMSO. The cells were frozen at -80°C for a minimum of 24 hrs.

2.2.3.2 Electrophoresis and staining

Cells were prepared as indicated above. All of the following steps were carried out on ice. Frozen cells were thawed and resuspended into a cell suspension of $2.5x10^4$ cells per ml in growth media. Cells were resuspended in 1 ml of molten 1% low-gelling-temperature agarose type VII (Sigma Aldrich, UK) and pipetted onto duplicate slides pre-coated with 1% type 1-A agarose (Sigma-Aldrich, UK). The cells were lysed in lysis buffer (100 mM disodium EDTA, 2.5 M sodium chloride, 10 mM pH 10.5 Tris-HCl) containing 1% triton X-100 on ice for 1 hr in the dark. Under dark conditions, the cells were then washed in distilled water every 15 min for 1 hr, incubated in ice-cold alkali buffer (50 mM sodium hydroxide, 1 mM pH 12.5 disodium EDTA) for 45 min and then electrophoresed for 25 min at 18V (0.6 V/cm), 250 mA. The slides were rinsed

once in neutralising buffer (0.5 M Tris-HCl, pH 7.5), once in 1 X PBS and left to dry overnight. The following day the slides were rehydrated with distilled water, stained with 2.5 μg/ml propidium iodide solution (Sigma- Aldrich, UK), rinsed again in distilled water and placed at 37°C until dry.

2.2.3.3 Data analysis

The comets were visualised by a Nikon inverted microscope with a super high pressure mercury lamp using a 580 nm dichromic mirror, 510 – 560 nm excitation filter and 590 barrier filter for propidium iodide staining. Measurements were taken by the KOMET version 6.0 software from Andor Technology. In total, 50 cells per sample (25 cells per slide) were analysed. Experiments were conducted independently three times in duplicates.

2.2.4 Immunofluorescence assay

2.2.4.1 Cell seeding and genotoxic treatment

2.5 x 10^4 and 3.5 x 10^4 of Ovca429 and Ovca433 knockdown cell pools, respectively, were seeded in 8 well chamber slides (PAA Laboratories Ltd., UK) and grown overnight at 37°C. The cells were then exposed to genotoxic stress under the following conditions: 2 Gy x-ray irradiation for γH2AX and 53BP1 detection; 10 Gy x-ray irradiation for RAD51 and BRCA1 foci detection; 1 hr incubation of 1 μM etoposide (Sigma-Aldrich, UK) for γH2AX and 10 μM etoposide for 53BP1 and RAD51 foci formation.

2.2.4.2 Foci detection

After treatment, the cells were incubated at 37°C to allow for DNA repair and the cells fixed at the following time points after DNA damage exposure: 0 hr, 30 min, 60 min, 180 min, 4 hrs, 8 hrs, 24 hrs, 48 hrs and 72 hrs. The cells were fixed in 4% paraformaldehyde (Alfa Aesar, UK) for 10 min, permeabilised for 10 min in 0.5% Triton X-100, and blocked in 10% normal goat serum (Invitrogen, UK) for 1 hr at room temperature. The slides were incubated with the appropriate primary antibody (Table 2.4) overnight at 4°C on a rotator, washed three time with 1 X PBS containing 0.1% Tween-20 (PBST) for 10 min each, and incubated with Alexa Fluor 488-conjugated goat α-rabbit or α-mouse secondary antibody (Invitrogen, UK) for 1 hr at room temperature in the dark. From this point forward, all methods were conducted in the dark. Cells were washed twice in 1 X PBST and once in 1 X PBS for 10 min each and mounted using EverBrite Mounting Medium with DAPI (Biotium, UK). Fluorescence images were captured with inverted microscope Zeiss Axio Observer Z1 (Zeiss) and visualised using AxioVision 4.8.2.0 software. At least images of 50 cells per condition were captured and foci counted manually by eye. Experiments were conducted independently three times. The antibodies used for immunofluorescence studies are listed in table 2.4.

Table 2.4. Immunofluorescence antibody dilutions

Primary Antibody	Primary antibody dilution	Primary antibody Supplier	Secondary Antibody	Secondary antibody dilution
53BP1	1:500	#4937, Cell Signaling, UK	rabbit	1:1000
BRCA1	1:500	sc-642, Santa Cruz, UK	rabbit	1:1000
H2AX	1:500	05-636, Millipore, UK	mouse	1:1000
RAD51	1:500	sc-8349, Santa Cruz, UK	rabbit	1:1000

2.2.5 Cell cycle analysis

2.2.5.1 Treatment conditions

Ovca433 parental and knockdown cell lines were seeded at a cell density of 5.0 x 10^4 cells per 100 mm plate, respectively, and allowed to adhere overnight at 37°C. To assess basal levels of cell cycle progression, cells were serum starved by the addition of RPMI media containing 2 mM L-glutamine and left to incubate for a further 18 hrs, before being replenished with growth media containing 10% FBS.

2.2.5.2 Sample Fixation

Cells were trypsinised, counted and 1x10^6 cells were centrifuged at 300 x g for 5 min, washed in 1 X PBS, further centrifuged at 300 x g for 5 min and resuspended in 50 μl of 1 X PBS. The resuspended cells were added drop-wise into 1 ml 70% absolute ethanol while being vortexed at a medium speed. The cells were frozen at -20°C for a minimum of 3 hrs prior to staining.

2.2.5.3 Staining and analysis

The cells were thoroughly resuspended and 200 μl of ethanol-fixed cells were added to a 12 x 75 mm polystyrene tube (BD Biosciences, UK). The cells were centrifuged at 300 x g for 5 min, washed in 500 μl 1 X PBS, further centrifuged at 300 x g for 5 min, and resuspended in 200 μl of staining solution (7.5 μg/ml propidium iodide, 20 μg/ml RNase A (Sigma-Aldrich, UK), 0.01% Triton-X, 0.05% sodium azide, stored in the dark at 4°C). The cells were incubated for 30 min in the dark at room temperature before being analysed on the Muse Cell Analyser (Millipore, UK). The gate settings were adjusted as depicted in figure 2.4.

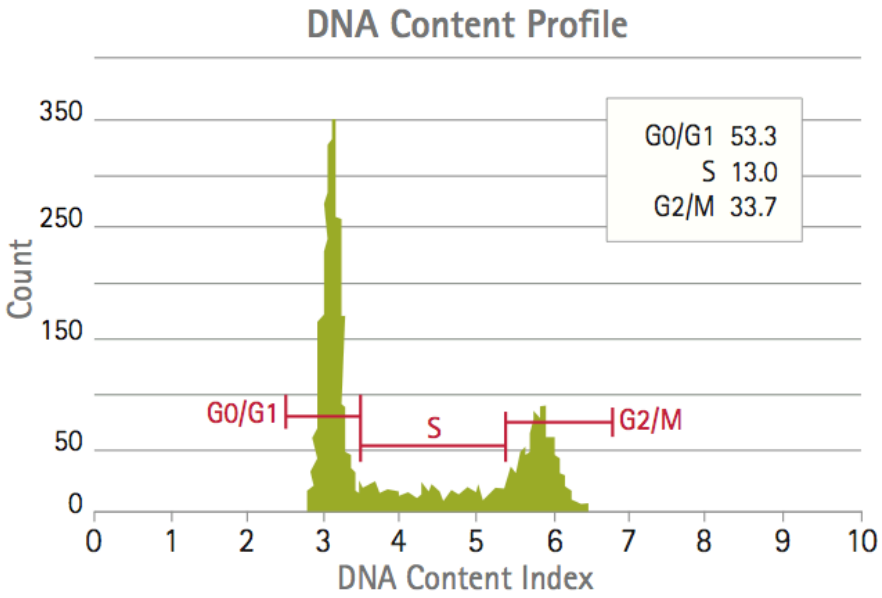

Figure 2.4. Example of gate settings for the MUSE cell sample analyser. Propidium iodide, staining of nuclear cellular content distinguish cells at different stages of the cell cycle, which differ in DNA content. Resting cells (G0/G1) contain two copies of each chromosome. As cells begin cycling, they synthesise chromosomal DNA (S phase). Fluorescence intensity from the DNA intercalating dye, propidium iodide, increases until all chromosomal DNA has doubled (G2/M phase). At this state, the G2/M cells fluoresce with twice the intensity of the G0/G1 population. The G2/M cells eventually divide into two cells. The assay thus utilises the differential staining of cells based on DNA content. Image source: http://www.emdmillipore.com/GB/en/product/Muse®-Cell-Cycle-Assay-Kit,MM_NF-MCH100106#overview

2.3 Chapter 4 materials and methods

The methods below represent all the methods used in chapter 4 ('Biological function of INPP4B').

2.3.1 Immunoprecipitation

293T cells were transiently transfected with 25μg pcDNA3-FLAG empty vector or peak-FLAG-INPP4B vector, as described in section 2.1.1.6. The lysates were incubated with 10 μl anti-FLAG M2 beads (Sigma-Aldrich, UK) for 2 hrs on a rotator at 4°C. The beads were spun down at 5000 rpm at 4°C for 1 min, then allowed to settle for 2 min on ice. The supernatant was carefully removed, ensuring no beads are removed. The beads were washed by the addition of 1 ml ice cold 1 X TBST, the closed microcentrifuge tube inverted several times, and centrifuged at 2,300 x g at 4°C for 1 min. This washing procedure was repeated twice in 1 X TBST and once in 1 X TBS. After removing the supernatant from the last wash, the immunoprecipitated complexes were eluted from the beads by the addition of 8 μl 5 X sample buffer. The beads in sample buffer was vortexed briefly, incubated at 95°C for 5 min and centrifuged at 16,000 x g for 2 min at room temperature. The immunoprecipitated complexes were analysed in a 5% acrylamide SDS-PAGE by immunoblotting, as described in section 2.1.3. Primary antibodies used were as follows: α-BRCA1, α-ATR, α-ATM, α-INPP4B, α-PTEN (see table 2.2. for dilutions and supplier).

2.3.2 MEF experiments

INPP4B$^{fl/fl}$ MEFs were infected with Adenovirus Cre recombinase ($1x10^3$pfu/ml, $1x10^4$pfu/ml, $1x10^5$pfu/ml, $1x10^6$pfu/ml Ad5CMVCre-eGFP, Gene Transfer Vector Core, University of Iowa, USA) overnight. 10 ml of the appropriate cell line growth media was added to the virus supernatant and allowed to incubate overnight at 37°C. The next day, the virus and media mixture was aspirated and replaced with 10 ml of regular growth media. Protein quantification was conducted following the protocol in section 2.1.3. Primary antibodies used were as follows: α-BRCA1, α-ATR, α-ATM, α-INPP4B (see table 2.2. for dilutions and supplier).

2.3.3 GST pull down assay

2.3.3.1 Generation of INPP4B fragments and preparation of entry and expression vectors

Fragments of INPP4B were generated by using pEAK FLAG-INPP4B as a template, as shown in figure 2.5. Primers (Eurofins MWG Operon, Germany) are listed in table 2.5. Polymerase chain reactions (PCR) were conducted using the Novagen KOD Hot Start DNA Polymerase (Millipore, UK) in a TProfessional Basic Gradient Thermocycler (Biometra, Germany). A high fidelity polymerase was used to ensure amplification the correct DNA sequences. 100 ng of pEAK INPP4B template and 200 ng of primer were used for the PCR reaction mix composition, along with the reaction components and volumes listed in the manufacturer's supplemented protocol, for a total reaction volume of 50 μl. The reaction was run according to the following conditions to generate the middle INPP4B fragment: 1 cycle of 2 min polymerase activation at 95°C; 30 cycles of 20 sec denaturation at 95°C, 30 sec annealing at 63°C and 2 min extension at 70°C; 1

cycle of 3 min of final extension at 70°C. Due to the differing annealing temperatures of the primer pairs, for the N-terminal and C-terminal INPP4B fragments, the PCR reaction was conducted in a multi-step gradient fashion as follows: 1 cycle of 2 min polymerase activation at 95°C; 30 cycles of 20 sec denaturation at 95°C, 30 sec annealing at 53 - 67°C, with 2 cycles conducted per temperature every 2 degrees, and 2 min extension at 70°C; 1 cycle of 3 min of final extension at 70°C. The PCR product was stored at 4°C until further use. The pENTR1A entry vector and the pGEX-KG expression vector were generous gifts from Dr Pablo Rodriguez (UCL, UK). Isolation and purification of the DNA plasmids were obtained as described in section 2.1.2.2.

Table 2.5. Primers used for amplifying INPP4B fragments

Primer	Sequence (5' → 3')	Tm°
INPP4B_1_aa_S sense primer	CCGTCGACATGGAAATTAAAGAG	58.9
INPP4B_460_aa_AS antisense primer	AAGCGGCCGCGGCATGTACAAAAAG	66.3
INPP4B_460_aa_S sense primer	CCGTCGACATGGAAAAAACAGAG	60.6
INPP4B_925_aa_AS antisense primer	AAGCGGCCGCTTAGGTGTCAGC	65.8
INPP4B_200_aa_AS antisense primer	AAGCGGCCGCATCTGTGGTGAT	64.0
INPP4B_200_aa_S sense primer	CCGTCGACATGGTACAGGGACAA	64.2
INPP4B_760_aa_AS antisense primer	AAGCGGCCGCAAACCTTTCAGC	64.0
INPP4B_760_aa_S sense primer	CCGTCGACATGGGAGATGTCTCT	64.2

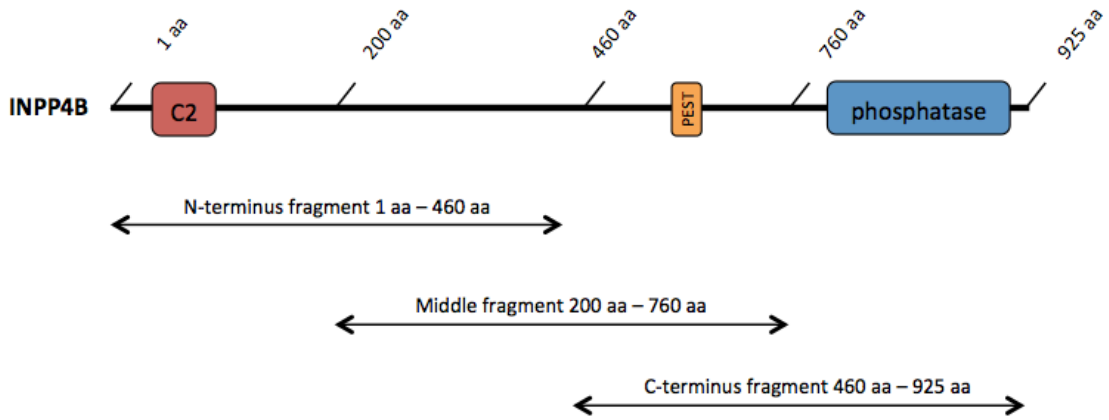

Figure 2.5. INPP4B fragments. pEAK FLAG-INPP4B was used as a template to generate three different INPP4B fragments by PCR: N-terminus fragment constituting 1 – 460 aa of INPP4B; Middle fragment constituting 200 – 760 aa of INPP4B; C-terminus fragment constituting 460 – 925 aa of INPP4B.

2.3.3.2 Cloning of INPP4B fragments into pENTR1A entry vector

The PCR product and digested entry vector were purified using the Nucleospin Extract II kit (Macherey Nagel, Germany) according to the supplemented protocol. The purified PCR product was then digested using restriction enzymes Sal I and Not I (New England Biolabs, UK) with the following reaction constituents: 200 µl purified PCR product, 2 µl Sal I (100,000 U/ml), 2 µl Not I (50,000 U/ml), 21 µl distilled H2O, 25 µl 10X restriction enzyme buffer 3.1 (New England Biolabs, UK). The reaction mixture was gently mixed and incubated overnight in a 37°C waterbath. The digested products were subjected to electrophoresis at 70V in a 1% agarose gel (1% w/v agarose (Sigma-Aldrich, UK), 1 X Tris Acetate EDTA (TAE) buffer (40 mM Tris-base, 20 mM glacial acetic acid (VWR Chemicals, UK), 1mM EDTA) alongside the peqGOLD 1kb DNA ladder (Peqlab, UK). Once the product was sufficiently run out, the bands were visualised on a UVIvue BTX 20M 312nm Transilluminator (Uvitec, UK), excised at the correct molecular weight and the gel purified using the Nucleospin Extract II kit (Macherey Nagel, Germany), according to the manufacturer's protocol. Similarly, the pENTR1A vectors were digested as follows: 10 µg DNA plasmid, 2 µl Sal I, 2 µl Not I, and the appropriate amount of distilled H_2O and 10X restriction enzyme buffer 3.1 (New England Biolabs, UK) to a total volume of 50 µl. As above, the digested product was electrophoresed at 70V in a 1% agarose gel, excised, purified, and stored at -20°C until further use. The sticky ends of the INPP4B fragments and pENTR1A vector formed, as a result of the restriction enzymes used, were ligated with T4 DNA ligase (New England Biolabs, UK) using 1 µg INPP4B fragment PCR product, 10 µg pENTR1A vector, 1 µl T4 ligase (400,000 U/ml), 5 µl 10X T4 DNA ligase reaction buffer and distilled water to a total volume of 50 µl. The reaction mix was gentle mixed by swirling, incubated at room temperature for an hr and concentrated using the

Vacufuge basic concentrator (Eppendorf, UK) to reduce the volume to approximately 20 µl. 10 µl of the concentrated ligation mixture was added into 50 µl gold efficiency α-select competent cells (Bioline, UK), and transformed as described in section 2.1.2. using LB-kanamycin agar plates. Positive colonies were selected and inoculated in a bacteria culture, the DNA isolated and purified, and checked for correct insertion size by digestion and visualisation on a 1% agarose gel.

2.3.3.3 LR recombination reaction

The INPP4B fragments inserted in the pENTR1A entry vector was transferred to destination vector pGEX-KG using the Gateway LR Clonase II Enzyme Mix (Invitrogen, UK) to catalyse the reaction. The reaction was set up with 400 ng entry clone, 300 ng destination vector, 4 µl 5 X clonase reaction buffer and Tris-EDTA (TE) buffer pH 8.0 up to a volume of 16 µl, and carried out according to the manufacturer's supplemented protocol. The LR reaction was transformed as described in section 2.1.2.2 and plated on LB-ampicillin agar plates to select for the ampicillin-resistant pGEX-KG plasmids. Positive colonies were selected and cloned, the DNA isolated and purified, and checked for correct insertion size by digestion and visualisation on a 1% agarose gel.

2.3.3.4 Purification of GST-tagged recombinant proteins

The colonies with the correct insertion size was transformed in *E. Coli* BL21 (Promega, UK) for maximal GST-tagged protein expression. The positive colonies were selected, inoculated in a 20 ml LB-ampicillin pre-culture and grown overnight in a 37°C incubated shaker. 5 ml of the densely grown culture were added to 200 ml ampicillin

LB-broth per fragment, and grown in the 37°C shaken until the culture reached an OD_{600} of 0.6 – 1.0. Desired GST protein expression was induced adding 0.1 mM Isopropyl β-D-1-thiogalactopyranoside (IPTG) (Thermo Scientific, UK) and cultured for an additional 3 hrs at 37°C in the shaker. The bacteria were pelleted by centrifugation at 3500 x g for 10 min at 4°C, resuspended in ice-cold PBS lysis buffer (1% Triton-X and protease inhibitors from Roche tablets in 1 x PBS), at a volume of 4 ml PBS lysis buffer per 200 ml bacteria culture. The bacterial suspension was sonicated on ice with 3-5 cycles of 10 sec sonication, followed by 10 sec rest. The sonicated lysate was pelleted again by centrifugation at 12,000 x g for 15 min at 4°C and the supernatant transferred to a fresh 15 ml falcon on ice.

2.3.3.5 Pull down of GST-tagged proteins

Glutathione Sepharose Fast Flow (GE Healthcare Life Sciences, UK) beads were precleared overnight on a rotator at 4°C in 5% skimmed milk in PBS lysis buffer; the beads were washed once in PBS lysis buffer and stored in a 1:1 slurry with PBS lysis buffer. Per 1 ml lysate used for each INPP4B fragment 250 μl of 1:1 sepharose bead slurry was added, and the beads were incubated at 4°C on a rotator for 2 hrs. A negative control was included by incubating the sepharose beads in PBS lysis buffer containing 5% skimmed milk. The lysate was centrifuged at 750 x g for 1 min at 4°C to pellet the beads, supernatant removed and beads washed once in 1 ml ice cold PBS lysis buffer, centrifuged again to pellet the beads, and incubated with FLAG-ATR lysate for 30 min at 4°C on a rotator (293T cells were transiently transfected with 25 μg pcDNA3.1 FLAG-ATR vector and lysed as described in section 2.1.1.6). The FLAG-ATR lysate was removed by centrifugation, and the beads washed three times in ice cold PBS lysis

buffer, before being eluted in 40 μl of 6 X sample buffer. Immunoblotting was carried out as described in section 2.1.3. Antibody detecting ATR (Bethyl Laboratories, UK; 1:10,000 primary antibody dilution) was used to detect interaction of ATR with GST-tagged INPP4B fragments. Input lanes were also detected and represents 1% of protein lysates in pulldown assays.

2.4 Chapter 5 materials and methods

The methods below represent all the methods used in chapter 5 ('Treatment of INPP4B deficiency with DNA repair inhibitors').

2.4.1 Drug handling and storage

10 mg of olaparib (KU-0059436, Selleck Chemicals, UK) was resuspended in DMSO to a stock concentration of 10 mM. Etoposide (Sigma-Aldrich, UK) was resuspended in DMSO to a stock concentration of 50 mM. Chk 1 inhibitors (LY2603618 and LY2940930, Eli Lilly, UK) was resuspended in DMSO to a stock concentration of 10 mM. Cisplatin (Teva UK Limited, UK) was generously provided by Dr. Victoria Spanswick (UCL, UK) in a 3.3 mM aqueous solution. Cisplatin was stored in the dark at room temperature. The remaining drugs were stored in 50 μl aliquots and stored at -20°C.

2.4.2 Cell proliferation assay

3000 and 4000 cells per well of Ovca429 and Ovca433 knockdown cell pools, respectively, were seeded in triplicates per condition in a 96-well plate (BD Falcon, UK) and grown overnight at 37°C. The cells were treated with drugs diluted in growth media in a range of concentrations as follows: Olaparib – 1 μM, 5 μM, 10 μM, 25 μM, 50 μM and 100 μM; LY2603618 – 250 nM, 500 nM, 750 nM, 1 μM, 5 μM, 10 μM and 25 μM; LY2940930 – 50 nM, 100 nM, 500 nM, 500 nM, 1 μM, 5 μM, 10 μM and 50μM. DMSO was used as a control. 24 hrs after seeding the cells, the cells were treated with drugs for 72 hrs. AlamarBlue (Thermo Scientific, UK) was used as a cell viability indicator to indirectly measure cell proliferation (metabolic readout). It uses

the natural reducing power of living cells to convert resazurin to the fluorescent molecule, resorufin. Resazurin is a nontoxic, cell permeable compound that is blue in color and virtually nonfluorescent. Upon entering cells, resazurin is reduced to resorufin, which produces very bright red fluorescence. Viable cells continuously convert resazurin to resorufin, thereby generating a quantitative measure of viability—and cytotoxicity. Fluorescence was measured by a spectrophotometer at an excitation wavelength of 590 nm and emission wavelength of 560 nm between 3 – 6 hrs after the addition of AlamarBlue.

2.4.3 Clonogenic survival assay

1000 cells per well were seeded in triplicates in a 6-well plate (BD Falcon, UK) and grown overnight at 37°C. Experiments were conducted using single agent treatments and double agent treatments. Dual drug treatment of cisplatin and olaparib was administered by adding 10 μM cisplatin on day 1 for 2 hrs, followed by continuous 1 μM olaparib treatment for 6 days. Cisplatin was removed by aspirating the media containing the drug, and washing the cells with fresh media before pipetting the media containing olaparib into the wells. Continuous treatment of olaparib was replenished every 48 hrs with fresh drug and media. DMSO was used as a control. The cells were grown until colonies of 50 or more cells were established. The cells were washed with 1 X PBS and fixed and stained with 1 X PBS containing 6% Glutaraldehyde (Sigma-Aldrich, UK) and 0.5% Crystal Violet (Sigma-Aldrich, UK) for 2 hrs at room temperature. The dye was removed and the cells were washed with deionised water and left to dry overnight. The number colonies were counted manually by eye. Experiments were conducted independently three times in triplicates.

2.4.4 Xenograft experiments

The xenograft experiments were conducted by Dr. Christina Gewinner (UCL, UK). Ovca429 shRNA-Renilla luciferase and Ovca429 shRNA-INPP4B expressing cells were injected subcutaneously in female NOD/SCID mice ($1x10^7$ cells/animal, n=8 each cell pool). Tumours were grown until a 50 to $60mm^3$ tumour volume was reached, then animals were treated with 50mg/kg olaparib daily consecutively for 5 days followed by two days break for two weeks. Tumour occurrence and size as well as animal weight and health were evaluated. All animal studies were approved by the UCL Biological Services Ethical Review Committee and licensed under UK Home Office regulations and the Guidance for the Operation of Animals (Scientific Procedures) Act 1986 (Home Office, London, UK). Project licence number PPL 70/7134.

CHAPTER 3. Establishment of a DNA repair defect in ovarian cancer cells

3.1 Introduction

Aberrant DNA repair processing and/or dysfunctional cell cycle checkpoint results in a predisposition to developing cancer, as well as altered responses to anti-cancer therapies, namely DNA-damaging chemotherapy and radiotherapy. The loss of function of a DNA repair pathway may result in increased activation of other pathways as a compensatory mechanism, and can cause resistance to DNA-damaging therapies. Inhibitors of these pathways may re-sensitise tumours to these treatments. Conversely, tumours that harbour dysfunctional DNA repair mechanisms may benefit from targeted therapies against the faulty pathway, which render the DNA damage irreparable by way of synthetic lethality. Establishing DNA repair defects to identify alternate DNA repair pathways for therapeutic exploitation may therefore result in clinical benefit for patients harbouring these defects.

Loss of INPP4B is associated with tumourigenesis, radio-resistance, aggressive cancer sub-types and poor survival in a wide variety of tissue types. Reduced INPP4B expression has been found across a variety of ovarian cancer subtype, mostly in ovarian serous and endometrioid adenocarcinomas, as depicted in figure 3.1-3.2.

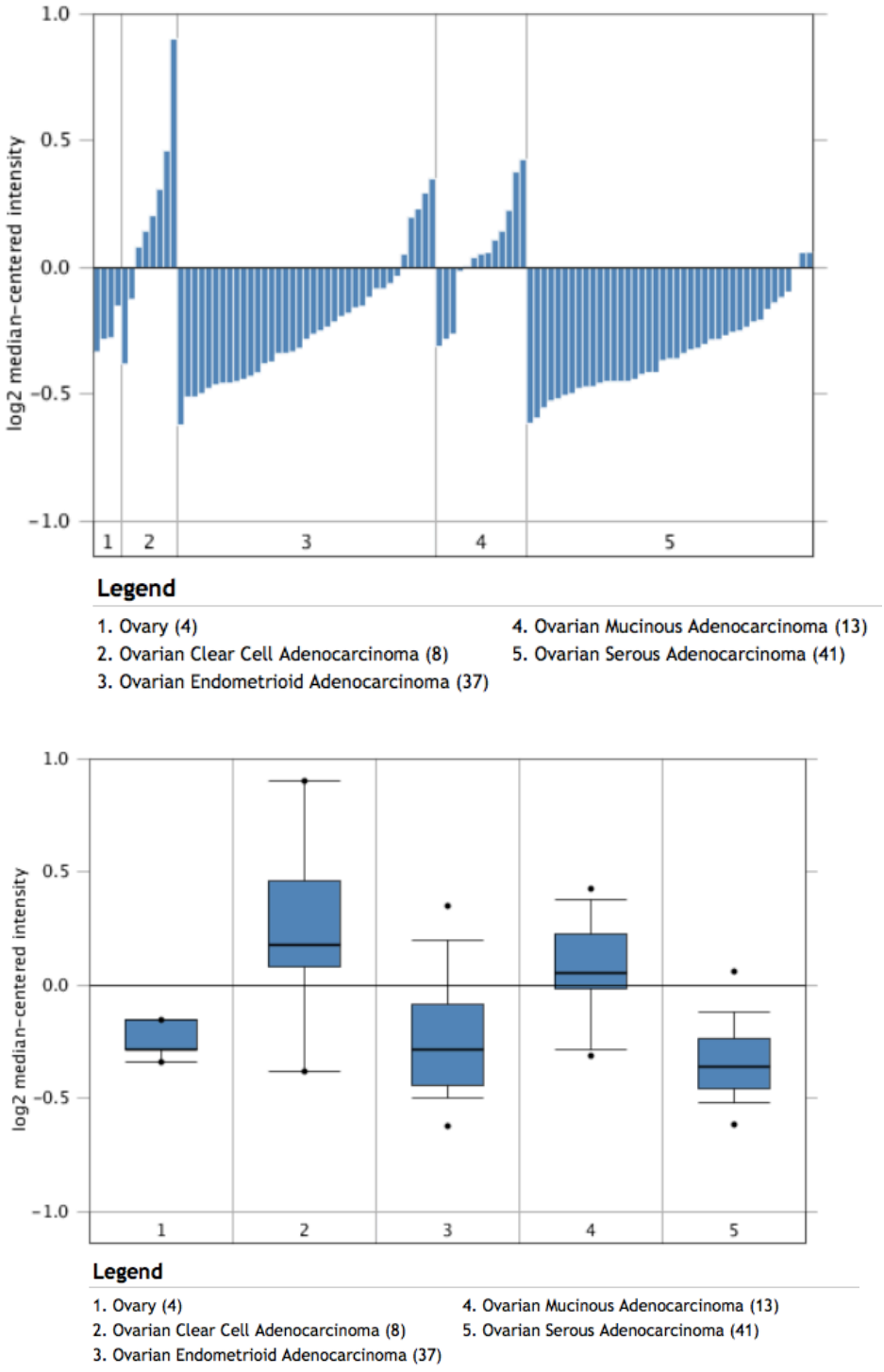

Figure 3.1. INPP4B expression across various ovarian cancer subtypes ('Hendrix Ovarian' dataset). Image source: www.oncomine.com depicting data from Hendrix et al. (Hendrix et al., 2006)

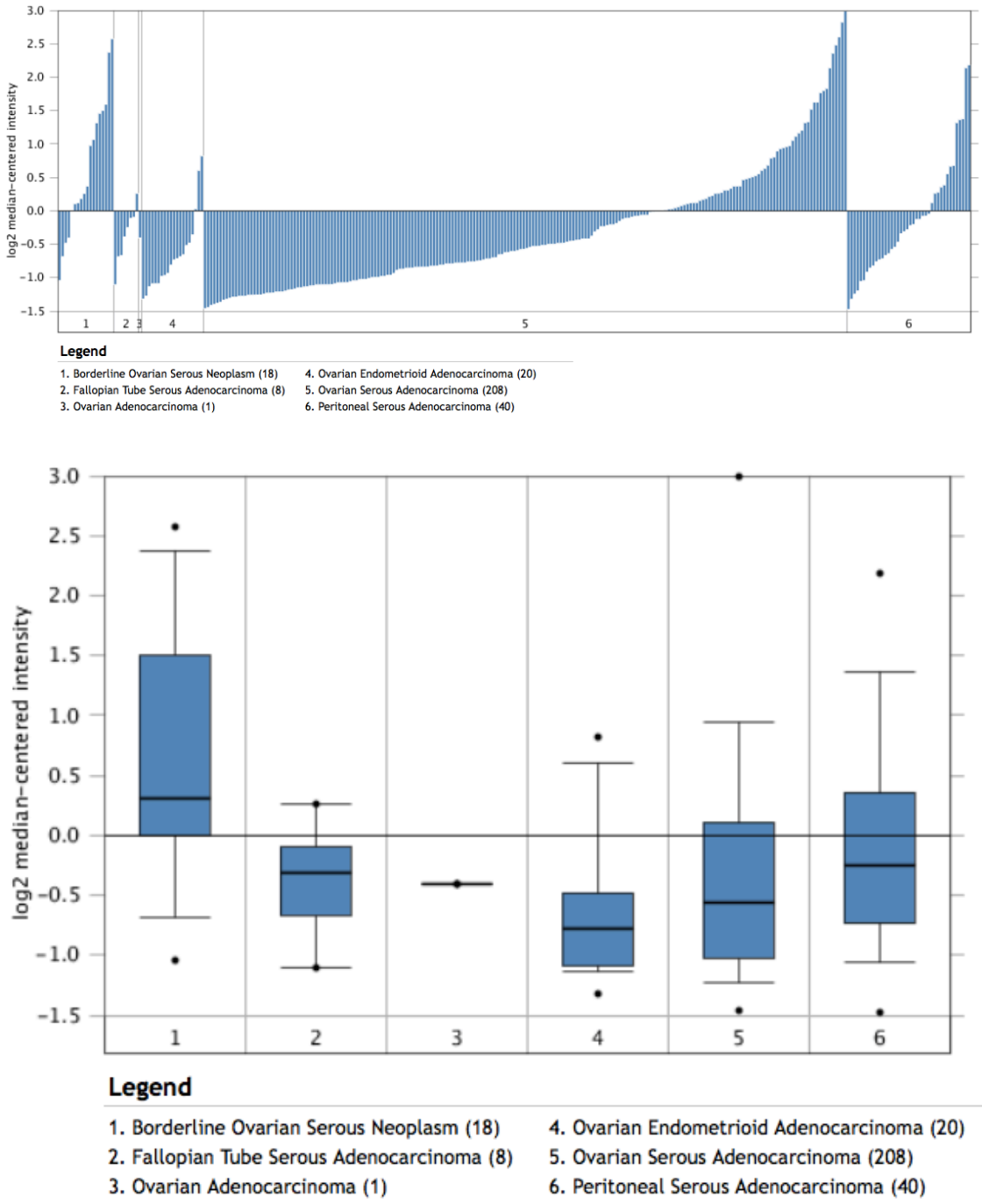

Figure 3.2. INPP4B expression across various ovarian cancer subtypes ('Tothill Ovarian' dataset). Image source: www.oncomine.com depicting data from Tothill et al. (Tothill et al., 2008)

However, validation of INPP4B in the context of DDR is yet to be reported in more detail in scientific literature. In order to further investigate and identify novel roles associated with loss of INPP4B, a microarray analysis was performed by Dr. George Pouligiannis (Harvard University, USA, current address: Institute for Cancer Research (ICR), London) and Dr. Christina Gewinner (UCL, UK). Stable knockdown cell pools expressing RNA hairpins against INPP4B or Renilla luciferase as a control were used to compare differential gene expression using the Affymetrix Human Genome U133 (HG-133) Plus array (Affymetrix, USA; appendix 1). Upon microarray analysis, BRCA1-mutant and poor survival gene signatures revealed in INPP4B deficient MCF-10A cells by microarray analysis**.** The full bioinformatics analysis of the microarray studies can be found in appendix 1 – 7.

Since BRCA1 mutations are a common occurrence in ovarian cancers, validation of the BRCA1 gene signature was conducted to assess the validity of the microarray findings. Data from each significant hit on the gene signature was collected from the microarray database, the protein functions researched and the hybridisation location for each probe was obtained. The primers used for qPCR experiments were selected from an established primer database (PrimerBank; http://pga.mgh.harvard.edu/primerbank/) such that they generated similar amplicon sizes, when available. To note, the hairpins used for this experiment were thoroughly tested for specificity and off-target effects (Gewinner et al., 2009; Westbrook et al., 2005). Knockdown cell pools of the MCF-10A cells were independently generated, and RNA carefully extracted. The RNA prepared for the microarray analysis was prepared in triplicates comprising sample preparations from two differently established knockdown cell pools and different RNA preparations. In addition to validation by qPCR, the microarray data were compared to a 60 gene

BRCAness gene signature defined by Konstantinopoulos et al. (Konstantinopoulos et al., 2010) to assess the gene signature by an alternative method.

The presence of a DNA-repair defect in the context of female-related cancers has great clinical implications due to the prevalence of BRCA1/2 mutations found in breast and ovarian cancers. With respect to ovarian tumours, *BRCA1/BRCA2* germline mutations represent up to 15% of high grade serous ovarian carcinomas (HGSC), and mounting evidence is pointing to a larger proportion of patients whose tumour biology reflects the 'BRCAness' phenotype. The 'BRCAness' phenotype has been defined by Chalasani et al. to be the phenotype of deficient BRCA function (Chalasani and Livingston, 2013). Muggia et al. further defines 'BRCAness' to include sporadic mutations and epigenetic alterations of the BRCA genes themselves, as well as other genes that contribute to a functionally deficient BRCA phenotype (Muggia and Safra, 2014). 5 – 31% of sporadic epithelial ovarian cancers (EOCs) exhibit dysfunctional BRCA1 through *BRCA1* promoter methylation (Baldwin et al., 2000; Esteller et al., 2000; Geisler et al., 2002). Amplification of *EMSY*, an inhibitor of BRCA2, was found amplified in 17% of sporadic ovarian tumours (Hughes-Davies et al., 2003). Defects in HR have been identified in up to 50% of EOC (CGARN, 2011), representing a large proportion of ovarian cancer patients which may benefit from treatment with therapies that target DNA repair.

Given the prevalence of 'BRCAness' found in ovarian tumours, in conjunction with the DNA repair defect identified in the microarray data upon loss of INPP4B, further investigations were carried out to examine the role of INPP4B in the context of DNA repair in ovarian cancer. For the assessment of DNA repair integrity and DNA damage

response (DDR) in relation to INPP4B loss, key experiments were conducted using comet assays and immunofluorescence assays. Comet assays, also known as single cell gel electrophoresis, is a tool to measure DNA damage in an individual cell. Initially developed by Ostling and Johanson in 1984 (Ostling and Johanson, 1984), and further modified a few years later by Singh et al. (Singh et al., 1988), the assay has the ability to identify broken DNA fragments through a series of procedures that involve lysis of agarose-embedded cells, gel electrophoresis, staining and microscopic analysis (described in detail in section 2.3.1). Lysis of the cells results in the removal of cellular membranes and release of soluble cell components, resulting in bare nucleoids remaining in the gel. The application of an electric field allows the migration of broken fragments of DNA, and damaged nucleoids can be visualised by propidium iodide staining. The resulting images can be divided into two parts: comet heads representing the intact DNA of a nucleiod, and comet tails representing broken fragments and damaged DNA "trailing" behind (figure 3.3). The olive tail moment is a measure of numerically assessing DNA damage by measuring percentage tail DNA and tail length and taking the product of these two values (Olive et al., 1990). Immunofluoresence assays were also conducted to assess the response of critical DNA repair proteins upon genotoxic stress. γH2AX has been commonly used as a marker of DSB through immunofluorescence assays that enable the visualisation and quantification of foci in individual cells (Kuo and Yang, 2008). RAD51 and 53BP1 are important DNA repair proteins involved in DSB repair in HR and NHEJ, respectively. In addition, cell cycle progression was investigated in INPP4B-deficient cells. DNA lesions activate checkpoint pathways that regulate specific DNA-repair mechanisms. The PI3K/Akt pathway has been implicated in the G1/S transition; Akt prevents cyclin D1 degradation

by regulating the activity of GSK3 (Diehl et al., 1998) and can negatively influence the expression of the CDK-inhibitor p27/kip1 protein (Shin et al., 2002).

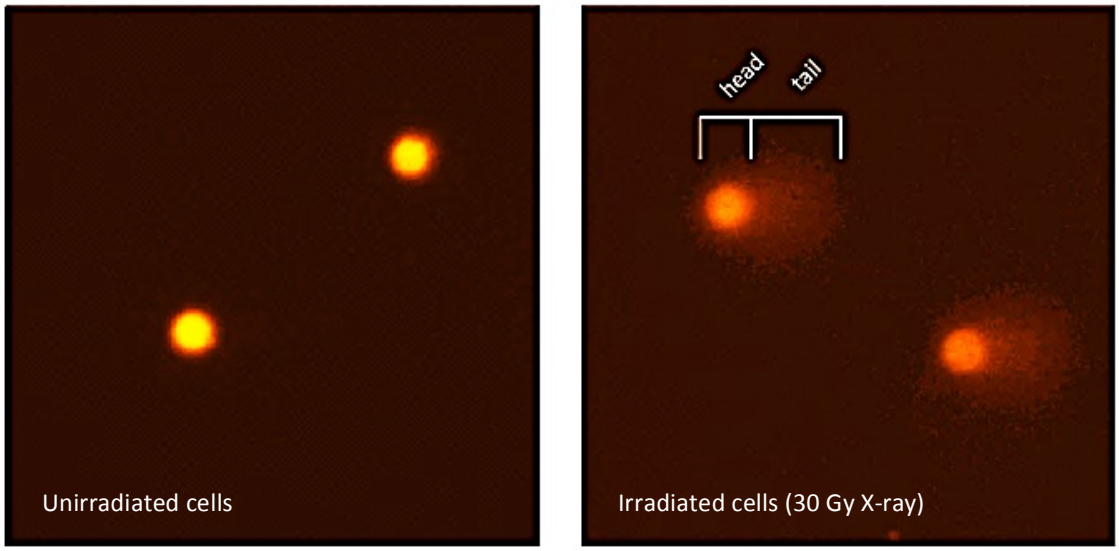

Figure 3.3. Comet head and comet tail images. The left image represents two nucleoids possessing no comet tails. The right image represents two nucleoids which possess a comet tail surrounding a comet head. The olive tail moment is calculated by multiplying the percentage tail DNA with the comet tail length. Cells used were Ovca433 (left image: unirradiated; right image: irradiated with 30 Gy X-ray) using the method details in 2.3.1.

A panel of ovarian cancer cell lines were obtained and characterised by assessing the protein expression levels of components of the PI3K/Akt pathway (INPP4B, PTEN and phospho-Serine 473 Akt), as well as activation of MAPK and mTOR pathways through phosphorylated p42/44 MAP kinases (phospho-p42/44) and phosphorylated ribosomal S6 (phospho-S6), respectively (figure 3.4). The characterisation of these cell lines was conducted by Dr. Christina Gewinner (UCL, UK). The PI3K/Akt pathway activation observed in the cell lines reflects the mutation/loss status of critical components in this pathway (PTEN or INPP4B loss, as well as *PIK3CA* mutations). From the ovarian cancer panel, epithelial cell lines Ovca429 and Ovca433 were selected for comparative experiments due to their robust protein expression of INPP4B and rapid growth rate. Knockdown cell pools of these cell lines were generated using shRNA hairpins directed against INPP4B and Renilla luciferase as a control (figure 3.5). Knockdown cell pools containing a heterogeneous population of cells that possess varying knockdown levels were purposely used to reflect tumour heterogeneity. Since knockdown of INPP4B diluted over time due to clonal selection shift, the cell pools were frequently re-derived and monitored for knockdown efficiency to guarantee reliability of experimental data. In general, a knockdown of 50% and more of reduced protein expression was generated for each knockdown cell pool generated. INPP4B knockdown in this study was achieved with the same retroviral hairpin directed against INPP4B as used in a study conducted by Gewinner et al. (Gewinner et al. 2009), where knockdown efficiency of 60% in two-dimensional studies pointed to a tumour suppressor function of INPP4B as well as a strong haploinsufficiency function of INPP4B. Furthermore, analyses of allelic loss of INPP4B in the cBioPortal for Cancer Genomics (MSKCC) and in collaboration with Dr. Andrea Richardson at Harvard University (Gewinner et al. 2009) resulted in only heterozygous loss of INPP4B in human epithelial tumours. Finally, Cre-

recombinase treatment of INPP4B$^{fl/fl}$ MEFs causing homozygous allelic deletion of INPP4B resulted in non-viability of these 'floxed' MEFs in long-term culture, suggesting that homozygous loss of INPP4B may be disadvantageous for cells and cells with haploinsufficiency have a growth advantage.

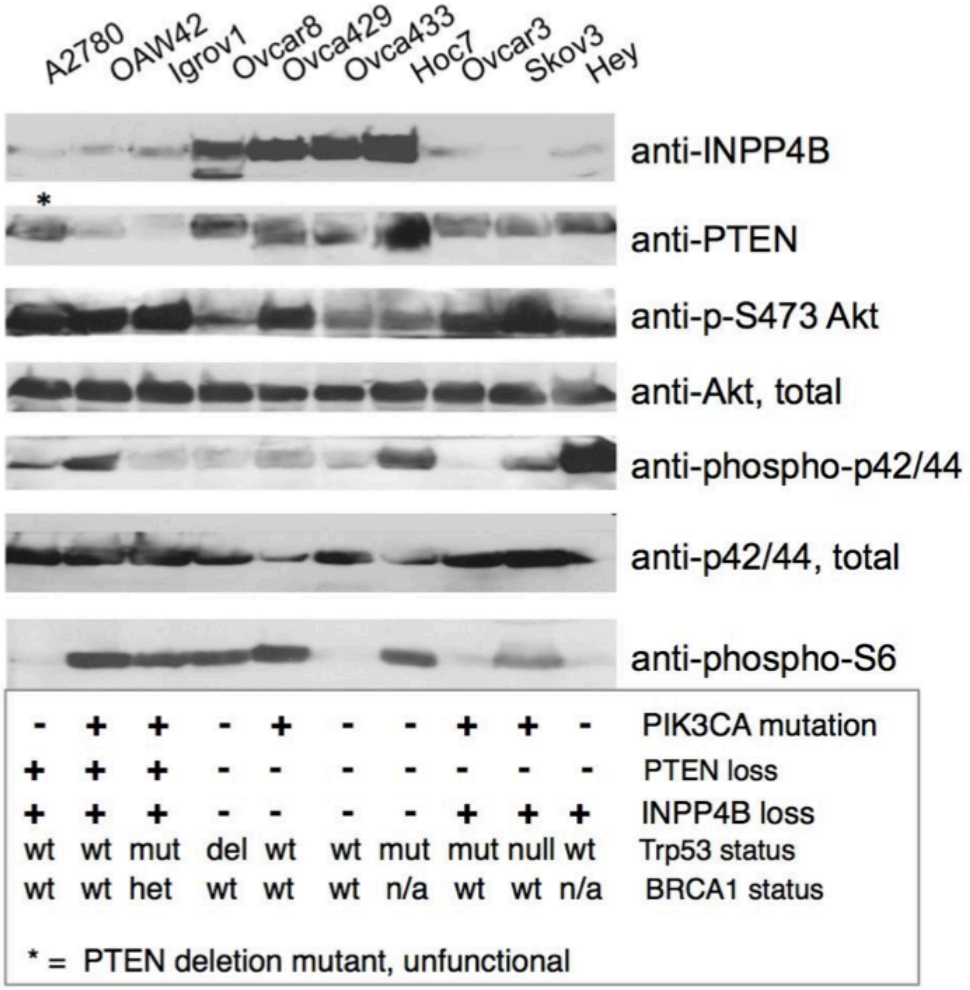

Figure 3.4. Characterisation of ovarian cancer cell lines. Immunoblotting of several ovarian cancer cell lines was performed to investigate protein expression levels and pathway activation of various components of the PI3K/Akt pathway and MAPK pathway. Protein expression levels of INPP4B, PTEN, pS473-Akt, total Akt, phosphor-p42/44, total p42/44 and pS6 were detected in ovarian cancer cell lines A2780, OAW42, Igrov1, Ovca429, Ovca433, Hoc7, Ovcar3, Skov3, Hey. In addition, *PIK3CA, Trp53,* and *BRCA1* mutation status are summarised. Cell line profiling was conducted by Dr. Christina Gewinner (UCL, UK).

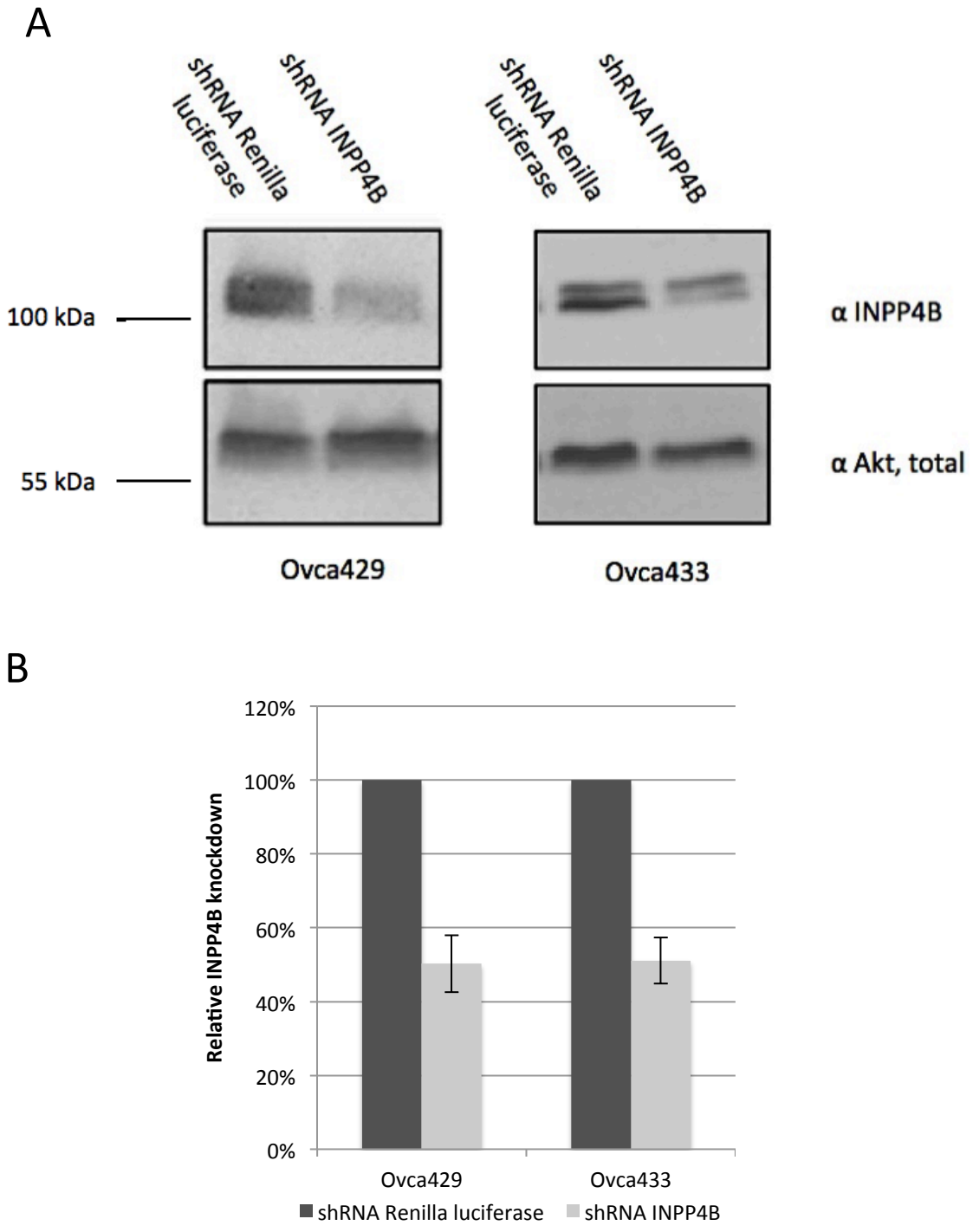

Figure 3.5. INPP4B knockdown of Ovca429 and Ovca433 cells. (A) Representative immunoblots displaying the knockdown efficiency of Ovca429 and Ovca433 cells using shRNA hairpins directed against INPP4B (110 kDa) and Renilla luciferase. Total Akt protein expression was used as a loading control. The knockdown effect was regularly monitored every two weeks. The doublet signal seen here is likely to be due to various post-translational modifications of the INPP4B protein such as acetylation or

phosphorylation, as suggested by Cell Signaling Inc.. The immunoblot for downstream phosphoSer473 Akt activation due to INPP4B knockdown can be found in figure 4.1. (B) The quantification of the protein levels revealed an INPP4B knockdown of 52% and 51% in Ovca429 and Ovca433 INPP4B knockdown cells pools, respectively. Semi-quantitative analysis was conducted using ImageJ. Quantification is representative of three independent experiments using three different knockdown cell pools.

3.2 Results

3.2.1 Validation of BRCA1 mutant gene signature

For this study, the set of 37 genes that encompass the BRCA1 mutant gene signature obtained from the microarray analysis was validated by qPCR (appendix 4). Appendix 5 lists individual microarray probe data of the genes that make up the BRCA1 mutant gene signature. Knockdown cell pools were independently generated using MCF-10A cells and shRNA hairpins against INPP4B or Renilla luciferase (figure 3.6B). 12 genes that were clearly over- or under-expressed in the microarray gene signature heat map were analysed by qPCR and relative gene expression was determined against expression of a housekeeping gene, β-actin, using the ΔΔCq method (Livak and Schmittgen, 2001) (appendix 6). The primers used were obtained from PrimerBank, which have been extensively tested for PCR specificity and efficiency (Spandidos et al., 2010; Wang and Seed, 2003; Wang et al., 2012). All of the 12 genes positively correlated with the microarray differential expression direction, as shown in figure 3.6A. The shRNA targeting INPP4B resulted in a 79% reduction in INPP4B mRNA expression. Interestingly, MCF-10A BRCA1 knockdown cell pools also harboured reduced INPP4B expression levels by 73% compared to the Renilla luciferase control (Figure 3.6B). In addition to validation by qPCR, the microarray data were compared to a 60 gene BRCAness gene signature defined by Konstantinopoulos et al. (Konstantinopoulos et al., 2010). 71% of the differentially expressed genes from the microarray data set correlated to the gene expression found in the 60 gene BRCAness signature (Figure 3.6C). A comprehensive list of differential gene expression between the two data sets is shown in appendix 7.

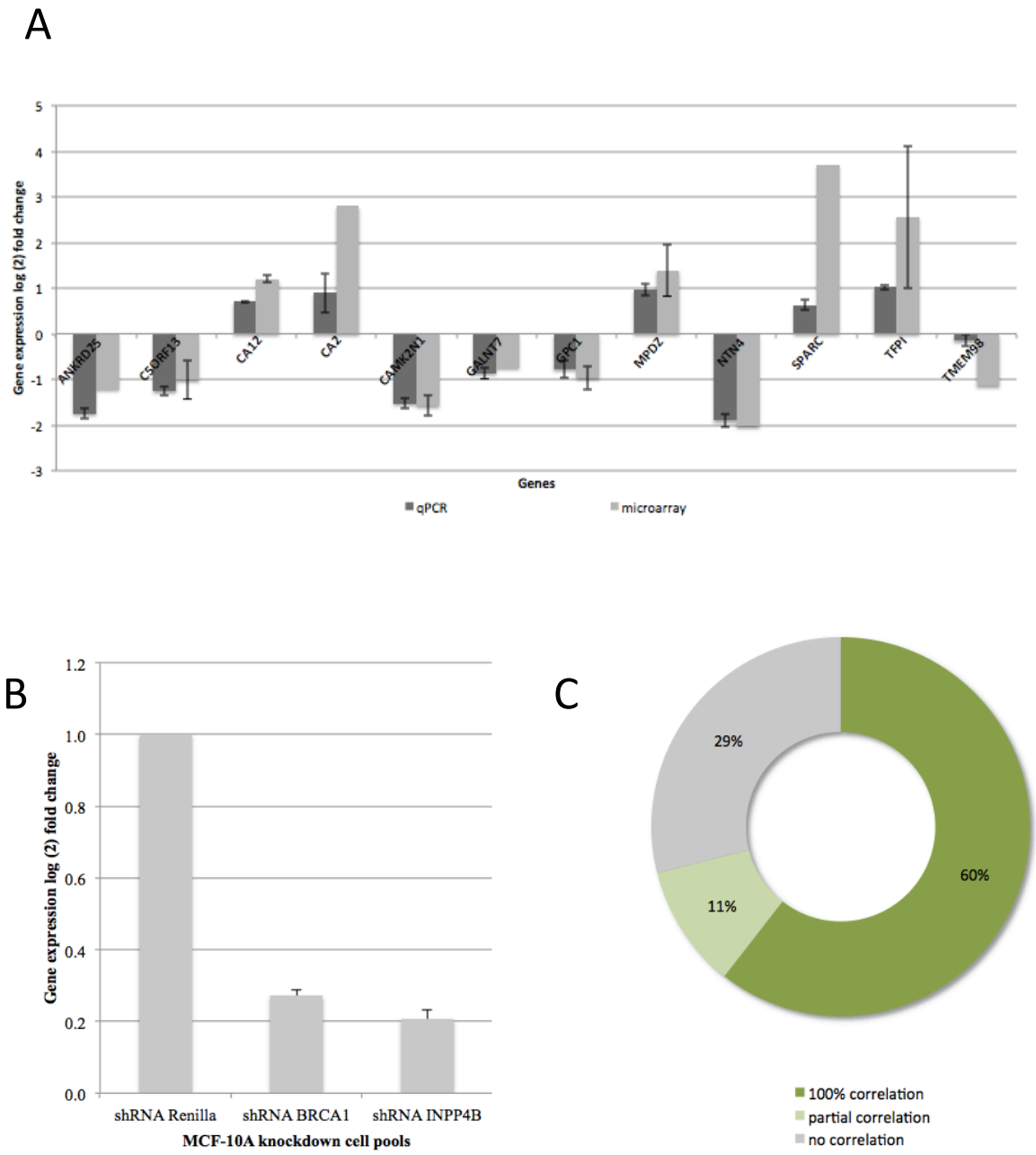

Figure 3.6. qPCR and microarray gene log (2) fold change comparison. (A) 12 genes were selected from the 37 BRCA1 mutant gene signature gene set and relative differential gene expression was quantified in MCF-10A INPP4B knockdown cell pools compared to the Renilla luciferase control. The gene expression log (2) fold change obtained from qPCR was compared to the log (2) fold change identified in the microarray data set. The qPCR results positively correlate with the microarray gene

expression values. (B) Knockdown efficiency of INPP4B in the MCF-10A shRNA INPP4B cell pools was relatively quantified against MCF-10A shRNA Renilla luciferase control. INPP4B mRNA expression was reduced by 79% in the INPP4B knockdown cell pools. Expression levels of INPP4B were also assessed in the BRCA1 knockdown cell pools and found to be reduced by of 73%. (C) The 60 gene BRCAness gene signature defined by Konstantinopoulos *et al.* was compared to the MCF-10A shRNA-INPP4B microarray data set (Konstantinopoulos et al., 2010). 71% of the differentially expressed genes from the MCF-10A shRNA INPP4B microarray data exhibited full correlation with the 60 gene signature weight, with respect to gene expression.

3.2.2 Loss of INPP4B results in a DNA repair defect in Ovca429 cells upon comet assay analysis

Ovca429 and Ovca433 shRNA Renilla luciferase cells were subjected to 16.2, 24.3, 32.4 Gy of X-ray irradiation to obtain dose response curves (figure 3.7), to define the appropriate level of DNA damage that would be sufficiently repairable. The olive tail moment is a measure of DNA damage that takes into account the tail length of the comet and the fraction of total DNA in the tail. The multiplication of these two factors gives rise to a numerical figure that assesses the extent of DNA damage of an individual cell. Both Ovca429 and Ovca433 knockdown cell pools exhibited olive tail moments above seven at 32.4 Gy irradiation, exhibiting a tail DNA percentage of 45.32% and 48.56%, respectively. Comet assays were also conducted to measure DNA repair. Cells were incubated at 37°C 15, 30, 45 and 60 min after irradiation, and the olive tail moment was plotted for each time point generating a DNA repair curve. A relative DNA repair curve was plotted, Upon 30 Gy X-ray radiation, Ovca429 shRNA INPP4B cells exhibited increased DNA damage 15 min post-irradiation, with an olive tail moment percentages of 3.67 compared to 2.31 and a p – value of 3×10^{-5} (figure 3.8A.). 30 min and 60 min post-irradiation, the shRNA INPP4B expressing cell pools compared to the control cells exhibited significantly different olive tail moment of 1.63 and 1.23, and 1.52 and 1.04, respectively, with a p – value of 0.04 and 0.05, respectively. Images from the analysis revealed a significantly enhanced comet tail in the INPP4B knockdown cell compared to the control 15 min, 30 min and 60 min after irradiation (figure 3.8B). DNA repair assays conducted with Ova433 knockdown cell pools treated with 35 Gy X-ray radiation revealed no difference in olive tail moment between the shRNA INPP4B and shRNA Renilla luciferase expressing cell pools (figure 3.8A).

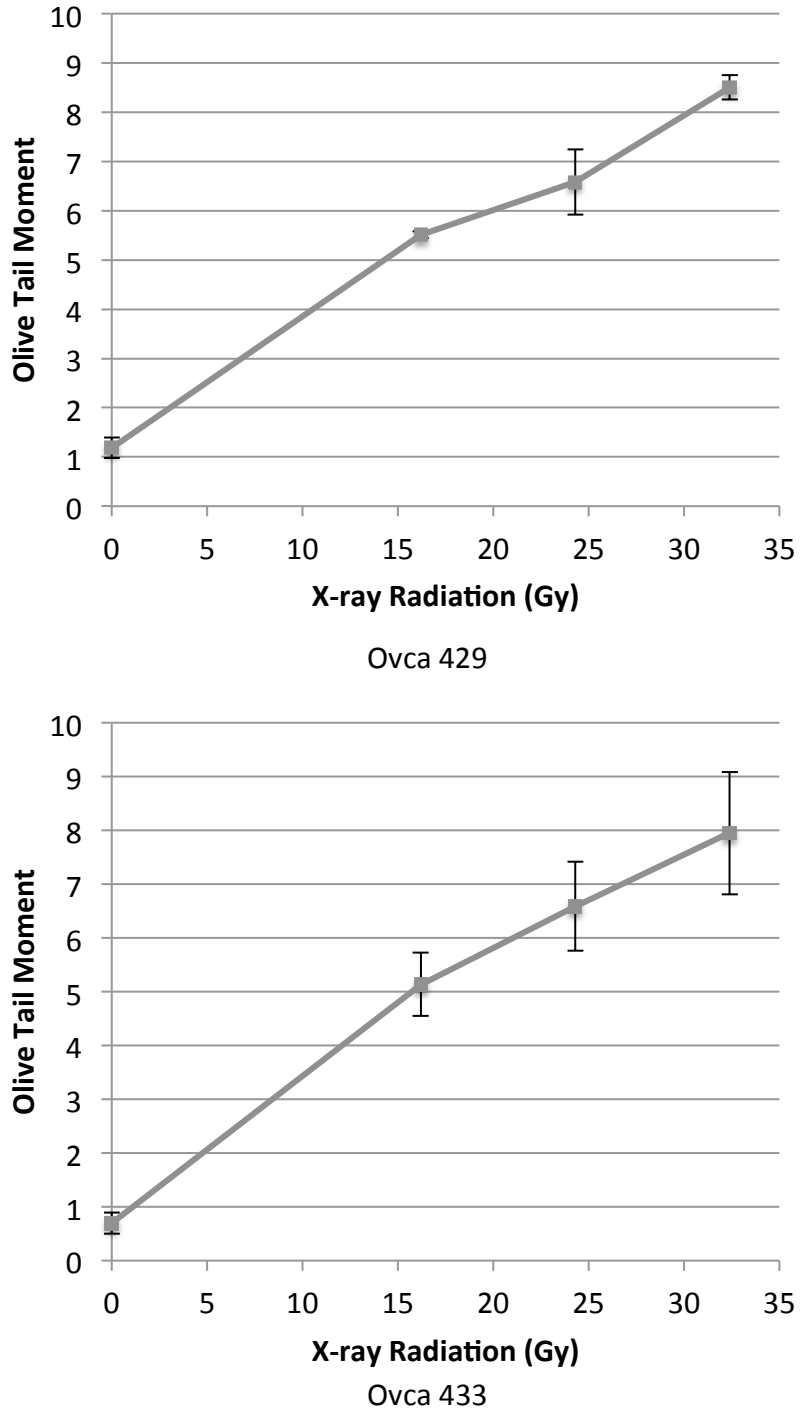

Figure 3.7. Comet assay dose response in Ovca429 and Ovca433 cells. Ovca429 and Ovca433 shRNA Renilla luciferase expressing cell pools were irradiated with 16.2, 24.3 and 32.4 Gy X-ray radiation and the respective olive tail moment plotted to form a dose response curve. Experiments were conducted independently three times. Error bars represent the standard deviation.

A

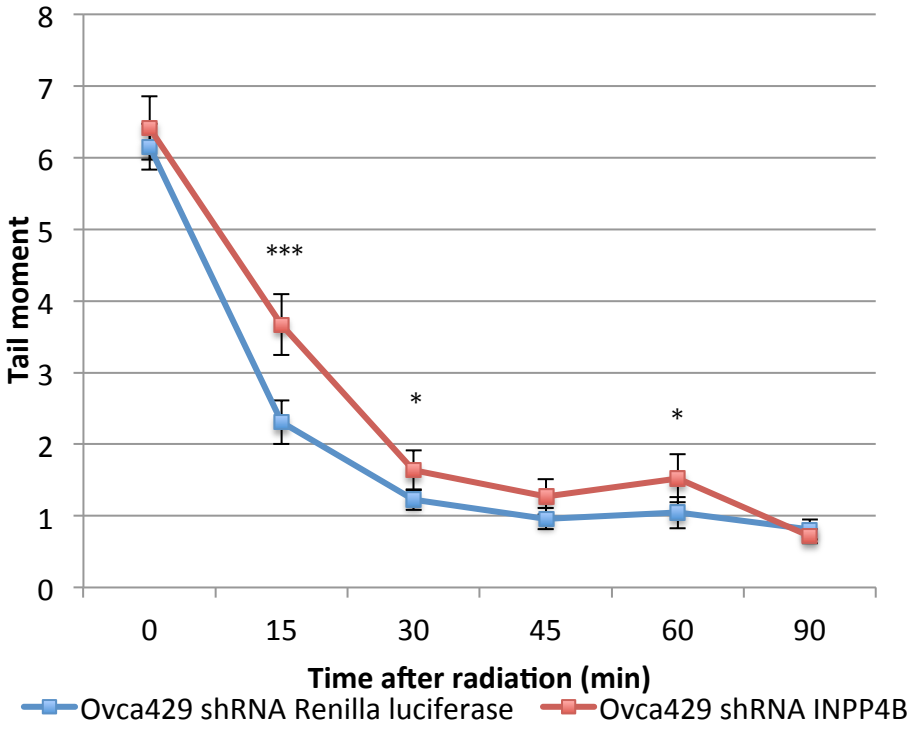
8
7
6
5
4
3
2
1
0
Tail moment
***
*
*
0
15
30
45
60
90
Time after radiation (min)
Ovca429 shRNA Renilla luciferase
Ovca429 shRNA INPP4B

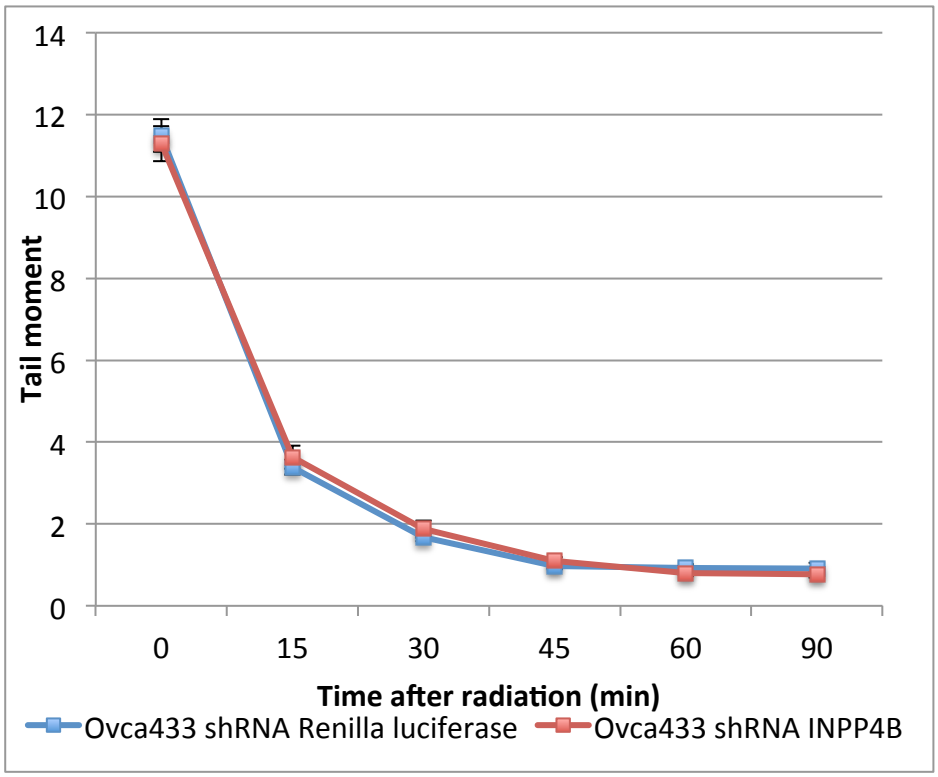
14
12
10
8
6
4
2
0
Tail moment
0
15
30
45
60
90
Time after radiation (min)
Ovca433 shRNA Renilla luciferase
Ovca433 shRNA INPP4B

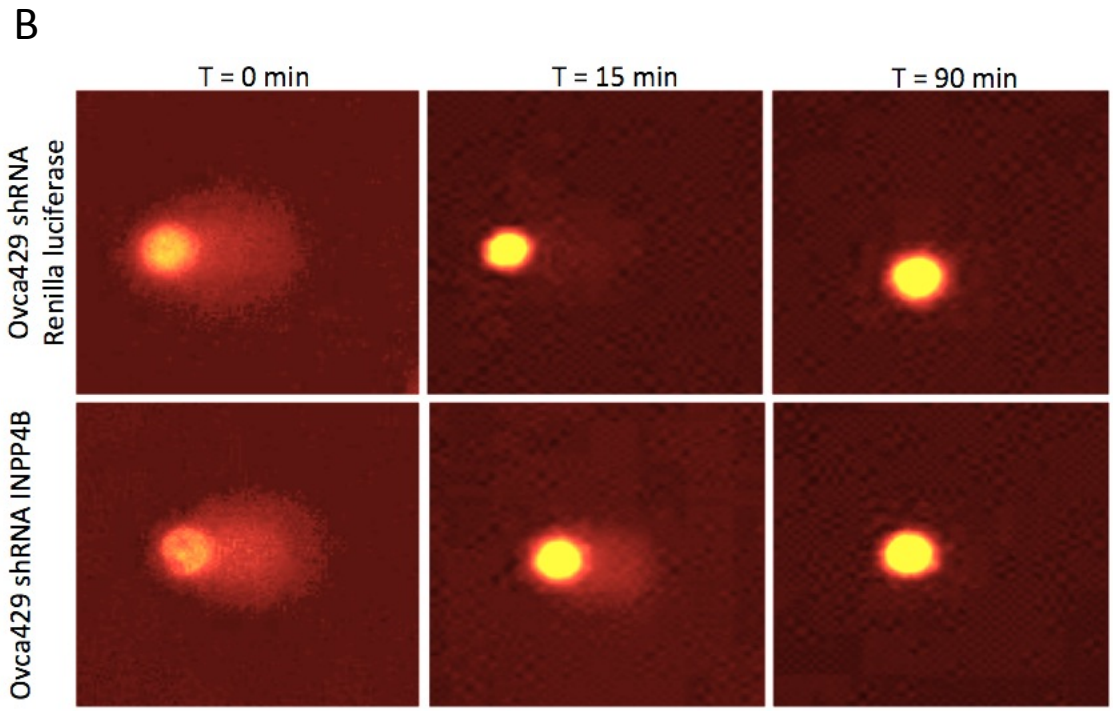

Figure 3.8. Ovca429 and Ovca433 DNA repair curves upon X-ray radiation. (A) Ovca429 and Ocva433 knockdown cell pools were treated with 30 and 35 Gy irradiation, respectively, and cells were left to repair at 37°C for 15, 30, 45 and 60 min after irradiation. Ovca429 shRNA INPP4B cells exhibited impaired DNA repair compared to the knockdown control. The p-values for conditions at 15 min, 30 min and 60 min are 3 x 10^{-5}, 0.04 and 0.05, respectively. Ovca433 shRNA INPP4B cells showed no significant differences in DNA repair compared to the control. In total 50 cells per sample (25 cells per slide) were analysed per experiment. Experiments were conducted independently three times. Error bars represent standard deviation and the t-test was used for statistical analysis (p-value of *≤0.05, ***≤0.0005). (B) Images capturing the comet tails of Ovca429 shRNA INPP4B cells and shRNA Renilla luciferase control 0, 15 and 90 min after irradiation.

3.2.3 Loss of INPP4B results in γH2AX foci retention upon treatment with etoposide in Ovca429 and Ovca433 knockdown cell pools

Immunofluorescence assays were conducted to investigate the effect loss of INPP4B has on the DNA damage response by quantification of γH2AX and RAD51 foci formation. Etoposide treatment was first optimised to determine the concentration to use in experiments (figure 3.9). Treatment of Ovca429 shRNA INPP4B expressing cell pools with 1 μM etoposide resulted in γH2AX foci retention compared to control cell pools (figure 3.10). For example, 30 min after treatment, INPP4B knockdown nuclei contained a mean value of 20.9 foci per nucleus compared to 16.2 foci in the control nuclei ($p = 0.001$); 60 min after treatment, INPP4B knockdown nuclei contained a mean value of 17.7 foci per nucleus compared to 14.3 foci in the control nuclei ($p = 0.01$); 180 min after treatment, nuclei from the Ovca429 shRNA INPP4B knockdown cell pools maintained a mean foci value of 14.8 compared to 11.7 foci in the control cells (p value = 0.005). Furthermore, the untreated INPP4B knockdown cell pools contained significantly increased mean foci per nucleus compared to the knockdown controls, and carried a mean value of 9.4 γH2AX foci per nucleus compared to 4.9 foci ($p = 4 \times 10^{-7}$). Ovca433 shRNA INPP4B knockdown cell pools harboured a significant increase in γH2AX foci retention 180 min after treatment with 14.3 foci per nucleus compared to 9.9 foci per nucleus in the knockdown control cells ($p = 9 \times 10^{-5}$) as depicted in figure 3.11. There was no statistical difference between the two knockdown cell pools in the untreated cells upon analysis, nor 0, 30, and 60 min after etoposide treatment.

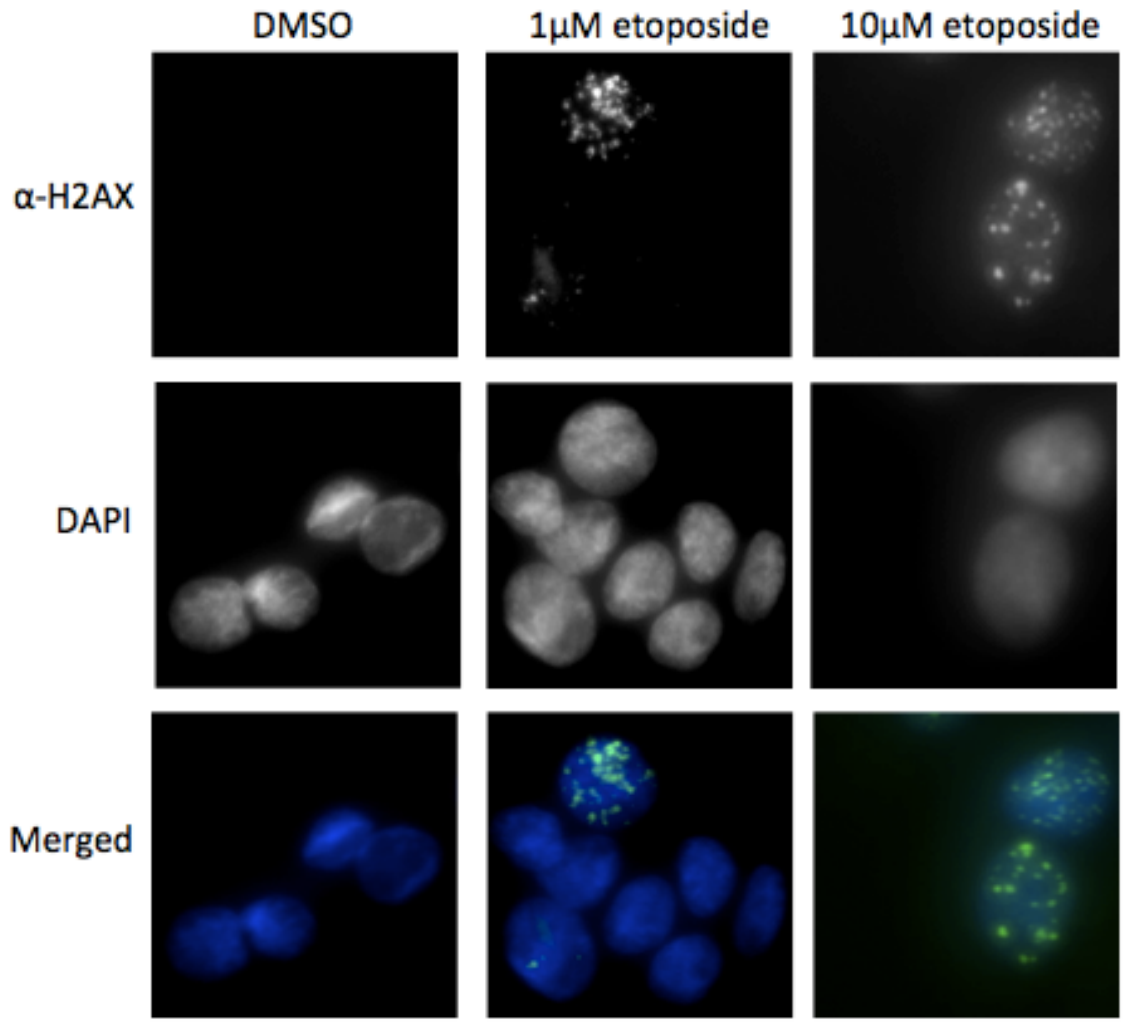

Figure 3.9. Optimisation of etoposide treatment. Ovca429 cells were treated for 1 hr with either DMSO, 1 μM or 10 μM etoposide. The rows of the figure represent staining of α-H2AX antibody, DAPI, and merged (DAPI and α-H2AX antibody) from top to bottom, respectively. The cells were washed, fixed and probed with the γH2AX antibody.

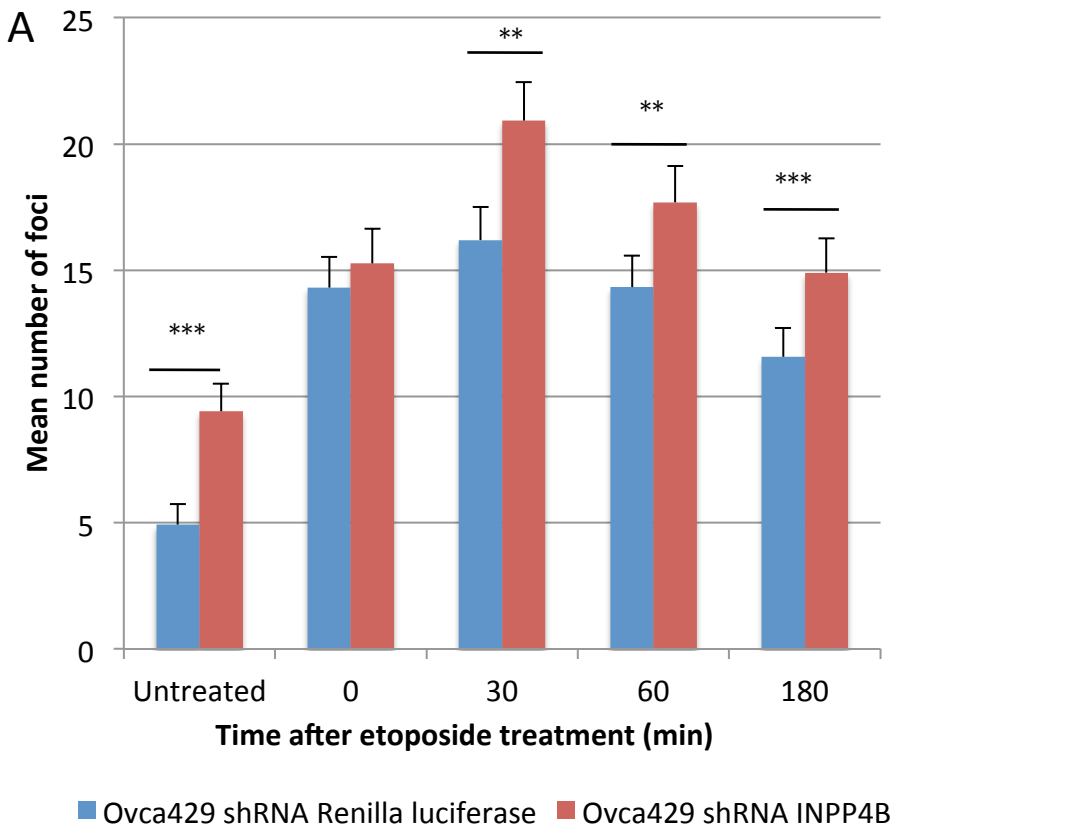
A
25
20
15
10
5
0
**
**
***
***
Mean number of foci
Untreated
0
30
60
180
Time after etoposide treatment (min)
Ovca429 shRNA Renilla luciferase
Ovca429 shRNA INPP4B

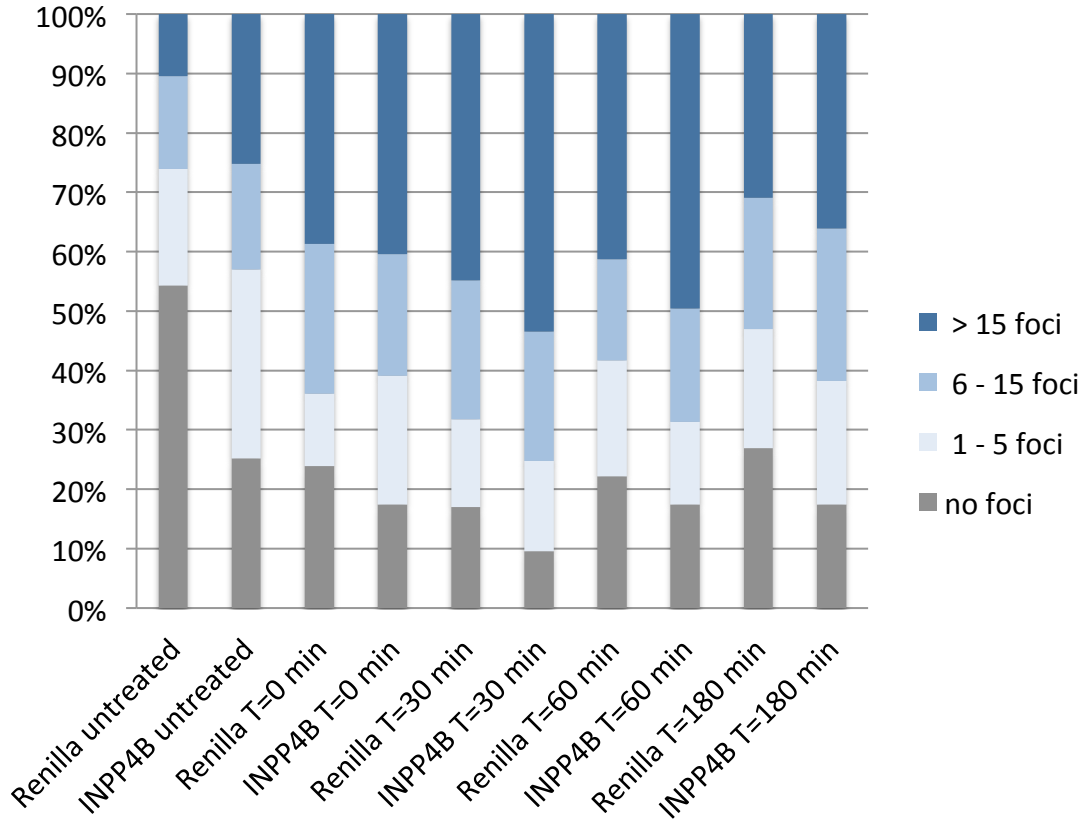
100%
90%
80%
70%
60%
50%
40%
30%
20%
10%
0%
> 15 foci
6 - 15 foci
1 - 5 foci
no foci
Renilla untreated
INPP4B untreated
Renilla T=0 min
INPP4B T=0 min
Renilla T=30 min
INPP4B T=30 min
Renilla T=60 min
INPP4B T=60 min
Renilla T=180 min
INPP4B T=180 min

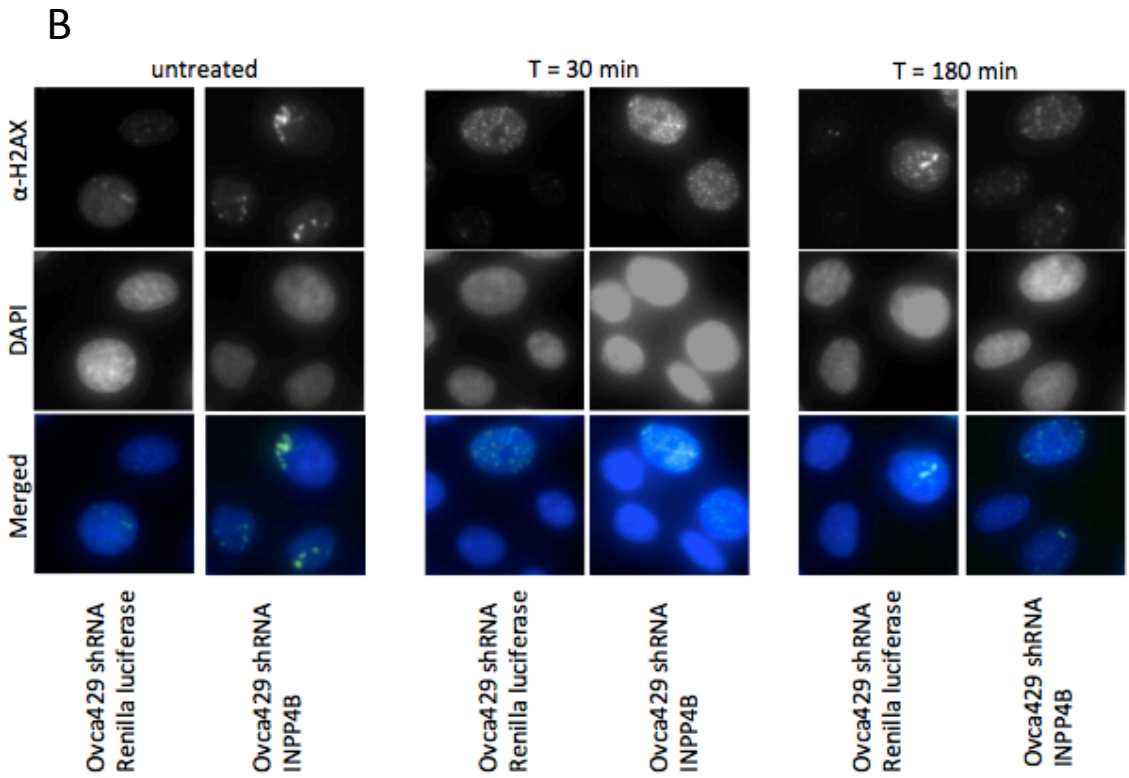

Figure 3.10. INPP4B knockdown in Ovca429 cells results in γH2AX foci retention upon etoposide treatment. (A) After treatment with 1 μM etoposide, Ovca429 knockdown cell pools were fixed 0, 30, 60 and 180 min after treatment. Ovca429 shRNA INPP4B expressing cell pools retained more foci per nucleus untreated, as well as 30, 60 and 180 min after treatment compared to the knockdown control. The p-value for untreated conditions and conditions at 30 min, 60 min and 180 min were 4 x 10^{-7}, 0.001, 0.01 and 0.005, respectively. The foci distribution graph on the right represents four foci groups categorised into number of nuclei containing 15 or more foci, 5 – 10 foci, 0 – 5 foci, and 0 foci. The sample size was a minimum of 30 cells and the t-test was used for statistical analysis (p-value of **≤0.005, ***≤0.0005). Foci were manually by eye. Experiment were conducted independently three times. (B) Image comparison of γH2AX foci formation in Ovca429 INPP4B and control knockdown cell pools. The

rows of the figure represent staining of α-H2AX antibody, DAPI, and merged (DAPI and α-H2AX antibody) from top to bottom, respectively.

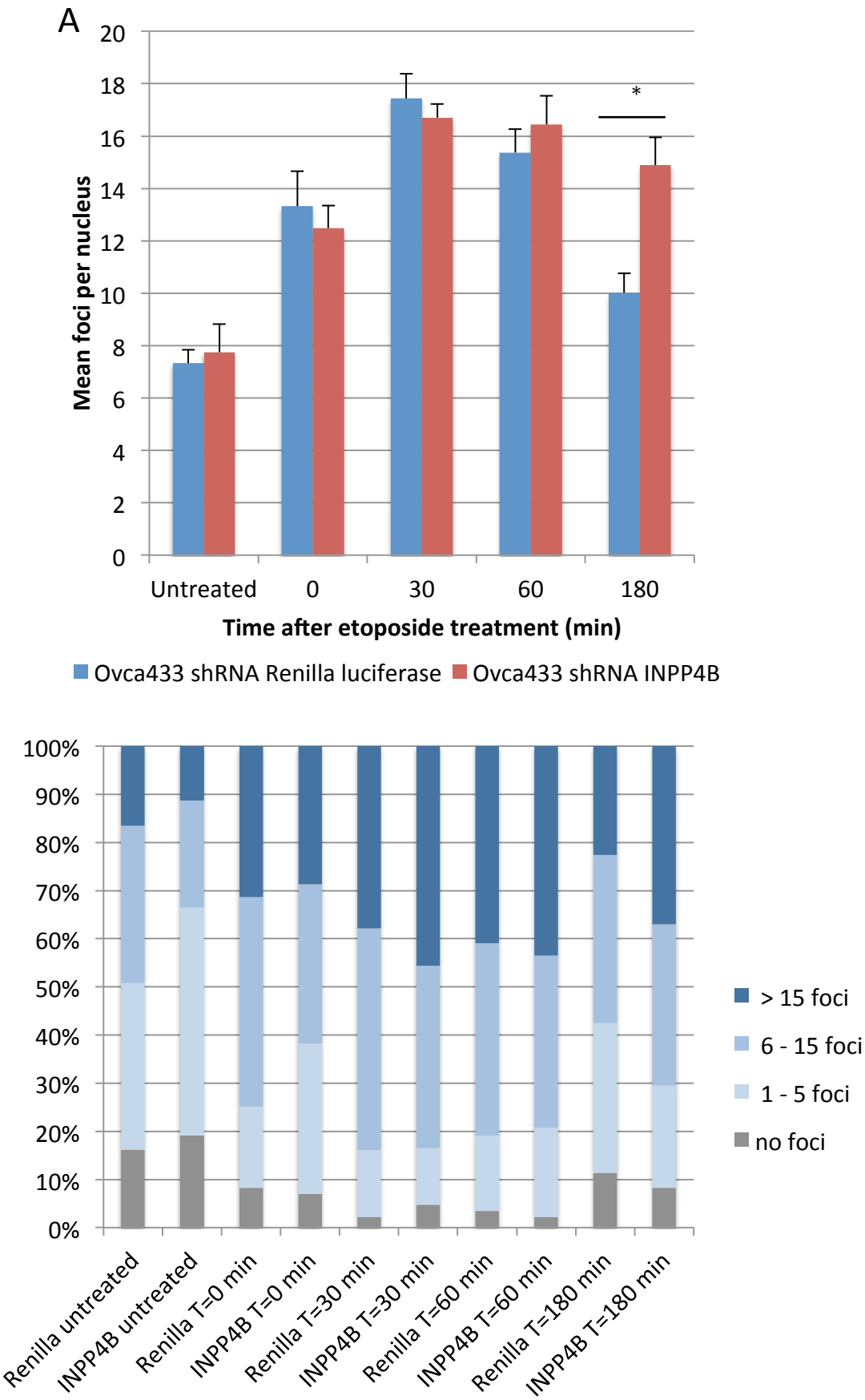
A
20
18
16
14
12
10
8
6
4
2
0
Mean foci per nucleus
*
Untreated
0
30
60
180
Time after etoposide treatment (min)
Ovca433 shRNA Renilla luciferase
Ovca433 shRNA INPP4B
100%
90%
80%
70%
60%
50%
40%
30%
20%
10%
0%
> 15 foci
6 - 15 foci
1 - 5 foci
no foci
Renilla untreated
INPP4B untreated
Renilla T=0 min
INPP4B T=0 min
Renilla T=30 min
INPP4B T=30 min
Renilla T=60 min
INPP4B T=60 min
Renilla T=180 min
INPP4B T=180 min

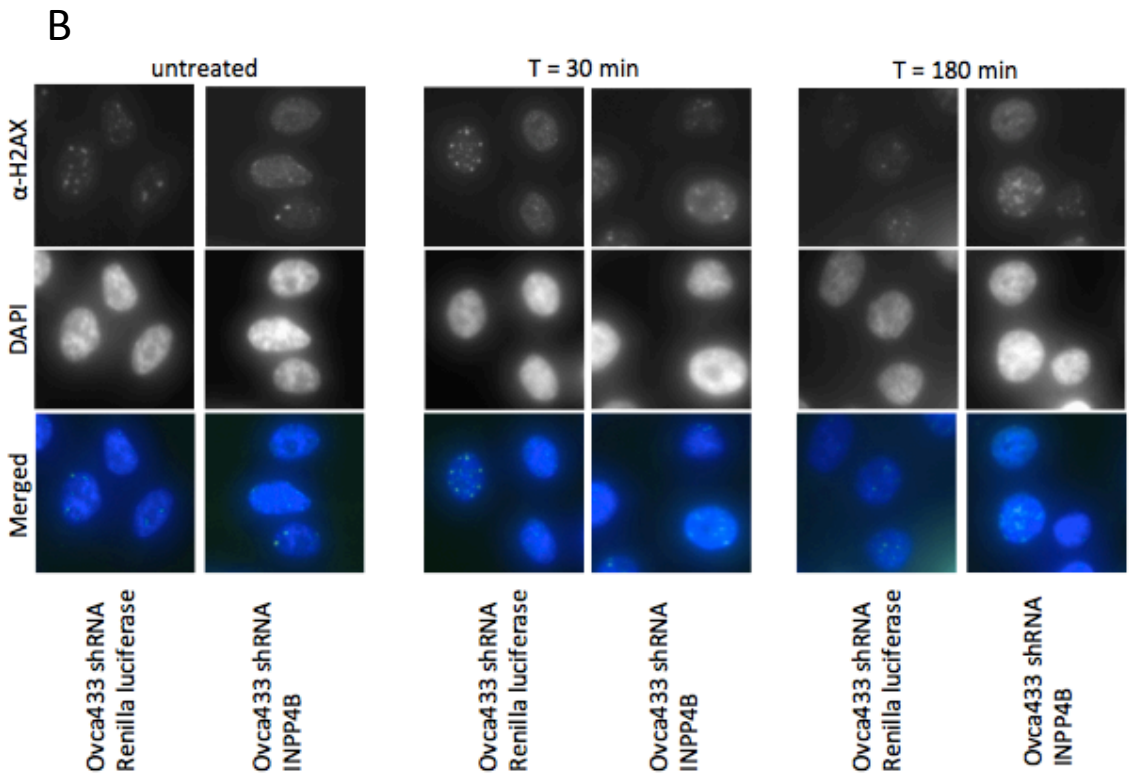

Figure 3.11. INPP4B knockdown in Ovca433 cells results in γH2AX foci retention upon etoposide treatment. (A) After treatment with 1 μM etoposide, Ovca433 knockdown cell pools were fixed 0, 30, 60 and 180 min after treatment. Ovca429 INPP4B knockdown cell pools retained more foci 180 min after treatment compared to the knockdown control. The p-value conditions at 180 min was $9x10^{-5}$. The sample size was a minimum of 30 cells and the t-test was used for statistical analysis (p-value of *≤0.05). Foci were manually by eye. Experiment were conducted independently three times. (B) Image comparison of γH2AX foci formation in Ovca433 INPP4B and control knockdown cell pools. The rows of the figure represent staining of α-H2AX antibody, DAPI, and merged (DAPI and α-H2AX antibody) from top to bottom, respectively.

3.2.4 Loss of INPP4B results in RAD51 and 53BP1 foci retention upon treatment with etoposide in Ovca429 knockdown cell pools

Similarly, immunofluorescence assays that detected foci formation of DSB repair protein RAD51 also found aberrant foci formation in Ovca429 INPP4B knockdown cell pools compared to the controls (figure 3.12). Cells were treated with 10 μM etoposide and incubated at 37°C 6, 12 and 24 hrs after treatment. Cells harbouring an INPP4B knockdown displayed increased mean RAD51 foci per nucleus quantities of 9.7 12 hrs after treatment compared to 7.1 foci per nucleus observed in the control cells ($p = 1.4 \times 10^{-7}$). 24 hrs after treatment, while RAD51 mean foci quantities remained at 6.7 foci per nucleus in the control cells, shRNA INPP4B cells displayed significantly increased foci quantities of 13.81 foci per nucleus ($p = 1.2 \times 10^{-16}$). In untreated cells, the two knockdown cell pools also exhibited statistical differences in the mean foci value with shRNA INPP4B cells harbouring a mean foci value of 2.7 compared to 3.4 in the control ($p = 0.002$).

Detection of 53BP1 in Ocva429 knockdown cell pools resulted in significant statistical differences at 6 and 12 hrs after 10 μM etoposide treatment, as well as in the untreated samples (figure 3.13). shRNA INPP4B knockdown cells possessed a mean foci value of 20.6 compared to 18.1 ($p = 0.008$) 6 hrs after treatment and 12 hrs after treatment. Cells with reduced INPP4B expression had a mean foci value of 23.1 compared to 18.4 ($p = 0.00005$) in the control cells. In the untreated samples, cells with less INPP4B contained a mean of 10.5 foci per nucleus, compared to 8.8 foci per nucleus in the control cells ($p = 0.01$).

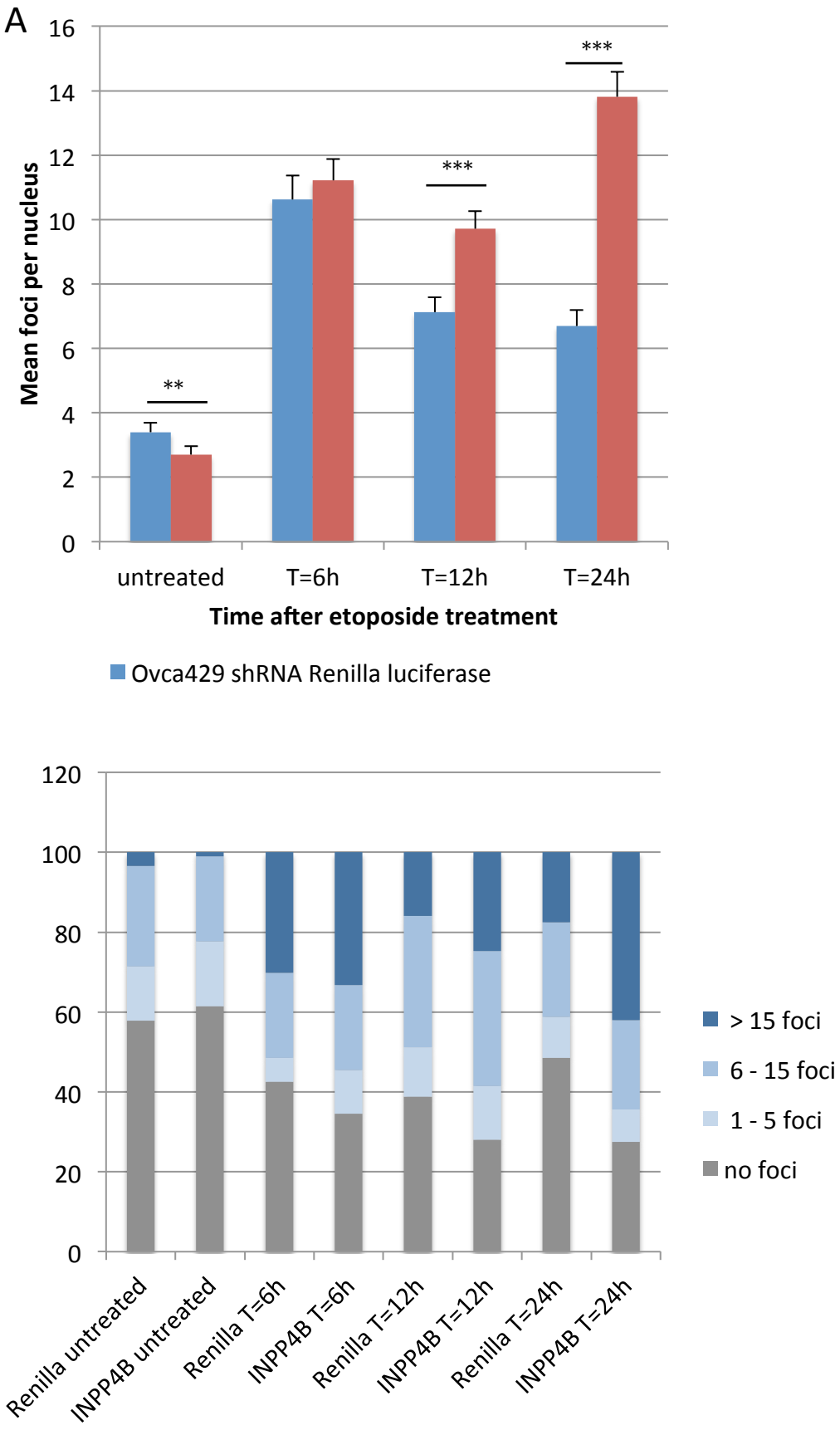
A
16
14
12
10
8
6
4
2
0
Mean foci per nucleus
**
***
***
untreated
T=6h
T=12h
T=24h
Time after etoposide treatment
Ovca429 shRNA Renilla luciferase
120
100
80
60
40
20
0
Renilla untreated
INPP4B untreated
Renilla T=6h
INPP4B T=6h
Renilla T=12h
INPP4B T=12h
Renilla T=24h
INPP4B T=24h
> 15 foci
6 - 15 foci
1 - 5 foci
no foci

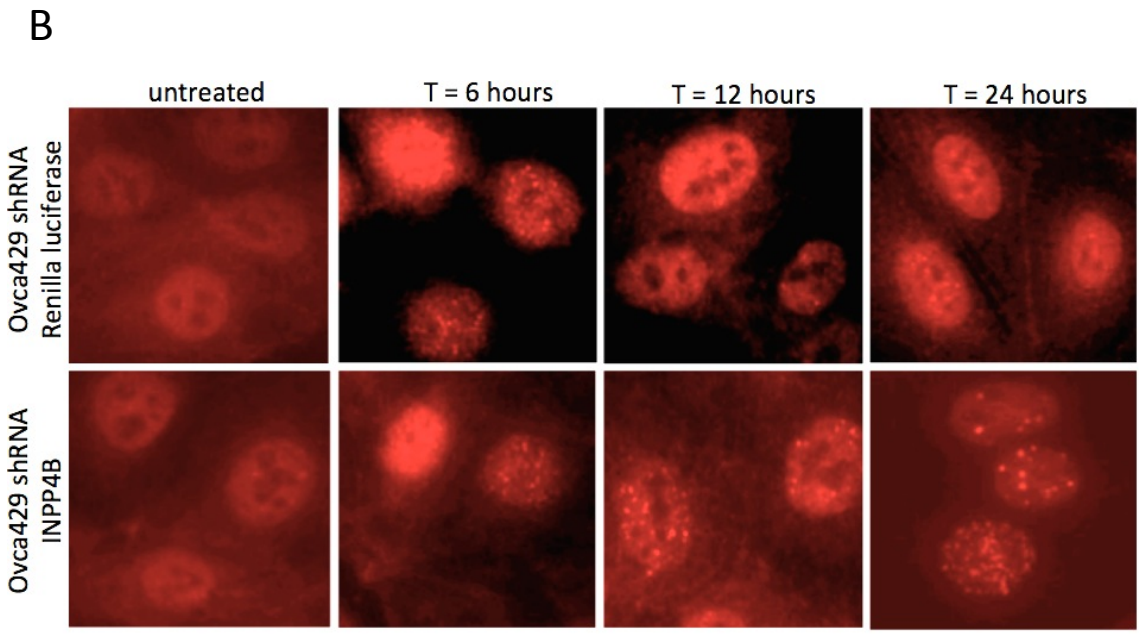

Figure 3.12. INPP4B knockdown in Ovca429 cells results in RAD51 foci retention upon etoposide treatment. (A) Upon treatment with 10 μM etoposide, RAD51 foci were quantified in Ovca429 knockdown cell pools 6, 12, and 24 hrs after treatment. Ovca429 INPP4B knockdown cell pools displayed RAD51 foci retention 12 and 24 hrs after treatment compared to the knockdown control. The p-value for the untreated condition and conditions at 12 hrs and 24 hrs were 0.002, 1.4×10^{-7} and 1.2×10^{-16}, respectively. The foci distribution graph reveals an increase in the number of nuclei containing more than 15 foci per nucleus at the same time points in INPP4B knockdown cells compared to the control. The sample size was a minimum of 50 cells and the t-test was used for statistical analysis (p-value of **≤0.005, ***≤0.0005). Foci were manually by eye. Experiments were conducted independently three times. (B) Image comparison of RAD51 foci formation in Ovca429 shRNA INPP4B and shRNA Renilla luciferase expressing cell pools. Here only the single-stained images are seen rather than the merged image for clearer observation of the foci.

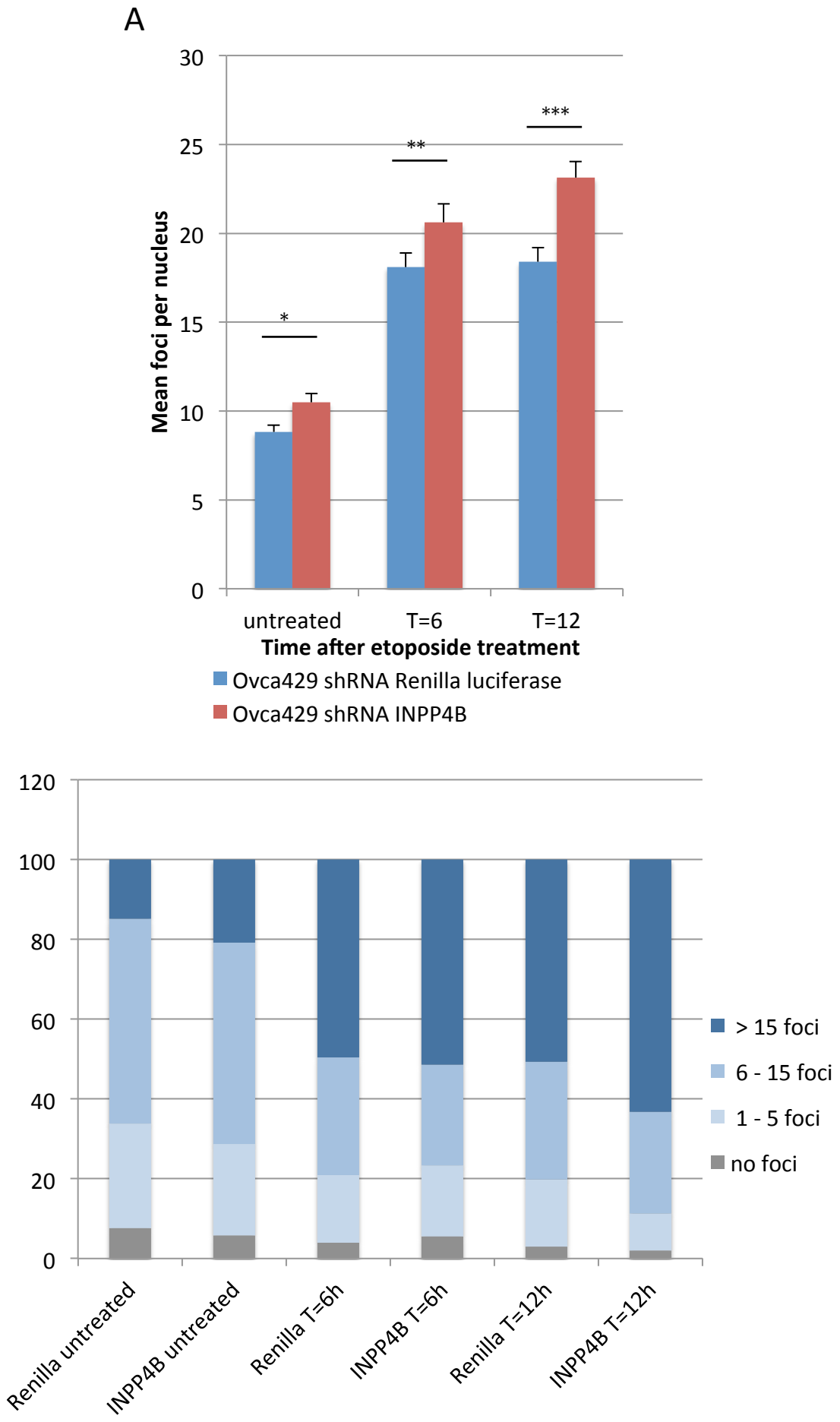
A
30
25
20
15
10
5
0
Mean foci per nucleus
*
**
***
untreated
T=6
T=12
Time after etoposide treatment
Ovca429 shRNA Renilla luciferase
Ovca429 shRNA INPP4B
120
100
80
60
40
20
0
> 15 foci
6 - 15 foci
1 - 5 foci
no foci
Renilla untreated
INPP4B untreated
Renilla T=6h
INPP4B T=6h
Renilla T=12h
INPP4B T=12h

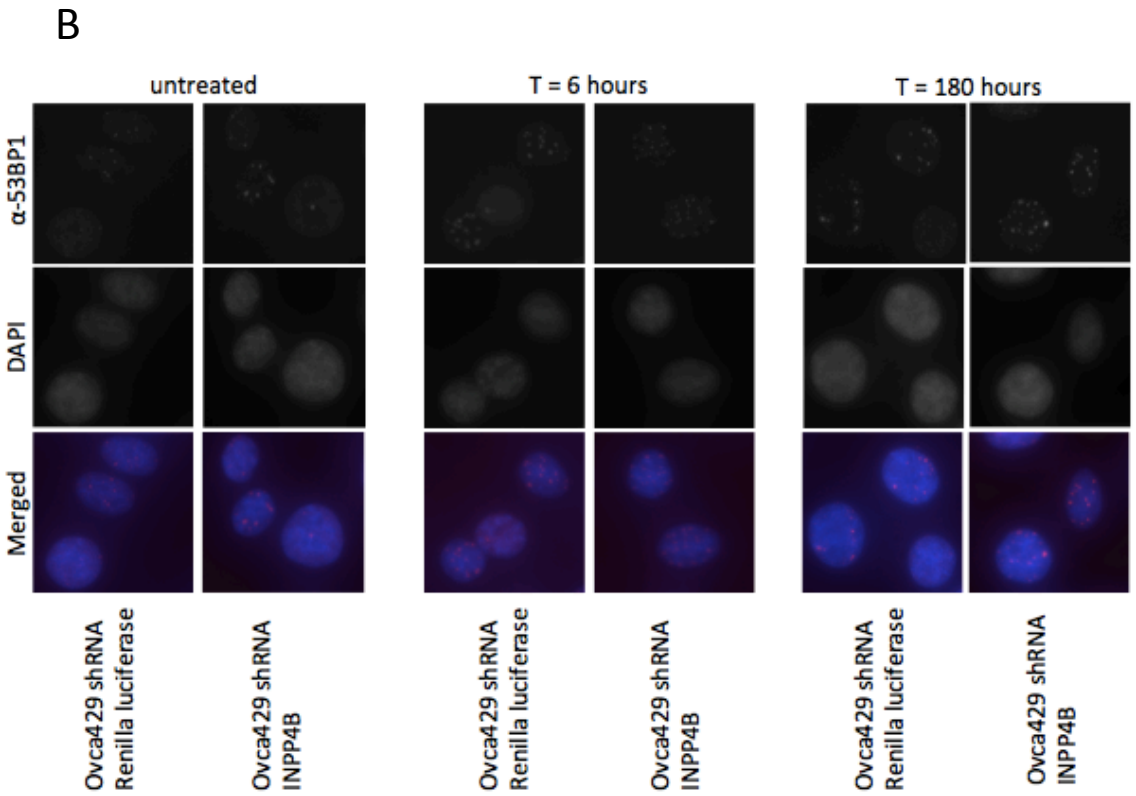

Figure 3.13. INPP4B knockdown in Ovca429 cells results in 53BP1 foci retention upon etoposide treatment. (A) Upon treatment with 10 μM etoposide, 53BP1 foci were quantified in Ovca429 knockdown cell pools 6 and 12 hrs after treatment. Ovca429 INPP4B knockdown cell pools displayed RAD51 foci retention across all time points after treatment compared to the knockdown control. The sample size was a minimum of 50 cells and the t-test was used for statistical analysis (p-value of *≤0.05, **≤0.005, ***≤0.0005). Foci were manually by eye. Experiments were conducted independently three times. (B) Image comparison of 53BP1 foci formation in Ovca429 shRNA INPP4B and shRNA Renilla luciferase expressing cell pools. The rows of the figure represent staining of α-53BP1 antibody, DAPI, and merged (DAPI and α-53BP1 antibody) from top to bottom, respectively.

3.2.5 Loss of INPP4B results in RAD51 foci retention upon irradiation in Ovca433 knockdown cell pools

Ovca433 knockdown cell pools were irradiated with 15 Gy X-ray radiation and incubated at 37°C for 24, 30 and 48 hrs after DNA damage. shRNA-INPP4B expressing cells displayed increased RAD51 foci formation 24 hrs after irradiation, harbouring a mean foci per nucleus value of 7.1 compared to 5.9 in the control cells (figure 3.14.; $p = 0.0004$). 48 hrs after treatment, the mean foci difference between the two knockdown cell pools was more apparent, with shRNA INPP4B cells possessing a mean of 7.0 foci per nucleus compared to 4.5 foci in the control knockdown cells ($p = 0.01$).

A

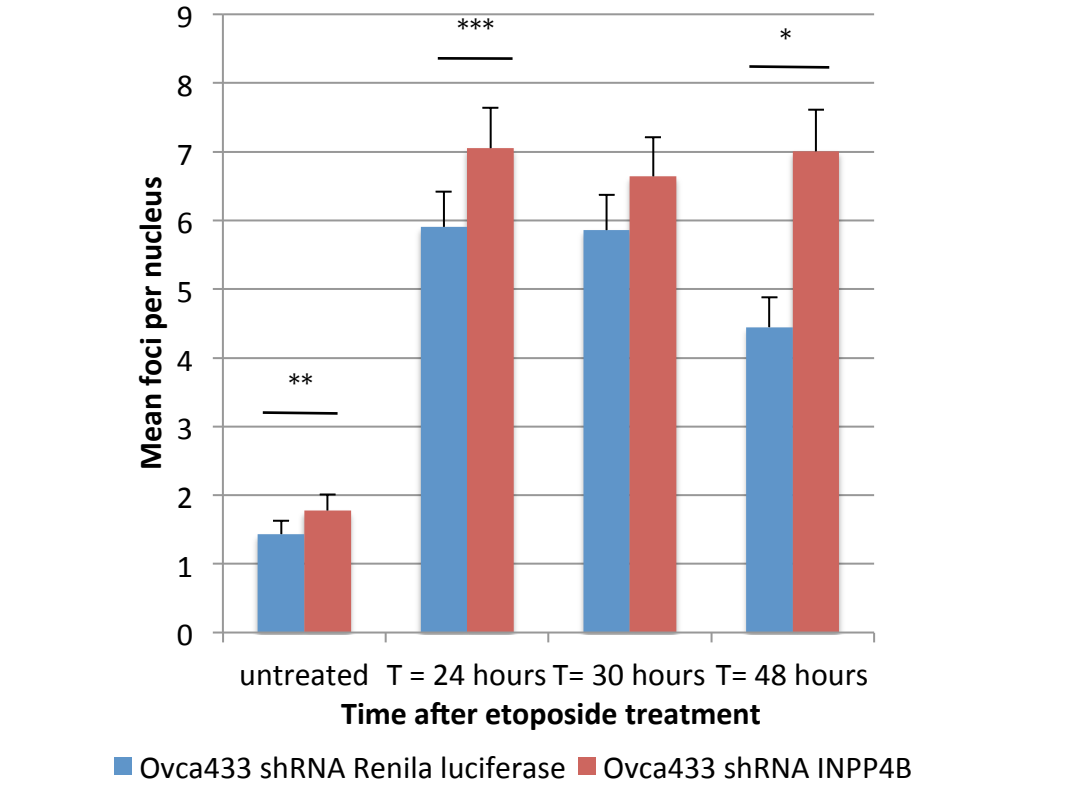
9
8
7
6
5
4
3
2
1
0
Mean foci per nucleus
***
*
**
untreated
T = 24 hours
T= 30 hours
T= 48 hours
Time after etoposide treatment
Ovca433 shRNA Renila luciferase
Ovca433 shRNA INPP4B

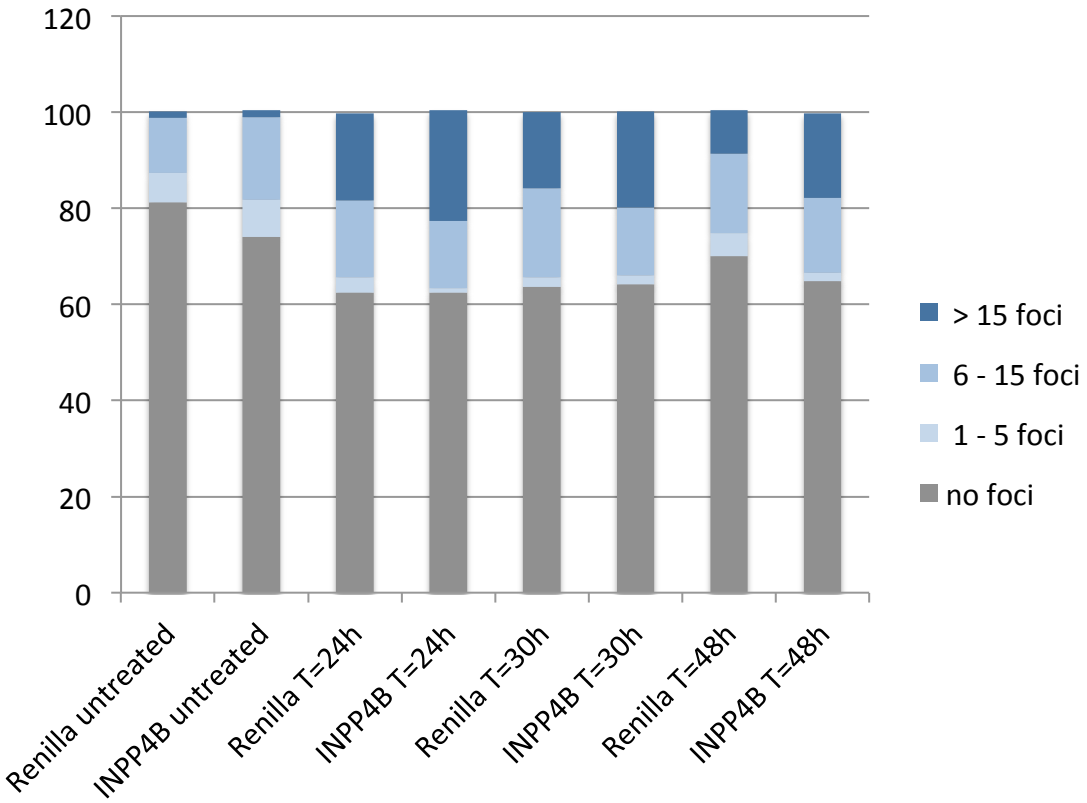
120
100
80
60
40
20
0
Renilla untreated
INPP4B untreated
Renilla T=24h
INPP4B T=24h
Renilla T=30h
INPP4B T=30h
Renilla T=48h
INPP4B T=48h
> 15 foci
6 - 15 foci
1 - 5 foci
no foci

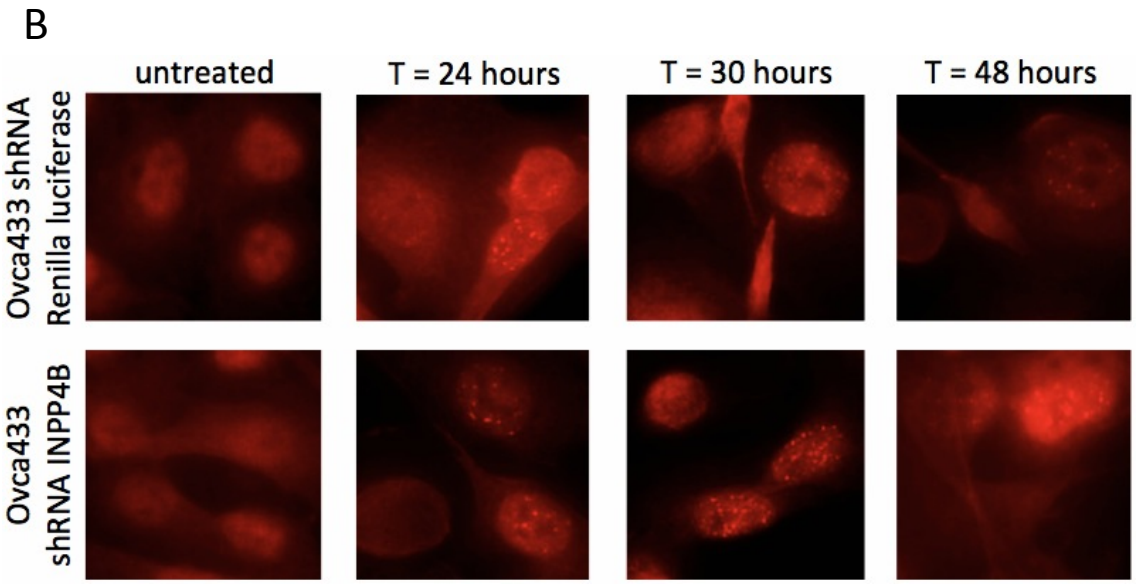

Figure 3.14. INPP4B knockdown in Ovca433 cells results in RAD51 foci retention upon irradiation. (A) Upon irradiation with 15 Gy X-ray RAD51 foci were quantified in Ovca433 knockdown cell pools 24, 30, and 48 hrs after treatment. Ovca433 INPP4B knockdown cell pools displayed RAD51 foci retention 24 and 48 hrs after treatment compared to the knockdown control, as well as in the untreated samples. The sample size was a minimum of 50 cells and the t-test was used for statistical analysis (p-value of *≤0.05, **≤0.005, ***≤0.0005). Foci were manually by eye. Experiments were conducted independently three times. (B) Image comparison of RAD51 foci formation in Ovca433 INPP4B and Renilla luciferase knockdown cell pools.

3.2.6 Loss of INPP4B in Ovca429 and Ovca433 cancer cell lines has no impact on BRCA1 foci formation upon irradiation

Plo et al. demonstrated that activated Akt1 repressed HR through cytoplasmic retention of BRCA1 and Rad51 resulting in a BRCA1-deficient phenotype in breast cancer (Plo et al., 2008a). Therefore, Ovca429 and Ovca433 knockdown cell lines were investigated for BRCA1 foci formation upon IR. Ovca429 and Ovca433 knockdown cell pools were irradiated with 2 Gy X-ray and incubated at 37°C for 7 and 24 hrs after radiation. Loss of INPP4B had no effect on BRCA1 foci formation in both ovarian cancer knockdown cell pools (figure 3.15– 3.16).

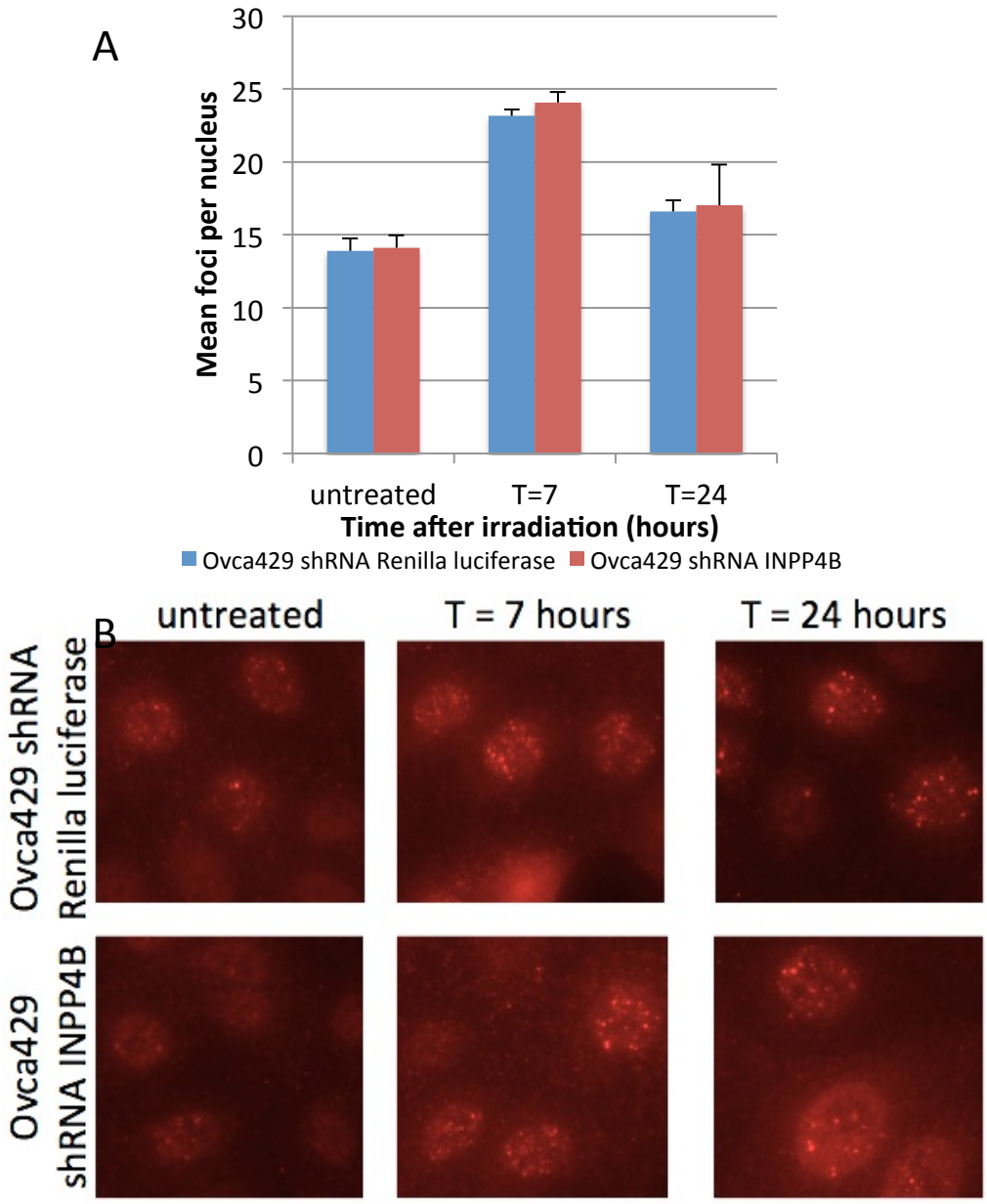

Figure 3.15. BRCA1 foci formation in Ovca429 knockdown cell pools. (A) Upon treatment with 2 Gy X-ray radiation, BRCA1 foci were quantified in Ovca429 Renilla luciferase (control) and INPP4B knockdown cell pools 7, and 24 hrs after treatment. No differences in mean foci values were detected between the knockdown cell pools. The sample size was a minimum of 50 cells and the t-test was used for statistical analysis (p-value of *≤0.05, **≤0.005, ***≤0.0005). Foci were counted by using Cell Profiler and the experiment was conducted independently three times. (B) Image comparison of

BRCA1 foci formation in Ovca429 INPP4B and Renilla luciferase knockdown cell pools.

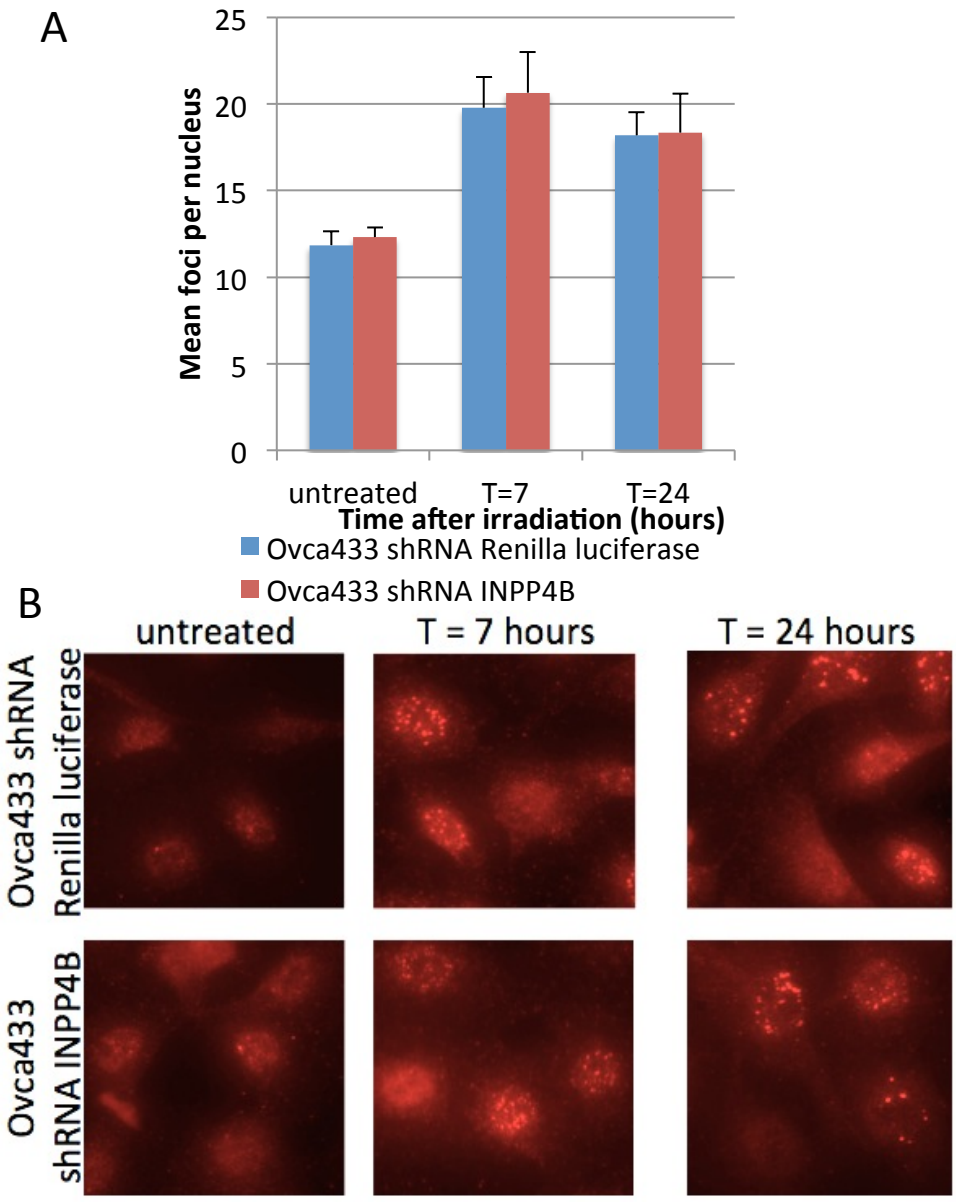

Figure 3.16. BRCA1 foci formation in Ovca433 knockdown cell pools. (A) Upon treatment with 2 Gy X-ray radiation, BRCA1 foci were quantified in Ovca433 Renilla luciferase (control) and INPP4B knockdown cell pools 7 and 24 hrs after treatment. No differences in mean foci values were detected between the knockdown cell pools. The sample size was a minimum of 50 cells and the t-test was used for statistical analysis (p-value of *≤0.05, **≤0.005, ***≤0.0005). Foci were counted by using Cell Profiler and the experiment was conducted independently three times. (B) Image comparison of

BRCA1 foci formation in Ovca433 shRNA INPP4B and shRNA Renilla luciferase knockdown cell pools.

3.2.7 INPP4B-deficient Ovca433 knockdown cell pools undergo aberrant cell cycle progression

The PI3K/Akt pathway has been implicated in regulation of cell cycle progression, and hence the cell cycle progression in relation to INPP4B loss was investigated. Ovca433 knockdown cell pools containing shRNA-INPP4B and shRNA-Renilla luciferase were subjected to cell cycle analyses using the Muse Cell Analyser machine (Milllpore, UK). Unchallenged Ovca433 knockdown cell pools were serum starved for 18 hrs to synchronise the cells and after replenishment of serum-containing media, the cells were fixed at various time points to track cell cycle progression. Cells were fixed at 0, 6, 12, 18, 24, 27, 30 hrs after serum starvation resulted in good analytical distribution of time points to examine cell cycle progression. The experiments revealed that loss of INPP4B in Ovca433 cells results in aberrant cell cycle progression compared to the knockdown control (figure 3.18). Unchallenged Ovca433 INPP4B-deficient cells displayed aberrant cell cycle progression compared to the knockdown control counterparts 24 hrs after serum replenishment ($p = 0.006$). Representative images of the primary data are depicted in figure 3.17. Cell cycle analysis of Ovca429 knockdown cell pools containing shRNA-INPP4B and shRNA-Renilla luciferase were not conducted due to time constraints.

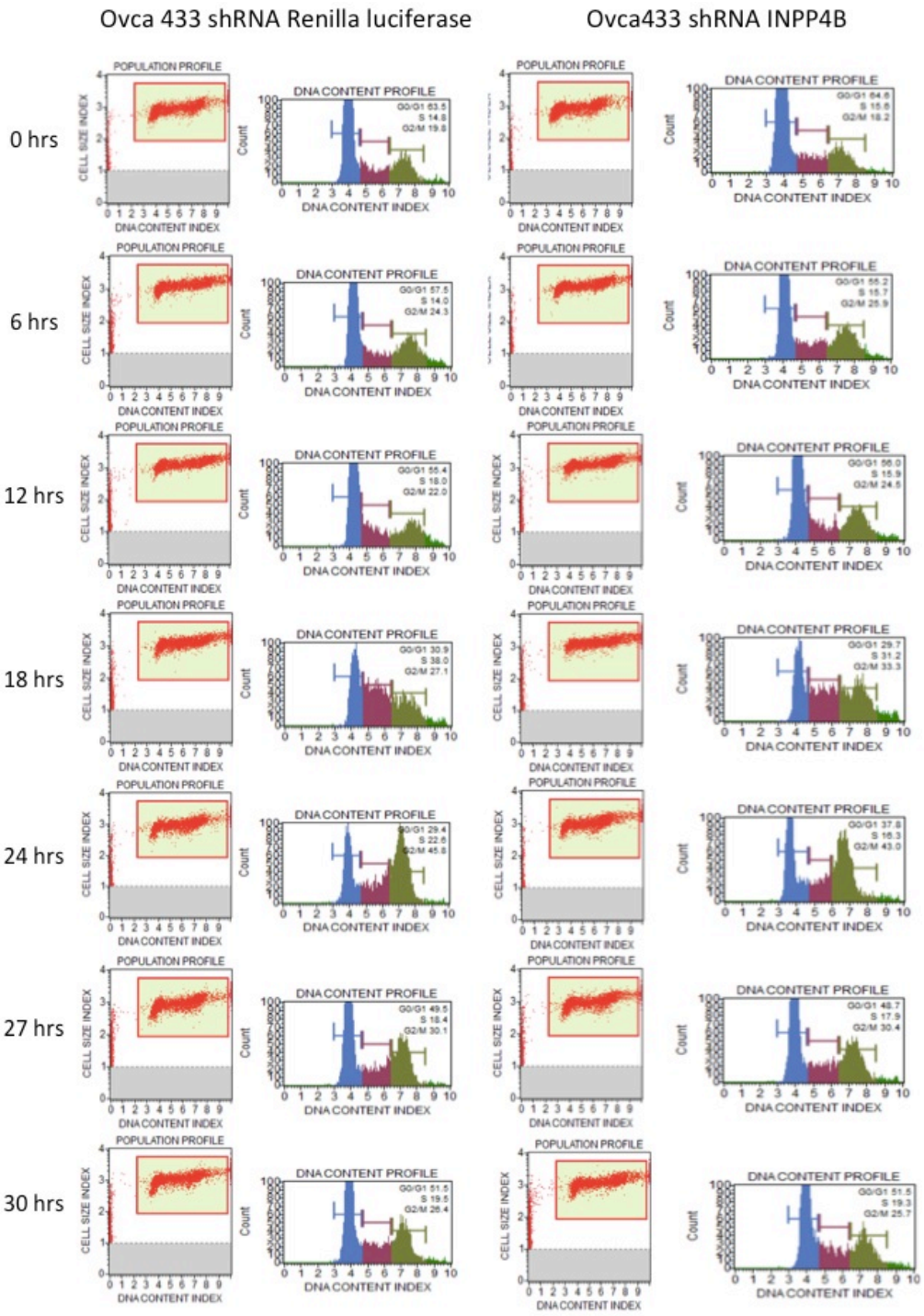

Figure 3.17. Cell cycle analysis of Ovca433 knockdown cell pool upon serum starvation. Ovca433 knockdown cell pools were serum starved for 18 hrs, fixed at the indicated time points and cell cycle stage analysed using the Muse Cell Analyzer. Experiments were conducted independently three times. The depicted graphs are representative primary data for one experiment used to assess cell cycle progression.

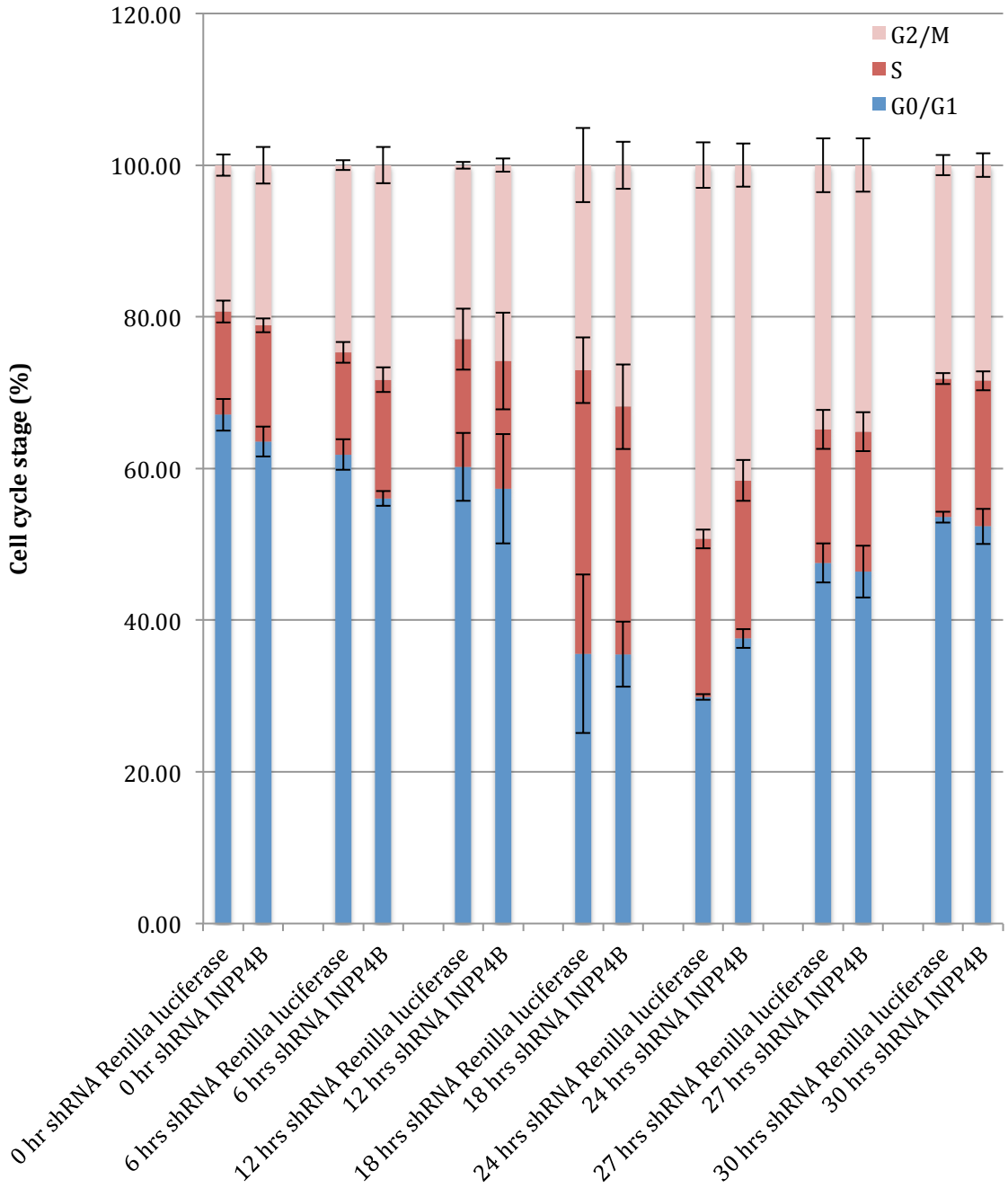

Figure 3.18. Cell cycle progression of Ovca433 knockdown cell pool upon serum starvation. Ovca433 knockdown cell pools were serum starved for 18 hrs, fixed at the indicated time points and cell cycle stage analyzed using the Muse Cell Analyzer. Unchallenged Ovca433 INPP4B-deficient cells displayed aberrant cell cycle progression compared to the knockdown control counterparts 24 hrs after serum replenishment ($p = 0.006$). One sample was used per condition. The t-test was used for statistical analysis and experiments were conducted independently three times. The

depicted graph is the average of all three experiments and representing the outcome of all three experiments.

3.3 Discussion

The tumour biology of ovarian cancer has been frequently associated with genetic alterations in components of DNA repair, the most well established genes being *BRCA1/2*. However, recent studies have revealed that women possess 'BRCAness' in up to a third of all ovarian cancers, as well harbour HR deficiency in almost half of ovarian carcinomas. Thus, investigation of INPP4B in the context of DNA repair in ovarian cancer could shed new light on its role in DDR, and its therapeutic relevance.

Microarray analyses comparing MCF-10A shRNA-INPP4B with MCF-10A shRNA Renilla luciferase expressing cell pool gene expression revealed two novel gene signature associations: 'poor survival' and 'BRCA1-mutant' gene signatures (appendix 4). These two gene sets have never previously been associated with knockdown of INPP4B in human mammary epithelial cells. The prevalence of *BRCA1* mutations within breast and ovarian cancer highlighted the importance of this finding, and consequently further analysis was conducted to verify the BRCA1-mutant signature through validation of the microarray results. The 37 gene-set that makes up this gene signature consists of a collection of transcription factors, proteases and ligases and protein kinases that are differentially expressed when BRCA1 is mutated, as defined by the KEGG pathway database. The microarray analysis revealed differential log(2) fold changes ranging from -3.78 to 4.00 (appendix 5). From the 37 gene set, 12 of the genes were selected for relative quantification via qPCR: NTN4, GPC1, CAMK2N1, CA2, MPDZ, TFPI, CA12, SPARC, TMEM98, GALNT7, C5ORF13, ANKRD35. These genes encode proteins involved in transcription regulation (ANKRD25), neural function (C5ORF13, MPDZ), glycosylation (GALNT7), extracellular matrix synthesis and cell shape change (SPARC), respiration (CA2, CA12), blood coagulation (TFPI), cell

growth (CAMK2N1) and cell migration/adhesion/proliferation/apoptosis (NTN4). While eight of the genes examined by qPCR exhibited similar differential gene expression (in direction and magnitude) to the microarray results, the qPCR gene expression values for genes CA2, TFPI, TMEM98 and SPARC were much lower compared to the log(2) fold changes found in the microarray analysis. While qPCR is a commonly used validation tool for confirming microarray results, data from these two methods of analyses often result in disagreement. Within the individual techniques themselves, they possess inherent pitfalls that may significantly influence the data obtained. The multiple sources of variability in microarray analysis include differences in arrays, dye labelling, efficiency in reverse transcription and hybridisation. Likewise, qPCR generated data also has several sources of error, namely amplification biases, exponential amplification of errors, mispriming, formation of primer dimers and the changing efficiency of qPCR at later cycles. High quality RNA is essential for accurate results, as gene expression can be affected by contaminating factors, salts, alcohols, phenols, all of which can affect the reverse transcriptases, and consequently RNA amplification in both methods. It should be noted that the MCF-10A knockdown cell pools derived for the microarray experiments and the ones used for qPCR were independently generated, and consequently, further adds to biological variances that contribute to discrepancies found between qPCR generated data and microarray data (Etienne et al., 2004).

Another explanation for the variability of results lies in the primer selection and microarray probe complementation. These probes have DNA oligomer sequences that target several splice variants of individual genes. Multiple probes for the same gene can target differing combinations of the gene splice variants and consequently the resulting

log(2) fold change can also be vastly different. An example of this includes the gene TFPI, which has four probes exhibiting log(2) fold changes of 0.68, 1.88, 4.00 and 3.64. These log(2) fold changes represent hybridisation of the probes for the following transcript variants (TV), respectively: TV2, TVX2; TV1, TVX1 – 3; TV1, TVX1, TVX2, TVX4; TVX1 – 4. Each of these probes target differing combinations of splice variants, and consequently the log(2) fold changes that arise are also different in magnitude. Furthermore, Etienee *et al.* reported that an increase in distance between the location of the PCR primers and the microarray probe on a given gene results in a decrease in correlation between the two methods (Etienne et al., 2004), which would also contribute to the discrepancies observed in the validation of the gene signature. Nevertheless, the gene expression trends obtained by qPCR echoed those found in the microarray data.

Down-regulation of INPP4B in MCF-10A shRNA BRCA1 cells was an interesting and novel finding; however, due to lab constraints this observation was not further investigated. While more experiments are required to further elucidate the relationship between INPP4B loss and BRCA1 loss in these cells, the results suggest that INPP4B may play a role in DNA damage repair in human mammary epithelial cells, in agreement with the finding of the BRCA1-mutant gene signature found in INPP4B deficient MCF-10A cells.

To further confirm that INPP4B loss in MCF-10A cells results in a BRCA1 mutant gene signature, the obtained microarray data were compared to a gene expression profile of BRCAness defined by Konstantinopoulos *et al.* that correlates with responsiveness to chemotherapy and with outcome in patients with epithelial ovarian cancer (EOC)

(Konstantinopoulos et al., 2010). A publicly available microarray data set containing tumour expression data from 61 EOC patients with either sporadic disease or BRCA1/2 germline mutations was used to derive the 60 gene signature into two clusters, BRCA-like (BL) and non-BRCA-like (NBL), of which the gene set was able to distinguish BL from NBL with 94% accuracy. Appendix 7 compares this 'BRCAness' signature with the MCF-10A shRNA INPP4B microarray data, and the summary of the data is depicted in Figure 3.6C. 71% of the differentially expressed genes found in the MCF-10A shRNA-INPP4B microarray data correlated with the gene expression change found in the BRCAness profile. 22 genes that were part of the 'BRCAness' signature were not differentially expressed in the microarray and therefore not included in this analysis. The two microarray datasets were derived from differing tissue types, as well as between malignant and non-malignant cells, which could explain why the correlation between the two datasets was not stronger. However, the comparison marks an important transition from investigating the DNA damage defect in mammary epithelial cells to ovarian cancer cells, which is the tissue type of interest for this study, and it is encouraging to observe significant correlation despite some biological differences between the two datasets.

In order to investigate DNA repair in individual cells, comet assays were conducted in both Ovca429 and Ovca433 knockdown cell pools to assess the repair of damage DNA over time after exposure to X-ray radiation. Ovca429 knockdown cell pools revealed a delay in DNA repair in cells harbouring decreased INPP4B expression compared to the shRNA Renilla luciferase control cells upon irradiation. Ionising radiation (IR) strand breaks primarily occur through reaction of reactive oxygen species (ROS) with the hydrogen radical on the surface areas of the DNA backbone (Balasubramanian et al.,

1998) and IR produces SSBs at a rate 20 times more than DSBs (Bradley and Kohn, 1979). With regards to both cell lines, the cells displayed a heterogeneous response to the DNA damage, with some cells possessing greater tail moments upon IR, and others, smaller tail moments. In experiments conducted using Ovca429 knockdown cell pools, the olive tail moments of both the shRNA INPP4B cells and the control cells were statistically different 15, 30 and 60 min after irradiation; However for the latter two time points, the olive tail moments were below 2, in which the cells visually did not possess a comet tail, and hence were assumed not to possess a large level of DNA damage. 15 min after damage the shRNA INPP4B cells clearly displayed larger tail moments, with cells retaining a mean tail moment of 3.67 compared to 2.31 in the control cells, indicating that cells with decreased INPP4B expression exhibits a delay in DNA repair compared to cells with normal INPP4B expression. While the results indicate that loss of INPP4B indeed results in a DNA repair defect, the specifics of the DNA lesions or mechanisms involved that caused this delay could not be defined due to the broad nature of the assay conducted. Also, due to the alkaline nature of the protocol implemented, the comet assay detects all forms of strand breaks, SSBs and DSBs, as well as alkali-labile lesions. The neutral comet assay, which was originally developed to detect primarily DSBs independent of SSBs (Olive and Banath, 2006), was not conducted due to the unreliable results of the protocol at hand. More extensive comet assays could be conducted to detect specific kinds of DNA damage, such as base damage, and interstrand cross-link, as follow up experiments. Finally, is important to note that the comet assay detects the rejoining of strand breaks and does not provide information on the fidelity of the repair (Olive et al., 1994). However, the results did provide a good indication that INPP4B plays a role in timely DNA repair and merited further investigation.

The Ovca433 shRNA INPP4B cells, on the other hand, did not display an aberration of DNA repair. This can be explained potentially by the biological differences between the two ovarian cancer cell lines. For example, the Ovca429 cell line carries a *PI3KCA* mutation that is not found in the Ovca433 cell line. The oncogenic nature of the constitutively active catalytic subunit of class IA PI3K in Ovca429 cell lines could aid in the sensitivity of the cells towards inefficient repair of DNA damage upon concomitant loss of INPP4B. Ovca433 cell lines may possess amplified repair mechanisms that dilute the effect of INPP4B knockdown, and therefore no DNA repair was observed in this particular cell line. To note, the disparity between the magnitude of the DNA damage induced by IR between the two cell lines analysed was a result of human error, a miscalculation of the intended dose imposed due to routine recalibration of the dosimeter.

To further investigate the DNA repair delay found upon comet assay analysis, detection of γH2AX, RAD51, and 53BP1 was conducted in Ovca429 knockdown cell pools to examine whether loss of INPP4B had an effect on the individual cell's immediate response to DNA damage, as well as the integrity of HR and NHEJ repair *in situ*. Etoposide was used to introduce strand breaks in the cells for these experiments. While conducting the experiment with IR would allow for a more comparative study of DNA repair in these cells with the results of the comet assays, due to laboratory limitations, etoposide was used as an alternative agent for DNA damage. Etoposide induces DNA damage by the inhibition of topoisomerase II (TOP2), an important enzyme that introduces transient DSBs and re-ligates them during DNA replication (TOP2α) and transcription (TOP2β) to relieve torsional stress. Etoposide has very low affinity for

intact DNA, but can readily insert into the DNA cleavage site formed by the TOP2 enzyme as it interacts with the DNA, preventing TOP2 from re-ligating the cleavage site (Wu et al., 2011). Hence, treatment of cells with etoposide results in DSB formation, although etoposide is also capable of generating SSBs (Bromberg et al., 2003).

Ovca429 shRNA INPP4B expressing cells were subjected to etoposide treatment for 1 hr to introduce strand breaks, and after the cells were washed thoroughly to remove the drug and foci were quantified to evaluate response to DNA damage over time. Without any DNA damage imposed, γH2AX foci were found significantly increased in Ovca429 shRNA INPP4B cells that were treated with DMSO only, and held a mean foci per nucleus value of 9.4, almost twice that of the control value, which is indicative of shRNA INPP4B expressing cells harbouring more genomic instability than their control knockdown counterparts. Interestingly, immediately after DNA damage was induced, both knockdown cells exhibited similar levels of damage, despite the increased mean foci per nucleus shRNA INPP4B cells retained in the control conditions. Thereafter, γH2AX mean foci values were significantly higher in shRNA INPP4B cells 30, 60 and 180 min after DNA damage compared to the control cells. Of note, the cells responded to the treatment in a heterogeneous manner. Ovca433 cells responded similarly, with the shINPP4B cells also retaining γH2AX 180 min after DNA damage. Akin to the γH2AX results, 53BP1 foci were found increased in Ovca429 shRNA INPP4B cells 6 and 12 hrs after treatment with 10 μM etoposide compared to the control cells, as well as DMSO treated conditions. The observations of the similarity in trend of 53BP1 foci formation to the γH2AX foci formation in shRNA INPP4B expressing cells are in line with evidence that 53BP1 accumulation at the DSBs is dependent on γH2AX formation

(Mallette et al., 2012). Treatment of Ovca429 knockdown cell pools with 10 μM etoposide and subsequent analysis of cells during DNA repair revealed a persistence of RAD51 foci 12 and 24 hrs after DNA damage in shRNA INPP4B cells compared to the control cells. Interestingly, 24 hrs after damage cells with reduced INPP4B expression displayed mean foci per nucleus values almost twice that of the control cells (13.81 vs 6.69, $p = 1.21x10^{-16}$), suggesting an increase in the number of DSBs generated after the initial genetic insult. Treatment of Ovca433 knockdown cell pools by IR also revealed similar findings of RAD51 persistence in cells with loss of INPP4B. While loss of BRCA1 function was shown to result in suppressed RAD51 foci formation, loss of ATR was linked to increased RAD51 foci formation in conjunction with increased γH2AX foci (Banath et al.; Chanoux et al., 2009). The experiments that address the relationship between INPP4B and ATR will be discussed in the next chapter. The above experiments clearly show that INPP4B regulates efficient DNA repair, including RAD51 related repair. Given that RAD51 is a crucial protein involved in homology-mediated pairing and strand exchange in HR, it can be proposed that loss of INPP4B is involved in regulation of HR repair efficiency. Finally, as aforementioned, Plo et al. demonstrated that activated Akt1 repressed HR through cytoplasmic retention of BRCA1 and Rad51 resulting in a BRCA1-deficient phenotype in breast cancer (Plo et al., 2008a). Thus, both Ovca429 and Ovca433 knockdown cell lines were investigated for BRCA1 foci formation upon IR. Knocking down INPP4B in both cell lines did not result in cytoplasmic retention of BRCA1 nor an aberration of BRCA1 foci formation, suggesting a different mechanism of defective DNA repair in INPP4B deficient cells.

Cell cycle studies were conducted to investigate if INPP4B loss impacted cell cycle progression. INPP4B-deficient Ovca433 cells resulted in a decrease in cell population

24 hrs after serum starvation in the S/G2/M phase (62.4%) compared to the control cells (70.2%) (p=0.006) indicating a faster progression through the cell cycle. While a further time point analysis between 18 hrs and 24 hrs is needed to conclude the meaning of this statistical difference, it was not conducted due to practical scheduling difficulties fixing the cells over a 30 hrs period. It is likely that INPP4B-deficiency results in an acceleration of cell cycle progression due to hyperactivation of the PI3K/Akt pathway. Another possibility is that loss of INPP4B may result in defective cell cycle checkpoints, since the cells displayed faster progression through the cell cycle. Investigating G1, S and G2 cell cycle control by flow cytometry in the context of INPP4B loss may provide more insight if there is any cell cycle checkpoint aberration. It would be of interest to investigate if DNA damage affects cell cycle progression in INPP4B-deficient cells. Affected cell cycle stages, if any, would give an indication as to which cell cycle specific proteins may also be affected by the loss of INPP4B. Additional cell cycles studies for INPP4B-deficient Ovca429 cells were not conducted due to time constraints.

Due to time restraint the DNA repair defect in Ovca429/Ovca433 INPP4B knockdown cell pools was not further investigated. Flow cytometry analysis could have been conducted to assess in which cell cycle does γH2AX, 53BP1 and RAD51 foci form in shRNA INPP4B cells relative to the control cells. GFP assays could have also been carried out to measure HR and NHEJ integrity specifically (Gunn and Stark, 2012). However, the evidence accumulated from the series of experiments conducted suggests that loss of INPP4B indeed leads to a DNA repair defect in the Ovca429 ovarian cancer cell line. While mechanisms for this defect have yet to be established, it is clear that INPP4B plays a role in HR efficiency and ovarian cancer patients harbouring a loss of

INPP4B may benefit from therapies that promote the use of DNA repair inhibitors in the context of synthetic lethality.

CHAPTER 4. Biological function of INPP4B

4.1 Introduction

One of the approaches in personalising cancer treatment is through stratification of DNA damage response (DDR) proteins based on their status, and subsequent implementation of appropriate therapies that exploit the defective DNA repair pathway. In the previous chapter a BRCA1-mutant gene signature was identified in INPP4B-deficient human mammary epithelial cells via microarray analysis, and then a DNA repair deficiency was confirmed in INPP4B-deficient ovarian cancer knockdown cells. Further investigation of INPP4B in the context of DNA repair would provide not only a more in depth understanding of the function of INPP4B, but also potentially widen the selection of therapeutic agents that would be effective in treating INPP4B-deficient tumours. Thus far, no studies have examined the mechanism of INPP4B and its role in DDR. Having established the cellular phenotypes associated with loss of INPP4B, further experiments were conducted to determine the molecular mechanisms that may result in the observed DNA repair defect. The cell systems were switched from the ovarian cancer cell lines to human embryonic kidney 293T cells due to its enhance transfection efficiency, which is needed for overexpression studies conducted to investigate interacting partners of INPP4B. Immunoblotting was conducted to investigate the loss of INPP4B in relation to the expression of other DDR proteins in MCF-10A cells, ovarian cancer cell lines, as well as in mouse embryonic fibroblasts (MEFs) containing loxP-flanked INPP4B. Potential phosphorylation sites of INPP4B as a substrate of ATR/ATM were also assessed. In addition, cell cycle studies were carried out to observe any aberration in cell cycle progression due to INPP4B loss. Finally, the interacting domain of INPP4B was determined using GST-pull down assays (Harper and Speicher; Katzen, 2007).

Results

4.1.1 Reduced ATR expression observed in INPP4B deficient Ovca429 knockdown cells.

Previous experiments revealed a DNA repair defect in INPP4B deficient breast and ovarian models. Supporting this finding, a reduction of INPP4B protein in MCF-10A shRNA-BRCA1 expressing cells was observed in immunoblots (figure 4.1A). In addition, reduced ATR protein levels were found in Ovca429 INPP4B knockdown cell pools compared to controls. No changes in BRCA1 protein expression were detected in Ovca429 and Ocva433 shRNA INPP4B knockdown cell lines relative to the control (figure 4.1B). These findings provide novel evidence that loss of INPP4B results in an aberration in DNA repair through reduced levels of key DNA protein, ATR, while BRCA1 protein levels remain unchanged. PhosphoSer473 Akt levels upon INPP4B knockdown were found significantly increased upon serum stimulation in Ovca433 cells in experiments conducted by Dr. Christina Gewinner, indicating that depletion of INPP4B is sufficient for increased lipid dependent signalling. Upon EGFR/Her2 inhibitor Erlotinib and Lapatinib treatment of Ovca433 shRNA-INPP4B cell pools show reduced/absent phosphoSer473 Akt (figure 4.1C).

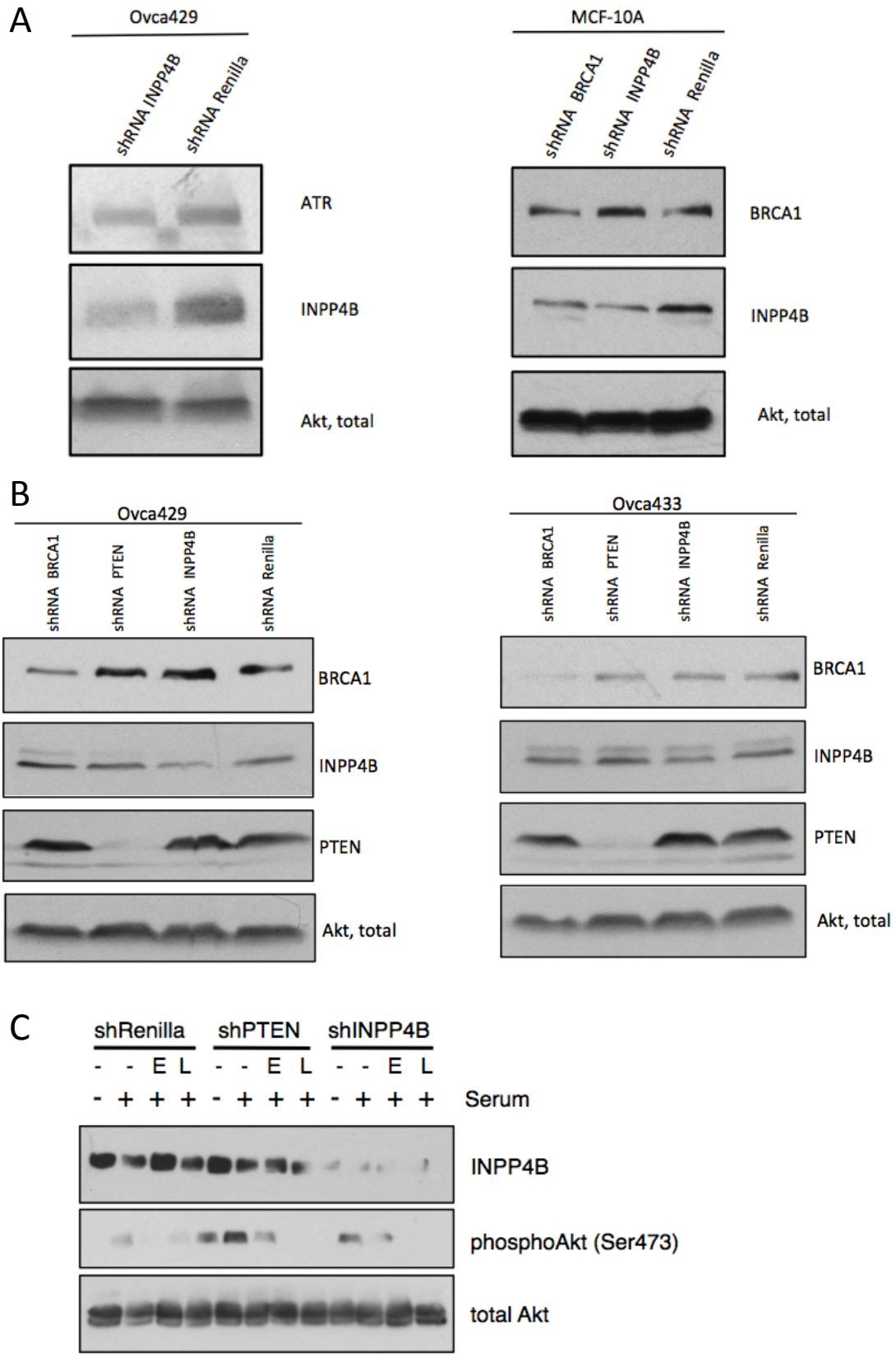
A
Ovca429
shRNA INPP4B
shRNA Renilla
ATR
INPP4B
Akt, total
MCF-10A
shRNA BRCA1
shRNA INPP4B
shRNA Renilla
BRCA1
INPP4B
Akt, total
B
Ovca429
shRNA BRCA1
shRNA PTEN
shRNA INPP4B
shRNA Renilla
BRCA1
INPP4B
PTEN
Akt, total
Ovca433
shRNA BRCA1
shRNA PTEN
shRNA INPP4B
shRNA Renilla
BRCA1
INPP4B
PTEN
Akt, total
C
shRenilla
shPTEN
shINPP4B
- - E L - - E L - - E L
- + + + - + + + - + + + Serum
INPP4B
phosphoAkt (Ser473)
total Akt

Figure 4.1. Immunoblots detecting ATR and BRCA1 protein expression in various cell lines. (A) A reduction of ATR and INPP4B protein expression was found in Ovca429 shRNA INPP4B and MCF-10A shRNA BRCA1 cells relative to the shRNA Renilla luciferase control, respectively. (B) No changes in BRCA1 protein expression were detected in Ovca429 and Ocva433 INPP4B knockdown cell lines were detected relative to the control. Immunoblotting was conducted independently three times. (C) Experiments conducted by Dr. Christina Gewinner revealed an increase of phosphoSer473 Akt levels upon INPP4B knockdown and serum stimulation in Ovca433 cells. In addition, Ovca433 cell pools were treated with the inhibition of the EGFR/Her2 pathway inhibitors Erlotinib and Lapatinib to study the effects of EGFR signalling in the context of INPP4B knockdown in Ovca433 cells. Erlotinib and Lapatinib treatment of Ovca433 shRNA-INPP4B cell pools show reduced/absent phosphoSer473 Akt. This experiment was conducted independently three times.

4.1.2 Loss of INPP4B in mouse embryonic fibroblasts results in concomitant loss of BRCA1, ATR and ATM protein levels

The experiments in this subsection were conducted by Dr. Christina Gewinner (UCL, UK). Floxed INPP4B (INPP4B$^{fl/fl}$) MEFs were obtained from Prof. Takehiko Sasaki, (Akita University, Japan). INPP4B expression was ablated in INPP4B$^{fl/fl}$ MEFs through infection with adenovirus Cre recombinase (Ad5Cre) and immortalised with shRNA against p53. Western blot analysis of dose-dependent Ad5Cre infection efficiency in INPP4B$^{fl/fl}$ shRNA-p53 MEFs resulted in loss of INPP4B greater than 50% 72 hrs post – infection (figure 4.2). Investigation of BRCA1, ATR and ATM protein levels revealed concomitant loss of BRCA1, ATR and ATM proteins. While modest downregulation of INPP4B protein expression resulted in reduced BRCA1 and ATM protein expression, a greater INPP4B protein level reduction was required to downregulate ATR protein levels. To control for a potential Ad5Cre off-target effect INPP4B, BRCA1, ATR and ATM protein levels of infected wildtype MEFs were compared to INPP4B$^{fl/fl}$ MEFs, however no changes in protein levels were detected in wild-type MEFs confirming the specificity of the observation described above (figure 4.3). These results suggest a key role for INPP4B in the stability three major DDR proteins BRCA1, ATM and ATR either on a protein level or mRNA level in transcription or translation.

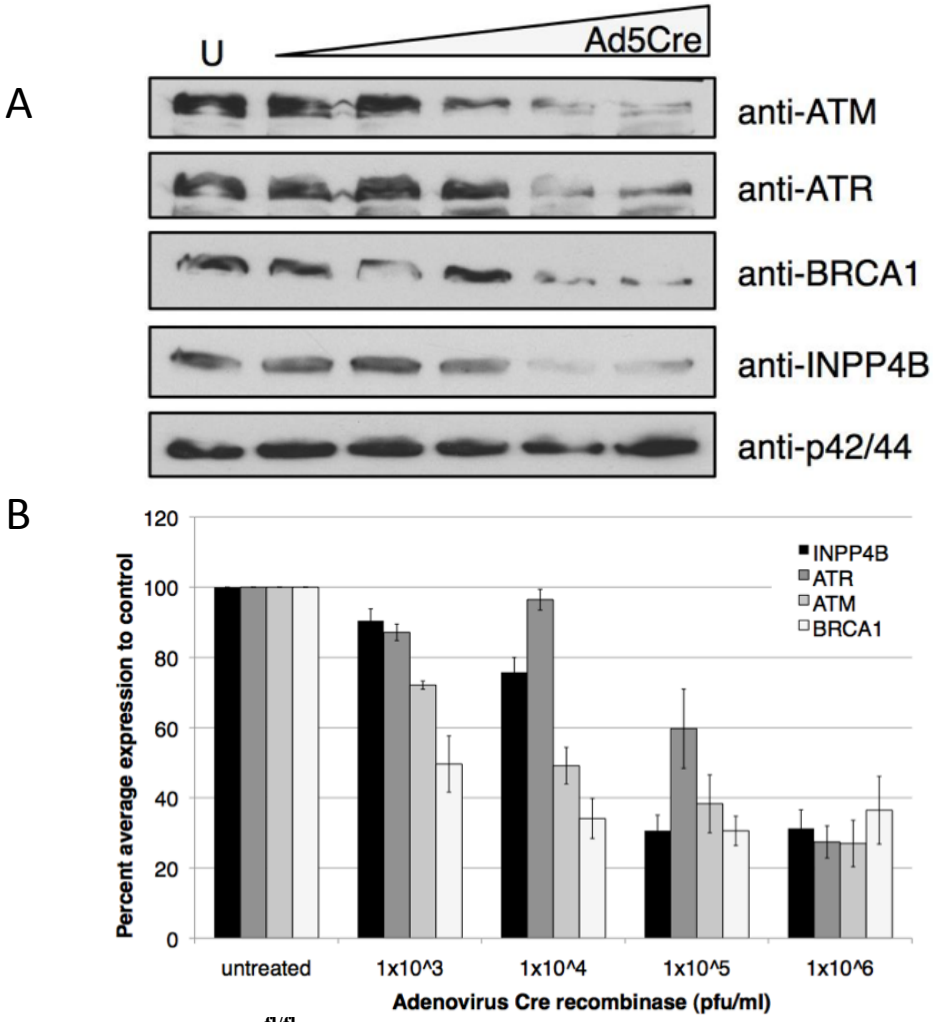

Figure 4.2. INPP4B$^{fl/fl}$ MEFs results in loss of ATM, ATR and BRCA1 protein expression with increasing concentrations of adenovirus Cre recombinase. (A) Immunoblots depicting increasing loss of INPP4B in conjunction with loss of ATR, ATM and BRCA1 protein expression. "U" represents the untreated MEFs. (B) Quantification of protein expression of INPP4B, ATR, ATM and BRCA1 relative to p42/44 loading control. Semi-quantitative analysis was conducted using ImageJ. Experiments were conducted independently three times by Dr. Christina Gewinner (UCL, UK).

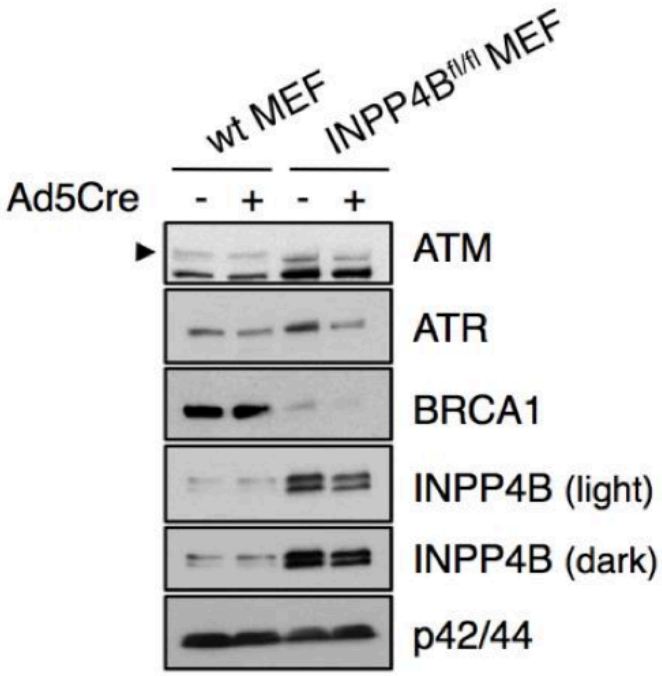

Figure 4.3. No off-target effects were observed in wild-type MEFs upon administration of adenovirus Cre recombinase. Infection of wild-type MEFs (wt MEFs) with adenovirus Cre recombinase did not result in changes in protein levels of ATM, ATR, BRCA1, and INPP4B, as depicted on the immunoblots. Experiments were conducted independently three times by Dr. Christina Gewinner (UCL, UK).

4.1.3 INPP4B, BRCA1, and ATR interact in a protein complex

Since loss of INPP4B in MEFs resulted in loss of key ATM, ATR and BRCA1, protein-protein interaction of INPP4B and the aforementioned DNA repair proteins was investigated to see if the loss was due to protein-protein interaction. 293T cells expressing Flag-tagged INPP4B (Flag-INPP4B) or empty Flag vector (control) were lysed and Flag-INPP4B protein complexes immunoprecipitated. Western blot analysis revealed specific interaction of INPP4B with ATR and BRCA1, but not with ATM or PTEN (figure 4.4). Interestingly, increased protein levels of BRCA1 in cell lysates overexpressing Flag-INPP4B was observed compared to control lysates. GST-pull down experiments using bacterial overexpressed GST-tagged fragments of N-terminal (aa1-460), middle (aa200-760) or C-terminal (aa460-924) INPP4B fragments (depicted in figure 4.5A) and Flag-tagged ATR or BRCA1 overexpressed in 293T cells revealed specific interactions of ATR and BRCA1 with the N-terminal and middle fragment of INPP4B but not with the C-terminal fragment in immunoblots (figure 4.5B). For these experiments it is important to note that the control used in this experiment consisted of sephorose beads incubated in FLAG-tagged lysates, rather than a GST-empty vector control. GST pull-down studies were conducted as published previously (Harper and Speicher; Katzen, 2007).

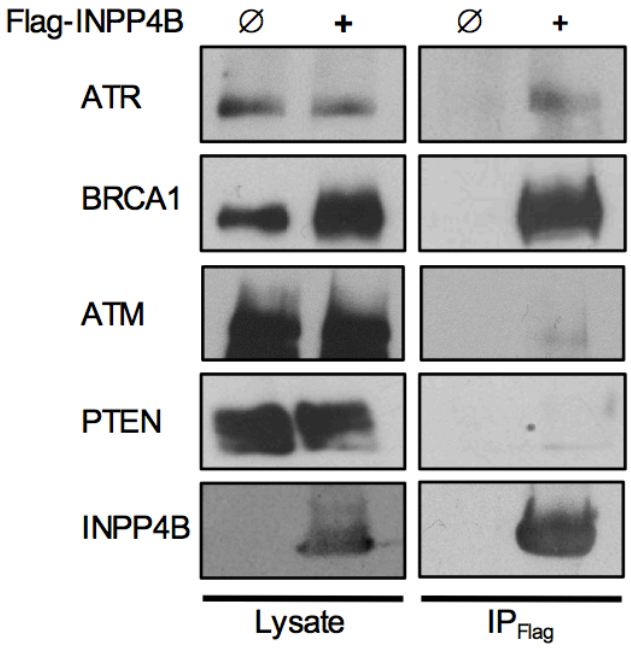

Figure 4.4. INPP4B forms a protein complex with endogenous ATR and BRCA1. 293T cells were transfected with pcDNA3/FLAG empty (indicated by Ø sign) or pEAK/FLAG-INPP4B (indicated by + sign) using PEI (9002-98-6, Polyscience). 48 hrs post – transfection cells were lysed and lysates incubated with anti-FLAG M2 beads. Input lanes represent 1% of protein lysates. Experiments were conducted independently three times.

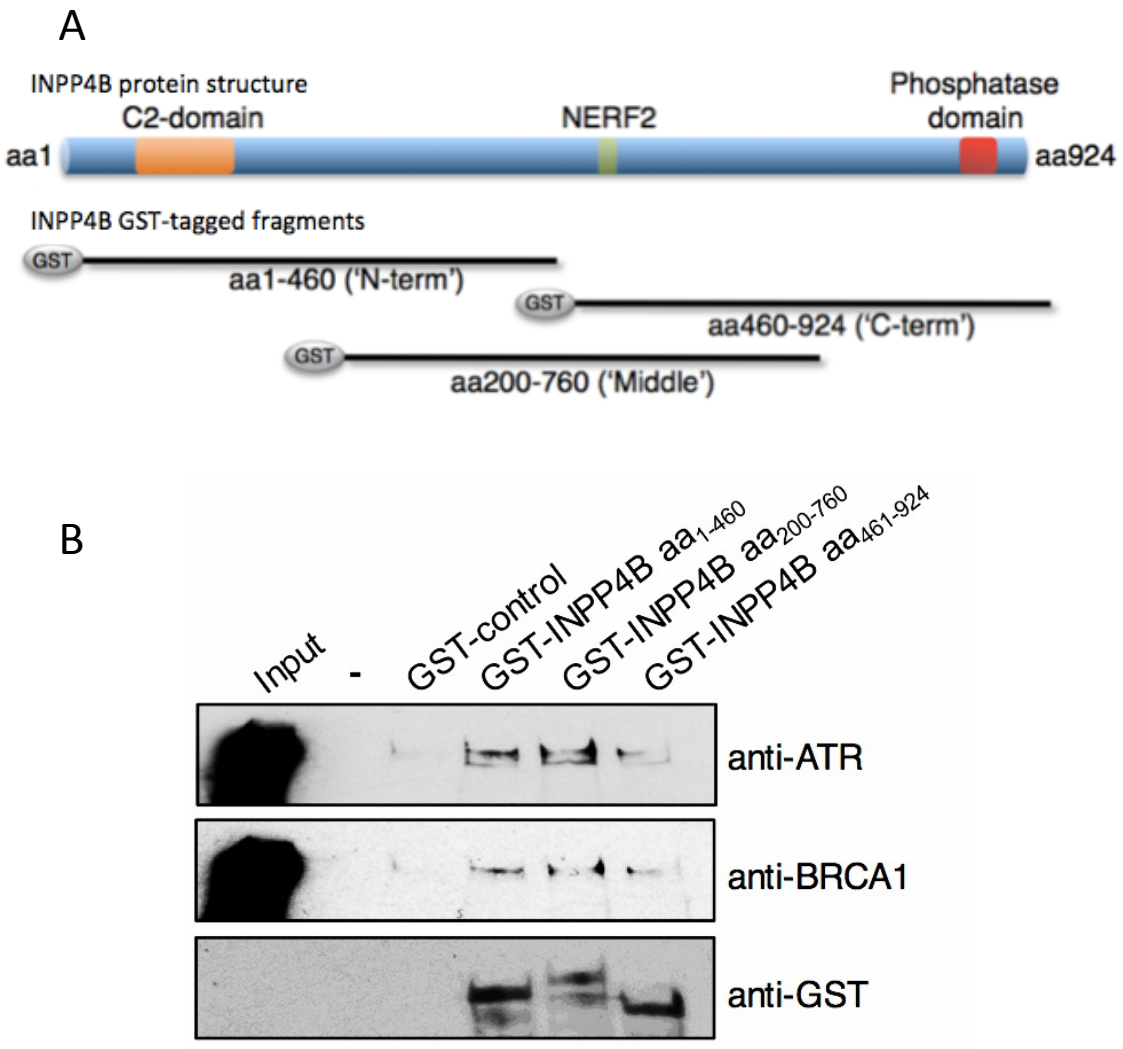

Figure 4.5. 293T cells overexpressing Flag-tagged ATR or BRCA1 revealed interactions of ATR and BRCA1 with the N-terminal and middle fragment of INPP4B but not with the C-terminal fragment. (A) GST-tagged fragments of N-terminal (aa1-460), middle (aa200-760) or C-terminal (aa460-924) were generated as depicted in the diagram. The aa1-460 N-terminal fragment contains the C2-domain of INPP4B, the aa200-760 middle fragment contains a NERF2 domain and the aa460-924 C-terminal domain contains the phosphatase domain of INPP4B. (B) GST-fusion constructs were used to 'fish' in extracts from 293T cells transfected with pcDNA3.1 FLAG-ATR. Each INPP4B fragment was incubated with precleared Glutathione

Sepharose Fast Flow (GE Healthcare Life Sciences, UK) slurry for 2 hrs, then after washing the beads were incubated with the ATR-lysate for 30 min. Immunoblotting was carried out as described in section 2.1.3. Antibody detecting ATR (Bethyl Laboratories, UK; 1:10,000 primary antibody dilution) was used to detect interaction of ATR with GST-tagged INPP4B fragments. Input lanes were also detected and represent 1% of protein lysates in pulldown assays. GST assays revealed BRCA1 and ATR interacting with the N-terminal and middle fragment of INPP4B, but not with the C-terminal fragment. Input lanes represent 1% of protein lysates. Experiments were conducted independently three times (UCL, UK). In these experiments, only empty agarose beads incubated with FLAG-tagged lysates were used as a control, rather than using a GST-empty vector control.

4.2 Discussion

We have shown in previous experiments a DNA repair defect in INPP4B-deficient ovarian cancer cell lines – Upon etoposide treatment INPP4B-deficient cells revealed an increase and retention of γH2AX, RAD51 and 53BP1 foci relative to controls indicating abnormal DNA repair and dysfunctional HR. Further experiments were carried out to investigate association of INPP4B with key DDR protein players and elucidate a mechanism that would explain the observed DNA defect.

Detection of DDR proteins in Ovca429 and Ovca433 unchallenged knockdown cell pools revealed a link between INPP4B and DDR protein expression levels. Specifically, MCF-10A cell pools containing BRCA1 knockdown possessed reduced INPP4B protein expression compared to the control knockdown cell pools. In addition, shRNA-INPP4B expressing Ovca429 cell pools harboured reduced ATR protein expression compared to the mock-knockdown controls. BRCA1 expression levels in ovca429 and ovca433 shRNA-INPP4B cell pools remained unchanged compared to the control. Depletion of INPP4B resulted in increased S473 phospho-Akt expression, revealing that loss of INPP4B is sufficient in increasing lipid-dependent signalling.

Experiments conducted in INPP4B deficient MEFs revealed concomitant loss of ATR, ATM and BRCA1 protein expression. Interestingly, increasing loss of INPP4B resulted in increasing loss of ATM, ATR and BRCA1, suggestive of a function of INPP4B protein in the expression-dependent stability of these critical DDR proteins. In order to address the mechanisms underlying the regulation of protein levels of ATR, ATM and BRCA1 proteins upon loss of INPP4B, protein-protein interaction in 293T cells overexpressing INPP4B were studied. While investigation of endogenous proteins

avoids any artificial effects of affinity tags or overexpression, endogenous protein-protein interaction was not conducted due to the unavailability of INPP4B antibody that functions effectively in immunoprecipitation experiments. In addition, the ovarian cancer cell lines used in this study could not be efficiently transfected and were consequently not used for overexpression studies. Instead, 293T cells were used for these experiments due to excellent transfection protein expression efficiency of the cell line. Immunoprecipitation studies revealed that 293T cells overexpressing INPP4B revealed an interaction of INPP4B with BRCA1 and ATR. Surprisingly, ATM was not found to interact with INPP4B, suggestive of different molecular mechanism that manifest with changing protein levels of INPP4B.

The protein section in which INPP4B interacts with ATR and BRCA1 was also investigated. INPP4B domains were cloned into bacterial GST overexpression plasmids and GST-tagged INPP4B fragments representing the N-, middle- and C-terminal sections of INPP4B were bacterially expressed and isolated. Protein-protein interactions of these bacterially expressed and isolated INPP4B fragments with BRCA1 and ATR were investigated in GST-pull down assays. The N-terminal region of INPP4B (aa1-460) and the middle region (aa200-760) of INPP4B were identified to be predominantly necessary for interaction with ATR and BRCA1. Further refining of the interacting domain could be investigated by cloning the overlapping region of the N- and middle fragment, isolating these fragments and assess interaction with BRCA1 and ATR in GST-pull down assays. It is worthy to note that in the GST pull-down assays, the control used consisted of sepharose beads incubated in FLAG-tagged lysates, and therefore does not take rule out possible sticky interaction of the FLAG-tagged ATR/BRCA1 with the GST-tag itself. However, given that three of the GST-tagged

INPP4B fragments resulted in varying levels of ATR and BRCA1 binding, it is likely that the effects are authentic.

Other questions that arise from the data obtained include investigating the exact mechanism of the interaction of INPP4B with BRCA1 and ATR. The protein interactions observed do not give a clear indication of whether or not INPP4B interacts directly or indirectly with BRCA1 and ATR. In order to determine if INPP4B interacts directly with BRCA1 and ATR, a yeast two-hybrid screening assay could be conducted. Yeast cells would be transfected with two plasmids consisting of INPP4B and ATR, coupled to the DNA-binding domain of a yeast transcription factor, like Gal4, and a cDNA fragment containing the activation domain on the transcription factor, respectively. If INPP4B and ATR interact directly, the DNA-binding domain and the activating domain would be in close proximity to each other resulting in the transcription activation of the reporter gene. It would also be worthy to investigate and identify other proteins that INPP4B may indirectly or directly be interacting with in a complex with ATR and BRCA1 by affinity purification of tagged INPP4B, followed by mass spectrometry (the same could be done with BRCA1). Also, subcellular localisation of INPP4B could be also determined using relevant lysis buffers to isolate nuclear proteins from cytoplasmic proteins and membrane proteins. Due to time constraints, however, the proposed experiments were not carried out. However, the novel interaction identified between INPP4B and ATR/BRCA1 shows that INPP4B plays a crucial role in modulating the stability of key players of the DDR pathway and may indicate a potential protein function of INPP4B. INPP4B deficiency in the context of ovarian cancer therapies that engage in the principle of synthetic lethality should

therefore be assessed to investigate the potential role of INPP4B as a biomarker of ovarian cancer treatment.

CHAPTER 5. Treatment of INPP4B deficient cells with DNA repair inhibitors

5.1 Introduction

Inhibition of DNA repair in cancer cells used to enhance the cytotoxicity of chemotherapies has been subjected to extensive scientific research over the last few decades. Amongst the numerous drugs that target critical DNA repair proteins as anti-cancer treatment, the most developed DNA repair inhibitors to date are the PARP inhibitors. There are currently nine PARP inhibitors in clinical development to treat a variety of cancer types that potentiate the effects of chemotherapy and radiation, as well as exploiting synthetic lethality in tumours with defective homologous recombination (HR) repair (PARP inhibitor trials in *BRCA*-mutated ovarian cancers, table 5.1; PARP inhibitor trials in sporadic ovarian cancers, table 5.2). The most promising results thus far stem from single-agent treatment of *BRCA1/2*-mutant breast and ovarian cancers in the clinic (Audeh et al., 2010; Fong et al., 2010; Tutt et al., 2010). *BRCA1/2* play an important role in HR and a substantial body of evidence describes ovarian tumours with aberrant HR function: up to 15% of ovarian cancers harbour *BRCA1/2*-mutations and up to 30% of sporadic ovarian cancers exhibit methylation of the *BRCA1* promoter (Baldwin et al., 2000; Catteau et al., 1999; Chan et al., 2002b; Esteller et al., 2000). Molecular aberrations were also investigated in 489 high grade serous ovarian carcinomas and approximately 50% of these samples harboured defective homologous recombination (CGARN, 2011), representing a larger proportion of patients than those currently being stratified for PARP inhibitor treatment. Novel predictive biomarkers are therefore required to accurately select patients who would benefit from PARP inhibitor treatment. Previous chapters have revealed a DNA repair defect in INPP4B deficient

ovarian cancer cells in response to genotoxic stress. In addition, INPP4B was found to interact with BRCA1 and ATR in overexpression studies. Since, INPP4B loss has been identified in 40% of ovarian tumours, the significance of INPP4B has great clinical implication, and therefore, the effect of INPP4B loss on tumour cell responses to the PARP inhibitor olaparib (Astrazeneca, UK) were assessed. INPP4B deficiency was also assessed in the context of other DNA damage response (DDR) protein inhibitors to screen for potential synthetic lethal interactions.

Table 5.1. PARP inhibitor trials in BRCA1/2-mutated ovarian cancers. Table source: (Burgess and Puhalla, 2014)

Trial	Study population	PARP inhibitor	Comparison therapy	Clinical responses[a]
Phase I De Bono et al. (71) NCT01286987	Advanced *BRCA*^{mut} tumors ($N = 39$, of which 8 BC and 23 OC)	BMN 673	None	*BRCA*^{mut} OC ORR: 11/17
Phase I Sandhu et al. (68) NCT00749502	Advanced solid tumors/hematologic malignancies ($N = 100$, of which 49 OC, including 22 *BRCA*^{mut})	Niraparib	None	*BRCA*^{mut} OC PR: 8/20
Phase I Fong et al. (62) NCT00516373	Advanced solid tumors $N = 60$, of which 21 OC, including 16 with *BRCA*^{mut}	Olaparib	None	*BRCA*^{mut} OC PR: 8/15 SD: 1/15
Phase II Gelmon et al. (65) NCT00679783	Recur, advanced *BRCA*^{mut} OC ($N = 17$)/BCs ($N = 10$), or *BRCA*^{wt} HGS and/or undifferentiated OC ($N = 47$)/TNBC ($N = 16$)	Olaparib	None	*BRCA*^{mut} OC CR: 0/17 PR: 7/17 SD: 6/17
Phase II Kaye et al. (66) NCT00628251	Advanced PRef or PRes *BRCA*^{mut} OC	Olaparib	Liposomal doxorubicin	Olaparib 200 mg twice daily PFS: 6.5 months ORR: 25% Olaparib 400 mg twice daily PFS: 8.8 months ORR: 31% Liposomal doxorubicin: PFS: 7.1 months ORR: 18%
Phase II Kaufman et al. (89) NCT01078662	*BRCA*^{mut} solid tumors (BC, $N = 62$, OC, $N = 193$)	Olaparib	None	*BRCA*^{mut} OC CR: 6/193 PR: 54/193 SD: 78/193 PFS rate: 54.6% for 6 months OS rate: 64.4% for 12 months
Phase II Audeh et al. (63) NCT00494442	Advanced *BRCA*^{mut} OC	Olaparib	None	ORR: 11/33 CR: 2/33 PR: 9/33 PFS: 5.8 months
Phase I Lee et al. (72) NCT00647062, NCT01445418	Met or unresect *BRCA*^{mut} BC and EOC ($N = 45$, of which 37 OC)	Olaparib + carboplatin	None	*BRCA*^{mut} OC CR: 0/34 PR: 15/34 SD: 14/34
Phase I van der Noll et al. (90) NCT00516724	Advanced solid tumors $N = 87$, including BC (26%) and OC (7%), of which 12 *BRCA*^{mut}	Olaparib + carboplatin ± paclitaxel	None	*BRCA*^{mut} CR: 17%[b] PR: 33%[b]
Phase I Liu et al. (82) NCT01116648	Recur or advanced EOC/TNBC $N = 28$, of which 12 *BRCA*^{mut} OC	Olaparib + cediranib (angiogenesis inhibitor)	None	*BRCA*^{mut} OC CR: 1/11 PR: 4/11
Phase I/II Kristeleit et al. (69) NCT01482715	Advanced solid tumors and relapsed PSens *BRCA*^{mut} OC $N = 29$, of which 17 BC and 7 OC, including *BRCA*^{mut} tumors	Rucaparib	None	*BRCA*^{mut} OC PR: 1/7 SD: 10/29 (of which 5 were OC, also 7 were *BRCA*^{mut})[b] CR + PR + SD: 6/7 in OC

Trial	Study population	PARP inhibitor	Comparison therapy	Clinical responses[a]
Phase I Huggins-Puhalla et al. (91) NCT00892736	Advanced *BRCA*^{mut} solid tumors ($N = 38$, of which 20 OC), or *BRCA*^{wt} BLBC or OC	Veliparib	None	*BRCA*^{mut} OC PR: 1/20 SD: 10/38[b]
Phase II Kummar et al. (97) NCT01306032	Refractory progressive *BRCA*^{mut} OC or HGS OC	Veliparib (V) + cyclophosphamide (C) $N = 36$	Cyclophosphamide (C) $N = 38$	V + C: PR: 3/36[b] C: PR: 5/38[b]
Phase I Bell-McGuinn et al. (98) NCT01063816	Met or unresect solid tumors $N = 59$, of which 39 OC, 24 of 39 OC *BRCA*^{mut}	Veliparib + carboplatin and gemcitabine	None	CR: 2/59[b] PR: 11/59[b] Of 13 responses, 8 *BRCA*^{mut} OC, 3 other OC

BC, breast cancer; OC, ovarian cancer; ORR, objective response rate; PR, partial response; SD, stable disease; recur, recurrent; BRCAwt, BRCA-wild type; HGS, high-grade serous; TNBC, triple negative breast cancer; PRef, platinum-refractory; PRes, platinum-resistant; PFS, progression free survival; OS, overall survival; CR, complete response; met, metastatic; unresect, unresectable; EOC, epithelial ovarian cancer; PSens, platinum-sensitive; BLBC, basal-like breast cancer.

Table 5.2. PARP inhibit trials in sporadic ovarian cancers. Table source: (Burgess and Puhalla, 2014)

Trial	Study population	PARP inhibitor	Comparison therapy	Clinical responses[a]
Phase II Gelmon et al. (65) NCT00679783	Recur, advanced *BRCA*^{mut} OC ($N=17$)/BCs ($N=10$), or *BRCA*^{wt} HGS and/or undifferentiated OC ($N=47$)/TNBC ($N=16$)	Olaparib	None	*BRCA*^{wt} OC CR: 0/46 PR: 11/46 SD: 18/46
Phase II Ledermann et al. (81) NCT00753545	Relapsed PSens serous OC after two courses of platinum-based chemotherapy	Olaparib	Placebo	PFS: 8.4 months OS 29.7 months ORR: 12.3% ORR + SD: 52.9%
Phase I Lee et al. (99) NCT01237067	Refractory or recur BC ($N=4$) and OC ($N=23$)	Olaparib + carboplatin	None	OC PR: 8/23 SD: 11/23
Phase I van der Noll et al. (90) NCT00516724	Advanced solid tumors $N=87$, including BC (26%) and OC (7%), of which 12 *BRCA*^{mut}	Olaparib + carboplatin ± paclitaxel	None	ORR: 14/87 (16%)[b] CR: 5% PR: 11% SD: 28%
Phase II Oza et al. (103) NCT01081951	Advanced PSens serous OC	Olaparib + carboplatin, paclitaxel	Carboplatin, paclitaxel alone	PFS: 12.2 months ORR: 64%
Phase I Liu et al. (82) NCT01116648	Recur or advanced EOC/TNBC $N=28$, of which 20 OC	Olaparib + cediranib (angiogenesis inhibitor)	None	OC CR: 1/18[b] PR: 7/18[b] SD: 3/18[b]
Phase I Balmana et al. (100) NCT00782574	Advanced solid tumors $N=54$, of which 10 OC	Olaparib + cisplatin	None	CR: 1/54[b] PR: 17/54[b] SD: 23/54[b]
Phase I Molife et al. (104) NCT01009190	Advanced solid tumors ($N=23$, of which 6 OC)	Rucaparib + carboplatin	None	OC PR: 1/6 SD: 2/6
Phase I Huggins-Puhalla et al. (91) NCT00892736	Advanced *BRCA*^{mut} solid tumors, or *BRCA*^{wt} tumors ($N=25$, of which 4 OC)	Veliparib	None	*BRCA*^{wt} SD: 7/25[b]
Phase I Kummar et al. (101) NCT00810966	Refractory solid tumors/lymphoma $N=35$, including BC and OC	Veliparib	Cyclophosphamide	PR: 7/35[b] SD: 6/35[b]
Phase II Kummar et al. (97) NCT01306032	Refractory progressive *BRCA*^{mut} OC or HGS OC	Veliparib (V) + cyclophosphamide (C) $N=36$	Cyclophosphamide (C) $N=38$	V + C: PR: 3/36[b] C: PR: 5/38[b]
Phase I Bell-McGuinn et al. (98) NCT01063816	Met or unresect solid tumors $N=59$, of which 39 OC, 24 of 39 *BRCA*^{mut}	Veliparib + carboplatin and gemcitabine	None	CR: 2/59[b] PR: 11/59[b] Of 13 responses, 8 *BRCA*^{mut} OC, 3 other OC, 2 others

recur, recurrent; BRCAmut , mutated BRCA; OC, ovarian cancer; BC, breast cancer; BRCAwt , BRCA-wild type; HGS, high-grade serous; TNBC, triple negative breast can- cer; CR, complete response; PR, partial response; SD, stable disease; PSens, platinum-sensitive; PFS, progression free survival; OS, overall survival; ORR, objective response rate; EOC, epithelial ovarian cancer; BLBC, basal-like breast cancer; met, metastatic; unresect, unresectable.

5.2 Results

5.2.1 Loss of INPP4B results in increased sensitivity towards olaparib

Cell proliferation assays were conducted to assess the effect of INPP4B loss in the context of PARP inhibitor treatment of ovarian cancer cells. Cells were treated continuously for 72 hrs with increasing concentrations of olaparib (dose-response) and cell viability assessed with a metabolic readout measured using Alamarblue. Ovca429 shRNA INPP4B cell pools displayed a dose-dependent and significantly increased sensitivity upon olaparib treatment compared to controls (figure 5.1). Treatment with 100 μM olaparib resulted in 38% reduction in growth in INPP4B deficient Ovca429 cells compared to 61% in the control cells ($p = 0.02$). Ovca433 knockdown cell pools were also assessed, however the shRNA INPP4B cells did not display as great a difference in olaparib sensitivity compared to the control.

The observed olaparib sensitivity in Ovca429 and Ovca433 INPP4B knockdown cell pools was also assessed in cell lines with varying endogenous expression levels of INPP4B or PTEN (experiments performed by Dr. Christina Gewinner). Cell proliferation assays were conducted in A2780 (INPP4B− / −, PTEN− / −), Ovcar3 (INPP4B− / −, PTEN+/+), and Ovca433 (INPP4B +/+, PTEN +/+) ovarian cancer cell lines in the same manner as previous experiments (see figure 3.4 for cell line protein expression). A2780 (INPP4B− / −, PTEN− / −) demonstrated the highest olaparib sensitivity followed by the INPP4B-negative Ovcar3 (INPP4B− / −, PTEN+/+). Ovca433 cells (INPP4B+/+, PTEN+/+) displayed greatest olaparib resistance (figure 5.2) Additional PTEN loss in INPP4B- deficient Ovcar3 cells resulted in additive olaparib sensitivity similar to the A2780 cell line (INPP4B− / −, PTEN− / −). PTEN knockdown in Ovcar3 cells resulted in additive olaparib sensitivity similar to the A2780

cell line (INPP4B− / −, PTEN− / −). In rescue experiments re-expression of Flag-tagged INPP4B in the INPP4B-deficient Igrov-1 cell line resulted in a 2-fold increase in olaparib resistance in cell proliferation assays (figure 5.2B)

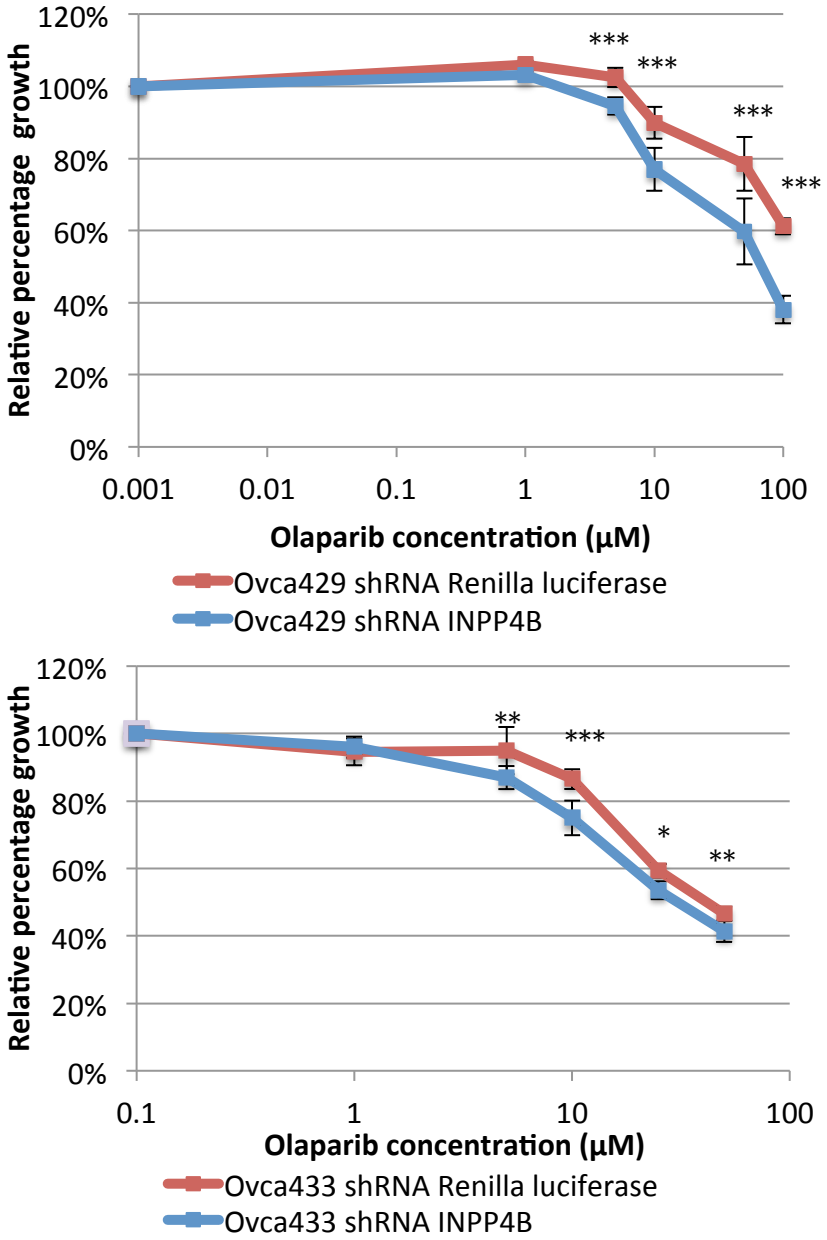

Figure 5.1. Dose response curve of olaparib treated Ovca429 and Ocva433 knockdown cell pools. Cell proliferation assays were conducted in Ovca429 knockdown cell pools subjected to 72 hrs continuous treatment of olaparib in increasing concentrations. Ovca429 shRNA INPP4B cell pools displayed a dose-dependent and significantly increased sensitivity upon olaparib treatment compared to controls. P-values for conditions at 1 µM, 5 µM, 10 µM and 100 µM were 0.027, 0.019, 0.039 and 0.026, respectively. IC50 for shRNA INPP4B cell pool is 61 µM, calculated using a

best-fit curve on Microsoft Excel. Ovca433 shRNA INPP4B cell pools also displayed increased sensitivity towards olaparib. P-values for conditions at 5 μM, 10 μM, 25 μM and 50 μM were 0.004, $5.79x10^{-5}$, 0.026 and $1.54x10^{-4}$, respectively. Experiments were conducted independently three times, in triplicates. Error bars indicate standard deviation. The t-test was used for statistical analysis (p-value of *≤0.05, **≤0.005, ***≤0.0005).

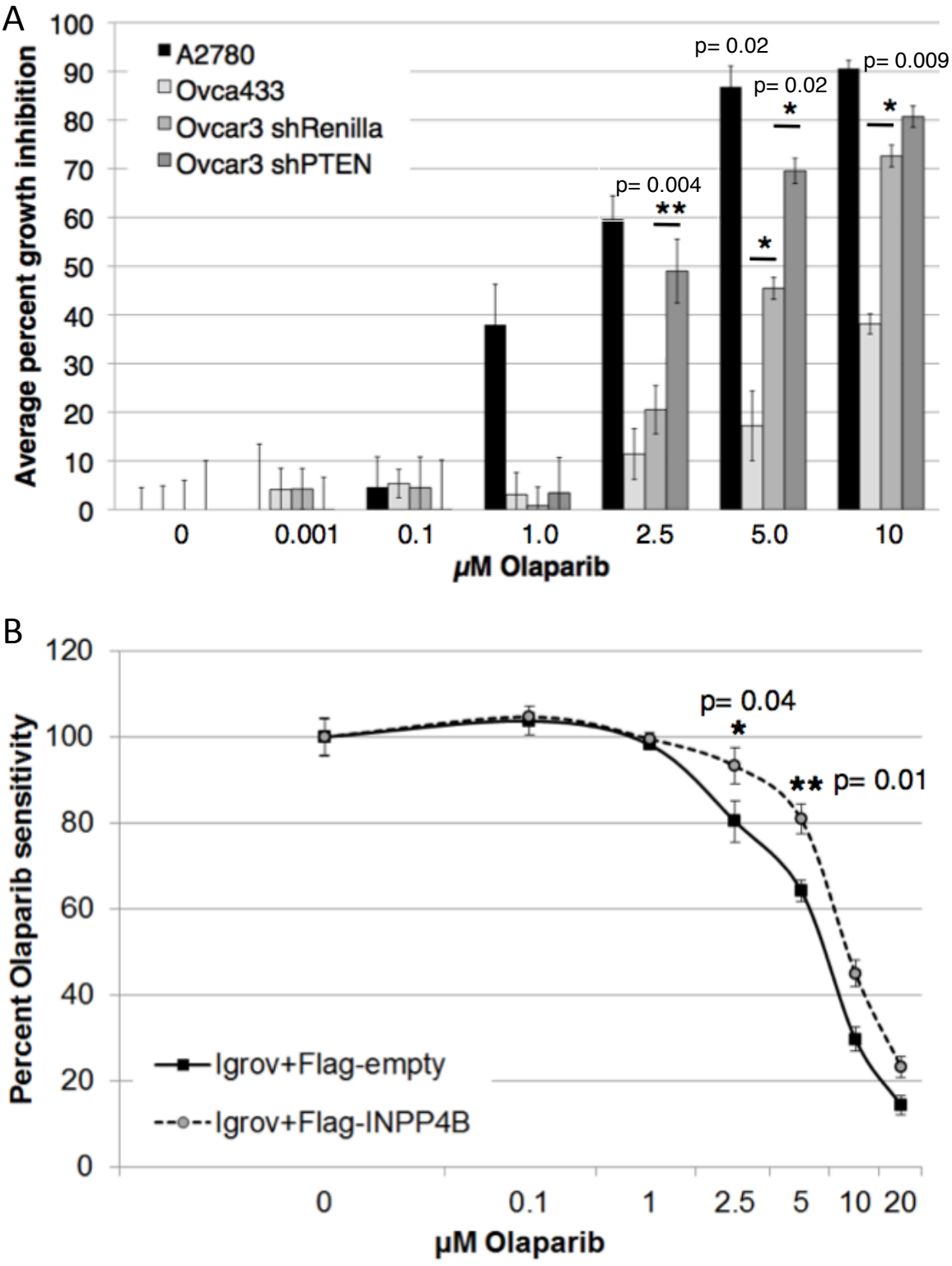

Figure 5.2. INPP4B loss in various ovarian cancer cell lines results in sensitivity towards PARP inhibitor treatment *in vitro*. (A) Cell proliferation assays were conducted in ovarian cancer cell line A2780 (INPP4B$^{-/-}$, PTEN$^{-/-}$), and these cells

demonstrated highest olaparib sensitivity followed by the INPP4B-negative Ovcar3 ($INPP4B^{-/-}$, $PTEN^{+/+}$). Ovca433 cells ($INPP4B^{+/+}$, $PTEN^{+/+}$) displayed greatest olaparib resistance. Additional PTEN loss in INPP4B-deficient Ovcar3 cells resulted in additive olaparib sensitivity similar to the A2780 cell line ($INPP4B^{-/-}$, $PTEN^{-/-}$). PTEN knockdown in Ovcar3 cells resulted in additive olaparib sensitivity similar to the A2780 cell line ($INPP4B^{-/-}$, $PTEN^{-/-}$). Experiment was conducted independently three times, in triplicate by Dr. Christina Gewinner (UCL, UK). Error bars represent standard deviation. The t-test was used for statistical analysis (p-value of *≤0.05, **≤0.005; P values for Ovca433 cells at conditions of 5 μM and 10 μM were 0.019 and 0.009, respectively. P-values for Ovca3 cells at conditions of 2.5 μM and 5 μM were 0.004 and 0.018, respectively). (B) Olaparib dose response curve of Igrov-1 cells ($INPP4B^{-/-}$, $PTEN^{+/+}$) expressing Flag-INPP4B or empty vector control. Percent growth is displayed. Experiment was conducted independently three times, in triplicate by Dr. Christina Gewinner (UCL, UK). P-values for conditions at 2.5 μM and 5 μM were 0.04 and 0.01, respectively. Error bars indicate standard deviation. The t-test was used for statistical analysis (p-value of *≤0.05).

5.2.2 Loss of INPP4B results in increase in cisplatin sensitivity and dual treatment of INPP4B-deficient cells with cisplatin and olaparib results in an additive effect

Clonogenic assays were conducted to assess the effectiveness of olaparib on the survival and proliferation of INPP4B-deficient cells under cisplatin-only, olaparib-only or dual treatment conditions (figure 5.3). Dual-treated cells were continuously treated with 1 μM olaparib for 6 days preceded by a single dose of 10 μM cisplatin on day 1. Ovca429 INPP4B knockdown cells showed significantly greater inhibition of clonogenic growth to single agent cisplatin or olaparib compared to controls. Combination treatment resulted in an additive effect, with significantly greater inhibition of growth in Ovca429 INPP4B knockdown pools compared to controls. Clonogenic assays in Ovca433 cells were attempted, but the cells were unable to grow into succinct colonies that could be accurately counted, hence experiments with this cell line were not continued. The t-test was used for statistical analysis (p-value of *$\leq$0.05, **$\leq$0.005, ***$\leq$0.0005).

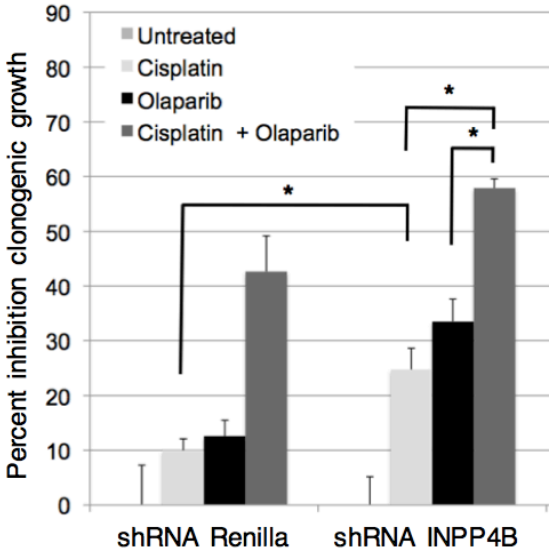

Figure 5.3. Clonogenic assays of Ovca429 knockdown cell pools using cisplatin alone or in combination with continuous olaparib treatment. Cells were treated with 10 μM cisplatin for 1 hr, continuously treated with 1 μM olaparib, or subjected to dual treatment of both cisplatin and olaparib. Single agent and dual agent treatments resulted in an additive and synergistic effect, respectively. Percent inhibition clonogenic growth is displayed. P-values for conditions between cisplatin treatments, cisplatin + dual treatment and olaparib + dual treatment were 0.006, 0.020 and 0.007, respectively. Experiments with all treatments pooled in one experiment were conducted independently three times, in triplicate. Error bars represent standard deviation. The t-test was used for statistical analysis (p-value of *≤0.05).

5.2.3 INPP4B knockdown in Ovca429 cells sensitises tumour growth to olaparib *in vivo*

Assessment of olaparib sensitivity *in vivo* was conducted by Dr. Christina Gewinner (UCL, UK). Ovca429 shRNA INPP4B or control cells were injected into nude mice subcutaneously and animals bearing established tumours were injected daily with either 50 mg/kg olaparib or DMSO. The mice were sacrificed two weeks post – treatment and their tumour burden quantified (figure 5.4). As expected, INPP4B deficient tumours were larger than tumours containing shRNA-Renilla luciferase cells with control treatment. Post-treatment, shRNA INPP4B tumours treated with olaparib revealed a significant reduction in tumour burden compared to control treated tumours, which further support the *in vitro* findings that loss of INPP4B results in enhanced sensitivity to olaparib treatment.

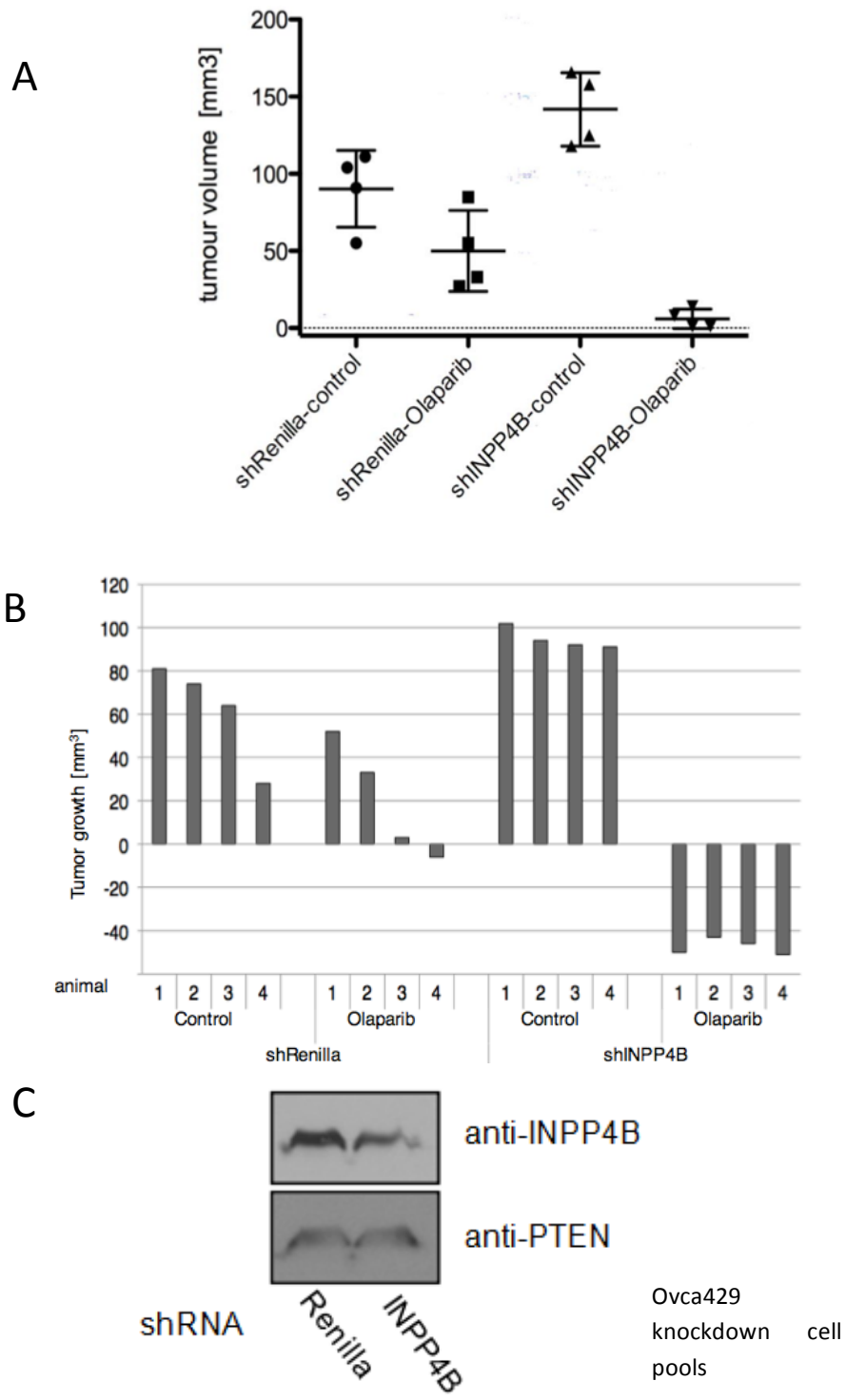

Figure 5.4. INPP4B knockdown in Ovca429 sensitises tumour growth to PARP inhibitor treatment *in vivo*. (A) Nude mice were injected subcutaneously with Ovca429 INPP4B or Renilla luciferase knockdown cells. Tumour bearing animals were injected daily with olaparib or DMSO. Quantification of tumour volume is shown (error

bars represent SD.). (B) Waterfall plot of tumour volume compared to treatment start. Xenograft experiments and quantification analysis were conducted by Dr. Christina Gewinner (UCL, UK). (C) Western blots of Ovca429 knockdown cells pools used for the *in vivo* experiments.

5.2.4 Treatment of INPP4B deficient Ovca429 knockdown cells with Chk1 inhibitor LY2940930 results in resistance in cell proliferation assays

The interaction of INPP4B with ATR identified in previous experiments led to the rationale of investigating other compounds that inhibit substrates of ATR, such as Chk1, to assess for synthetic lethal effects. Cell proliferation assays using two Chk1 inhibitors, LY2940930 and LY2603618 (Eli Lilly, USA), were conducted in Ovca429 and Ovca433 knockdown cell pools to investigate potential synthetic lethal interaction. Cells were treated continuously for 72 hrs with increasing concentrations of the inhibitors (dose-response curve), and cell viability via metabolic readout was measured. Upon treatment, INPP4B-deficient ovca429 cells exhibited reduced sensitivity towards LY2940930 compared to the control. Compared to the control, shRNA INPP4B cells revealed a 107% growth increase vs. 98% ($p = 0.038$), 102% vs 83% ($p = 0.0040$, 60% vs 41% ($p = 0.051$), and 32% vs 25% ($p = 0.014$). On the other hand, treatment of Ovca433 shRNA INPP4B cells with LY2940930 resulted in no significant difference compared to the control (figure 5.5). Investigation of LY2603618 in both Ovca429 and Ovca433 knockdown cell pools resulted in no statistical difference between INPP4B-deficient knockdown cell pools and the mock knockdown control (figure 5.6). Further investigation of LY2603618 treated Ovca429 shRNA INPP4B cells in clonogenic assays revealed no statistical difference between the cells and the controls (figure 5.7), although the trend was for INPP4B knockdown Ovca433 cells to be more sensitive; the opposite of that was observed in Ovcax429 cells with LY2940930.

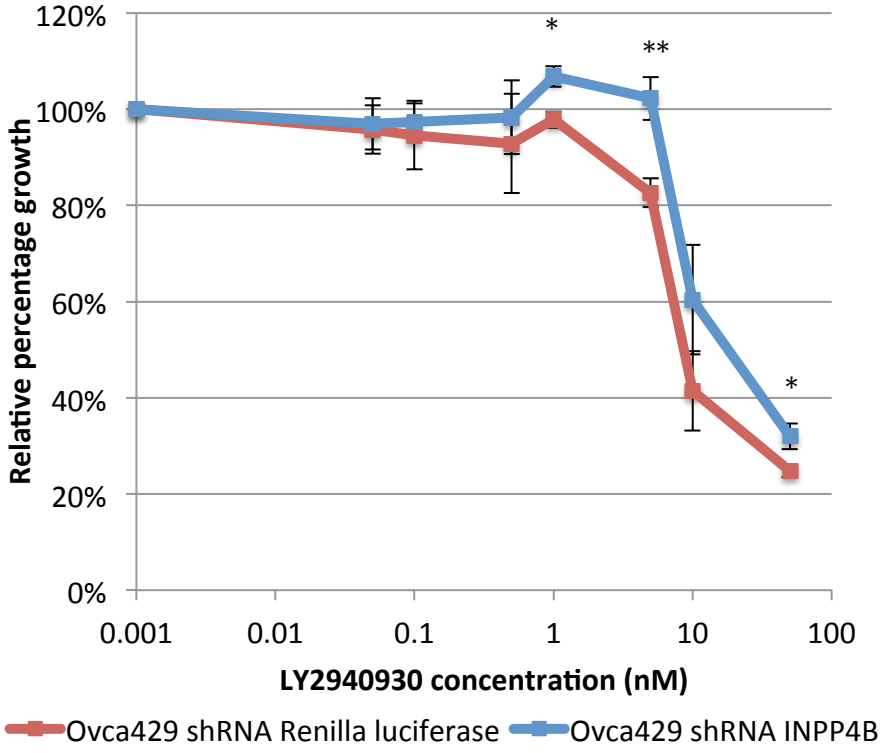

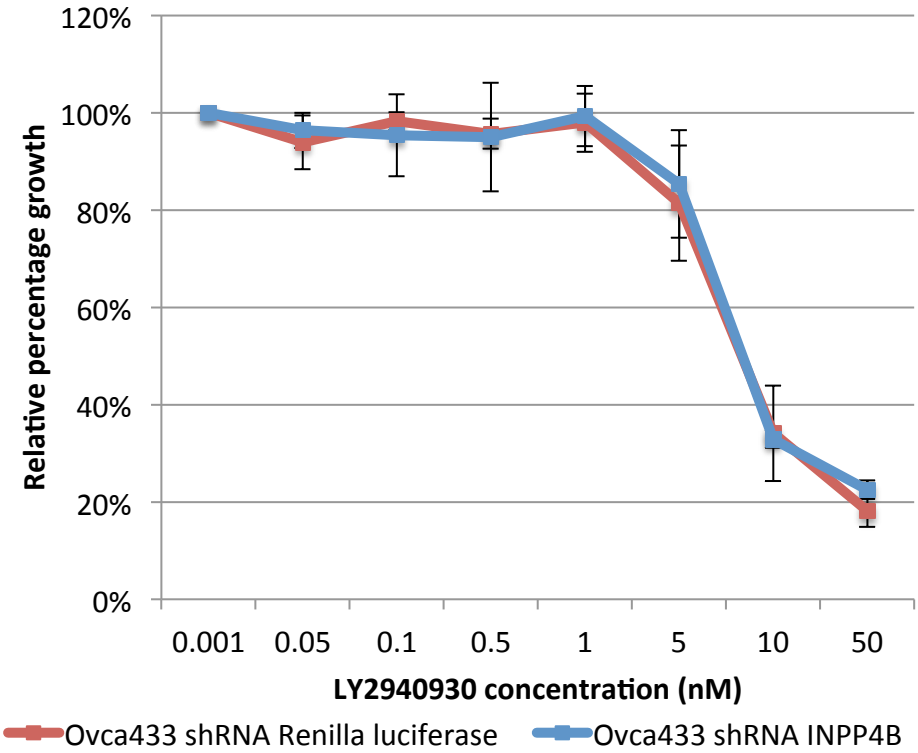

Figure 5.5. Ovca429 and Ovca433 knockdown cell pool dose response curves upon LY2940930 treatment. Ovca429 and ovca433 knockdown cell pools were continuously treated with varying concentrations of Chk1 inhibitors LY2940930 and

metabolic activity was measured 72 hrs post-treatment. Ovca429 shRNA INPP4B cells displayed decreased growth inhibition upon LY2940930 treatment compared to the controls. P-values for conditions at 1 μM, 5μM and 50 μM were 0.038, 0.004 and 0.014, respectively. Experiments with Ovca433 INPP4B deficient cells displayed no statistical difference and mock knockdown control. All experiments were conducted independently three times, in triplicates. Error bars represent standard deviation. The t-test was used for statistical analysis (p-value of *≤0.05, **≤0.005).

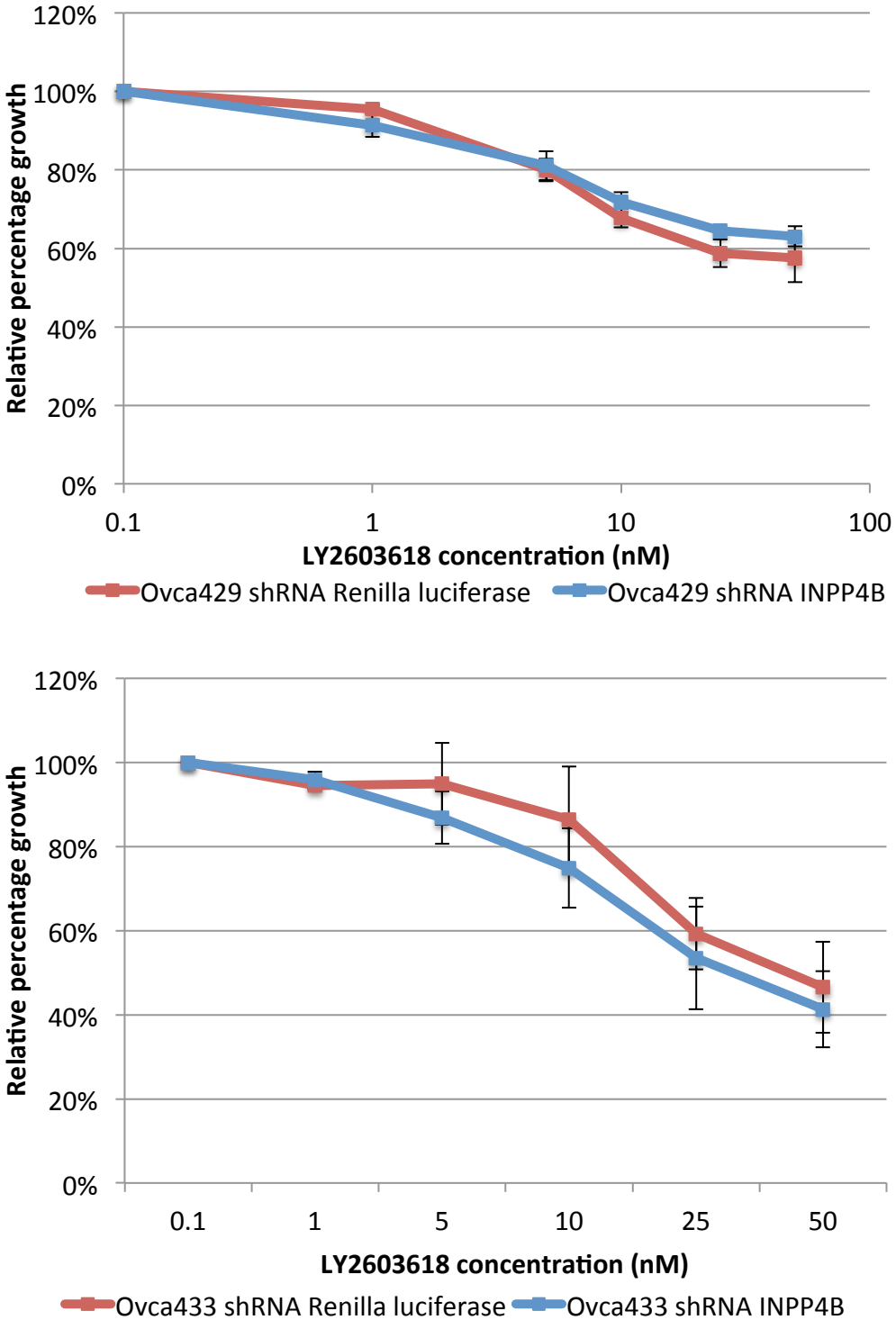

Figure 5.6. Ovca429 and Ovca433 knockdown cell pool dose response curves upon LY2603618 treatment. Ovca429 and ovca433 knockdown cell pools were continuously treated with varying concentrations of Chk1 inhibitors LY2603618 and metabolic activity was measured 72 hrs post-treatment. No statistic difference was

observed between the INPP4B deficient cells and mock knockdown control. All experiments were conducted independently three times, in triplicates. Error bars represent standard deviation. The t-test was used for statistical analysis.

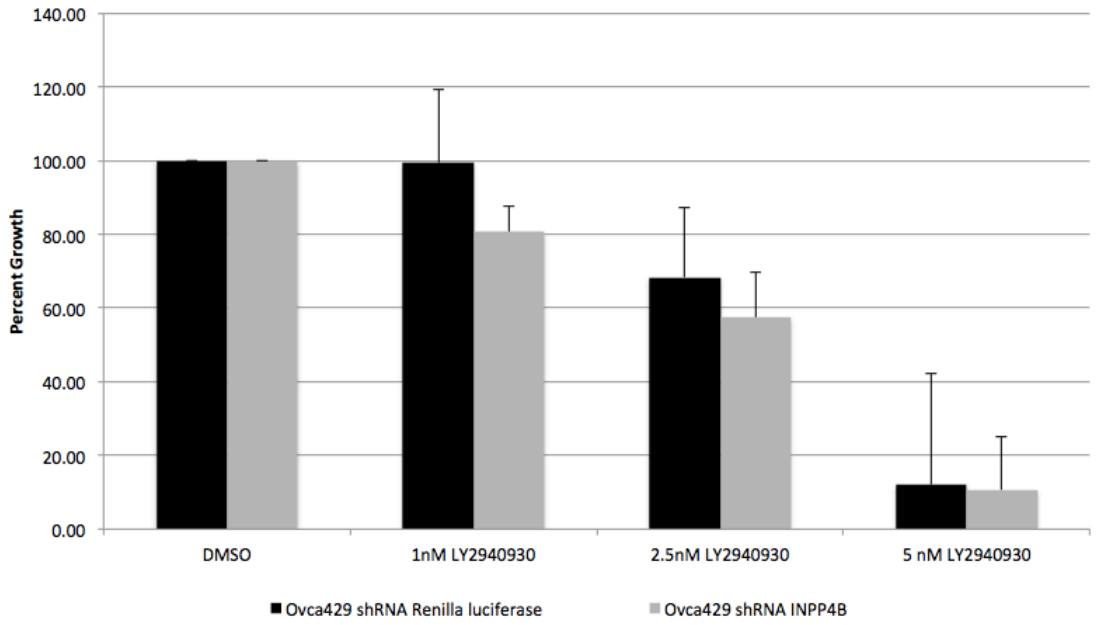

Figure 5.7. LY2940930 treated Ovca429 cells possessing shRNA INPP4B resulted in no statistical difference in clonogenic growth compared to the controls. 1,000 Ovca429 knockdown cells were seeded per well in a 6-well dish and attached cells were treated with 1 nM, 2.5 nM and 5 nM LY2940930 every other day for 6 days, then stained and counted. No statistical difference was seen between INPP4B-deficient and control Ovca429 cells. Experiment was conducted independently three times, in triplicates. Error bars represent standard deviation. The t-test was used for statistical analysis.

5.3 Discussion

Previous experiments have revealed a protein-protein interaction between INPP4B and ATR, and loss of INPP4B resulted in diminished protein expression of ATR in mouse embryonic fibroblast models. One of the key substrates of ATR is the serine threonine checkpoint kinase Chk1. Chk1 plays a central role in normal DNA replication, mitosis, and cytokinesis. Inhibition of Chk1 in the absence of DNA damage can cause impaired DNA replication, loss of DNA damage checkpoints, premature entry into mitosis, and cell death (Bucher and Britten, 2008; Thompson and Eastman, 2013). The effect of INPP4B knockdown on Chk1 inhibitors was investigated to screen for potential synthetic lethal interaction. For the experiments, two potent small molecule inhibitors of Chk1 were used, LY2940930 (also known as LY2606368) and LY2603618, which inhibit Chk1/2 and Chk1, respectively (Eli Lilly, UK). Both compounds are currently being assessed in phase I clinical trials for advanced cancers (NCT01115790, 2010; NCT01341457, 2011). Cell proliferation assays of LY2940930 treated Ovca433 cell pools did not result in any statistical difference between shRNA INPP4B cells and the control. Similarly, no statistical difference was found in cell proliferation assays conducted in both Ovca429 and Ovca433 knockdown cell pools. Downregulation of ATR and ATM protein levels due to INPP4B loss may contribute to decreased activation of Chk1 and Chk2, and hence, loss of sensitivity towards Chk1/2 inhibitors. On the other hand, Ovca429 shRNA-INPP4B cells displayed reduced sensitivity towards LY2940930 treatment compared to the controls in cell proliferation assays. The precise mechanism for the observed reduced sensitivity was not deduced due to time constraints. However, a study conducted observed that oncogenic KRAS and dominant negative TP53 render BRCA2-depleted HEK293 cells resistant to Chk1 inhibition, which suggests that modulations in other pathways due to INPP4B loss may contribute

to the reduced sensitivity towards Chk1 inhibition (Hattori et al., 2011). Further experiments will need to be conducted to examine DDR pathway activation and phosphorylation status of relevant proteins in the context of INPP4B loss, which may provide insight into which pathways are involved in this reduced sensitivity.

The effect of INPP4B loss and PARP inhibition was also investigated in this study. Identification of HR defects has gained traction in cancer therapy research due to their potential exploitation by PARP inhibitors, as well as by conventional treatment. Pre-clinically, PARP inhibitors have shown efficacy not only in cells lacking BRCA1/2, but also in cells with other defective HR proteins, such as RAD51, ATR, ATM, Chk1, and FANCA or FANCC (Bryant et al., 2005; Farmer et al., 2005; McCabe et al., 2006), which provided the rational for assessing PARP inhibitors clinically in *BRCA1/2*-mutant tumours. The phase II trial data of PARP inhibitor olaparib in ovarian cancer patients that received treatment based on *BRCA1/2* mutation status revealed a median improvement of 6.9 months in progression-free survival and an overall survival improvement of 3 months compared with placebo (Ledermann et al., 2012). While 10 – 15% of ovarian tumours harbour germline mutations in *BRCA1/2*, there is a growing body of evidence that suggests additional mechanisms of BRCA1/2 dysfunction and HR-deficiency are involved in the pathogenesis of ovarian cancer (George et al., 2013; Turner et al., 2004; Weberpals et al., 2008). Therefore, there is a great need to identify patients who would benefit most from PARP inhibitor treatment and be included in these in clinical trials currently designed for BRCA-related cancers. Upon treatment with the PARP inhibitor olaparib, INPP4B deficient Ovca429 and Ovca433 ovarian cancer cells displayed a modest increase in sensitivity towards the drug compared to control cells in cell proliferation assays. In addition, studies in other ovarian serous

adenocarcinoma based cell lines (A2780, Ovcar-3), have also confirmed that loss of INPP4B is associated with olaparib sensitivity and re-expression of INPP4B in the INPP4B-deficient IGROV-1 endometrioid carcinoma cell line resulted in decreased olaparib sensitivity. Therefore, the integrity of INPP4B expression and its effect on olaparib sensitivity can be observed across a range of ovarian cancer cell lines and subtypes. However, it must be noted that the limitation of this study remains being unable to determine whether the two cell ovarian cancer cell lines represent either high grade or low grade serous ovarian carcinomas, two distinct diseases with differing molecular and clinical pathological profiles. Clonogenic growth assessment in Ocva429 shRNA INPP4B cells revealed not only an increased sensitivity towards single agent treatment of olaparib, but interestingly, also a heightened sensitivity towards single agent cisplatin treatment. The sensitivity of INPP4B deficient cells towards cisplatin treatment mirrors the responsiveness of germline *BRCA1/2*-mutant ovarian tumours to platinum-based regimens, whereby the DNA damage induced by the platinum is more efficacious in cells harbouring DNA repair defects (Cass et al., 2003). In addition, dual treatment of both drugs resulted in an additive effect in INPP4B deficient cells compared to the controls. *In vivo* experiments in immunosuppressed mice further confirmed great sensitivity of INPP4B-deficient tumours towards olaparib compared to the control treatment.

The clinical implications of using PARP inhibitors in cancer therapy have been promising, albeit not without adversity. Several clinical trials have provided greater insight into problems of drug toxicity and resistance. When used as monotherapy, PARP inhibitors are generally well tolerated with the most common side effects including fatigue, nausea, and vomiting; dose-limiting toxicities of cognitive

dysfunction and mood alterations have also been described (Audeh et al., 2010; Fong et al., 2009; Gelmon et al., 2011). PARP inhibitors combined with chemotherapy in *BRCA*-mutated ovarian malignancies, on the other hand, have resulted in myelosuppression with grade 3/4 adverse events (neutropenia (42%)), as well as thrombocytopenia (20%), and anaemia (13%) (Jung-min Lee, 2013). Combination therapies of PARP inhibitors and novel targeted agents have also been assessed. Cadiranib, an anti-angiogenic agent was used in conjunction with olaparib in recurrent epithelial ovarian cancers, and while the overall response rate was 44%, patients frequently experienced grade 3 or higher haematologic and non-haematologic toxicities (Liu et al., 2013). Further examination of drug combinations and toxicities will need to be conducted to implement effective treatment of patients with PARP inhibitors while keeping side effects at a minimum.

Furthermore, the issue of drug resistance has pervaded the study of ovarian cancer, with the majority of patients likely to develop resistance against first line platinum therapy. The continuation of clinical trials exploring the effects of PARP inhibitors targeting *BRCA*-mutant tumours also highlights the need to address drug resistance in this context. While the phase II study led be Lederman et al. revealed a 40% response to olaparib in germline *BRCA* mutation carriers with breast or ovarian cancer, several mechanisms of resistance have been hypothesised to take account of the remainder of patients who do not respond to PARP inhibitor treatment. Amongst the numerous resistance mechanisms that have been proposed, secondary mutation of *BRCA2* is the most well validated mechanism of PARP-inhibitor resistance. Two groups independently discovered that PARP inhibitor resistance came about due to mutation in the *BRCA2* gene itself that resulted in the restoration of the opening reading frame for

BRCA2 was frequently observed in resistant tumour cell lines (Edwards et al., 2008; Sakai et al., 2008). Whether the secondary mutations are present before or arise during PARP-inhibitor therapy is currently unknown. It may be possible that rare resistant cells harbouring secondary mutations before treatment are selected by the PARP inhibitor treatment itself resulting in developed resistance. Additional studies are required to identify approaches that would result in more effective PARP inhibitor treatment, reduce *de novo* resistance to the drug, and provide alternative therapies to circumvent inherent or acquired resistance.

Despite the toxicities and resistance encountered by these drugs in clinic, the relevance of INPP4B with respect to PARP inhibitors is one of great importance. Reliable biomarkers are currently needed to identify DDR defects to best select and stratify patients on the basis of the molecular phenotype of the tumour in order to improve therapeutic response, as well as reduce healthcare costs of administering drugs that are likely to have little effect. Additional studies are necessary to establish the level of INPP4B protein expression that would result in optimum sensitivity towards PARP inhibitor treatment. The mechanisms of PARP inhibitor sensitivity should also be firmly defined, which include assessing via immunoblotting the cellular response of various DDR proteins, as well as other players in major signalling pathways, since crosstalk between pathways is a common feature in drug response and resistance. Gaining a deeper understanding of these cellular changes would also provide further insight into potential synergistic effects with other clinical inhibitors. Given that INPP4B loss has been found in 40% of ovarian cancer patients, the experiments conducted provide the rationale for establishing INPP4B as a biomarker of PARP inhibitor response, and consequently offers novel therapeutic options for a significant subset of patients.

CHAPTER 6. Final Discussion

Current standard of care ovarian cancer treatment involves optimal cytoreductive surgery and adjuvant platinum- and taxane-based chemotherapy. While the majority of patients are initially responsive to treatment, over 70% develop disease recurrence and platinum-resistance, revealing an urgent need to develop alternative treatment options for these patients.

The study of ovarian cancer and the lack of advancement in providing treatment options with better outcomes are in part due to the lack of appropriate models available in the laboratory setting. Conventional models have been limited to a set of relatively poorly characterised immortalised cell lines, to which the true origins of the cell lines have recently been called into question (Anglesio et al., 2013; Domcke et al., 2013). A study conducted by Domcke et al. found that 60% of all published research articles on high grade serous ovarian carcinomas (HGSC) are inaccurate representations of the disease, and the 12 most suitable ovarian cancer cell lines that best characterise HGSC were used in only 1% of publications (Domcke et al., 2013). In addition, the redefinition of ovarian cancer as a collective term for molecularly and aetiologically distinct diseases that share a common anatomical location, has also caused further confusion as to the origins of the cell lines on hand (Bast et al., 2009). The progress of establishing animal models that mimic ovarian cancer pathogenesis is also being redefined. Mouse models for endometrioid ovarian cancer subtype have been successfully implemented to identify the site of origin and disease pathogenesis of this particular subtype (Dinulescu et al., 2005; Wu et al., 2013; Wu et al., 2007). However, the development of accurate mouse models that recapitulate the early molecular alterations and disease progress of HGSC, have been slow to progress, likely due to previous models targeting the ovarian

surface epithelium as the site of origin. A recent study conducted by Perets et al. has challenged the traditional model of the ovaries being the site of carcinogenesis by demonstrating that HGSC can originate from the secretory cells of the fallopian tubes. By generating a de novo mouse model of HGSC that targets commonly altered HGSC genes specifically to secretory epithelial cells within the fallopian tube, they observed the development of precursor serous tubule intraepithelial carcinomas lesions, HGSC, and the progression to advanced stage disease, including ovarian and peritoneal metastases (Perets et al., 2013). More methodological studies are required to firstly re-verify the origins of ovarian cancer cell lines that are currently available, and secondly to further evaluate the site origins of the different subtype of ovarian cancer to provide the appropriate cellular context for assessing therapeutic strategies more accurately.

Using synthetic lethality as a basis for therapy in order to exploit inherent differences between cancer cells and normal cells provides an attractive opportunity to develop novel treatments for cancer that is tailored and highly selective. The best example of synthetic lethality use is PARP inhibitor treatment for ovarian tumours harbouring *BRCA1/2* mutations. Given the promising results of several PARP inhibitors currently in phase III trails, identifying other genetic determinants of PARP inhibitor sensitivity may enhance treatment options for women with ovarian cancer. Identifying the relevance of a DNA repair defect due to INPP4B loss prevails in the context of ovarian cancer, where *BRCA1* mutations, "BRCAness" and homologous recombination (HR) repair deficiency is common feature of ovarian tumours. The novel function of INPP4B in maintaining HR integrity identified in this study results in a therapeutic opportunity through the delivery of therapeutic strategies on this same basis of synthetic lethality. The effect of INPP4B loss resulting in increased sensitivity to the PARP inhibitor

olaparib in ovarian cancer cells and in xenograft models as evidenced from this study has great implications for using INPP4B as a novel biomarker of PARP inhibitor sensitivity in ovarian cancer. Current clinical trials that involve the use of PARP inhibitors as monotherapy or in conjunction with other treatments have previously enrolled patients primarily based on their *BRCA* status. Newer studies have also incorporated patient selection based on their disease subtype and platinum-sensitivity. Stratifying patients based on INPP4B expression may have a profound impact on the inclusion of more patients likely to benefit from PARP inhibitor treatment. Using the recently established revised ovarian cancer models and redefined cell lines, it would be profitable to investigate the effects of INPP4B on DNA repair in each of the five main subtypes of ovarian cancer, HGSC, LGSC, clear cell carcinoma, mucinous carcinoma and endometriod carcinoma, which would better appropriate relevant therapeutic strategies to patients based specifically on their disease subtype. From a clinical perspective, this study provides the rationale to investigate olaparib sensitivity in INPP4B-deficient serous ovarian tumours in phase 0 trials.

This study also identified a potential mechanism for the DNA repair defect through the identification of protein-protein interaction of INPP4B with ATR and BRCA1 and provides a platform for further research to be conducted to construe the details of this mechanism and how it temporally and spatially relates in response to DNA damage, as well as in an unchallenged environment. In addition, elucidation of whether or not the function of INPP4B in this context is dependent on its catalytic activity or its protein function still needs to be defined. While INPP4B loss affected HR repair, assessing the function of INPP4B in other DNA repair pathways in detail may identify other DNA repair inhibitors that would also show therapeutic efficacy. It is of interest to note that

the experiments in this study were conducted in a variety of tissue types apart from the ovarian cell lines used, including human mammary cell line MCF-10A, where INPP4B loss and its tumour suppressor function was initially characterised, and INPP4B floxed mouse embryonic fibroblasts. Regardless of the cell lines used, the results across all experiments pointed to the involvement of INPP4B with a DNA repair defect. In addition, since INPP4B loss is found in various epithelial cancers, these observations raise further questions as to whether this DNA repair deficiency can be found in cancers of different tissue types, and whether or not the protein-protein interaction of INPP4B with ATR and BRCA1 is conserved. Speculation for INPP4B's mechanism of action could be that INPP4B plays a role in the stability of ATR and BRCA1 in the context of proteosomal degradation; loss of INPP4B as a protein that interacts with ATR and BRCA1 directly or indirectly could lead to an acceleration of degradation of the DNA repair proteins, therefore resulting in a DNA repair defect. The loss of INPP4B expression resulting in cisplatin sensitivity observed in this study merits in depth assessment within the ovarian cancer setting. Data obtained in collaboration with Dr. Andrew Feber (University College London, UK) have revealed that re-expression of INPP4B in bladder cancer patients resulted in developed resistance to platinum drugs, indicative of a role of INPP4B in platinum sensitivity in other cancer tissue types. This study investigated the loss of INPP4B and its effect on DNA repair and treatment strategies in ovarian cancer; however the effect of INPP4B loss and INPP4A levels were not addressed and potentially could in part compensate for INPP4B loss.

In the last decade the establishment of targeted therapies in ovarian cancer treatment has reignited advances in developing effective treatment options for patients. In parallel with determining the clinical efficacy of the inhibitors, the establishment of predictive

biomarkers are needed not only to enrich trials with more patients that would likely respond to the treatment, but also to provide a greater chance in furthering clinical development and ultimately achieving drug registration (Carden et al., 2010). Current models of identifying tumours with non-germline HR repair defects include immunohistochemistry (IHC) analysis of tissue microarrays (TMAs), gene expression profiling, and methylation-specific arrays, all of which have been reported to have varying degrees of predictive power (Ahluwalia et al., 2001; Jazaeri et al., 2002; Konstantinopoulos et al., 2010; Vollebergh et al., 2012). In addition to knowledge driven gene-based markers, other strategies for assessing HR integrity include the use of genomic instability as a general hallmark of HR deficiency through copy number aberration analysis by array comparative genomic hybridisation (aCGH), and the use of pharmacodynamics biomarkers as a readout of HR activity through the measurement of RAD51 foci following *ex vivo* DNA damage induction (Mukhopadhyay et al., 2010). A study conducted by the Cancer Genome Atlas Research Network identified HR deficiency in approximately 50% of HGSC and specifically found genetic mutations and epigenetic silencing in numerous HR genes, including BRCA1, BRCA2, EMSY, RAD51C, ATR, ATM, PALB2, and several FA genes (CGARN, 2011). This study provides the rationale for including INPP4B as a biomarker of HR deficiency that should be further investigated in preclinical and clinical settings.

A comprehensive analysis of *INPP4B* overall gene expression in metastatic melanomas compared to primary melanomas was performed and significantly lower *INPP4B* expression was found in metastatic melanomas compared to primary lesions corroborating earlier findings that loss of *INPP4B* expression may modulate the metastatic potential of tumours (figure 6.1A) (Gewinner et al., 2009). Loss of *INPP4B*

expression was associated with poor overall survival in patients bearing ductal invasive breast carcinomas, as evidenced from earlier studies (figure 6.1B) (Gewinner et al., 2009). Taken together, these findings point to a critical role of INPP4B in overall patient survival and metastatic disease. It will be profitable to address if INPP4B correlates with patient outcome in clinical trials using HR inhibitors and if it can be used as a prognostic marker in ovarian cancer as well.

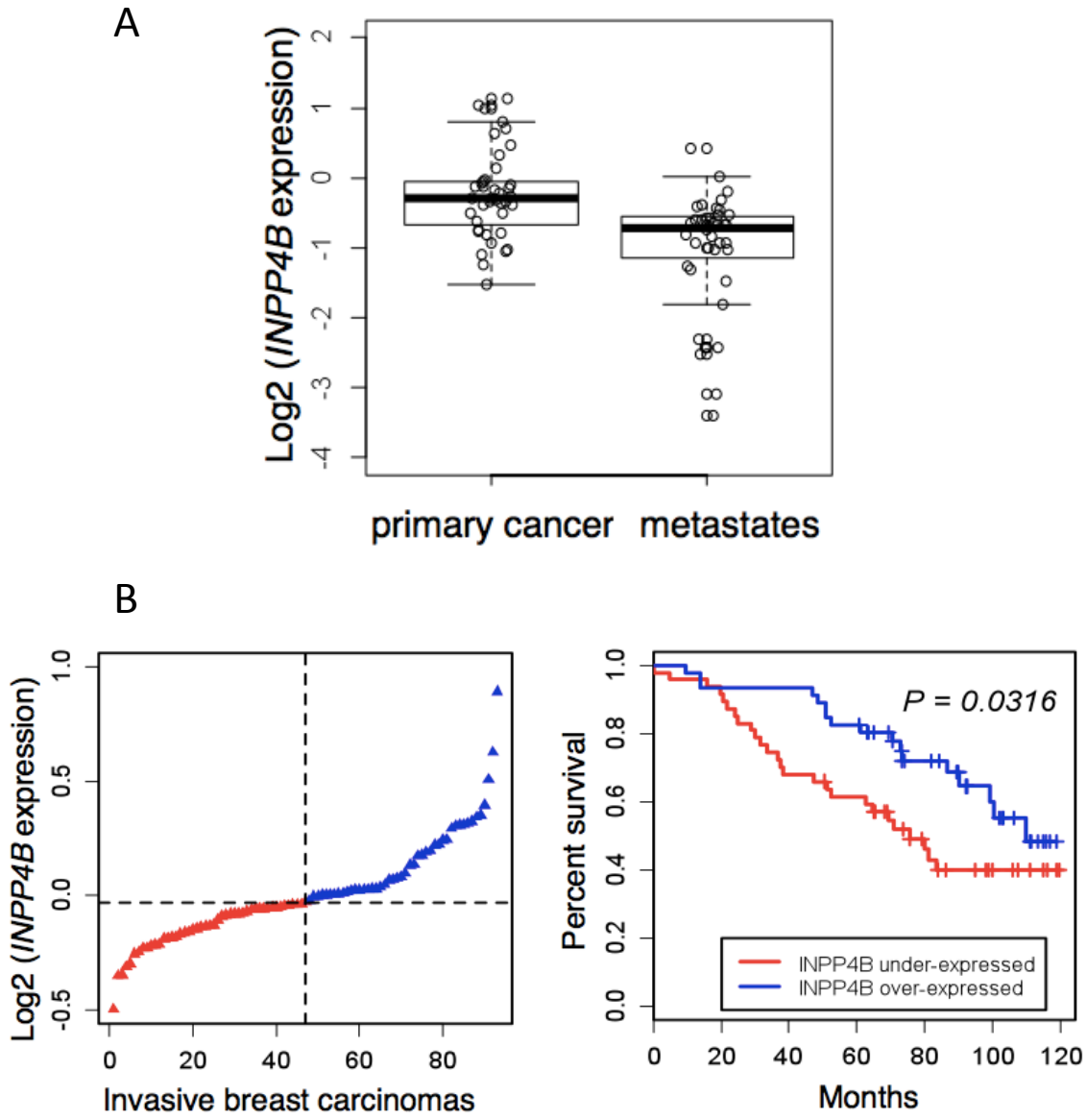

Figure 6.1. *INPP4B* is lost in human tumours and metastases. (A) Box-plots indicating significantly overall lower *INPP4B* expression in metastatic compared to primary melanomas (overall *INPP4B* loss: 48.6%). (B) Ranked *INPP4B* expression in ductal invasive breast carcinomas (n=93) and Kaplan-Meier survival curves comparing disease-free survival between cases with the lowest (<50th percentile) vs. highest (>50th percentile) *INPP4B* expression (P= 0.0316, log-rank test). Bioinformatic analysis was conducted by Dr. George Pouligiannis (Harvard University, USA).

In addition, the relevance of INPP4B within the context of the PI3K/Akt pathway and ovarian cancer requires further investigation. In a comprehensive analysis of 93 primary ovarian tumours, aCGH analysis was used to identify copy number changes amongst nine canonical signalling pathways (PI3K/AKT/mTOR, MAPK, TGF-B, p38/MAPK, JNK, JAK/STAT, WNT/β-Catenin, and NFκB) and the PI3K/AKT/mTOR pathway was the most frequently altered cancer related pathway (Huang et al., 2011). Currently, clinical trials that are combining PI3K/Akt/mTOR inhibitors with other targeted therapies are enrolling patients for the study regardless of the PI3K/Akt pathway component status within their tumours. Identifying biomarkers that would accurately predict patient response through assessment of PI3K/Akt component integrity, and hence also identify the relevant subset of patients for enrolment may increase the efficacy of clinical trials. In breast and gynaecological malignancies, *PI3KCA* mutation and PTEN loss correlated with patient response to doxorubicin, bevacizumab, and temsirolimus (Moroney et al., 2011). Preliminary studies treating INPP4B-deficient ovarian cancer cells with dual PI3K/mTOR inhibitor NVP-BEZ235 (Novartis, Switzerland) resulted in increased sensitivity compared to the control treated cells. It would be of interest to see whether the incorporation of PARP inhibitors would be a synergistic treatment addition in this context.

The limitations of this study from a therapeutic perspective revolve around the long-term impact of PARP inhibition of ovarian tumours. While novel predictive markers are needed to accurately include patients likely to respond to PARP inhibitor treatments, current predictors of sensitivity and the one proposed in this study do not necessarily represent predictors of long lasting therapy sensitivity. Evidence of PARP inhibitor resistance has emerged, through resistance of secondary mutations of *BRCA2*, and also

resistance through loss of 53BP1 expression (Bouwman et al., 2010; Bunting et al., 2012). Continuing research is required to provide a better framework of understanding the function of INPP4B in ovarian cancer as well as present potential therapeutic alternatives to circumvent arising drug resistance. Gaining greater insight into the regulation of INPP4B, defining the cytoplasmic and nuclear roles of the protein, and discerning how INPP4B contributes to other signalling pathways directly and indirectly will provide a more well-rounded understanding of the impact of INPP4B on ovarian cancer and how it can be best exploited therapeutically to provide a specific and long lasting benefit for patients.

CHAPTER 7. Appendix

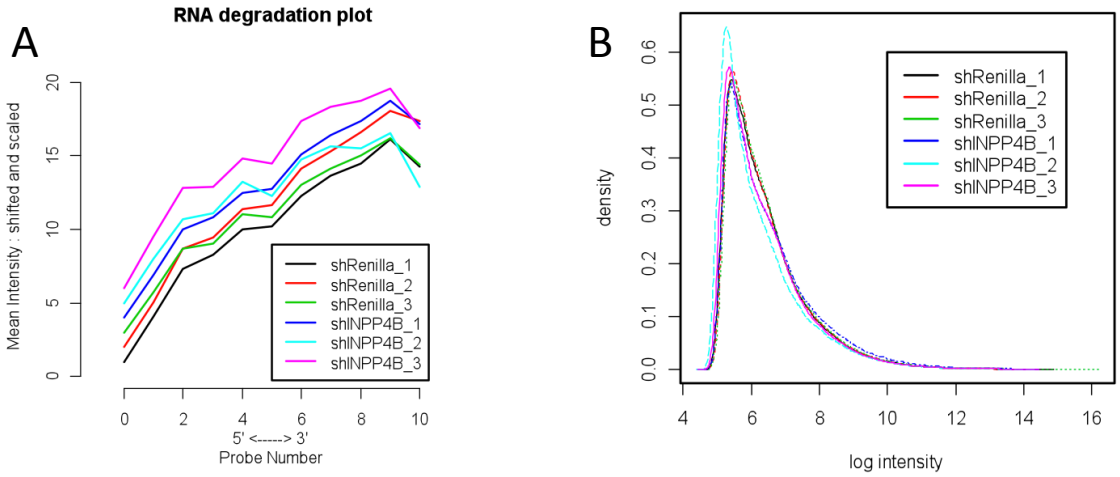

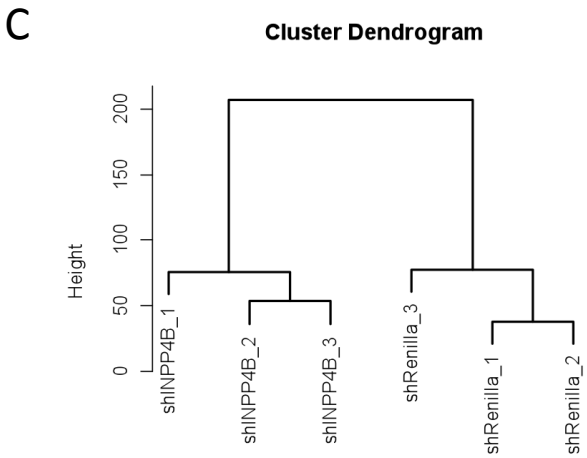

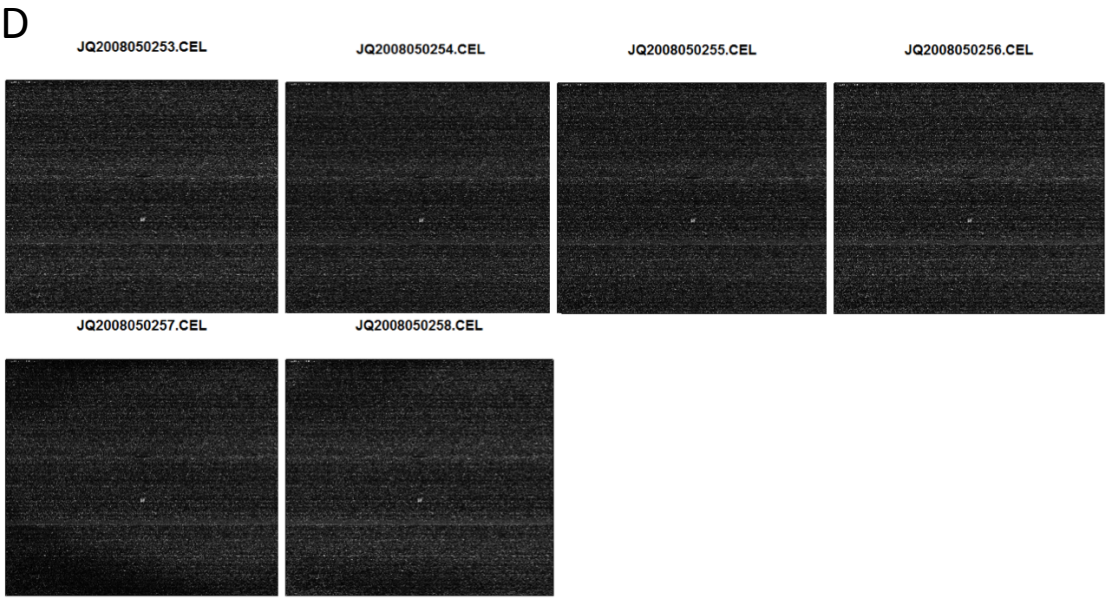

Appendix 1. Qualitative analyses of the microarray experiments that were used to assess the transcriptional changes of MCF-10A shRNA INPP4B or Renilla luciferase expressing cell pools. (A) RNA degradation plots indicating the relative intensities of individual probes ordered from 5′ to 3′ averaged over all probe sets. (B) Scatter plots of the log – intensity values of the genes across all microarray experiments. (C) Unsupervised hierarchical clustering across the 54,675 gene probes that were included in the microarray platform indicating good clustering among the replicate samples. (D) Image plots of the arrays that were used in this experiment indicating no major artifacts. Analysis was performed by Dr. George Pouligiannis (Harvard University, USA). Experiments were conducted in triplicates (n = 6). Data pre-processing and quality control were performed in R (http://www.r-project.org/) and Bioconductor.

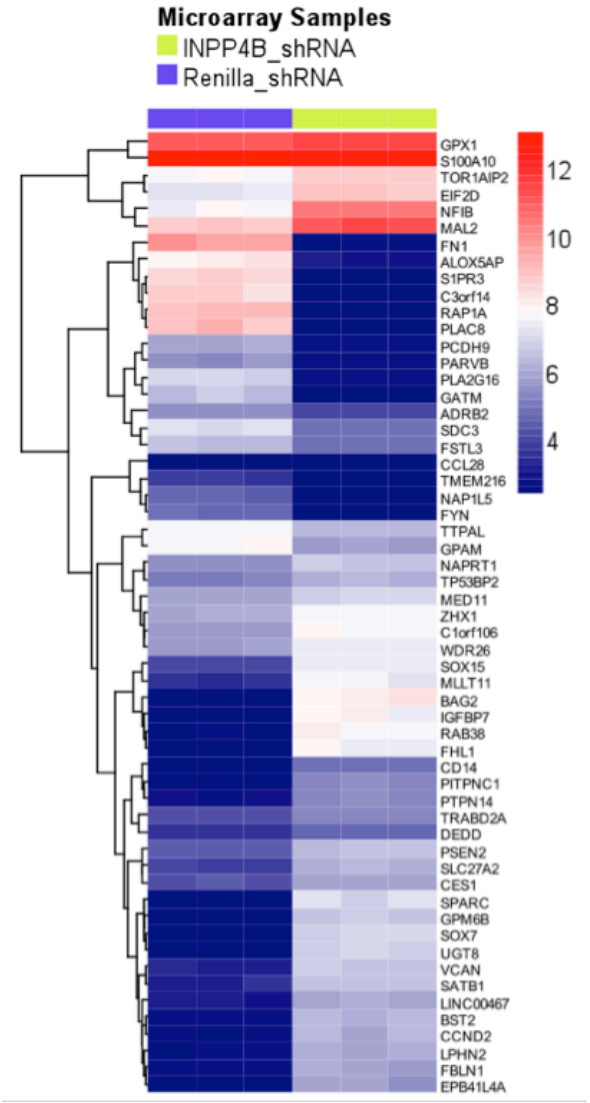

Appendix 2. Heatmap of the most significantly differentially expressed genes (adjusted P-value < 0.05) between Renilla luciferase and INPP4B knockdown MCF-10A cells. Red and blue bars represent high and low gene expression relative to the median expression, respectively. Cell preparation and bioinformatic analysis were conducted by Dr Christina Gewinner (UCL, UK) and Dr George Pouligiannis (Harvard University, USA). The differentially expressed genes were computed by an empirical Bayes shrinkage of the standard errors toward a common value approach embedded within the

Limma package (Smyth, 2004). P-values were adjusted for multiple comparisons using the false discovery rate approach implemented by Benjamini & Hochberg (Klipper-Aurbach et al., 1995).

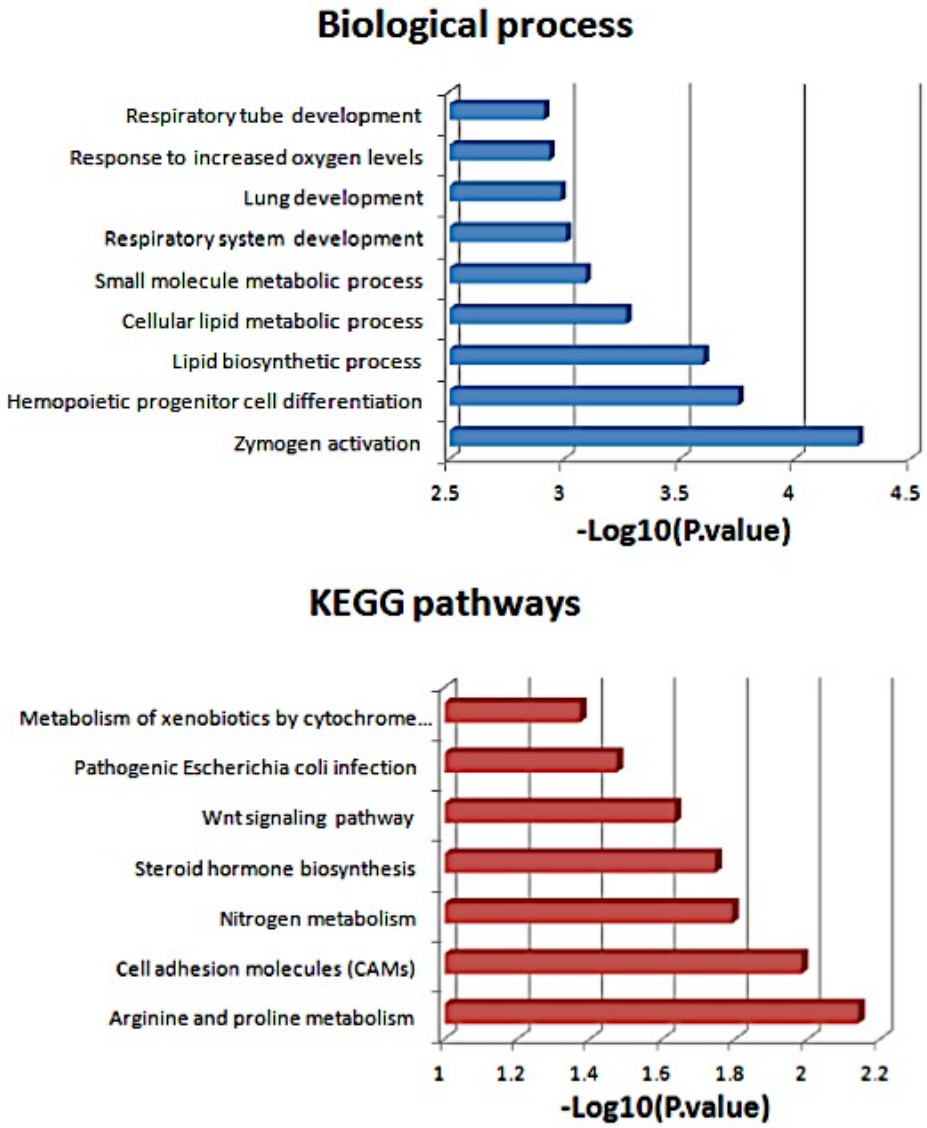

Appendix 3. Biological processes and Kyoto encyclopaedia of genes and genomes (KEGG) pathways enriched in the genes associated with INPP4B knockdown. Gene ontology and pathway enrichment analysis was performed using a classical hypergeometric test and the gene ontologies or pathways with the highest negative log(10) P value were plotted. Bioinformatic analysis was conducted by Dr George Pouligiannis (Harvard University, USA).

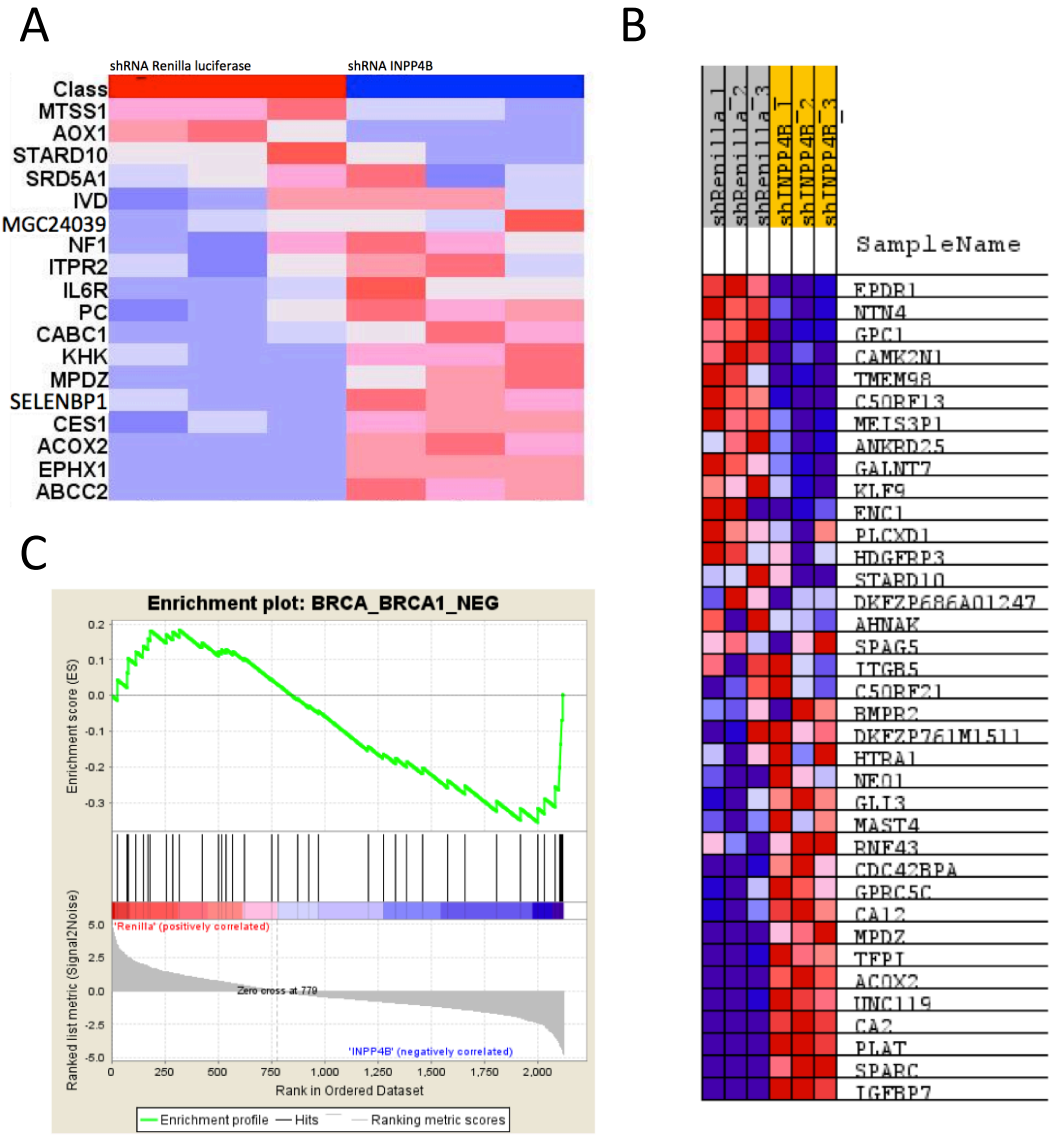

Appendix 4. BRCA1-mutant and poor survival gene signatures revealed in INPP4B deficient MCF-10A cells by microarray analysis. (A) Heatmap highlighting differences of the differentially expressed genes in the poor survival gene set. Red and blue bars represent high and low gene expression relative to the median expression, respectively. (**B**) Heatmap highlighting coordinated differential expression of the BRCA_BRCA1_NEG gene signature in MCF-10A shRNA INPP4B knockdown cells. **(C**) Gene set enrichment analysis (GSEA) of the BRCA_BRCA1_NEG gene signature. Method was performed as described previously (Subramanian et al., 2005). Bioinformatic analysis was conducted by Dr George Pouligiannis (Harvard University,

USA). The differentially expressed genes were computed by an empirical Bayes shrinkage of the standard errors toward a common value approach embedded within the Limma package (Smyth, 2004). P – values were adjusted for multiple comparison using the false discovery rate approach implemented by Benjamini & Hochberg (Klipper-Aurbach et al., 1995).

Appendix 5. BRCA1-mutant gene signature microarray data

Gene name	Probe ID	Log (2) Fold Change	P Value	Adjusted P Value
ACOX2	205364_at	1.48	1.62E-06	2.80E-04
AHNAK	220016_at	-0.62	6.19E-02	3.12E-01
AHNAK	211986_at	-0.33	1.23E-01	4.41E-01
AHNAK	238855_at	-0.05	6.97E-01	8.95E-01
AHNAK	1563560_at	-0.01	9.51E-01	9.85E-01
AHNAK	235281_x_at	-0.01	9.67E-01	9.89E-01
ANKRD25	218418_s_at	-1.21	2.02E-05	1.57E-03
ANKRD25	221068_at	-0.13	4.51E-01	7.70E-01
ANKRD25	1569602_at	-0.02	9.00E-01	9.70E-01
BMPR2	1556075_at	-0.17	1.93E-01	5.46E-01
BMPR2	210214_s_at	-0.05	7.54E-01	9.19E-01
BMPR2	238516_at	0.00	9.90E-01	9.97E-01
C5ORF13	201310_s_at	-1.31	1.60E-04	6.54E-03
C5ORF13	201309_x_at	-0.72	8.48E-04	2.06E-02
C5ORF13	230424_at	-0.21	1.86E-01	5.36E-01
C5ORF13	238411_x_at	0.17	2.45E-01	6.04E-01
C5ORF13	238410_x_at	-0.04	7.46E-01	9.16E-01
C5ORF13	222344_at	0.04	7.49E-01	9.17E-01
C5ORF21	212936_at	0.15	5.01E-01	8.01E-01
C5ORF21	223882_at	-0.08	5.87E-01	8.47E-01
CA12	203963_at	1.35	9.84E-06	9.44E-04
CA12	214164_x_at	1.13	2.36E-05	1.75E-03
CA12	210735_s_at	1.19	4.87E-05	2.89E-03
CA12	215867_x_at	1.15	5.35E-05	3.07E-03
CA12	204508_s_at	1.19	7.45E-05	3.87E-03
CA2	209301_at	2.80	2.96E-07	9.36E-05
CAMK2N1	229163_at	-1.79	4.57E-07	1.19E-04
CAMK2N1	218309_at	-1.61	3.00E-06	4.14E-04
CAMK2N1	228302_x_at	-1.34	1.99E-05	1.56E-03
DKFZP686A01247	212328_at	0.51	2.16E-02	1.71E-01
DKFZP686A01247	232457_at	0.14	3.19E-01	6.73E-01
DKFZP686A01247	1569208_a_at	0.08	5.19E-01	8.10E-01
DKFZP686A01247	212325_at	0.11	5.28E-01	8.15E-01
DKFZP686A01247	1566248_at	0.08	5.41E-01	8.23E-01
DKFZP686A01247	1566249_at	-0.07	6.35E-01	8.68E-01
DKFZP686A01247	244554_at	-0.06	6.46E-01	8.73E-01
DKFZP686A01247	241459_at	0.05	6.92E-01	8.93E-01

Gene name	Probe ID	Log (2) Fold Change	P Value	Adjusted P Value
DKFZP686A01247	212327_at	0.07	7.31E-01	9.10E-01
DKFZP761M1511	225355_at	0.43	1.98E-02	1.63E-01
ENC1	201341_at	-0.58	4.35E-02	2.56E-01
ENC1	201340_s_at	-0.66	6.03E-02	3.07E-01
EPDR1	223253_at	-3.78	6.71E-09	6.55E-06
EPDR1	240297_at	-0.26	8.05E-02	3.57E-01
GALNT7	218313_s_at	-0.74	2.11E-03	3.84E-02
GALNT7	222587_s_at	-0.47	4.60E-02	2.63E-01
GLI3	227376_at	1.04	3.29E-04	1.08E-02
GLI3	1569342_at	-0.30	3.45E-02	2.25E-01
GLI3	205201_at	0.35	3.46E-02	2.26E-01
GPC1	202756_s_at	-1.15	1.94E-05	1.53E-03
GPC1	202755_s_at	-0.79	8.06E-05	4.06E-03
GPC1	214858_at	0.44	5.82E-02	3.01E-01
HDGFRP3	209524_at	-1.46	2.99E-02	2.08E-01
HDGFRP3	228266_s_at	0.25	1.05E-01	4.09E-01
HDGFRP3	221976_s_at	-0.17	2.86E-01	6.45E-01
HDGFRP3	209525_at	-0.19	3.17E-01	6.71E-01
HDGFRP3	209526_s_at	0.11	4.70E-01	7.83E-01
HDGFRP3	216693_x_at	0.10	5.37E-01	8.20E-01
HTRA1	201185_at	0.98	2.01E-03	3.71E-02
ITGB5	214021_x_at	-0.68	2.52E-04	8.99E-03
ITGB5	201124_at	0.18	3.20E-01	6.73E-01
ITGB5	214020_x_at	-0.12	3.71E-01	7.16E-01
ITGB5	201125_s_at	0.09	5.26E-01	8.14E-01
KLF9	203542_s_at	-1.29	4.69E-03	6.49E-02
KLF9	203543_s_at	-1.09	8.22E-03	9.42E-02
KLF9	203541_s_at	0.27	7.50E-02	3.46E-01
KLF9	230636_s_at	-0.20	2.70E-01	6.30E-01
KLF9	228474_s_at	0.00	9.86E-01	9.95E-01
MAST4	225613_at	1.25	1.17E-04	5.21E-03
MAST4	225611_at	1.06	6.00E-04	1.63E-02
MAST4	40016_g_at	0.78	8.51E-04	2.06E-02
MAST4	210958_s_at	0.58	1.04E-02	1.09E-01
MAST4	243575_at	0.14	3.44E-01	6.94E-01
MAST4	222348_at	0.10	6.15E-01	8.59E-01
MAST4	1554652_s_at	-0.03	8.57E-01	9.56E-01
MEIS3P1	214077_x_at	-0.50	6.17E-03	7.79E-02
MPDZ	213306_at	1.80	2.08E-06	3.17E-04

Gene name	Probe ID	Log (2) Fold Change	P Value	Adjusted P Value
MPDZ	205079_s_at	0.99	2.88E-05	2.02E-03
NTN4	223315_at	-2.03	3.75E-08	2.33E-05
NTN4	234202_at	0.14	3.97E-01	7.35E-01
PLCXD1	218951_s_at	-0.48	6.86E-03	8.39E-02
RNF43	218704_at	0.56	2.01E-03	3.71E-02
RNF43	228828_at	-0.23	1.89E-01	5.40E-01
RNF43	239588_s_at	0.15	3.11E-01	6.66E-01
RNF43	244226_s_at	-0.10	4.20E-01	7.50E-01
RNF43	228826_at	-0.07	6.31E-01	8.67E-01
RNF43	239589_at	0.05	7.26E-01	9.08E-01
SPAG5	203145_at	0.10	6.99E-01	8.96E-01
SPARC	200665_s_at	3.70	1.17E-10	4.87E-07
STARD10	223103_at	-0.79	4.08E-02	2.47E-01
STARD10	232322_x_at	-0.48	5.34E-02	2.86E-01
STARD10	1557661_at	0.08	4.78E-01	7.87E-01
STARD10	238911_at	0.04	7.99E-01	9.36E-01
TFPI	210664_s_at	3.64	2.91E-10	9.34E-07
TFPI	213258_at	4.00	3.31E-09	4.64E-06
TFPI	209676_at	1.88	2.47E-04	8.89E-03
TFPI	210665_at	0.68	1.18E-03	2.55E-02
TMEM98	223170_at	-1.14	3.92E-05	2.50E-03

Appendix 6. BRCA1 mutant microarray gene set used for microarray validation.

Gene name	Log (2) Fold Change	Standard Deviation	P Value	Adjusted P Value
ANKRD25	-1.21		2.02E-05	1.57E-03
C5ORF13	-1.02	0.42	5.04E-04	1.35E-02
CA12	1.20	0.08	4.20E-05	2.51E-03
CA2	2.80		2.96E-07	9.36E-05
CAMK2N1	-1.58	0.13	7.78E-06	6.96E-04
GALNT7	-0.74		2.11E-03	3.84E-02
GPC1	-0.97		5.00E-05	2.80E-03
MPDZ	1.39	0.57	1.55E-05	1.17E-03
NTN4	-2.03		3.75E-08	2.33E-05
SPARC	3.70		1.17E-10	4.87E-07
TFPI	2.55	1.55	3.56E-04	8.60E-03
TMEM98	-1.14		3.92E-05	2.50E-03

Appendix 7. Konstantinopoulos *et al.* BRCAness gene profile comparison with the MCF-10A shRNA INPP4B microarray data set.

Gene Symbol	Weight BRCA1-mutant (Konstanopoulos et al.)	Log-fold change in MCF-10A shRNA INPP4B microarray
DAD1	0.10	N/A
RAD21	0.17	1.09
		0.69
LDHA	0.02	N/A
SPARC	0.16	3.70
		0.95
SKP1	0.14	0.17
PPP1CC	0.02	N/A
RAN	0.10	0.22
USP9X	-0.01	-0.31
ECHS1	-0.05	0.58
GNAI3	0.14	N/A
HDAC1	-0.03	0.26
LGMN	-0.07	0.49
CYR61	-0.05	-0.94
		-1.01
SH3BGRL	0.07	0.60
MGST3	-0.02	1.39
RCN2	0.21	0.23
SMC1A	0.03	0.40
		0.36
BST2	0.21	2.96
ENG	0.06	N/A
SRGN	-0.16	-2.75
		-3.55
GBP1	0.08	-0.39
		-0.20
UNC119B	0.14	0.22
RGS1	-0.26	N/A
CDC2	0.11	N/A
SAT1	-0.04	-0.71
		-0.40
		-0.41
		-0.27
GGH	-0.02	-0.25
GUCY1B3	0.02	0.67
		0.45
WFDC2	0.07	N/A
NMI	0.09	1.56

Gene Symbol	Weight BRCA1-mutant (Konstanopoulos et al.)	Log-fold change in MCF-10A shINPP4B microarray
PRAME	0.03	N/A
CCL4	-0.15	0.23
MGST2	0.00	0.47
MMP7	0.00	N/A
SNCA	-0.16	0.78 0.53 0.65 0.46
VTN	-0.04	N/A
ALPP	-0.03	-0.67
MTAP	-0.05	0.38 0.22
IDUA	0.10	0.26
SERPINF2	-0.01	0.37
WAS	-0.02	0.41
CD1D	-0.14	-0.25
GFI1	-0.03	N/A
P11	0.01	N/A
SEMA3F	0.08	0.49 0.63 0.34
TNF	-0.02	N/A
ROS1	0.17	-0.24 -0.23
MADCAM1	-0.03	N/A
PDIA4	0.16	N/A
HMGN2	-0.02	-0.43
HLA-B	0.10	1.48 1.27 1.48
TM9SF1	0.11	N/A
CCDC93	-0.09	0.31
APEX1	0.02	N/A
VEGFA	0.06	0.32 0.20
POSTN	0.21	N/A
PSTPIP1	-0.04	N/A
PMS1	-0.06	N/A
HLA-A	0.02	1.83 1.13
PCTP	-0.05	0.92
SEH1L	0.11	N/A

N/A represents genes present in the BRCAness gene profile but not in the MCF-10A shRNA INPP4B microarray data set, therefore no comparison of gene expression trends could be made.

References

Abadir, R., and Hakami, N. (1983). Ataxia telangiectasia with cancer. An indication for reduced radiotherapy and chemotherapy doses. Br J Radiol *56*, 343-345.

Accili, D., and Arden, K.C. (2004). FoxOs at the crossroads of cellular metabolism, differentiation, and transformation. Cell *117*, 421-426.

Ackah, E., Yu, J., Zoellner, S., Iwakiri, Y., Skurk, C., Shibata, R., Ouchi, N., Easton, R.M., Galasso, G., Birnbaum, M.J.*, et al.* (2005). Akt1/protein kinase Balpha is critical for ischemic and VEGF-mediated angiogenesis. J Clin Invest *115*, 2119-2127.

Agoulnik, I.U., Hodgson, M.C., Bowden, W.A., and Ittmann, M.M. (2011). INPP4B: the new kid on the PI3K block. Oncotarget *2*, 321-328.

Agranoff, B.W., Bradley, R.M., and Brady, R.O. (1958). The enzymatic synthesis of inositol phosphatide. J Biol Chem *233*, 1077-1083.

Ahluwalia, A., Hurteau, J.A., Bigsby, R.M., and Nephew, K.P. (2001). DNA methylation in ovarian cancer. II. Expression of DNA methyltransferases in ovarian cancer cell lines and normal ovarian epithelial cells. Gynecol Oncol *82*, 299-304.

Ahn, J.Y., Li, X., Davis, H.L., and Canman, C.E. (2002). Phosphorylation of threonine 68 promotes oligomerization and autophosphorylation of the Chk2 protein kinase via the forkhead-associated domain. J Biol Chem *277*, 19389-19395.

Ahn, J.Y., Schwarz, J.K., Piwnica-Worms, H., and Canman, C.E. (2000). Threonine 68 phosphorylation by ataxia telangiectasia mutated is required for efficient activation of Chk2 in response to ionizing radiation. Cancer Res *60*, 5934-5936.

Alessi, D.R., Andjelkovic, M., Caudwell, B., Cron, P., Morrice, N., Cohen, P., and Hemmings, B.A. (1996). Mechanism of activation of protein kinase B by insulin and IGF-1. EMBO J *15*, 6541-6551.

Alimonti, A., Carracedo, A., Clohessy, J.G., Trotman, L.C., Nardella, C., Egia, A., Salmena, L., Sampieri, K., Haveman, W.J., Brogi, E.*, et al.* (2010). Subtle variations in Pten dose determine cancer susceptibility. Nat Genet *42*, 454-458.

Alsop, K., Fereday, S., Meldrum, C., deFazio, A., Emmanuel, C., George, J., Dobrovic, A., Birrer, M.J., Webb, P.M., Stewart, C.*, et al.* (2012). BRCA mutation frequency and patterns of treatment response in BRCA mutation-positive women with ovarian cancer: a report from the Australian Ovarian Cancer Study Group. Journal of clinical oncology : official journal of the American Society of Clinical Oncology *30*, 2654-2663.

Altomare, D.A., Guo, K., Cheng, J.Q., Sonoda, G., Walsh, K., and Testa, J.R. (1995). Cloning, chromosomal localization and expression analysis of the mouse Akt2 oncogene. Oncogene *11*, 1055-1060.

Altomare, D.A., Lyons, G.E., Mitsuuchi, Y., Cheng, J.Q., and Testa, J.R. (1998). Akt2 mRNA is highly expressed in embryonic brown fat and the AKT2 kinase is activated by insulin. Oncogene *16*, 2407-2411.

Alvarez-Nunez, F., Bussaglia, E., Mauricio, D., Ybarra, J., Vilar, M., Lerma, E., de Leiva, A., Matias-Guiu, X., and Thyroid Neoplasia Study, G. (2006). PTEN promoter methylation in sporadic thyroid carcinomas. Thyroid *16*, 17-23.

Andressoo, J.O., Hoeijmakers, J.H., and de Waard, H. (2005). Nucleotide excision repair and its connection with cancer and ageing. Adv Exp Med Biol *570*, 45-83.

Anglesio, M.S., Wiegand, K.C., Melnyk, N., Chow, C., Salamanca, C., Prentice, L.M., Senz, J., Yang, W., Spillman, M.A., Cochrane, D.R.*, et al.* (2013). Type-specific cell line models for type-specific ovarian cancer research. PLoS One *8*, e72162.

Antoni, L., Sodha, N., Collins, I., and Garrett, M.D. (2007). CHK2 kinase: cancer susceptibility and cancer therapy - two sides of the same coin? Nat Rev Cancer *7*, 925-936.

Antoniou, A., Pharoah, P.D., Narod, S., Risch, H.A., Eyfjord, J.E., Hopper, J.L., Loman, N., Olsson, H., Johannsson, O., Borg, A.*, et al.* (2003). Average risks of breast and ovarian cancer associated with BRCA1 or BRCA2 mutations detected in case Series unselected for family history: a combined analysis of 22 studies. Am J Hum Genet *72*, 1117-1130.

Arboleda, M.J., Lyons, J.F., Kabbinavar, F.F., Bray, M.R., Snow, B.E., Ayala, R., Danino, M., Karlan, B.Y., and Slamon, D.J. (2003). Overexpression of AKT2/protein kinase Bbeta leads to up-regulation of beta1 integrins, increased invasion, and metastasis of human breast and ovarian cancer cells. Cancer Res *63*, 196-206.

Armour, S.M., Baur, J.A., Hsieh, S.N., Land-Bracha, A., Thomas, S.M., and Sinclair, D.A. (2009). Inhibition of mammalian S6 kinase by resveratrol suppresses autophagy. Aging (Albany NY) *1*, 515-528.

Audeh, M.W., Carmichael, J., Penson, R.T., Friedlander, M., Powell, B., Bell-McGuinn, K.M., Scott, C., Weitzel, J.N., Oaknin, A., Loman, N.*, et al.* (2010). Oral poly(ADP-ribose) polymerase inhibitor olaparib in patients with BRCA1 or BRCA2 mutations and recurrent ovarian cancer: a proof-of-concept trial. Lancet *376*, 245-251.

Auersperg, N., Wong, A.S., Choi, K.C., Kang, S.K., and Leung, P.C. (2001). Ovarian surface epithelium: biology, endocrinology, and pathology. Endocr Rev *22*, 255-288.

Azad, N.S., Posadas, E.M., Kwitkowski, V.E., Steinberg, S.M., Jain, L., Annunziata, C.M., Minasian, L., Sarosy, G., Kotz, H.L., Premkumar, A.*, et al.* (2008). Combination targeted therapy with sorafenib and bevacizumab results in enhanced toxicity and antitumor activity. Journal of clinical oncology : official journal of the American Society of Clinical Oncology *26*, 3709-3714.

Bahassi, E.M., Ovesen, J.L., Riesenberg, A.L., Bernstein, W.Z., Hasty, P.E., and Stambrook, P.J. (2008). The checkpoint kinases Chk1 and Chk2 regulate the functional associations between hBRCA2 and Rad51 in response to DNA damage. Oncogene *27*, 3977-3985.

Bakkenist, C.J., and Kastan, M.B. (2003). DNA damage activates ATM through intermolecular autophosphorylation and dimer dissociation. Nature *421*, 499-506.

Balasubramanian, B., Pogozelski, W.K., and Tullius, T.D. (1998). DNA strand breaking by the hydroxyl radical is governed by the accessible surface areas of the hydrogen atoms of the DNA backbone. Proc Natl Acad Sci U S A *95*, 9738-9743.

Baldwin, R.L., Nemeth, E., Tran, H., Shvartsman, H., Cass, I., Narod, S., and Karlan, B.Y. (2000). BRCA1 promoter region hypermethylation in ovarian carcinoma: a population-based study. Cancer Res *60*, 5329-5333.

Balendran, A., Casamayor, A., Deak, M., Paterson, A., Gaffney, P., Currie, R., Downes, C.P., and Alessi, D.R. (1999). PDK1 acquires PDK2 activity in the presence of a synthetic peptide derived from the carboxyl terminus of PRK2. Curr Biol *9*, 393-404.

Banath, J.P., Klokov, D., MacPhail, S.H., Banuelos, C.A., and Olive, P.L. Residual gammaH2AX foci as an indication of lethal DNA lesions. BMC Cancer *10*, 4.

Bartkova, J., Horejsi, Z., Sehested, M., Nesland, J.M., Rajpert-De Meyts, E., Skakkebaek, N.E., Stucki, M., Jackson, S., Lukas, J., and Bartek, J. (2007). DNA damage response mediators MDC1 and 53BP1: constitutive activation and aberrant loss in breast and lung cancer, but not in testicular germ cell tumours. Oncogene *26*, 7414-7422.

Bartlett, J.M., Langdon, S.P., Simpson, B.J., Stewart, M., Katsaros, D., Sismondi, P., Love, S., Scott, W.N., Williams, A.R., Lessells, A.M*., et al.* (1996). The prognostic value of epidermal growth factor receptor mRNA expression in primary ovarian cancer. British journal of cancer *73*, 301-306.

Bast, R.C., Jr., Feeney, M., Lazarus, H., Nadler, L.M., Colvin, R.B., and Knapp, R.C. (1981). Reactivity of a monoclonal antibody with human ovarian carcinoma. The Journal of clinical investigation *68*, 1331-1337.

Bast, R.C., Jr., Hennessy, B., and Mills, G.B. (2009). The biology of ovarian cancer: new opportunities for translation. Nat Rev Cancer *9*, 415-428.

Bast, R.C., Jr., and Spriggs, D.R. (2011). More than a biomarker: CA125 may contribute to ovarian cancer pathogenesis. Gynecol Oncol *121*, 429-430.

Bell D, B.A., Birrer M, Chien J, Cramer D, Dao F, Dhir R, DiSaia P, Gabra H, Glenn P, Godwin A, Gross J, Hartmann L, Huang M, Huntsman D, Iacocca M, Imielinski M, Kalloger S, Karlan B, Levine D, Mills G, Morrison C, Mutch D, Olvera N, Orsulic S, Park K, Petrelli N, Rabeno B, Rader J, Sikic B, Smith-McCune K, Sood A, Bowtell D, Penny R, Testa J, Chang K, Dinh H, Drummond J, Fowler G, Gunaratne P, Hawes A, Kovar C, Lewis L, Morgan M, Newsham I, Santibanez J, Reid J, Trevino L, Wu Y-, Wang M, Muzny D, Wheeler D, Gibbs R, Getz G, Lawrence M, Cibulskis K, Sivachenko A, Sougnez C, Voet D, Wilkinson J, Bloom T, Ardlie K, Fennell T, Baldwin J, Gabriel S, Lander E, Ding LL, Fulton R, Koboldt D, McLellan M, Wylie T, Walker J, O'Laughlin M, Dooling D, Fulton L, Abbott R, Dees N, Zhang Q, Kandoth C, Wendl M, Schierding W, Shen D, Harris C, Schmidt H, Kalicki J, Delehaunty K, Fronick C, Demeter R, Cook L, Wallis J, Lin L, Magrini V, Hodges J, Eldred J, Smith S, Pohl C, Vandin F, Raphael B, Weinstock G, Mardis E, Wilson R, Meyerson M, Winckler W, Getz G, Verhaak R, Carter S, Mermel C, Saksena G, Nguyen H, Onofrio R, Lawrence M, Hubbard D, Gupta S, Crenshaw A, Ramos A, Ardlie K, Chin L,

Protopopov A, Zhang J, Kim T, Perna I, Xiao Y, Zhang H, Ren G, Sathiamoorthy N, Park R, Lee E, Park P, Kucherlapati R, Absher M, Waite L, Sherlock G, Brooks J, Li J, Xu J, Myers R, Laird PW, Cope L, Herman J, Shen H, Weisenberger D, Noushmehr H, Pan F, Triche T Jr, Berman B, Van Den Berg D, Buckley J, Baylin S, Spellman P, Purdom E, Neuvial P, Bengtsson H, Jakkula L, Durinck S, Han J, Dorton S, Marr H, Choi Y, Wang V, Wang N, Ngai J, Conboy J, Parvin B, Feiler H, Speed T, Gray J, Levine A, Socci N, Liang Y, Taylor B, Schultz N, Borsu L, Lash A, Brennan C, Viale A, Sander C, Ladanyi M, Hoadley K, Meng S, Du Y, Shi Y, Li L, Turman Y, Zang D, Helms E, Balu S, Zhou X, Wu J, Topal M, Hayes D, Perou C, Getz G, Voet D, Saksena G, Zhang J, Zhang H, Wu C, Shukla S, Cibulskis K, Lawrence M, Sivachenko A, Jing R, Park R, Liu Y, Park P, Noble M, Chin L, Carter H, Kim D, Karchin R, Spellman P, Purdom E, Neuvial P, Bengtsson H, Durinck S, Han J, Korkola J, Heiser L, Cho R, Hu Z, Parvin B, Speed T, Gray J, Schultz N, Cerami E, Taylor B, Olshen A, Reva B, Antipin Y, Shen R, Mankoo P, Sheridan R, Ciriello G, Chang W, Bernanke J, Borsu L, Levine D, Ladanyi M, Sander C, Haussler D, Benz C, Stuart J, Benz S, Sanborn J, Vaske C, Zhu J, Szeto C, Scott G, Yau C, Hoadley K, Du Y, Balu S, Hayes D, Perou C, Wilkerson M, Zhang N, Akbani R, Baggerly K, Yung W, Mills G, Weinstein J, Penny R, Shelton T, Grimm D, Hatfield M, Morris S, Yena P, Rhodes P, Sherman M, Paulauskis J, Millis S, Kahn A, Greene J, Sfeir R, Jensen M, Chen J, Whitmore J, Alonso S, Jordan J, Chu A, Zhang J, Barker A, Compton C, Eley G, Ferguson M, Fielding P, Gerhard D, Myles R, Schaefer C, Mills Shaw K, Vaught J, Vockley J, Good P, Guyer M, Ozenberger B, Peterson J, Thomson E. (2011). Integrated genomic analyses of ovarian carcinoma. Nature *474*, 609-615.

Bender, C.F., Sikes, M.L., Sullivan, R., Huye, L.E., Le Beau, M.M., Roth, D.B., Mirzoeva, O.K., Oltz, E.M., and Petrini, J.H. (2002). Cancer predisposition and hematopoietic failure in Rad50(S/S) mice. Genes Dev *16*, 2237-2251.

Berns, K., Horlings, H.M., Hennessy, B.T., Madiredjo, M., Hijmans, E.M., Beelen, K., Linn, S.C., Gonzalez-Angulo, A.M., Stemke-Hale, K., Hauptmann, M.*, et al.* (2007). A functional genetic approach identifies the PI3K pathway as a major determinant of trastuzumab resistance in breast cancer. Cancer Cell *12*, 395-402.

Bhattacharyya, A., Ear, U.S., Koller, B.H., Weichselbaum, R.R., and Bishop, D.K. (2000). The breast cancer susceptibility gene BRCA1 is required for subnuclear assembly of Rad51 and survival following treatment with the DNA cross-linking agent cisplatin. J Biol Chem *275*, 23899-23903.

Bianco, R., Shin, I., Ritter, C.A., Yakes, F.M., Basso, A., Rosen, N., Tsurutani, J., Dennis, P.A., Mills, G.B., and Arteaga, C.L. (2003). Loss of PTEN/MMAC1/TEP in EGF receptor-expressing tumor cells counteracts the antitumor action of EGFR tyrosine kinase inhibitors. Oncogene *22*, 2812-2822.

Bigner, S.H., Mark, J., Mahaley, M.S., and Bigner, D.D. (1984). Patterns of the early, gross chromosomal changes in malignant human gliomas. Hereditas *101*, 103-113.

Birch, J.M. (1994). Li-Fraumeni syndrome. Eur J Cancer *30A*, 1935-1941.

Blasina, A., de Weyer, I.V., Laus, M.C., Luyten, W.H., Parker, A.E., and McGowan, C.H. (1999). A human homologue of the checkpoint kinase Cds1 directly inhibits Cdc25 phosphatase. Curr Biol *9*, 1-10.

Blasina, A., Hallin, J., Chen, E., Arango, M.E., Kraynov, E., Register, J., Grant, S., Ninkovic, S., Chen, P., Nichols, T.*, et al.* (2008). Breaching the DNA damage checkpoint via PF-00477736, a novel small-molecule inhibitor of checkpoint kinase 1. Mol Cancer Ther *7*, 2394-2404.

Blommaart, E.F., Luiken, J.J., Blommaart, P.J., van Woerkom, G.M., and Meijer, A.J. (1995). Phosphorylation of ribosomal protein S6 is inhibitory for autophagy in isolated rat hepatocytes. J Biol Chem *270*, 2320-2326.

Bolis, G., Parazzini, F., Scarfone, G., Villa, A., Amoroso, M., Rabaiotti, E., Polatti, A., Reina, S., and Pirletti, E. (1999). Paclitaxel vs epidoxorubicin plus paclitaxel as second-line therapy for platinum-refractory and -resistant ovarian cancer. Gynecol Oncol *72*, 60-64.

Bookman, M.A., Brady, M.F., McGuire, W.P., Harper, P.G., Alberts, D.S., Friedlander, M., Colombo, N., Fowler, J.M., Argenta, P.A., De Geest, K.*, et al.* (2009). Evaluation of new platinum-based treatment regimens in advanced-stage ovarian cancer: a Phase III Trial of the Gynecologic Cancer Intergroup. Journal of clinical oncology : official journal of the American Society of Clinical Oncology *27*, 1419-1425.

Bookman, M.A., Greer, B.E., and Ozols, R.F. (2003). Optimal therapy of advanced ovarian cancer: carboplatin and paclitaxel vs. cisplatin and paclitaxel (GOG 158) and an update on GOG0 182-ICON5. International journal of gynecological cancer : official journal of the International Gynecological Cancer Society *13*, 735-740.

Boutros, R., Lobjois, V., and Ducommun, B. (2007). CDC25 phosphatases in cancer cells: key players? Good targets? Nat Rev Cancer *7*, 495-507.

Bouwman, P., Aly, A., Escandell, J.M., Pieterse, M., Bartkova, J., van der Gulden, H., Hiddingh, S., Thanasoula, M., Kulkarni, A., Yang, Q.*, et al.* (2010). 53BP1 loss rescues BRCA1 deficiency and is associated with triple-negative and BRCA-mutated breast cancers. Nat Struct Mol Biol *17*, 688-695.

Bradley, M.O., and Kohn, K.W. (1979). X-ray induced DNA double strand break production and repair in mammalian cells as measured by neutral filter elution. Nucleic Acids Res *7*, 793-804.

Branzei, D., and Foiani, M. (2009). The checkpoint response to replication stress. DNA Repair (Amst) *8*, 1038-1046.

Briani, C., Schlotter, M., Lichter, P., and Kalla, C. (2006). Development of a mantle cell lymphoma in an ATM heterozygous woman after occupational exposure to ionising radiation and somatic mutation of the second allele. Leuk Res *30*, 1193-1196.

Brodbeck, D., Cron, P., and Hemmings, B.A. (1999). A human protein kinase Bgamma with regulatory phosphorylation sites in the activation loop and in the C-terminal hydrophobic domain. J Biol Chem *274*, 9133-9136.

Brodbeck, D., Hill, M.M., and Hemmings, B.A. (2001). Two splice variants of protein kinase B gamma have different regulatory capacity depending on the presence or absence of the regulatory phosphorylation site serine 472 in the carboxyl-terminal hydrophobic domain. J Biol Chem *276*, 29550-29558.

Bromberg, K.D., Burgin, A.B., and Osheroff, N. (2003). A two-drug model for etoposide action against human topoisomerase IIalpha. J Biol Chem *278*, 7406-7412.

Brown, E.J., and Baltimore, D. (2000). ATR disruption leads to chromosomal fragmentation and early embryonic lethality. Genes Dev *14*, 397-402.

Brunet, A., Bonni, A., Zigmond, M.J., Lin, M.Z., Juo, P., Hu, L.S., Anderson, M.J., Arden, K.C., Blenis, J., and Greenberg, M.E. (1999). Akt promotes cell survival by phosphorylating and inhibiting a Forkhead transcription factor. Cell *96*, 857-868.

Bryant, H.E., Schultz, N., Thomas, H.D., Parker, K.M., Flower, D., Lopez, E., Kyle, S., Meuth, M., Curtin, N.J., and Helleday, T. (2005). Specific killing of BRCA2-deficient tumours with inhibitors of poly(ADP-ribose) polymerase. Nature *434*, 913-917.

Bucher, N., and Britten, C.D. (2008). G2 checkpoint abrogation and checkpoint kinase-1 targeting in the treatment of cancer. Br J Cancer *98*, 523-528.

Buda, A., Floriani, I., Rossi, R., Colombo, N., Torri, V., Conte, P.F., Fossati, R., Ravaioli, A., and Mangioni, C. (2004). Randomised controlled trial comparing single agent paclitaxel vs epidoxorubicin plus paclitaxel in patients with advanced ovarian cancer in early progression after platinum-based chemotherapy: an Italian Collaborative Study from the Mario Negri Institute, Milan, G.O.N.O. (Gruppo Oncologico Nord Ovest) group and I.O.R. (Istituto Oncologico Romagnolo) group. Br J Cancer *90*, 2112-2117.

Bunney, T.D., and Katan, M. (2010). Phosphoinositide signalling in cancer: beyond PI3K and PTEN. Nat Rev Cancer *10*, 342-352.

Bunting, S.F., Callen, E., Kozak, M.L., Kim, J.M., Wong, N., Lopez-Contreras, A.J., Ludwig, T., Baer, R., Faryabi, R.B., Malhowski, A.*, et al.* (2012). BRCA1 functions independently of homologous recombination in DNA interstrand crosslink repair. Mol Cell *46*, 125-135.

Burger, R.A., Brady, M.F., Bookman, M.A., Fleming, G.F., Monk, B.J., Huang, H., Mannel, R.S., Homesley, H.D., Fowler, J., Greer, B.E.*, et al.* (2011). Incorporation of bevacizumab in the primary treatment of ovarian cancer. N Engl J Med *365*, 2473-2483.

Burger, R.A., Sill, M.W., Monk, B.J., Greer, B.E., and Sorosky, J.I. (2007). Phase II trial of bevacizumab in persistent or recurrent epithelial ovarian cancer or primary peritoneal cancer: a Gynecologic Oncology Group Study. Journal of clinical oncology : official journal of the American Society of Clinical Oncology *25*, 5165-5171.

Burgess, M., and Puhalla, S. (2014). BRCA 1/2-Mutation Related and Sporadic Breast and Ovarian Cancers: More Alike than Different. Front Oncol *4*, 19.

Byfield, M.P., Murray, J.T., and Backer, J.M. (2005). hVps34 is a nutrient-regulated lipid kinase required for activation of p70 S6 kinase. J Biol Chem *280*, 33076-33082.

Calera, M.R., Martinez, C., Liu, H., Jack, A.K., Birnbaum, M.J., and Pilch, P.F. (1998). Insulin increases the association of Akt-2 with Glut4-containing vesicles. J Biol Chem *273*, 7201-7204.

Campbell, I.G., Russell, S.E., Choong, D.Y., Montgomery, K.G., Ciavarella, M.L., Hooi, C.S., Cristiano, B.E., Pearson, R.B., and Phillips, W.A. (2004). Mutation of the PIK3CA gene in ovarian and breast cancer. Cancer research *64*, 7678-7681.

Cannistra, S.A., Matulonis, U.A., Penson, R.T., Hambleton, J., Dupont, J., Mackey, H., Douglas, J., Burger, R.A., Armstrong, D., Wenham, R.*, et al.* (2007). Phase II study of bevacizumab in patients with platinum-resistant ovarian cancer or peritoneal serous cancer. Journal of clinical oncology : official journal of the American Society of Clinical Oncology *25*, 5180-5186.

Carden, C.P., Sarker, D., Postel-Vinay, S., Yap, T.A., Attard, G., Banerji, U., Garrett, M.D., Thomas, G.V., Workman, P., Kaye, S.B.*, et al.* (2010). Can molecular biomarker-based patient selection in Phase I trials accelerate anticancer drug development? Drug Discov Today *15*, 88-97.

Carlson, K.J., Skates, S.J., and Singer, D.E. (1994). Screening for ovarian cancer. Annals of internal medicine *121*, 124-132.

Carpten, J.D., Faber, A.L., Horn, C., Donoho, G.P., Briggs, S.L., Robbins, C.M., Hostetter, G., Boguslawski, S., Moses, T.Y., Savage, S.*, et al.* (2007). A transforming mutation in the pleckstrin homology domain of AKT1 in cancer. Nature *448*, 439-444.

Carracedo, A., Ma, L., Teruya-Feldstein, J., Rojo, F., Salmena, L., Alimonti, A., Egia, A., Sasaki, A.T., Thomas, G., Kozma, S.C.*, et al.* (2008). Inhibition of mTORC1 leads to MAPK pathway activation through a PI3K-dependent feedback loop in human cancer. J Clin Invest *118*, 3065-3074.

Cass, I., Baldwin, R.L., Varkey, T., Moslehi, R., Narod, S.A., and Karlan, B.Y. (2003). Improved survival in women with BRCA-associated ovarian carcinoma. Cancer *97*, 2187-2195.

Catteau, A., Harris, W.H., Xu, C.F., and Solomon, E. (1999). Methylation of the BRCA1 promoter region in sporadic breast and ovarian cancer: correlation with disease characteristics. Oncogene *18*, 1957-1965.

CGARN, C.G.A.R.N. (2008). Comprehensive genomic characterization defines human glioblastoma genes and core pathways. Nature *455*, 1061-1068.

CGARN, T.C.G.A.R.N. (2011). Integrated genomic analyses of ovarian carcinoma. Nature *474*, 609-615.

Chalasani, P., and Livingston, R. (2013). Differential chemotherapeutic sensitivity for breast tumors with "BRCAness": a review. Oncologist *18*, 909-916.

Chan, D.W., Chen, B.P., Prithivirajsingh, S., Kurimasa, A., Story, M.D., Qin, J., and Chen, D.J. (2002a). Autophosphorylation of the DNA-dependent protein kinase catalytic subunit is required for rejoining of DNA double-strand breaks. Genes Dev *16*, 2333-2338.

Chan, K.Y., Ozcelik, H., Cheung, A.N., Ngan, H.Y., and Khoo, U.S. (2002b). Epigenetic factors controlling the BRCA1 and BRCA2 genes in sporadic ovarian cancer. Cancer Res *62*, 4151-4156.

Chanoux, R.A., Yin, B., Urtishak, K.A., Asare, A., Bassing, C.H., and Brown, E.J. (2009). ATR and H2AX cooperate in maintaining genome stability under replication stress. J Biol Chem *284*, 5994-6003.

Chen, T., Stephens, P.A., Middleton, F.K., and Curtin, N.J. (2012). Targeting the S and G2 checkpoint to treat cancer. Drug Discov Today *17*, 194-202.

Chen, V.W., Ruiz, B., Killeen, J.L., Cote, T.R., Wu, X.C., and Correa, C.N. (2003). Pathology and classification of ovarian tumors. Cancer *97*, 2631-2642.

Chen, W.S., Xu, P.Z., Gottlob, K., Chen, M.L., Sokol, K., Shiyanova, T., Roninson, I., Weng, W., Suzuki, R., Tobe, K.*, et al.* (2001). Growth retardation and increased apoptosis in mice with homozygous disruption of the Akt1 gene. Genes Dev *15*, 2203-2208.

Chen, X., Zhong, S., Zhu, X., Dziegielewska, B., Ellenberger, T., Wilson, G.M., MacKerell, A.D., Jr., and Tomkinson, A.E. (2008). Rational design of human DNA ligase inhibitors that target cellular DNA replication and repair. Cancer Res *68*, 3169-3177.

Cheng, J.Q., Godwin, A.K., Bellacosa, A., Taguchi, T., Franke, T.F., Hamilton, T.C., Tsichlis, P.N., and Testa, J.R. (1992). AKT2, a putative oncogene encoding a member of a subfamily of protein-serine/threonine kinases, is amplified in human ovarian carcinomas. Proc Natl Acad Sci U S A *89*, 9267-9271.

Chiang, G.G., and Abraham, R.T. (2005). Phosphorylation of mammalian target of rapamycin (mTOR) at Ser-2448 is mediated by p70S6 kinase. J Biol Chem *280*, 25485-25490.

Cho, H., Mu, J., Kim, J.K., Thorvaldsen, J.L., Chu, Q., Crenshaw, E.B., 3rd, Kaestner, K.H., Bartolomei, M.S., Shulman, G.I., and Birnbaum, M.J. (2001a). Insulin resistance and a diabetes mellitus-like syndrome in mice lacking the protein kinase Akt2 (PKB beta). Science *292*, 1728-1731.

Cho, H., Thorvaldsen, J.L., Chu, Q., Feng, F., and Birnbaum, M.J. (2001b). Akt1/PKBalpha is required for normal growth but dispensable for maintenance of glucose homeostasis in mice. J Biol Chem *276*, 38349-38352.

Choudhury, A., Zhao, H., Jalali, F., Al Rashid, S., Ran, J., Supiot, S., Kiltie, A.E., and Bristow, R.G. (2009). Targeting homologous recombination using imatinib results in enhanced tumor cell chemosensitivity and radiosensitivity. Mol Cancer Ther *8*, 203-213.

Ciardiello, F., Caputo, R., Bianco, R., Damiano, V., Pomatico, G., De Placido, S., Bianco, A.R., and Tortora, G. (2000). Antitumor effect and potentiation of cytotoxic drugs activity in human cancer cells by ZD-1839 (Iressa), an epidermal growth factor receptor-selective tyrosine kinase inhibitor. Clinical cancer research : an official journal of the American Association for Cancer Research *6*, 2053-2063.

Clement, S., Krause, U., Desmedt, F., Tanti, J.F., Behrends, J., Pesesse, X., Sasaki, T., Penninger, J., Doherty, M., Malaisse, W.*, et al.* (2001). The lipid phosphatase SHIP2 controls insulin sensitivity. Nature *409*, 92-97.

Cockcroft, S., and Carvou, N. (2007). Biochemical and biological functions of class I phosphatidylinositol transfer proteins. Biochim Biophys Acta *1771*, 677-691.

Coffer, P.J., and Woodgett, J.R. (1991). Molecular cloning and characterisation of a novel putative protein-serine kinase related to the cAMP-dependent and protein kinase C families. Eur J Biochem *201*, 475-481.

Collazo, M.M., Wood, D., Paraiso, K.H., Lund, E., Engelman, R.W., Le, C.T., Stauch, D., Kotsch, K., and Kerr, W.G. (2009). SHIP limits immunoregulatory capacity in the T-cell compartment. Blood *113*, 2934-2944.

Cramer, D.W., Bast, R.C., Jr., Berg, C.D., Diamandis, E.P., Godwin, A.K., Hartge, P., Lokshin, A.E., Lu, K.H., McIntosh, M.W., Mor, G.*, et al.* (2011). Ovarian cancer biomarker performance in prostate, lung, colorectal, and ovarian cancer screening trial specimens. Cancer prevention research *4*, 365-374.

Curtin, N.J. (2012). DNA repair dysregulation from cancer driver to therapeutic target. Nat Rev Cancer *12*, 801-817.

D'Amours, D., Desnoyers, S., D'Silva, I., and Poirier, G.G. (1999). Poly(ADP-ribosyl)ation reactions in the regulation of nuclear functions. Biochem J *342 (Pt 2)*, 249-268.

Daley, J.M., Kwon, Y., Niu, H., and Sung, P. (2013). Investigations of Homologous Recombination Pathways and Their Regulation. Yale J Biol Med *86*, 453-461.

Datta, S.R., Dudek, H., Tao, X., Masters, S., Fu, H., Gotoh, Y., and Greenberg, M.E. (1997). Akt phosphorylation of BAD couples survival signals to the cell-intrinsic death machinery. Cell *91*, 231-241.

Datta, S.R., Katsov, A., Hu, L., Petros, A., Fesik, S.W., Yaffe, M.B., and Greenberg, M.E. (2000). 14-3-3 proteins and survival kinases cooperate to inactivate BAD by BH3 domain phosphorylation. Mol Cell *6*, 41-51.

Davies, M.A., Stemke-Hale, K., Tellez, C., Calderone, T.L., Deng, W., Prieto, V.G., Lazar, A.J., Gershenwald, J.E., and Mills, G.B. (2008). A novel AKT3 mutation in melanoma tumours and cell lines. Br J Cancer *99*, 1265-1268.

De Placido, S., Scambia, G., Di Vagno, G., Naglieri, E., Lombardi, A.V., Biamonte, R., Marinaccio, M., Carteni, G., Manzione, L., Febbraro, A.*, et al.* (2004). Topotecan compared with no therapy after response to surgery and carboplatin/paclitaxel in patients with ovarian cancer: Multicenter Italian Trials in Ovarian Cancer (MITO-1) randomized study. Journal of clinical oncology : official journal of the American Society of Clinical Oncology *22*, 2635-2642.

Deans, A.J., and West, S.C. (2011). DNA interstrand crosslink repair and cancer. Nat Rev Cancer *11*, 467-480.

Debnath, J., Muthuswamy, S.K., and Brugge, J.S. (2003). Morphogenesis and oncogenesis of MCF-10A mammary epithelial acini grown in three-dimensional basement membrane cultures. Methods *30*, 256-268.

del Peso, L., Gonzalez-Garcia, M., Page, C., Herrera, R., and Nunez, G. (1997). Interleukin-3-induced phosphorylation of BAD through the protein kinase Akt. Science *278*, 687-689.

Delacroix, S., Wagner, J.M., Kobayashi, M., Yamamoto, K., and Karnitz, L.M. (2007). The Rad9-Hus1-Rad1 (9-1-1) clamp activates checkpoint signaling via TopBP1. Genes Dev *21*, 1472-1477.

Delcommenne, M., Tan, C., Gray, V., Rue, L., Woodgett, J., and Dedhar, S. (1998). Phosphoinositide-3-OH kinase-dependent regulation of glycogen synthase kinase 3 and protein kinase B/AKT by the integrin-linked kinase. Proc Natl Acad Sci U S A *95*, 11211-11216.

Di Paolo, G., and De Camilli, P. (2006). Phosphoinositides in cell regulation and membrane dynamics. Nature *443*, 651-657.

Dibble, C.C., and Manning, B.D. (2013). Signal integration by mTORC1 coordinates nutrient input with biosynthetic output. Nat Cell Biol *15*, 555-564.

Diehl, J.A., Cheng, M., Roussel, M.F., and Sherr, C.J. (1998). Glycogen synthase kinase-3beta regulates cyclin D1 proteolysis and subcellular localization. Genes Dev *12*, 3499-3511.

Ding, L., Getz, G., Wheeler, D.A., Mardis, E.R., McLellan, M.D., Cibulskis, K., Sougnez, C., Greulich, H., Muzny, D.M., Morgan, M.B.*, et al.* (2008). Somatic mutations affect key pathways in lung adenocarcinoma. Nature *455*, 1069-1075.

Ding, Q., Reddy, Y.V., Wang, W., Woods, T., Douglas, P., Ramsden, D.A., Lees-Miller, S.P., and Meek, K. (2003). Autophosphorylation of the catalytic subunit of the DNA-dependent protein kinase is required for efficient end processing during DNA double-strand break repair. Mol Cell Biol *23*, 5836-5848.

Dinulescu, D.M., Ince, T.A., Quade, B.J., Shafer, S.A., Crowley, D., and Jacks, T. (2005). Role of K-ras and Pten in the development of mouse models of endometriosis and endometrioid ovarian cancer. Nat Med *11*, 63-70.

Domcke, S., Sinha, R., Levine, D.A., Sander, C., and Schultz, N. (2013). Evaluating cell lines as tumour models by comparison of genomic profiles. Nat Commun *4*, 2126.

Domin, J., and Waterfield, M.D. (1997). Using structure to define the function of phosphoinositide 3-kinase family members. FEBS letters *410*, 91-95.

du Bois, A., Floquet, A., Kim, J.W., Rau, J., del Campo, J.M., Friedlander, M., Pignata, S., Fujiwara, K., Vergote, I., Colombo, N.*, et al.* (2014). Incorporation of pazopanib in maintenance therapy of ovarian cancer. J Clin Oncol *32*, 3374-3382.

du Bois, A., Luck, H.J., Meier, W., Adams, H.P., Mobus, V., Costa, S., Bauknecht, T., Richter, B., Warm, M., Schroder, W.*, et al.* (2003). A randomized clinical trial of cisplatin/paclitaxel versus carboplatin/paclitaxel as first-line treatment of ovarian cancer. Journal of the National Cancer Institute *95*, 1320-1329.

Dupre, A., Boyer-Chatenet, L., Sattler, R.M., Modi, A.P., Lee, J.H., Nicolette, M.L., Kopelovich, L., Jasin, M., Baer, R., Paull, T.T., *et al.* (2008). A forward chemical genetic screen reveals an inhibitor of the Mre11-Rad50-Nbs1 complex. Nat Chem Biol *4*, 119-125.

Edinger, A.L., and Thompson, C.B. (2002). Akt maintains cell size and survival by increasing mTOR-dependent nutrient uptake. Mol Biol Cell *13*, 2276-2288.

Edwards, S.L., Brough, R., Lord, C.J., Natrajan, R., Vatcheva, R., Levine, D.A., Boyd, J., Reis-Filho, J.S., and Ashworth, A. (2008). Resistance to therapy caused by intragenic deletion in BRCA2. Nature *451*, 1111-1115.

Elstrom, R.L., Bauer, D.E., Buzzai, M., Karnauskas, R., Harris, M.H., Plas, D.R., Zhuang, H., Cinalli, R.M., Alavi, A., Rudin, C.M., *et al.* (2004). Akt stimulates aerobic glycolysis in cancer cells. Cancer Res *64*, 3892-3899.

Engelman, J.A., Luo, J., and Cantley, L.C. (2006). The evolution of phosphatidylinositol 3-kinases as regulators of growth and metabolism. Nature reviews Genetics *7*, 606-619.

Eric Pujade-Lauraine, F.H., Béatrice Weber, Alexander Reuss, Andres Poveda, Gunnar Kristensen, Roberto Sorio, Ignace B. Vergote, Petronella Witteveen, Aristotelis Bamias, Deolinda Pereira, Pauline Wimberger, Ana Oaknin, Mansoor Raza Mirza, Philippe Follana, David T. Bollag, Isabelle Ray-Coquard and AURELIA Investigators (2012). AURELIA: A randomized phase III trial evaluating bevacizumab (BEV) plus chemotherapy (CT) for platinum (PT)-resistant recurrent ovarian cancer (OC). Journal of Clinical Oncology, 2012 ASCO Annual Meeting Abstracts *Vol 30*.

Esteller, M., Silva, J.M., Dominguez, G., Bonilla, F., Matias-Guiu, X., Lerma, E., Bussaglia, E., Prat, J., Harkes, I.C., Repasky, E.A., *et al.* (2000). Promoter hypermethylation and BRCA1 inactivation in sporadic breast and ovarian tumors. J Natl Cancer Inst *92*, 564-569.

Etemadmoghadam, D., deFazio, A., Beroukhim, R., Mermel, C., George, J., Getz, G., Tothill, R., Okamoto, A., Raeder, M.B., Harnett, P., *et al.* (2009). Integrated genome-wide DNA copy number and expression analysis identifies distinct mechanisms of primary chemoresistance in ovarian carcinomas. Clin Cancer Res *15*, 1417-1427.

Etienne, W., Meyer, M.H., Peppers, J., and Meyer, R.A., Jr. (2004). Comparison of mRNA gene expression by RT-PCR and DNA microarray. Biotechniques *36*, 618-620, 622, 624-616.

Evers, B., Helleday, T., and Jonkers, J. (2010). Targeting homologous recombination repair defects in cancer. Trends Pharmacol Sci *31*, 372-380.

Falck, J., Petrini, J.H., Williams, B.R., Lukas, J., and Bartek, J. (2002). The DNA damage-dependent intra-S phase checkpoint is regulated by parallel pathways. Nat Genet *30*, 290-294.

Farmer, H., McCabe, N., Lord, C.J., Tutt, A.N., Johnson, D.A., Richardson, T.B., Santarosa, M., Dillon, K.J., Hickson, I., Knights, C., *et al.* (2005). Targeting the DNA repair defect in BRCA mutant cells as a therapeutic strategy. Nature *434*, 917-921.

Fedele, C.G., Ooms, L.M., Ho, M., Vieusseux, J., O'Toole, S.A., Millar, E.K., Lopez-Knowles, E., Sriratana, A., Gurung, R., Baglietto, L.*, et al.* (2010). Inositol polyphosphate 4-phosphatase II regulates PI3K/Akt signaling and is lost in human basal-like breast cancers. Proceedings of the National Academy of Sciences of the United States of America *107*, 22231-22236.

Feng, J., Park, J., Cron, P., Hess, D., and Hemmings, B.A. (2004). Identification of a PKB/Akt hydrophobic motif Ser-473 kinase as DNA-dependent protein kinase. J Biol Chem *279*, 41189-41196.

Ferlay J, S.H., Bray F, Forman D, Mathers C and Parkin DM (2010). GLOBOCAN 2008 v1.2, Cancer Incidence and Mortality Worldwide.

Ferron, M., Boudiffa, M., Arsenault, M., Rached, M., Pata, M., Giroux, S., Elfassihi, L., Kisseleva, M., Majerus, P.W., Rousseau, F.*, et al.* (2011). Inositol polyphosphate 4-phosphatase B as a regulator of bone mass in mice and humans. Cell Metab *14*, 466-477.

Ferron, M., and Vacher, J. (2006). Characterization of the murine Inpp4b gene and identification of a novel isoform. Gene *376*, 152-161.

Filippa, N., Sable, C.L., Filloux, C., Hemmings, B., and Van Obberghen, E. (1999). Mechanism of protein kinase B activation by cyclic AMP-dependent protein kinase. Mol Cell Biol *19*, 4989-5000.

Fischer-Colbrie, J., Witt, A., Heinzl, H., Speiser, P., Czerwenka, K., Sevelda, P., and Zeillinger, R. (1997). EGFR and steroid receptors in ovarian carcinoma: comparison with prognostic parameters and outcome of patients. Anticancer research *17*, 613-619.

Fong, P.C., Boss, D.S., Yap, T.A., Tutt, A., Wu, P., Mergui-Roelvink, M., Mortimer, P., Swaisland, H., Lau, A., O'Connor, M.J.*, et al.* (2009). Inhibition of poly(ADP-ribose) polymerase in tumors from BRCA mutation carriers. N Engl J Med *361*, 123-134.

Fong, P.C., Yap, T.A., Boss, D.S., Carden, C.P., Mergui-Roelvink, M., Gourley, C., De Greve, J., Lubinski, J., Shanley, S., Messiou, C.*, et al.* (2010). Poly(ADP)-ribose polymerase inhibition: frequent durable responses in BRCA carrier ovarian cancer correlating with platinum-free interval. J Clin Oncol *28*, 2512-2519.

Fordham, S.E., Matheson, E.C., Scott, K., Irving, J.A., and Allan, J.M. (2011). DNA mismatch repair status affects cellular response to Ara-C and other anti-leukemic nucleoside analogs. Leukemia *25*, 1046-1049.

Franke, T.F., Kaplan, D.R., Cantley, L.C., and Toker, A. (1997). Direct regulation of the Akt proto-oncogene product by phosphatidylinositol-3,4-bisphosphate. Science *275*, 665-668.

Fruman, D.A., Meyers, R.E., and Cantley, L.C. (1998). Phosphoinositide kinases. Annual review of biochemistry *67*, 481-507.

Furgason, J.M., and Bahassi el, M. (2013). Targeting DNA repair mechanisms in cancer. Pharmacol Ther *137*, 298-308.

Gaidarov, I., Smith, M.E., Domin, J., and Keen, J.H. (2001). The class II phosphoinositide 3-kinase C2alpha is activated by clathrin and regulates clathrin-mediated membrane trafficking. Mol Cell *7*, 443-449.

Gao, Z., Maloney, D.J., Dedkova, L.M., and Hecht, S.M. (2008). Inhibitors of DNA polymerase beta: activity and mechanism. Bioorg Med Chem *16*, 4331-4340.

Garcia, A.A., Hirte, H., Fleming, G., Yang, D., Tsao-Wei, D.D., Roman, L., Groshen, S., Swenson, S., Markland, F., Gandara, D.*, et al.* (2008). Phase II clinical trial of bevacizumab and low-dose metronomic oral cyclophosphamide in recurrent ovarian cancer: a trial of the California, Chicago, and Princess Margaret Hospital phase II consortia. Journal of clinical oncology : official journal of the American Society of Clinical Oncology *26*, 76-82.

Garcia, J.M., Silva, J., Pena, C., Garcia, V., Rodriguez, R., Cruz, M.A., Cantos, B., Provencio, M., Espana, P., and Bonilla, F. (2004). Promoter methylation of the PTEN gene is a common molecular change in breast cancer. Genes Chromosomes Cancer *41*, 117-124.

Garofalo, R.S., Orena, S.J., Rafidi, K., Torchia, A.J., Stock, J.L., Hildebrandt, A.L., Coskran, T., Black, S.C., Brees, D.J., Wicks, J.R.*, et al.* (2003). Severe diabetes, age-dependent loss of adipose tissue, and mild growth deficiency in mice lacking Akt2/PKB beta. J Clin Invest *112*, 197-208.

Garrett, A.P., Lee, K.R., Colitti, C.R., Muto, M.G., Berkowitz, R.S., and Mok, S.C. (2001). k-ras mutation may be an early event in mucinous ovarian tumorigenesis. International journal of gynecological pathology : official journal of the International Society of Gynecological Pathologists *20*, 244-251.

Garrett, M.D., and Collins, I. (2011). Anticancer therapy with checkpoint inhibitors: what, where and when? Trends Pharmacol Sci *32*, 308-316.

Geering, B., Cutillas, P.R., Nock, G., Gharbi, S.I., and Vanhaesebroeck, B. (2007). Class IA phosphoinositide 3-kinases are obligate p85-p110 heterodimers. Proc Natl Acad Sci U S A *104*, 7809-7814.

Geisler, J.P., Hatterman-Zogg, M.A., Rathe, J.A., and Buller, R.E. (2002). Frequency of BRCA1 dysfunction in ovarian cancer. J Natl Cancer Inst *94*, 61-67.

Gelmon, K.A., Tischkowitz, M., Mackay, H., Swenerton, K., Robidoux, A., Tonkin, K., Hirte, H., Huntsman, D., Clemons, M., Gilks, B.*, et al.* (2011). Olaparib in patients with recurrent high-grade serous or poorly differentiated ovarian carcinoma or triple-negative breast cancer: a phase 2, multicentre, open-label, non-randomised study. Lancet Oncol *12*, 852-861.

Gemignani, M.L., Schlaerth, A.C., Bogomolniy, F., Barakat, R.R., Lin, O., Soslow, R., Venkatraman, E., and Boyd, J. (2003). Role of KRAS and BRAF gene mutations in mucinous ovarian carcinoma. Gynecologic oncology *90*, 378-381.

George, J., Alsop, K., Etemadmoghadam, D., Hondow, H., Mikeska, T., Dobrovic, A., deFazio, A., Australian Ovarian Cancer Study, G., Smyth, G.K., Levine, D.A.*, et al.* (2013). Nonequivalent gene expression and copy number alterations in high-grade

serous ovarian cancers with BRCA1 and BRCA2 mutations. Clin Cancer Res *19*, 3474-3484.

George, S., Rochford, J.J., Wolfrum, C., Gray, S.L., Schinner, S., Wilson, J.C., Soos, M.A., Murgatroyd, P.R., Williams, R.M., Acerini, C.L.*, et al.* (2004). A family with severe insulin resistance and diabetes due to a mutation in AKT2. Science *304*, 1325-1328.

Gewinner, C., Wang, Z.C., Richardson, A., Teruya-Feldstein, J., Etemadmoghadam, D., Bowtell, D., Barretina, J., Lin, W.M., Rameh, L., Salmena, L.*, et al.* (2009). Evidence that inositol polyphosphate 4-phosphatase type II is a tumor suppressor that inhibits PI3K signaling. Cancer Cell *16*, 115-125.

Gharbi, S.I., Zvelebil, M.J., Shuttleworth, S.J., Hancox, T., Saghir, N., Timms, J.F., and Waterfield, M.D. (2007). Exploring the specificity of the PI3K family inhibitor LY294002. Biochem J *404*, 15-21.

GlaxoSmithKline (2010). Efficacy and Safety of Pazopanib Monotherapy After First-line Chemotherapy in Ovarian, Fallopian Tube, or Primary Peritoneal Cancer in Asian Women
.

Goel, A., Arnold, C.N., Niedzwiecki, D., Carethers, J.M., Dowell, J.M., Wasserman, L., Compton, C., Mayer, R.J., Bertagnolli, M.M., and Boland, C.R. (2004). Frequent inactivation of PTEN by promoter hypermethylation in microsatellite instability-high sporadic colorectal cancers. Cancer Res *64*, 3014-3021.

Gonzalez-Martin, A. (2013). Update on randomized trials on recurrent disease. Ann Oncol *24 Suppl 10*, x48-x52.

Gordan, J.D., and Simon, M.C. (2007). Hypoxia-inducible factors: central regulators of the tumor phenotype. Curr Opin Genet Dev *17*, 71-77.

Gordon, A.N., Finkler, N., Edwards, R.P., Garcia, A.A., Crozier, M., Irwin, D.H., and Barrett, E. (2005). Efficacy and safety of erlotinib HCl, an epidermal growth factor receptor (HER1/EGFR) tyrosine kinase inhibitor, in patients with advanced ovarian carcinoma: results from a phase II multicenter study. International journal of gynecological cancer : official journal of the International Gynecological Cancer Society *15*, 785-792.

Gore, M.E., Fryatt, I., Wiltshaw, E., and Dawson, T. (1990). Treatment of relapsed carcinoma of the ovary with cisplatin or carboplatin following initial treatment with these compounds. Gynecologic oncology *36*, 207-211.

Grallert, B., and Boye, E. (2008). The multiple facets of the intra-S checkpoint. Cell Cycle *7*, 2315-2320.

Greenlee, R.T., Hill-Harmon, M.B., Murray, T., and Thun, M. (2001). Cancer statistics, 2001. CA: a cancer journal for clinicians *51*, 15-36.

Guarente, L. (1993). Synthetic enhancement in gene interaction: a genetic tool come of age. Trends Genet *9*, 362-366.

Gumy-Pause, F., Wacker, P., and Sappino, A.P. (2004). ATM gene and lymphoid malignancies. Leukemia *18*, 238-242.

Gunn, A., and Stark, J.M. (2012). I-SceI-based assays to examine distinct repair outcomes of mammalian chromosomal double strand breaks. Methods Mol Biol *920*, 379-391.

Hamilton, M.J., Ho, V.W., Kuroda, E., Ruschmann, J., Antignano, F., Lam, V., and Krystal, G. (2011). Role of SHIP in cancer. Exp Hematol *39*, 2-13.

Hanahan, D., and Weinberg, R.A. (2011). Hallmarks of cancer: the next generation. Cell *144*, 646-674.

Harper, S., and Speicher, D.W. Purification of proteins fused to glutathione S-transferase. Methods Mol Biol *681*, 259-280.

Hartman, J.L.t., Garvik, B., and Hartwell, L. (2001). Principles for the buffering of genetic variation. Science *291*, 1001-1004.

Harvell, D.M., Richer, J.K., Allred, D.C., Sartorius, C.A., and Horwitz, K.B. (2006). Estradiol regulates different genes in human breast tumor xenografts compared with the identical cells in culture. Endocrinology *147*, 700-713.

Hattori, H., Skoulidis, F., Russell, P., and Venkitaraman, A.R. (2011). Context dependence of checkpoint kinase 1 as a therapeutic target for pancreatic cancers deficient in the BRCA2 tumor suppressor. Mol Cancer Ther *10*, 670-678.

Hegi, M.E., Diserens, A.C., Gorlia, T., Hamou, M.F., de Tribolet, N., Weller, M., Kros, J.M., Hainfellner, J.A., Mason, W., Mariani, L.*, et al.* (2005). MGMT gene silencing and benefit from temozolomide in glioblastoma. N Engl J Med *352*, 997-1003.

Heikkinen, K., Mansikka, V., Karppinen, S.M., Rapakko, K., and Winqvist, R. (2005). Mutation analysis of the ATR gene in breast and ovarian cancer families. Breast Cancer Res *7*, R495-501.

Hendrix, N.D., Wu, R., Kuick, R., Schwartz, D.R., Fearon, E.R., and Cho, K.R. (2006). Fibroblast growth factor 9 has oncogenic activity and is a downstream target of Wnt signaling in ovarian endometrioid adenocarcinomas. Cancer Res *66*, 1354-1362.

Hennessy, B.T., Smith, D.L., Ram, P.T., Lu, Y., and Mills, G.B. (2005). Exploiting the PI3K/AKT pathway for cancer drug discovery. Nat Rev Drug Discov *4*, 988-1004.

Henriksen, R., Funa, K., Wilander, E., Backstrom, T., Ridderheim, M., and Oberg, K. (1993). Expression and prognostic significance of platelet-derived growth factor and its receptors in epithelial ovarian neoplasms. Cancer research *53*, 4550-4554.

Hickson, I., Zhao, Y., Richardson, C.J., Green, S.J., Martin, N.M., Orr, A.I., Reaper, P.M., Jackson, S.P., Curtin, N.J., and Smith, G.C. (2004). Identification and characterization of a novel and specific inhibitor of the ataxia-telangiectasia mutated kinase ATM. Cancer Res *64*, 9152-9159.

Hirte, H., Oza, A., Swenerton, K., Ellard, S.L., Grimshaw, R., Fisher, B., Tsao, M., and Seymour, L. (2010). A phase II study of erlotinib (OSI-774) given in combination with carboplatin in patients with recurrent epithelial ovarian cancer (NCIC CTG IND.149). Gynecologic oncology *118*, 308-312.

Ho, C.M., Lin, M.C., Huang, S.H., Huang, C.J., Lai, H.C., Chien, T.Y., and Chang, S.F. (2009). PTEN promoter methylation and LOH of 10q22-23 locus in PTEN expression of ovarian clear cell adenocarcinomas. Gynecol Oncol *112*, 307-313.

Hodgson, M.C., Shao, L.J., Frolov, A., Li, R., Peterson, L.E., Ayala, G., Ittmann, M.M., Weigel, N.L., and Agoulnik, I.U. (2011). Decreased expression and androgen regulation of the tumor suppressor gene INPP4B in prostate cancer. Cancer research *71*, 572-582.

Hoeijmakers, J.H. (2001). Genome maintenance mechanisms for preventing cancer. Nature *411*, 366-374.

Hoeijmakers, J.H. (2009). DNA damage, aging, and cancer. N Engl J Med *361*, 1475-1485.

Holz, M.K., and Blenis, J. (2005). Identification of S6 kinase 1 as a novel mammalian target of rapamycin (mTOR)-phosphorylating kinase. J Biol Chem *280*, 26089-26093.

Hosokawa, N., Hara, T., Kaizuka, T., Kishi, C., Takamura, A., Miura, Y., Iemura, S., Natsume, T., Takehana, K., Yamada, N.*, et al.* (2009). Nutrient-dependent mTORC1 association with the ULK1-Atg13-FIP200 complex required for autophagy. Mol Biol Cell *20*, 1981-1991.

Howell, J.J., Ricoult, S.J., Ben-Sahra, I., and Manning, B.D. (2013). A growing role for mTOR in promoting anabolic metabolism. Biochem Soc Trans *41*, 906-912.

Huang, J., Zhang, L., Greshock, J., Colligon, T.A., Wang, Y., Ward, R., Katsaros, D., Lassus, H., Butzow, R., Godwin, A.K.*, et al.* (2011). Frequent genetic abnormalities of the PI3K/AKT pathway in primary ovarian cancer predict patient outcome. Genes Chromosomes Cancer *50*, 606-618.

Hughes-Davies, L., Huntsman, D., Ruas, M., Fuks, F., Bye, J., Chin, S.F., Milner, J., Brown, L.A., Hsu, F., Gilks, B.*, et al.* (2003). EMSY links the BRCA2 pathway to sporadic breast and ovarian cancer. Cell *115*, 523-535.

Hutchinson, J.N., Jin, J., Cardiff, R.D., Woodgett, J.R., and Muller, W.J. (2004). Activation of Akt-1 (PKB-alpha) can accelerate ErbB-2-mediated mammary tumorigenesis but suppresses tumor invasion. Cancer Res *64*, 3171-3178.

Ile, K.E., Schaaf, G., and Bankaitis, V.A. (2006). Phosphatidylinositol transfer proteins and cellular nanoreactors for lipid signaling. Nat Chem Biol *2*, 576-583.

Irie, H.Y., Pearline, R.V., Grueneberg, D., Hsia, M., Ravichandran, P., Kothari, N., Natesan, S., and Brugge, J.S. (2005). Distinct roles of Akt1 and Akt2 in regulating cell migration and epithelial-mesenchymal transition. J Cell Biol *171*, 1023-1034.

J. Ang, T.A.Y., P. Fong, C. P. Carden, D. S. Tan, J. Hanwell, J. Carmichael, J. S. De Bono, M. E. Gore and S. B. Kaye (2010). Preliminary experience with the use of

chemotherapy (CT) following treatment with olaparib, a poly(ADP-ribose) polymerase inhibitor (PARPi), in patients with BRCA1/2-deficient ovarian cancer (BDOC).
.

J. H. M. Schellens, G.S., A. C. Pavlick, R. Tibes, S. Leijen, S. M. Tolaney, I. Diaz-Padilla, R. K. Ramanathan, T. Demuth, J. Viscusi, J. D. Cheng, R. Lam, Y. Xu and A. M. Oza (2011). Update on a phase I pharmacologic and pharmacodynamic study of MK-1775, a Wee1 tyrosine kinase inhibitor, in monotherapy and combination with gemcitabine, cisplatin, or carboplatin in patients with advanced solid tumors.
.

JA Ledermann, T.P., FA Raja, AC Embleton, GJS Rustin, G Jayson, SB Kaye, A Swart, M Vaughan, H Hirte (2013). Randomised double-blind phase III trial of cediranib (AZD 2171) in relapsed platinum sensitive ovarian cancer: Results of the ICON6 trial

. 2013 NCRI Cancer Conference
.

Jazaeri, A.A., Yee, C.J., Sotiriou, C., Brantley, K.R., Boyd, J., and Liu, E.T. (2002). Gene expression profiles of BRCA1-linked, BRCA2-linked, and sporadic ovarian cancers. J Natl Cancer Inst *94*, 990-1000.

Jemal, A., Bray, F., Center, M.M., Ferlay, J., Ward, E., and Forman, D. (2011). Global cancer statistics. CA Cancer J Clin *61*, 69-90.

Jemal, A., Siegel, R., Ward, E., Murray, T., Xu, J., and Thun, M.J. (2007). Cancer statistics, 2007. CA: a cancer journal for clinicians *57*, 43-66.

Jemal, A., Siegel, R., Xu, J., and Ward, E. (2010). Cancer statistics, 2010. CA: a cancer journal for clinicians *60*, 277-300.

Jensen, R.B., Carreira, A., and Kowalczykowski, S.C. (2010). Purified human BRCA2 stimulates RAD51-mediated recombination. Nature *467*, 678-683.

Johnson, N., Li, Y.C., Walton, Z.E., Cheng, K.A., Li, D., Rodig, S.J., Moreau, L.A., Unitt, C., Bronson, R.T., Thomas, H.D.*, et al.* (2011). Compromised CDK1 activity sensitizes BRCA-proficient cancers to PARP inhibition. Nat Med *17*, 875-882.

Jones, P.F., Jakubowicz, T., and Hemmings, B.A. (1991). Molecular cloning of a second form of rac protein kinase. Cell Regul *2*, 1001-1009.

Jung, C.H., Jun, C.B., Ro, S.H., Kim, Y.M., Otto, N.M., Cao, J., Kundu, M., and Kim, D.H. (2009). ULK-Atg13-FIP200 complexes mediate mTOR signaling to the autophagy machinery. Mol Biol Cell *20*, 1992-2003.

Jung-min Lee, C.M.A., John L. Hays, Anne M. Noonan, Lori M. Minasian, JoAnne Zujewski, Minshu Yu, Jiuping Jay Ji, Tristan Sissung, Nicole D. Houston, Elise C. Kohn (2013). Phase I/Ib study of the PARP inhibitor olaparib (O) with carboplatin (C) in BRCA1/2 mutation carriers with breast or ovarian cancer. J Clin Oncol 31, 2013 (suppl; abstr 2514)

.

Kagawa, S., Soeda, Y., Ishihara, H., Oya, T., Sasahara, M., Yaguchi, S., Oshita, R., Wada, T., Tsuneki, H., and Sasaoka, T. (2008). Impact of transgenic overexpression of SH2-containing inositol 5'-phosphatase 2 on glucose metabolism and insulin signaling in mice. Endocrinology *149*, 642-650.

Kandel, E.S., Skeen, J., Majewski, N., Di Cristofano, A., Pandolfi, P.P., Feliciano, C.S., Gartel, A., and Hay, N. (2002). Activation of Akt/protein kinase B overcomes a G(2)/m cell cycle checkpoint induced by DNA damage. Mol Cell Biol *22*, 7831-7841.

Kang, J., Bronson, R.T., and Xu, Y. (2002). Targeted disruption of NBS1 reveals its roles in mouse development and DNA repair. EMBO J *21*, 1447-1455.

Karran, P., and Bignami, M. (1994). DNA damage tolerance, mismatch repair and genome instability. Bioessays *16*, 833-839.

Karran, P., and Marinus, M.G. (1982). Mismatch correction at O6-methylguanine residues in E. coli DNA. Nature *296*, 868-869.

Kashiwada, M., Cattoretti, G., McKeag, L., Rouse, T., Showalter, B.M., Al-Alem, U., Niki, M., Pandolfi, P.P., Field, E.H., and Rothman, P.B. (2006). Downstream of tyrosine kinases-1 and Src homology 2-containing inositol 5'-phosphatase are required for regulation of CD4+CD25+ T cell development. J Immunol *176*, 3958-3965.

Kastan, M.B., and Bartek, J. (2004). Cell-cycle checkpoints and cancer. Nature *432*, 316-323.

Katso, R., Okkenhaug, K., Ahmadi, K., White, S., Timms, J., and Waterfield, M.D. (2001). Cellular function of phosphoinositide 3-kinases: implications for development, homeostasis, and cancer. Annu Rev Cell Dev Biol *17*, 615-675.

Katzen, F. (2007). Gateway((R)) recombinational cloning: a biological operating system. Expert Opin Drug Discov *2*, 571-589.

Kelemen, L.E., and Kobel, M. (2011). Mucinous carcinomas of the ovary and colorectum: different organ, same dilemma. Lancet Oncol *12*, 1071-1080.

Kihara, A., Noda, T., Ishihara, N., and Ohsumi, Y. (2001). Two distinct Vps34 phosphatidylinositol 3-kinase complexes function in autophagy and carboxypeptidase Y sorting in Saccharomyces cerevisiae. J Cell Biol *152*, 519-530.

Kim, J.S., Yun, H.S., Um, H.D., Park, J.K., Lee, K.H., Kang, C.M., Lee, S.J., and Hwang, S.G. (2012). Identification of inositol polyphosphate 4-phosphatase type II as a novel tumor resistance biomarker in human laryngeal cancer HEp-2 cells. Cancer biology & therapy *13*, 1307-1318.

King, F.W., Skeen, J., Hay, N., and Shtivelman, E. (2004). Inhibition of Chk1 by activated PKB/Akt. Cell Cycle *3*, 634-637.

King, M.C., Marks, J.H., Mandell, J.B., and New York Breast Cancer Study, G. (2003). Breast and ovarian cancer risks due to inherited mutations in BRCA1 and BRCA2. Science *302*, 643-646.

Klippel, A., Kavanaugh, W.M., Pot, D., and Williams, L.T. (1997). A specific product of phosphatidylinositol 3-kinase directly activates the protein kinase Akt through its pleckstrin homology domain. Mol Cell Biol *17*, 338-344.

Klipper-Aurbach, Y., Wasserman, M., Braunspiegel-Weintrob, N., Borstein, D., Peleg, S., Assa, S., Karp, M., Benjamini, Y., Hochberg, Y., and Laron, Z. (1995). Mathematical formulae for the prediction of the residual beta cell function during the first two years of disease in children and adolescents with insulin-dependent diabetes mellitus. Medical hypotheses *45*, 486-490.

Koberle, B., Grimaldi, K.A., Sunters, A., Hartley, J.A., Kelland, L.R., and Masters, J.R. (1997). DNA repair capacity and cisplatin sensitivity of human testis tumour cells. Int J Cancer *70*, 551-555.

Kondratov, R.V., and Antoch, M.P. (2007). Circadian proteins in the regulation of cell cycle and genotoxic stress responses. Trends Cell Biol *17*, 311-317.

Konstantinopoulos, P.A., Spentzos, D., Karlan, B.Y., Taniguchi, T., Fountzilas, E., Francoeur, N., Levine, D.A., and Cannistra, S.A. (2010). Gene expression profile of BRCAness that correlates with responsiveness to chemotherapy and with outcome in patients with epithelial ovarian cancer. Journal of clinical oncology : official journal of the American Society of Clinical Oncology *28*, 3555-3561.

Koren, I., Reem, E., and Kimchi, A. (2010). DAP1, a novel substrate of mTOR, negatively regulates autophagy. Curr Biol *20*, 1093-1098.

Krishna, M., and Narang, H. (2008). The complexity of mitogen-activated protein kinases (MAPKs) made simple. Cellular and molecular life sciences : CMLS *65*, 3525-3544.

Krishnakumar, R., and Kraus, W.L. (2010). The PARP side of the nucleus: molecular actions, physiological outcomes, and clinical targets. Mol Cell *39*, 8-24.

Kumagai, A., and Dunphy, W.G. (2003). Repeated phosphopeptide motifs in Claspin mediate the regulated binding of Chk1. Nat Cell Biol *5*, 161-165.

Kumagai, A., Kim, S.M., and Dunphy, W.G. (2004). Claspin and the activated form of ATR-ATRIP collaborate in the activation of Chk1. J Biol Chem *279*, 49599-49608.

Kumamoto-Yonezawa, Y., Sasaki, R., Suzuki, Y., Matsui, Y., Hada, T., Uryu, K., Sugimura, K., Yoshida, H., and Mizushina, Y. (2010). Enhancement of human cancer cell radiosensitivity by conjugated eicosapentaenoic acid - a mammalian DNA polymerase inhibitor. Int J Oncol *36*, 577-584.

Kuo, L.J., and Yang, L.X. (2008). Gamma-H2AX - a novel biomarker for DNA double-strand breaks. In Vivo *22*, 305-309.

Kuschal, C., Thoms, K.M., Boeckmann, L., Laspe, P., Apel, A., Schon, M.P., and Emmert, S. (2011). Cyclosporin A inhibits nucleotide excision repair via downregulation of the xeroderma pigmentosum group A and G proteins, which is mediated by calcineurin inhibition. Exp Dermatol *20*, 795-799.

Landen, C.N., Jr., Birrer, M.J., and Sood, A.K. (2008). Early events in the pathogenesis of epithelial ovarian cancer. Journal of clinical oncology : official journal of the American Society of Clinical Oncology *26*, 995-1005.

Langelier, M.F., Planck, J.L., Roy, S., and Pascal, J.M. (2011). Crystal structures of poly(ADP-ribose) polymerase-1 (PARP-1) zinc fingers bound to DNA: structural and functional insights into DNA-dependent PARP-1 activity. J Biol Chem *286*, 10690-10701.

Lapenna, S., and Giordano, A. (2009). Cell cycle kinases as therapeutic targets for cancer. Nat Rev Drug Discov *8*, 547-566.

Lavecchia, A., Di Giovanni, C., and Novellino, E. (2010). Inhibitors of Cdc25 phosphatases as anticancer agents: a patent review. Expert Opin Ther Pat *20*, 405-425.

Lavin, M.F., and Kozlov, S. (2007). ATM activation and DNA damage response. Cell Cycle *6*, 931-942.

Ledermann, J., Harter, P., Gourley, C., Friedlander, M., Vergote, I., Rustin, G., Scott, C., Meier, W., Shapira-Frommer, R., Safra, T.*, et al.* (2012). Olaparib maintenance therapy in platinum-sensitive relapsed ovarian cancer. N Engl J Med *366*, 1382-1392.

Lee, J., Kumagai, A., and Dunphy, W.G. (2001). Positive regulation of Wee1 by Chk1 and 14-3-3 proteins. Mol Biol Cell *12*, 551-563.

Lee, J.H., and Paull, T.T. (2005). ATM activation by DNA double-strand breaks through the Mre11-Rad50-Nbs1 complex. Science *308*, 551-554.

Li, G.M. (1999). The role of mismatch repair in DNA damage-induced apoptosis. Oncol Res *11*, 393-400.

Li, J., Yen, C., Liaw, D., Podsypanina, K., Bose, S., Wang, S.I., Puc, J., Miliaresis, C., Rodgers, L., McCombie, R.*, et al.* (1997). PTEN, a putative protein tyrosine phosphatase gene mutated in human brain, breast, and prostate cancer. Science *275*, 1943-1947.

Liang, J., Zubovitz, J., Petrocelli, T., Kotchetkov, R., Connor, M.K., Han, K., Lee, J.H., Ciarallo, S., Catzavelos, C., Beniston, R.*, et al.* (2002). PKB/Akt phosphorylates p27, impairs nuclear import of p27 and opposes p27-mediated G1 arrest. Nat Med *8*, 1153-1160.

Liaw, D., Marsh, D.J., Li, J., Dahia, P.L., Wang, S.I., Zheng, Z., Bose, S., Call, K.M., Tsou, H.C., Peacocke, M.*, et al.* (1997). Germline mutations of the PTEN gene in Cowden disease, an inherited breast and thyroid cancer syndrome. Nat Genet *16*, 64-67.

Lijinsky, W., Pegg, A.E., Anver, M.R., and Moschel, R.C. (1994). Effects of inhibition of O6-alkylguanine-DNA alkyltransferase in rats on carcinogenesis by methylnitrosourea and ethylnitrosourea. Jpn J Cancer Res *85*, 226-230.

Lin, W.M., Baker, A.C., Beroukhim, R., Winckler, W., Feng, W., Marmion, J.M., Laine, E., Greulich, H., Tseng, H., Gates, C.*, et al.* (2008). Modeling genomic diversity and tumor dependency in malignant melanoma. Cancer Res *68*, 664-673.

Liu, J.F., Tolaney, S.M., Birrer, M., Fleming, G.F., Buss, M.K., Dahlberg, S.E., Lee, H., Whalen, C., Tyburski, K., Winer, E.*, et al.* (2013). A Phase 1 trial of the poly(ADP-ribose) polymerase inhibitor olaparib (AZD2281) in combination with the anti-angiogenic cediranib (AZD2171) in recurrent epithelial ovarian or triple-negative breast cancer. Eur J Cancer *49*, 2972-2978.

Liu, Q., Guntuku, S., Cui, X.S., Matsuoka, S., Cortez, D., Tamai, K., Luo, G., Carattini-Rivera, S., DeMayo, F., Bradley, A.*, et al.* (2000). Chk1 is an essential kinase that is regulated by Atr and required for the G(2)/M DNA damage checkpoint. Genes Dev *14*, 1448-1459.

Liu, Q., Sasaki, T., Kozieradzki, I., Wakeham, A., Itie, A., Dumont, D.J., and Penninger, J.M. (1999). SHIP is a negative regulator of growth factor receptor-mediated PKB/Akt activation and myeloid cell survival. Genes Dev *13*, 786-791.

Liu, X., Shi, Y., Maag, D.X., Palma, J.P., Patterson, M.J., Ellis, P.A., Surber, B.W., Ready, D.B., Soni, N.B., Ladror, U.S.*, et al.* (2012). Iniparib nonselectively modifies cysteine-containing proteins in tumor cells and is not a bona fide PARP inhibitor. Clin Cancer Res *18*, 510-523.

Livak, K.J., and Schmittgen, T.D. (2001). Analysis of relative gene expression data using real-time quantitative PCR and the 2(-Delta Delta C(T)) Method. Methods *25*, 402-408.

Lo, T.C., Barnhill, L.M., Kim, Y., Nakae, E.A., Yu, A.L., and Diccianni, M.B. (2009). Inactivation of SHIP1 in T-cell acute lymphoblastic leukemia due to mutation and extensive alternative splicing. Leuk Res *33*, 1562-1566.

Lord, C.J., and Ashworth, A. (2012). The DNA damage response and cancer therapy. Nature *481*, 287-294.

Lukas, C., Falck, J., Bartkova, J., Bartek, J., and Lukas, J. (2003). Distinct spatiotemporal dynamics of mammalian checkpoint regulators induced by DNA damage. Nat Cell Biol *5*, 255-260.

Luo, J.M., Yoshida, H., Komura, S., Ohishi, N., Pan, L., Shigeno, K., Hanamura, I., Miura, K., Iida, S., Ueda, R.*, et al.* (2003). Possible dominant-negative mutation of the SHIP gene in acute myeloid leukemia. Leukemia *17*, 1-8.

Lutz, A.M., Willmann, J.K., Drescher, C.W., Ray, P., Cochran, F.V., Urban, N., and Gambhir, S.S. (2011). Early diagnosis of ovarian carcinoma: is a solution in sight? Radiology *259*, 329-345.

M. J. Birrer, P.K., R. T. Penson, M. Roche, A. Ambrosio, T. E. Stallings, U. Matulonis and C. R. Bradley (2011). A phase II trial of iniparib (BSI-201) in combination with gemcitabine/carboplatin (GC) in patients with platinum-resistant recurrent ovarian cancer. Journal of Clinical Oncology, 2011 ASCO Annual Meeting Abstracts *Vol 29*.

Macrae, C.J., McCulloch, R.D., Ylanko, J., Durocher, D., and Koch, C.A. (2008). APLF (C2orf13) facilitates nonhomologous end-joining and undergoes ATM-dependent hyperphosphorylation following ionizing radiation. DNA Repair (Amst) *7*, 292-302.

Magnussen A., K.C., Söderkvist P., Karlsson M. G., and Thunell L. K. (2011). Alterations of INPP4B, PIK3CA and pAkt of the PI3K pathway are associated with squamous cell carcinoma of the lung. Cancer Research *71*, 1041.

Mahaney, B.L., Meek, K., and Lees-Miller, S.P. (2009). Repair of ionizing radiation-induced DNA double-strand breaks by non-homologous end-joining. Biochem J *417*, 639-650.

Mallette, F.A., Mattiroli, F., Cui, G., Young, L.C., Hendzel, M.J., Mer, G., Sixma, T.K., and Richard, S. (2012). RNF8- and RNF168-dependent degradation of KDM4A/JMJD2A triggers 53BP1 recruitment to DNA damage sites. EMBO J *31*, 1865-1878.

Marechal, A., and Zou, L. (2013). DNA damage sensing by the ATM and ATR kinases. Cold Spring Harb Perspect Biol *5*.

Massague, J. (2004). G1 cell-cycle control and cancer. Nature *432*, 298-306.

Matheny, R.W., Jr., and Adamo, M.L. (2009). Current perspectives on Akt Akt-ivation and Akt-ions. Exp Biol Med (Maywood) *234*, 1264-1270.

Mathieu Ferron, M.B., Michel Arsenault, Mohamed Rached, Monica Pata,Sylvie Giroux, Latifa Elfassihi, Marina Kisseleva, Philip W. Majerus, Franc¸ois Rousseau, and Jean Vacher (2011). Inositol Polyphosphate 4-Phosphatase B as a Regulator of Bone Mass in Mice and Humans. Cell

Matsuoka, S., Rotman, G., Ogawa, A., Shiloh, Y., Tamai, K., and Elledge, S.J. (2000). Ataxia telangiectasia-mutated phosphorylates Chk2 in vivo and in vitro. Proc Natl Acad Sci U S A *97*, 10389-10394.

Matthews, D.J., Yakes, F.M., Chen, J., Tadano, M., Bornheim, L., Clary, D.O., Tai, A., Wagner, J.M., Miller, N., Kim, Y.D.*, et al.* (2007). Pharmacological abrogation of S-phase checkpoint enhances the anti-tumor activity of gemcitabine in vivo. Cell Cycle *6*, 104-110.

McCabe, N., Turner, N.C., Lord, C.J., Kluzek, K., Bialkowska, A., Swift, S., Giavara, S., O'Connor, M.J., Tutt, A.N., Zdzienicka, M.Z.*, et al.* (2006). Deficiency in the repair of DNA damage by homologous recombination and sensitivity to poly(ADP-ribose) polymerase inhibition. Cancer Res *66*, 8109-8115.

Meek, K., Dang, V., and Lees-Miller, S.P. (2008). DNA-PK: the means to justify the ends? Adv Immunol *99*, 33-58.

Mellinghoff, I.K., Wang, M.Y., Vivanco, I., Haas-Kogan, D.A., Zhu, S., Dia, E.Q., Lu, K.V., Yoshimoto, K., Huang, J.H., Chute, D.J.*, et al.* (2005). Molecular determinants of the response of glioblastomas to EGFR kinase inhibitors. N Engl J Med *353*, 2012-2024.

Menon, S., Dibble, C.C., Talbott, G., Hoxhaj, G., Valvezan, A.J., Takahashi, H., Cantley, L.C., and Manning, B.D. (2014). Spatial control of the TSC complex integrates insulin and nutrient regulation of mTORC1 at the lysosome. Cell *156*, 771-785.

Menoyo, A., Alazzouzi, H., Espin, E., Armengol, M., Yamamoto, H., and Schwartz, S., Jr. (2001). Somatic mutations in the DNA damage-response genes ATR and CHK1 in sporadic stomach tumors with microsatellite instability. Cancer Res *61*, 7727-7730.

Micha, J.P., Goldstein, B.H., Rettenmaier, M.A., Genesen, M., Graham, C., Bader, K., Lopez, K.L., Nickle, M., and Brown, J.V., 3rd (2007). A phase II study of outpatient first-line paclitaxel, carboplatin, and bevacizumab for advanced-stage epithelial ovarian, peritoneal, and fallopian tube cancer. International journal of gynecological cancer : official journal of the International Gynecological Cancer Society *17*, 771-776.

Minesh P. Mehta, W.J.C., Ding Wang, Fen Wang, Lawrence Kleinberg, Anthony M. Brade, Nael Mostafa, Xiangdong Zhou, Jiang Qian, Terri Leahy, Bhardwaj Desai, Vincent L. Giranda; Northwestern University, Chicago, IL; Radiation Therapy Oncology Group and Emory University, Atlanta, GA; Josephine Ford Cancer Center/Henry Ford Health System, Detroit, MI; University of Kansas Medical Center, Kansas City, KS; The Johns Hopkins University, Baltimore, MD; Princess Margaret Hospital, University of Toronto, Toronto, ON, Canada; Abbott Laboratories, Abbott Park, IL (2012). Phase I safety and pharmacokinetic (PK) study of veliparib in combination with whole brain radiation therapy (WBRT) in patients (pts) with brain metastases.

. J Clin Oncol 30, 2012 (suppl; abstr 2013)

.

Modrich, P., and Lahue, R. (1996). Mismatch repair in replication fidelity, genetic recombination, and cancer biology. Annu Rev Biochem *65*, 101-133.

Mohammed, M.Z., Vyjayanti, V.N., Laughton, C.A., Dekker, L.V., Fischer, P.M., Wilson, D.M., 3rd, Abbotts, R., Shah, S., Patel, P.M., Hickson, I.D.*, et al.* (2011). Development and evaluation of human AP endonuclease inhibitors in melanoma and glioma cell lines. Br J Cancer *104*, 653-663.

Monk, B.J., Herzog, T.J., Kaye, S.B., Krasner, C.N., Vermorken, J.B., Muggia, F.M., Pujade-Lauraine, E., Lisyanskaya, A.S., Makhson, A.N., Rolski, J.*, et al.* (2010). Trabectedin plus pegylated liposomal Doxorubicin in recurrent ovarian cancer. J Clin Oncol *28*, 3107-3114.

Morbidelli, L., Donnini, S., and Ziche, M. (2003). Role of nitric oxide in the modulation of angiogenesis. Curr Pharm Des *9*, 521-530.

Moroney, J.W., Schlumbrecht, M.P., Helgason, T., Coleman, R.L., Moulder, S., Naing, A., Bodurka, D.C., Janku, F., Hong, D.S., and Kurzrock, R. (2011). A phase I trial of liposomal doxorubicin, bevacizumab, and temsirolimus in patients with advanced gynecologic and breast malignancies. Clin Cancer Res *17*, 6840-6846.

Morrell, D., Cromartie, E., and Swift, M. (1986). Mortality and cancer incidence in 263 patients with ataxia-telangiectasia. J Natl Cancer Inst *77*, 89-92.

Muggia, F., and Safra, T. (2014). 'BRCAness' and its implications for platinum action in gynecologic cancer. Anticancer Res *34*, 551-556.

Mukhopadhyay, A., Elattar, A., Cerbinskaite, A., Wilkinson, S.J., Drew, Y., Kyle, S., Los, G., Hostomsky, Z., Edmondson, R.J., and Curtin, N.J. (2010). Development of a functional assay for homologous recombination status in primary cultures of epithelial ovarian tumor and correlation with sensitivity to poly(ADP-ribose) polymerase inhibitors. Clin Cancer Res *16*, 2344-2351.

Munck, J.M., Batey, M.A., Zhao, Y., Jenkins, H., Richardson, C.J., Cano, C., Tavecchio, M., Barbeau, J., Bardos, J., Cornell, L.*, et al.* (2012). Chemosensitization of cancer cells by KU-0060648, a dual inhibitor of DNA-PK and PI-3K. Mol Cancer Ther *11*, 1789-1798.

Murray, D., and Honig, B. (2002). Electrostatic control of the membrane targeting of C2 domains. Mol Cell *9*, 145-154.

Mutch, D.G. (2002). Surgical management of ovarian cancer. Seminars in oncology *29*, 3-8.

Nagata, Y., Lan, K.H., Zhou, X., Tan, M., Esteva, F.J., Sahin, A.A., Klos, K.S., Li, P., Monia, B.P., Nguyen, N.T.*, et al.* (2004). PTEN activation contributes to tumor inhibition by trastuzumab, and loss of PTEN predicts trastuzumab resistance in patients. Cancer Cell *6*, 117-127.

Nakayama, K., Nakayama, N., Kurman, R.J., Cope, L., Pohl, G., Samuels, Y., Velculescu, V.E., Wang, T.L., and Shih Ie, M. (2006). Sequence mutations and amplification of PIK3CA and AKT2 genes in purified ovarian serous neoplasms. Cancer biology & therapy *5*, 779-785.

Nasuhoglu, C., Feng, S., Mao, J., Yamamoto, M., Yin, H.L., Earnest, S., Barylko, B., Albanesi, J.P., and Hilgemann, D.W. (2002). Nonradioactive analysis of phosphatidylinositides and other anionic phospholipids by anion-exchange high-performance liquid chromatography with suppressed conductivity detection. Anal Biochem *301*, 243-254.

NCT00748527, C.R.U. (2008). Carboplatin With or Without Decitabine in Treating Patients With Progressive, Advanced Ovarian Epithelial Cancer, Fallopian Tube Cancer, or Primary Peritoneal Cancer
.

NCT00886691, G.O.G. (2009). Bevacizumab With or Without Everolimus in Treating Patients With Recurrent or Persistent Ovarian Epithelial Cancer, Fallopian Tube Cancer, or Primary Peritoneal Cancer
.

NCT01031381, U.o.P. (2009). Study of RAD001 and Bevacizumab in Recurrent Ovarian, Peritoneal, and Fallopian Tube Cancer (RADBEV)
.

NCT01081951, A. (2010). Study to Compare the Efficacy and Safety of Olaparib When Given in Combination With Carboplatin and Paclitaxel, Compared With Carboplatin and Paclitaxel in Patients With Advanced Ovarian Cancer
.

NCT01115790, E.L.a.C. (2010). A Phase 1 Study in Participants With Advanced Cancer
.

NCT01164995, T.N.C.I. (2010). Study With Wee-1 Inhibitor MK-1775 and Carboplatin to Treat p53 Mutated Refractory and Resistant Ovarian Cancer (M10MKO)
.

NCT01281514, F.C.C.C. (2011). Carboplatin, Pegylated Liposomal Doxorubicin Hydrochloride, and Everolimus in Treating Patients With Relapsed Ovarian Epithelial, Fallopian Tube, or Peritoneal Cavity Cancer
.

NCT01283035, N.C.I.N. (2011). A Phase II Study of Akt Inhibitor MK2206 in the Treatment of Recurrent Platinum-Resistant Ovarian, Fallopian Tube, or Peritoneal Cancer
.

NCT01341457, E.L.a.C. (2011). A Study of LY2603618 in Combination With Gemcitabine in Patients With Solid Tumors
.

NCT01353625, C.C. (2011). Study to Assess Safety and Tolerability of Oral CC-115 for Patients With Advanced Solid Tumors, and Hematologic Malignancies.
.

NCT01684878, H.-L.R. (2012). A Study of Pertuzumab in Combination With Standard Chemotherapy in Women With Recurrent Platinum-Resistant Epithelian Ovarian Cancer and Low HER3 mRNA Expression
.

Neijt, J.P., Engelholm, S.A., Tuxen, M.K., Sorensen, P.G., Hansen, M., Sessa, C., de Swart, C.A., Hirsch, F.R., Lund, B., and van Houwelingen, H.C. (2000). Exploratory phase III study of paclitaxel and cisplatin versus paclitaxel and carboplatin in advanced ovarian cancer. Journal of clinical oncology : official journal of the American Society of Clinical Oncology *18*, 3084-3092.

Nigg, E.A. (2001). Mitotic kinases as regulators of cell division and its checkpoints. Nat Rev Mol Cell Biol *2*, 21-32.

Niida, H., Katsuno, Y., Banerjee, B., Hande, M.P., and Nakanishi, M. (2007). Specific role of Chk1 phosphorylations in cell survival and checkpoint activation. Mol Cell Biol *27*, 2572-2581.

Nitiss, J.L. (2009). DNA topoisomerase II and its growing repertoire of biological functions. Nat Rev Cancer *9*, 327-337.

Nobukuni, T., Joaquin, M., Roccio, M., Dann, S.G., Kim, S.Y., Gulati, P., Byfield, M.P., Backer, J.M., Natt, F., Bos, J.L.*, et al.* (2005). Amino acids mediate mTOR/raptor signaling through activation of class 3 phosphatidylinositol 3OH-kinase. Proc Natl Acad Sci U S A *102*, 14238-14243.

Norris, F.A., Atkins, R.C., and Majerus, P.W. (1997a). The cDNA cloning and characterization of inositol polyphosphate 4-phosphatase type II. Evidence for conserved alternative splicing in the 4-phosphatase family. J Biol Chem *272*, 23859-23864.

Norris, F.A., Atkins, R.C., and Majerus, P.W. (1997b). Inositol polyphosphate 4-phosphatase is inactivated by calpain-mediated proteolysis in stimulated human platelets. J Biol Chem *272*, 10987-10989.

Norris, F.A., Auethavekiat, V., and Majerus, P.W. (1995a). The isolation and characterization of cDNA encoding human and rat brain inositol polyphosphate 4-phosphatase. J Biol Chem *270*, 16128-16133.

Norris, F.A., and Majerus, P.W. (1994). Hydrolysis of phosphatidylinositol 3,4-bisphosphate by inositol polyphosphate 4-phosphatase isolated by affinity elution chromatography. J Biol Chem *269*, 8716-8720.

Norris, F.A., Ungewickell, E., and Majerus, P.W. (1995b). Inositol hexakisphosphate binds to clathrin assembly protein 3 (AP-3/AP180) and inhibits clathrin cage assembly in vitro. J Biol Chem *270*, 214-217.

Nouspikel, T. (2009). DNA repair in mammalian cells : Nucleotide excision repair: variations on versatility. Cell Mol Life Sci *66*, 994-1009.

Nystuen, A., Legare, M.E., Shultz, L.D., and Frankel, W.N. (2001). A null mutation in inositol polyphosphate 4-phosphatase type I causes selective neuronal loss in weeble mutant mice. Neuron *32*, 203-212.

O'Connell, M.J., Walworth, N.C., and Carr, A.M. (2000). The G2-phase DNA-damage checkpoint. Trends Cell Biol *10*, 296-303.

O'Reilly, K.E., Rojo, F., She, Q.B., Solit, D., Mills, G.B., Smith, D., Lane, H., Hofmann, F., Hicklin, D.J., Ludwig, D.L.*, et al.* (2006). mTOR inhibition induces upstream receptor tyrosine kinase signaling and activates Akt. Cancer Res *66*, 1500-1508.

Odorizzi, G., Babst, M., and Emr, S.D. (2000). Phosphoinositide signaling and the regulation of membrane trafficking in yeast. Trends Biochem Sci *25*, 229-235.

Olive, P.L., and Banath, J.P. (2006). The comet assay: a method to measure DNA damage in individual cells. Nat Protoc *1*, 23-29.

Olive, P.L., Banath, J.P., and Durand, R.E. (1990). Heterogeneity in radiation-induced DNA damage and repair in tumor and normal cells measured using the "comet" assay. Radiat Res *122*, 86-94.

Olive, P.L., Banath, J.P., and MacPhail, H.S. (1994). Lack of a correlation between radiosensitivity and DNA double-strand break induction or rejoining in six human tumor cell lines. Cancer Res *54*, 3939-3946.

Oliver, A.W., Paul, A., Boxall, K.J., Barrie, S.E., Aherne, G.W., Garrett, M.D., Mittnacht, S., and Pearl, L.H. (2006). Trans-activation of the DNA-damage signalling protein kinase Chk2 by T-loop exchange. EMBO J *25*, 3179-3190.

Olson, T.A., Mohanraj, D., Carson, L.F., and Ramakrishnan, S. (1994). Vascular permeability factor gene expression in normal and neoplastic human ovaries. Cancer research *54*, 276-280.

ONS, U.N.S. (2010). Cancer Statistics registrations: registrations of cancer diagnosed in 2008, England. , O.f.N. Statistics, ed.

Osorio, A., de la Hoya, M., Rodriguez-Lopez, R., Martinez-Ramirez, A., Cazorla, A., Granizo, J.J., Esteller, M., Rivas, C., Caldes, T., and Benitez, J. (2002). Loss of heterozygosity analysis at the BRCA loci in tumor samples from patients with familial breast cancer. Int J Cancer *99*, 305-309.

Ostling, O., and Johanson, K.J. (1984). Microelectrophoretic study of radiation-induced DNA damages in individual mammalian cells. Biochem Biophys Res Commun *123*, 291-298.

Ozols, R.F., Bundy, B.N., Greer, B.E., Fowler, J.M., Clarke-Pearson, D., Burger, R.A., Mannel, R.S., DeGeest, K., Hartenbach, E.M., and Baergen, R. (2003). Phase III trial of carboplatin and paclitaxel compared with cisplatin and paclitaxel in patients with optimally resected stage III ovarian cancer: a Gynecologic Oncology Group study. Journal of clinical oncology : official journal of the American Society of Clinical Oncology *21*, 3194-3200.

Pal, T., Permuth-Wey, J., Betts, J.A., Krischer, J.P., Fiorica, J., Arango, H., LaPolla, J., Hoffman, M., Martino, M.A., Wakeley, K.*, et al.* (2005). BRCA1 and BRCA2 mutations account for a large proportion of ovarian carcinoma cases. Cancer *104*, 2807-2816.

Panda, H., Jaiswal, A.S., Corsino, P.E., Armas, M.L., Law, B.K., and Narayan, S. (2009). Amino acid Asp181 of 5'-flap endonuclease 1 is a useful target for chemotherapeutic development. Biochemistry *48*, 9952-9958.

Parsons, D.W., Wang, T.L., Samuels, Y., Bardelli, A., Cummins, J.M., DeLong, L., Silliman, N., Ptak, J., Szabo, S., Willson, J.K.*, et al.* (2005). Colorectal cancer: mutations in a signalling pathway. Nature *436*, 792.

Patel, A.G., De Lorenzo, S.B., Flatten, K.S., Poirier, G.G., and Kaufmann, S.H. (2012). Failure of iniparib to inhibit poly(ADP-Ribose) polymerase in vitro. Clin Cancer Res *18*, 1655-1662.

Patel, A.G., Sarkaria, J.N., and Kaufmann, S.H. (2011). Nonhomologous end joining drives poly(ADP-ribose) polymerase (PARP) inhibitor lethality in homologous recombination-deficient cells. Proc Natl Acad Sci U S A *108*, 3406-3411.

Pautier, P., Joly, F., Kerbrat, P., Bougnoux, P., Fumoleau, P., Petit, T., Rixe, O., Ringeisen, F., Carrasco, A.T., and Lhomme, C. (2010). Phase II study of gefitinib in combination with paclitaxel (P) and carboplatin (C) as second-line therapy for ovarian,

tubal or peritoneal adenocarcinoma (1839IL/0074). Gynecologic oncology *116*, 157-162.

Peasland, A., Wang, L.Z., Rowling, E., Kyle, S., Chen, T., Hopkins, A., Cliby, W.A., Sarkaria, J., Beale, G., Edmondson, R.J*., et al.* (2011). Identification and evaluation of a potent novel ATR inhibitor, NU6027, in breast and ovarian cancer cell lines. Br J Cancer *105*, 372-381.

Pena-Diaz, J., and Jiricny, J. (2012). Mammalian mismatch repair: error-free or error-prone? Trends Biochem Sci *37*, 206-214.

Perets, R., Wyant, G.A., Muto, K.W., Bijron, J.G., Poole, B.B., Chin, K.T., Chen, J.Y., Ohman, A.W., Stepule, C.D., Kwak, S*., et al.* (2013). Transformation of the fallopian tube secretory epithelium leads to high-grade serous ovarian cancer in Brca;Tp53;Pten models. Cancer Cell *24*, 751-765.

Perez-Lorenzo, R., Gill, K.Z., Shen, C.H., Xian Zhao, F., Zheng, B., Schulze, H.J., Silvers, D.N., Brunner, G., and Horst, B.A. (2013a). A Tumor Suppressor Function for the Lipid Phosphatase INPP4B in Melanocytic Neoplasms. J Invest Dermatol.

Perez-Lorenzo, R., Gill, K.Z., Shen, C.H., Zhao, F.X., Zheng, B., Schulze, H.J., Silvers, D.N., Brunner, G., and Horst, B.A. (2013b). A Tumor Suppressor Function for the Lipid Phosphatase INPP4B in Melanocytic Neoplasms. The Journal of investigative dermatology.

Perren, T.J., Swart, A.M., Pfisterer, J., Ledermann, J.A., Pujade-Lauraine, E., Kristensen, G., Carey, M.S., Beale, P., Cervantes, A., Kurzeder, C*., et al.* (2011). A phase 3 trial of bevacizumab in ovarian cancer. N Engl J Med *365*, 2484-2496.

Pesesse, X., Deleu, S., De Smedt, F., Drayer, L., and Erneux, C. (1997). Identification of a second SH2-domain-containing protein closely related to the phosphatidylinositol polyphosphate 5-phosphatase SHIP. Biochem Biophys Res Commun *239*, 697-700.

Philp, A.J., Campbell, I.G., Leet, C., Vincan, E., Rockman, S.P., Whitehead, R.H., Thomas, R.J., and Phillips, W.A. (2001). The phosphatidylinositol 3'-kinase p85alpha gene is an oncogene in human ovarian and colon tumors. Cancer Res *61*, 7426-7429.

Planas-Silva, M.D., and Weinberg, R.A. (1997). The restriction point and control of cell proliferation. Curr Opin Cell Biol *9*, 768-772.

Plo, I., Laulier, C., Gauthier, L., Lebrun, F., Calvo, F., and Lopez, B.S. (2008a). AKT1 inhibits homologous recombination by inducing cytoplasmic retention of BRCA1 and RAD51. Cancer Res *68*, 9404-9412.

Plo, I., Laulier, C., Gauthier, L., Lebrun, F., Calvo, F., and Lopez, B.S. (2008b). AKT1 inhibits homologous recombination by inducing cytoplasmic retention of BRCA1 and RAD51. Cancer research *68*, 9404-9412.

Plumb, J.A., Strathdee, G., Sludden, J., Kaye, S.B., and Brown, R. (2000). Reversal of drug resistance in human tumor xenografts by 2'-deoxy-5-azacytidine-induced demethylation of the hMLH1 gene promoter. Cancer Res *60*, 6039-6044.

Plummer, R., Jones, C., Middleton, M., Wilson, R., Evans, J., Olsen, A., Curtin, N., Boddy, A., McHugh, P., Newell, D*., et al.* (2008). Phase I study of the poly(ADP-ribose) polymerase inhibitor, AG014699, in combination with temozolomide in patients with advanced solid tumors. Clin Cancer Res *14*, 7917-7923.

Podsypanina, K., Ellenson, L.H., Nemes, A., Gu, J., Tamura, M., Yamada, K.M., Cordon-Cardo, C., Catoretti, G., Fisher, P.E., and Parsons, R. (1999). Mutation of Pten/Mmac1 in mice causes neoplasia in multiple organ systems. Proc Natl Acad Sci U S A *96*, 1563-1568.

Posadas, E.M., Liel, M.S., Kwitkowski, V., Minasian, L., Godwin, A.K., Hussain, M.M., Espina, V., Wood, B.J., Steinberg, S.M., and Kohn, E.C. (2007). A phase II and pharmacodynamic study of gefitinib in patients with refractory or recurrent epithelial ovarian cancer. Cancer *109*, 1323-1330.

Prasad, N.K., Tandon, M., Badve, S., Snyder, P.W., and Nakshatri, H. (2008). Phosphoinositol phosphatase SHIP2 promotes cancer development and metastasis coupled with alterations in EGF receptor turnover. Carcinogenesis *29*, 25-34.

Press, J.Z., De Luca, A., Boyd, N., Young, S., Troussard, A., Ridge, Y., Kaurah, P., Kalloger, S.E., Blood, K.A., Smith, M*., et al.* (2008). Ovarian carcinomas with genetic and epigenetic BRCA1 loss have distinct molecular abnormalities. BMC cancer *8*, 17.

Prewett, M., Deevi, D.S., Bassi, R., Fan, F., Ellis, L.M., Hicklin, D.J., and Tonra, J.R. (2007). Tumors established with cell lines selected for oxaliplatin resistance respond to oxaliplatin if combined with cetuximab. Clin Cancer Res *13*, 7432-7440.

Puc, J., Keniry, M., Li, H.S., Pandita, T.K., Choudhury, A.D., Memeo, L., Mansukhani, M., Murty, V.V., Gaciong, Z., Meek, S.E*., et al.* (2005). Lack of PTEN sequesters CHK1 and initiates genetic instability. Cancer Cell *7*, 193-204.

Qiu, L., Wang, S., Lang, J.H., Shen, K., Huang, H.F., Pan, L.Y., Wu, M., and Yang, J.X. (2013). The occurrence of endometriosis with ovarian carcinomas is not purely coincidental. Eur J Obstet Gynecol Reprod Biol *170*, 225-228.

R. Morgan, A.M.O., R. Qin, K. M. Laumann, H. Mackay, E. L. Strevel, S. Welch, D. Sullivan, R. M. Wenham, H. X. Chen, L. A. Doyle, D. R. Gandara and C. Erlichman (2011). A phase II trial of temsirolimus and bevacizumab in patients with endometrial, ovarian, hepatocellular carcinoma, carcinoid, or islet cell cancer: Ovarian cancer (OC) subset—A study of the Princess Margaret, Mayo, Southeast phase II, and California Cancer (CCCP) N01 Consortia NCI#8233.
. Journal of Clinical Oncology, 2011 ASCO Annual Meeting Abstracts
Vol 29, No 15_suppl (May 20 Supplement), 2011: 5015.

R. Plummer, P.L., J. Evans, N. Steven, M. Middleton, R. Wilson, K. Snow, R. Dewji and H. Calvert (2006). First and final report of a phase II study of the poly(ADP-ribose) polymerase (PARP) inhibitor, AG014699, in combination with temozolomide (TMZ) in patients with metastatic malignant melanoma (MM)
. Journal of Clinical Oncology, 2006 ASCO Annual Meeting Proceedings (Post-Meeting Edition) *Vol 24, No 18S (June 20 Supplement), 2006: 8013*.

R. T. Penson, C.W., B. Lasonde, C. N. Krasner, P. Konstantinopoulos, T. E. Stallings, C. R. Bradley, M. J. Birrer and U. Matulonis (2011). A phase II trial of iniparib (BSI-201) in combination with gemcitabine/carboplatin (GC) in patients with platinum-sensitive recurrent ovarian cancer. Journal of Clinical Oncology, 2011 ASCO Annual Meeting Abstracts
Vol 29.

Rabik, C.A., Njoku, M.C., and Dolan, M.E. (2006). Inactivation of O6-alkylguanine DNA alkyltransferase as a means to enhance chemotherapy. Cancer Treat Rev *32*, 261-276.

Ranson, M., Middleton, M.R., Bridgewater, J., Lee, S.M., Dawson, M., Jowle, D., Halbert, G., Waller, S., McGrath, H., Gumbrell, L.*, et al.* (2006). Lomeguatrib, a potent inhibitor of O6-alkylguanine-DNA-alkyltransferase: phase I safety, pharmacodynamic, and pharmacokinetic trial and evaluation in combination with temozolomide in patients with advanced solid tumors. Clin Cancer Res *12*, 1577-1584.

Reaper, P.M., Griffiths, M.R., Long, J.M., Charrier, J.D., Maccormick, S., Charlton, P.A., Golec, J.M., and Pollard, J.R. (2011). Selective killing of ATM- or p53-deficient cancer cells through inhibition of ATR. Nat Chem Biol *7*, 428-430.

Rechsteiner, M., and Rogers, S.W. (1996). PEST sequences and regulation by proteolysis. Trends Biochem Sci *21*, 267-271.

Richardson, A.L., Wang, Z.C., De Nicolo, A., Lu, X., Brown, M., Miron, A., Liao, X., Iglehart, J.D., Livingston, D.M., and Ganesan, S. (2006). X chromosomal abnormalities in basal-like human breast cancer. Cancer Cell *9*, 121-132.

Robertson, A.B., Klungland, A., Rognes, T., and Leiros, I. (2009). DNA repair in mammalian cells: Base excision repair: the long and short of it. Cell Mol Life Sci *66*, 981-993.

Robey, R.B., and Hay, N. (2006). Mitochondrial hexokinases, novel mediators of the antiapoptotic effects of growth factors and Akt. Oncogene *25*, 4683-4696.

Romero, I., and Bast, R.C., Jr. (2012). Minireview: human ovarian cancer: biology, current management, and paths to personalizing therapy. Endocrinology *153*, 1593-1602.

Rouleau, M., Patel, A., Hendzel, M.J., Kaufmann, S.H., and Poirier, G.G. (2010). PARP inhibition: PARP1 and beyond. Nat Rev Cancer *10*, 293-301.

Ruschmann, J., Ho, V., Antignano, F., Kuroda, E., Lam, V., Ibaraki, M., Snyder, K., Kim, C., Flavell, R.A., Kawakami, T.*, et al.* (2010). Tyrosine phosphorylation of SHIP promotes its proteasomal degradation. Exp Hematol *38*, 392-402, 402 e391.

Rustin, G.J., van der Burg, M.E., Griffin, C.L., Guthrie, D., Lamont, A., Jayson, G.C., Kristensen, G., Mediola, C., Coens, C., Qian, W.*, et al.* (2010). Early versus delayed treatment of relapsed ovarian cancer (MRC OV05/EORTC 55955): a randomised trial. Lancet *376*, 1155-1163.

Ruzankina, Y., Pinzon-Guzman, C., Asare, A., Ong, T., Pontano, L., Cotsarelis, G., Zediak, V.P., Velez, M., Bhandoola, A., and Brown, E.J. (2007). Deletion of the developmentally essential gene ATR in adult mice leads to age-related phenotypes and stem cell loss. Cell Stem Cell *1*, 113-126.

Sable, C.L., Filippa, N., Hemmings, B., and Van Obberghen, E. (1997). cAMP stimulates protein kinase B in a Wortmannin-insensitive manner. FEBS Lett *409*, 253-257.

Sakai, W., Swisher, E.M., Karlan, B.Y., Agarwal, M.K., Higgins, J., Friedman, C., Villegas, E., Jacquemont, C., Farrugia, D.J., *et al.* (2008). Secondary mutations as a mechanism of cisplatin resistance in BRCA2-mutated cancers. Nature *451*, 1116-1120.

Salmena, L., Carracedo, A., and Pandolfi, P.P. (2008). Tenets of PTEN tumor suppression. Cell *133*, 403-414.

Salvesen, H.B., MacDonald, N., Ryan, A., Jacobs, I.J., Lynch, E.D., Akslen, L.A., and Das, S. (2001). PTEN methylation is associated with advanced stage and microsatellite instability in endometrial carcinoma. Int J Cancer *91*, 22-26.

Sancak, Y., Thoreen, C.C., Peterson, T.R., Lindquist, R.A., Kang, S.A., Spooner, E., Carr, S.A., and Sabatini, D.M. (2007). PRAS40 is an insulin-regulated inhibitor of the mTORC1 protein kinase. Mol Cell *25*, 903-915.

Sandercock, J., Parmar, M.K., Torri, V., and Qian, W. (2002). First-line treatment for advanced ovarian cancer: paclitaxel, platinum and the evidence. British journal of cancer *87*, 815-824.

Sansal, I., and Sellers, W.R. (2004). The biology and clinical relevance of the PTEN tumor suppressor pathway. J Clin Oncol *22*, 2954-2963.

Sarbassov, D.D., Guertin, D.A., Ali, S.M., and Sabatini, D.M. (2005). Phosphorylation and regulation of Akt/PKB by the rictor-mTOR complex. Science *307*, 1098-1101.

Sartori, A.A., Lukas, C., Coates, J., Mistrik, M., Fu, S., Bartek, J., Baer, R., Lukas, J., and Jackson, S.P. (2007). Human CtIP promotes DNA end resection. Nature *450*, 509-514.

Sasaki, J., Kofuji, S., Itoh, R., Momiyama, T., Takayama, K., Murakami, H., Chida, S., Tsuya, Y., Takasuga, S., Eguchi, S., *et al.* (2010). The PtdIns(3,4)P(2) phosphatase INPP4A is a suppressor of excitotoxic neuronal death. Nature *465*, 497-501.

Sasaoka, T., Hori, H., Wada, T., Ishiki, M., Haruta, T., Ishihara, H., and Kobayashi, M. (2001). SH2-containing inositol phosphatase 2 negatively regulates insulin-induced glycogen synthesis in L6 myotubes. Diabetologia *44*, 1258-1267.

Sasieni, P.D., Shelton, J., Ormiston-Smith, N., Thomson, C.S., and Silcocks, P.B. (2011). What is the lifetime risk of developing cancer?: the effect of adjusting for multiple primaries. British journal of cancer *105*, 460-465.

Sattler, M., Verma, S., Byrne, C.H., Shrikhande, G., Winkler, T., Algate, P.A., Rohrschneider, L.R., and Griffin, J.D. (1999). BCR/ABL directly inhibits expression of SHIP, an SH2-containing polyinositol-5-phosphatase involved in the regulation of hematopoiesis. Mol Cell Biol *19*, 7473-7480.

Savic, V., Yin, B., Maas, N.L., Bredemeyer, A.L., Carpenter, A.C., Helmink, B.A., Yang-Iott, K.S., Sleckman, B.P., and Bassing, C.H. (2009). Formation of dynamic gamma-H2AX domains along broken DNA strands is distinctly regulated by ATM and MDC1 and dependent upon H2AX densities in chromatin. Mol Cell *34*, 298-310.

Schilder, R.J., Sill, M.W., Chen, X., Darcy, K.M., Decesare, S.L., Lewandowski, G., Lee, R.B., Arciero, C.A., Wu, H., and Godwin, A.K. (2005). Phase II study of gefitinib in patients with relapsed or persistent ovarian or primary peritoneal carcinoma and evaluation of epidermal growth factor receptor mutations and immunohistochemical expression: a Gynecologic Oncology Group Study. Clinical cancer research : an official journal of the American Association for Cancer Research *11*, 5539-5548.

Schlegel, B.P., Jodelka, F.M., and Nunez, R. (2006). BRCA1 promotes induction of ssDNA by ionizing radiation. Cancer Res *66*, 5181-5189.

Schorge, J.O., McCann, C., and Del Carmen, M.G. (2010). Surgical debulking of ovarian cancer: what difference does it make? Rev Obstet Gynecol *3*, 111-117.

Schreiber, V., Dantzer, F., Ame, J.C., and de Murcia, G. (2006). Poly(ADP-ribose): novel functions for an old molecule. Nat Rev Mol Cell Biol *7*, 517-528.

Scott, P.H., Brunn, G.J., Kohn, A.D., Roth, R.A., and Lawrence, J.C., Jr. (1998). Evidence of insulin-stimulated phosphorylation and activation of the mammalian target of rapamycin mediated by a protein kinase B signaling pathway. Proc Natl Acad Sci U S A *95*, 7772-7777.

Scully, R., Chen, J., Plug, A., Xiao, Y., Weaver, D., Feunteun, J., Ashley, T., and Livingston, D.M. (1997). Association of BRCA1 with Rad51 in mitotic and meiotic cells. Cell *88*, 265-275.

Sehouli, J., Stengel, D., Oskay-Oezcelik, G., Zeimet, A.G., Sommer, H., Klare, P., Stauch, M., Paulenz, A., Camara, O., Keil, E.*, et al.* (2008). Nonplatinum topotecan combinations versus topotecan alone for recurrent ovarian cancer: results of a phase III study of the North-Eastern German Society of Gynecological Oncology Ovarian Cancer Study Group. J Clin Oncol *26*, 3176-3182.

Seiden, M.V., Burris, H.A., Matulonis, U., Hall, J.B., Armstrong, D.K., Speyer, J., Weber, J.D., and Muggia, F. (2007). A phase II trial of EMD72000 (matuzumab), a humanized anti-EGFR monoclonal antibody, in patients with platinum-resistant ovarian and primary peritoneal malignancies. Gynecologic oncology *104*, 727-731.

Seiler, J.A., Conti, C., Syed, A., Aladjem, M.I., and Pommier, Y. (2007). The intra-S-phase checkpoint affects both DNA replication initiation and elongation: single-cell and -DNA fiber analyses. Mol Cell Biol *27*, 5806-5818.

Sekimoto, T., Fukumoto, M., and Yoneda, Y. (2004). 14-3-3 suppresses the nuclear localization of threonine 157-phosphorylated p27(Kip1). EMBO J *23*, 1934-1942.

Sekulic, A., Hudson, C.C., Homme, J.L., Yin, P., Otterness, D.M., Karnitz, L.M., and Abraham, R.T. (2000). A direct linkage between the phosphoinositide 3-kinase-AKT signaling pathway and the mammalian target of rapamycin in mitogen-stimulated and transformed cells. Cancer Res *60*, 3504-3513.

Semenza, G.L. (2003). Targeting HIF-1 for cancer therapy. Nat Rev Cancer *3*, 721-732.

Shah, Z.H., Jones, D.R., Sommer, L., Foulger, R., Bultsma, Y., D'Santos, C., and Divecha, N. (2013). Nuclear phosphoinositides and their impact on nuclear functions. FEBS J *280*, 6295-6310.

Shih Ie, M., and Kurman, R.J. (2004). Ovarian tumorigenesis: a proposed model based on morphological and molecular genetic analysis. The American journal of pathology *164*, 1511-1518.

Shimada, M., Niida, H., Zineldeen, D.H., Tagami, H., Tanaka, M., Saito, H., and Nakanishi, M. (2008). Chk1 is a histone H3 threonine 11 kinase that regulates DNA damage-induced transcriptional repression. Cell *132*, 221-232.

Shin, I., Yakes, F.M., Rojo, F., Shin, N.Y., Bakin, A.V., Baselga, J., and Arteaga, C.L. (2002). PKB/Akt mediates cell-cycle progression by phosphorylation of p27(Kip1) at threonine 157 and modulation of its cellular localization. Nat Med *8*, 1145-1152.

Shiotani, B., and Zou, L. (2009). Single-stranded DNA orchestrates an ATM-to-ATR switch at DNA breaks. Mol Cell *33*, 547-558.

Shrivastav, M., De Haro, L.P., and Nickoloff, J.A. (2008). Regulation of DNA double-strand break repair pathway choice. Cell Res *18*, 134-147.

Shtivelman, E., Sussman, J., and Stokoe, D. (2002). A role for PI 3-kinase and PKB activity in the G2/M phase of the cell cycle. Curr Biol *12*, 919-924.

Simpkins, F., Garcia-Soto, A., and Slingerland, J. (2013). New insights on the role of hormonal therapy in ovarian cancer. Steroids *78*, 530-537.

Simpkins, F., Hevia-Paez, P., Sun, J., Ullmer, W., Gilbert, C.A., da Silva, T., Pedram, A., Levin, E.R., Reis, I.M., Rabinovich, B.*, et al.* (2012). Src Inhibition with saracatinib reverses fulvestrant resistance in ER-positive ovarian cancer models in vitro and in vivo. Clin Cancer Res *18*, 5911-5923.

Singer, G., Oldt, R., 3rd, Cohen, Y., Wang, B.G., Sidransky, D., Kurman, R.J., and Shih Ie, M. (2003a). Mutations in BRAF and KRAS characterize the development of low-grade ovarian serous carcinoma. Journal of the National Cancer Institute *95*, 484-486.

Singer, G., Shih Ie, M., Truskinovsky, A., Umudum, H., and Kurman, R.J. (2003b). Mutational analysis of K-ras segregates ovarian serous carcinomas into two types: invasive MPSC (low-grade tumor) and conventional serous carcinoma (high-grade tumor). International journal of gynecological pathology : official journal of the International Society of Gynecological Pathologists *22*, 37-41.

Singh, N.P., McCoy, M.T., Tice, R.R., and Schneider, E.L. (1988). A simple technique for quantitation of low levels of DNA damage in individual cells. Exp Cell Res *175*, 184-191.

Sirotnak, F.M. (2003). Studies with ZD1839 in preclinical models. Seminars in oncology *30*, 12-20.

Sirotnak, F.M., Zakowski, M.F., Miller, V.A., Scher, H.I., and Kris, M.G. (2000). Efficacy of cytotoxic agents against human tumor xenografts is markedly enhanced by coadministration of ZD1839 (Iressa), an inhibitor of EGFR tyrosine kinase. Clinical cancer research : an official journal of the American Association for Cancer Research *6*, 4885-4892.

Sleeman, M.W., Wortley, K.E., Lai, K.M., Gowen, L.C., Kintner, J., Kline, W.O., Garcia, K., Stitt, T.N., Yancopoulos, G.D., Wiegand, S.J.*, et al.* (2005). Absence of the lipid phosphatase SHIP2 confers resistance to dietary obesity. Nat Med *11*, 199-205.

Smith, H.O., Berwick, M., Verschraegen, C.F., Wiggins, C., Lansing, L., Muller, C.Y., and Qualls, C.R. (2006). Incidence and survival rates for female malignant germ cell tumors. Obstetrics and gynecology *107*, 1075-1085.

Smith, J., Tho, L.M., Xu, N., and Gillespie, D.A. (2010). The ATM-Chk2 and ATR-Chk1 pathways in DNA damage signaling and cancer. Adv Cancer Res *108*, 73-112.

Smyth, G.K. (2004). Linear models and empirical bayes methods for assessing differential expression in microarray experiments. Statistical applications in genetics and molecular biology *3*, Article3.

Song, G., Ouyang, G., and Bao, S. (2005). The activation of Akt/PKB signaling pathway and cell survival. J Cell Mol Med *9*, 59-71.

Songyang, Z., Shoelson, S.E., Chaudhuri, M., Gish, G., Pawson, T., Haser, W.G., King, F., Roberts, T., Ratnofsky, S., Lechleider, R.J.*, et al.* (1993). SH2 domains recognize specific phosphopeptide sequences. Cell *72*, 767-778.

Sorensen, C.S., Hansen, L.T., Dziegielewski, J., Syljuasen, R.G., Lundin, C., Bartek, J., and Helleday, T. (2005). The cell-cycle checkpoint kinase Chk1 is required for mammalian homologous recombination repair. Nat Cell Biol *7*, 195-201.

Spandidos, A., Wang, X., Wang, H., and Seed, B. (2010). PrimerBank: a resource of human and mouse PCR primer pairs for gene expression detection and quantification. Nucleic Acids Res *38*, D792-799.

Steck, P.A., Pershouse, M.A., Jasser, S.A., Yung, W.K., Lin, H., Ligon, A.H., Langford, L.A., Baumgard, M.L., Hattier, T., Davis, T.*, et al.* (1997). Identification of a candidate tumour suppressor gene, MMAC1, at chromosome 10q23.3 that is mutated in multiple advanced cancers. Nat Genet *15*, 356-362.

Stephens, L.R., Eguinoa, A., Erdjument-Bromage, H., Lui, M., Cooke, F., Coadwell, J., Smrcka, A.S., Thelen, M., Cadwallader, K., Tempst, P.*, et al.* (1997). The G beta gamma sensitivity of a PI3K is dependent upon a tightly associated adaptor, p101. Cell *89*, 105-114.

Stewart, G.S., Maser, R.S., Stankovic, T., Bressan, D.A., Kaplan, M.I., Jaspers, N.G., Raams, A., Byrd, P.J., Petrini, J.H., and Taylor, A.M. (1999). The DNA double-strand break repair gene hMRE11 is mutated in individuals with an ataxia-telangiectasia-like disorder. Cell *99*, 577-587.

Stewart, G.S., Wang, B., Bignell, C.R., Taylor, A.M., and Elledge, S.J. (2003). MDC1 is a mediator of the mammalian DNA damage checkpoint. Nature *421*, 961-966.

Stjernstrom, A., Karlsson, C., Fernandez, O.J., Soderkvist, P., Karlsson, M.G., and Thunell, L.K. (2014). Alterations of INPP4B, PIK3CA and pAkt of the PI3K pathway are associated with squamous cell carcinoma of the lung. Cancer Med.

Stommel, J.M., Kimmelman, A.C., Ying, H., Nabioullin, R., Ponugoti, A.H., Wiedemeyer, R., Stegh, A.H., Bradner, J.E., Ligon, K.L., Brennan, C.*, et al.* (2007). Coactivation of receptor tyrosine kinases affects the response of tumor cells to targeted therapies. Science *318*, 287-290.

Subramanian, A., Tamayo, P., Mootha, V.K., Mukherjee, S., Ebert, B.L., Gillette, M.A., Paulovich, A., Pomeroy, S.L., Golub, T.R., Lander, E.S.*, et al.* (2005). Gene set enrichment analysis: a knowledge-based approach for interpreting genome-wide expression profiles. Proc Natl Acad Sci U S A *102*, 15545-15550.

Suire, S., Coadwell, J., Ferguson, G.J., Davidson, K., Hawkins, P., and Stephens, L. (2005). p84, a new Gbetagamma-activated regulatory subunit of the type IB phosphoinositide 3-kinase p110gamma. Curr Biol *15*, 566-570.

Sun, Y., Jiang, X., Xu, Y., Ayrapetov, M.K., Moreau, L.A., Whetstine, J.R., and Price, B.D. (2009). Histone H3 methylation links DNA damage detection to activation of the tumour suppressor Tip60. Nat Cell Biol *11*, 1376-1382.

Sundqvist, A., Bengoechea-Alonso, M.T., Ye, X., Lukiyanchuk, V., Jin, J., Harper, J.W., and Ericsson, J. (2005). Control of lipid metabolism by phosphorylation-dependent degradation of the SREBP family of transcription factors by SCF(Fbw7). Cell Metab *1*, 379-391.

Swift, M., Morrell, D., Massey, R.B., and Chase, C.L. (1991). Incidence of cancer in 161 families affected by ataxia-telangiectasia. N Engl J Med *325*, 1831-1836.

Swisher, E.M., Sakai, W., Karlan, B.Y., Wurz, K., Urban, N., and Taniguchi, T. (2008). Secondary BRCA1 mutations in BRCA1-mutated ovarian carcinomas with platinum resistance. Cancer Res *68*, 2581-2586.

Taha, C., Liu, Z., Jin, J., Al-Hasani, H., Sonenberg, N., and Klip, A. (1999). Opposite translational control of GLUT1 and GLUT4 glucose transporter mRNAs in response to insulin. Role of mammalian target of rapamycin, protein kinase b, and phosphatidylinositol 3-kinase in GLUT1 mRNA translation. J Biol Chem *274*, 33085-33091.

Taylor, A.M., Harnden, D.G., Arlett, C.F., Harcourt, S.A., Lehmann, A.R., Stevens, S., and Bridges, B.A. (1975). Ataxia telangiectasia: a human mutation with abnormal radiation sensitivity. Nature *258*, 427-429.

Taylor, B.S., Schultz, N., Hieronymus, H., Gopalan, A., Xiao, Y., Carver, B.S., Arora, V.K., Kaushik, P., Cerami, E., Reva, B.*, et al.* (2010). Integrative genomic profiling of human prostate cancer. Cancer Cell *18*, 11-22.

Temkin, S.M., Yamada, S.D., and Fleming, G.F. (2010). A phase I study of weekly temsirolimus and topotecan in the treatment of advanced and/or recurrent gynecologic malignancies. Gynecol Oncol *117*, 473-476.

Thompson, D., Duedal, S., Kirner, J., McGuffog, L., Last, J., Reiman, A., Byrd, P., Taylor, M., and Easton, D.F. (2005). Cancer risks and mortality in heterozygous ATM mutation carriers. J Natl Cancer Inst *97*, 813-822.

Thompson, R., and Eastman, A. (2013). The cancer therapeutic potential of Chk1 inhibitors: how mechanistic studies impact on clinical trial design. Br J Clin Pharmacol *76*, 358-369.

Tibarewal, P., Zilidis, G., Spinelli, L., Schurch, N., Maccario, H., Gray, A., Perera, N.M., Davidson, L., Barton, G.J., and Leslie, N.R. (2012). PTEN protein phosphatase activity correlates with control of gene expression and invasion, a tumor-suppressing phenotype, but not with AKT activity. Sci Signal *5*, ra18.

Toker, A., and Cantley, L.C. (1997). Signalling through the lipid products of phosphoinositide-3-OH kinase. Nature *387*, 673-676.

Tothill, R.W., Tinker, A.V., George, J., Brown, R., Fox, S.B., Lade, S., Johnson, D.S., Trivett, M.K., Etemadmoghadam, D., Locandro, B.*, et al.* (2008). Novel molecular subtypes of serous and endometrioid ovarian cancer linked to clinical outcome. Clin Cancer Res *14*, 5198-5208.

Tran, H., Brunet, A., Griffith, E.C., and Greenberg, M.E. (2003). The many forks in FOXO's road. Sci STKE *2003*, RE5.

Trimmer, E.E., and Essigmann, J.M. (1999). Cisplatin. Essays Biochem *34*, 191-211.

Trotman, L.C., Niki, M., Dotan, Z.A., Koutcher, J.A., Di Cristofano, A., Xiao, A., Khoo, A.S., Roy-Burman, P., Greenberg, N.M., Van Dyke, T.*, et al.* (2003). Pten dose dictates cancer progression in the prostate. PLoS Biol *1*, E59.

Turner, N., Tutt, A., and Ashworth, A. (2004). Hallmarks of 'BRCAness' in sporadic cancers. Nature reviews Cancer *4*, 814-819.

Tutt, A., Robson, M., Garber, J.E., Domchek, S.M., Audeh, M.W., Weitzel, J.N., Friedlander, M., Arun, B., Loman, N., Schmutzler, R.K.*, et al.* (2010). Oral poly(ADP-ribose) polymerase inhibitor olaparib in patients with BRCA1 or BRCA2 mutations and advanced breast cancer: a proof-of-concept trial. Lancet *376*, 235-244.

Tutt, A.N., van Oostrom, C.T., Ross, G.M., van Steeg, H., and Ashworth, A. (2002). Disruption of Brca2 increases the spontaneous mutation rate in vivo: synergism with ionizing radiation. EMBO Rep *3*, 255-260.

Umar, A., Boland, C.R., Terdiman, J.P., Syngal, S., de la Chapelle, A., Ruschoff, J., Fishel, R., Lindor, N.M., Burgart, L.J., Hamelin, R.*, et al.* (2004). Revised Bethesda

Guidelines for hereditary nonpolyposis colorectal cancer (Lynch syndrome) and microsatellite instability. J Natl Cancer Inst *96*, 261-268.

Usanova, S., Piee-Staffa, A., Sied, U., Thomale, J., Schneider, A., Kaina, B., and Koberle, B. (2010). Cisplatin sensitivity of testis tumour cells is due to deficiency in interstrand-crosslink repair and low ERCC1-XPF expression. Mol Cancer *9*, 248.

Uziel, T., Lerenthal, Y., Moyal, L., Andegeko, Y., Mittelman, L., and Shiloh, Y. (2003). Requirement of the MRN complex for ATM activation by DNA damage. EMBO J *22*, 5612-5621.

Vander Haar, E., Lee, S.I., Bandhakavi, S., Griffin, T.J., and Kim, D.H. (2007). Insulin signalling to mTOR mediated by the Akt/PKB substrate PRAS40. Nat Cell Biol *9*, 316-323.

Vanhaesebroeck, B., and Alessi, D.R. (2000). The PI3K-PDK1 connection: more than just a road to PKB. Biochem J *346 Pt 3*, 561-576.

Vanhaesebroeck, B., Leevers, S.J., Panayotou, G., and Waterfield, M.D. (1997). Phosphoinositide 3-kinases: a conserved family of signal transducers. Trends Biochem Sci *22*, 267-272.

Varon, R., Vissinga, C., Platzer, M., Cerosaletti, K.M., Chrzanowska, K.H., Saar, K., Beckmann, G., Seemanova, E., Cooper, P.R., Nowak, N.J.*, et al.* (1998). Nibrin, a novel DNA double-strand break repair protein, is mutated in Nijmegen breakage syndrome. Cell *93*, 467-476.

Vassileva, V., Millar, A., Briollais, L., Chapman, W., and Bapat, B. (2002). Genes involved in DNA repair are mutational targets in endometrial cancers with microsatellite instability. Cancer Res *62*, 4095-4099.

Viglietto, G., Motti, M.L., Bruni, P., Melillo, R.M., D'Alessio, A., Califano, D., Vinci, F., Chiappetta, G., Tsichlis, P., Bellacosa, A.*, et al.* (2002). Cytoplasmic relocalization and inhibition of the cyclin-dependent kinase inhibitor p27(Kip1) by PKB/Akt-mediated phosphorylation in breast cancer. Nat Med *8*, 1136-1144.

Vilar, E., Bartnik, C.M., Stenzel, S.L., Raskin, L., Ahn, J., Moreno, V., Mukherjee, B., Iniesta, M.D., Morgan, M.A., Rennert, G.*, et al.* (2011). MRE11 deficiency increases sensitivity to poly(ADP-ribose) polymerase inhibition in microsatellite unstable colorectal cancers. Cancer Res *71*, 2632-2642.

Voigt, P., Dorner, M.B., and Schaefer, M. (2006). Characterization of p87PIKAP, a novel regulatory subunit of phosphoinositide 3-kinase gamma that is highly expressed in heart and interacts with PDE3B. J Biol Chem *281*, 9977-9986.

Vollebergh, M.A., Jonkers, J., and Linn, S.C. (2012). Genomic instability in breast and ovarian cancers: translation into clinical predictive biomarkers. Cell Mol Life Sci *69*, 223-245.

Wada, T., Sasaoka, T., Funaki, M., Hori, H., Murakami, S., Ishiki, M., Haruta, T., Asano, T., Ogawa, W., Ishihara, H.*, et al.* (2001). Overexpression of SH2-containing inositol phosphatase 2 results in negative regulation of insulin-induced metabolic

actions in 3T3-L1 adipocytes via its 5'-phosphatase catalytic activity. Mol Cell Biol *21*, 1633-1646.

Walker, M., Black, E.J., Oehler, V., Gillespie, D.A., and Scott, M.T. (2009). Chk1 C-terminal regulatory phosphorylation mediates checkpoint activation by de-repression of Chk1 catalytic activity. Oncogene *28*, 2314-2323.

Wang, J.W., Howson, J.M., Ghansah, T., Desponts, C., Ninos, J.M., May, S.L., Nguyen, K.H., Toyama-Sorimachi, N., and Kerr, W.G. (2002). Influence of SHIP on the NK repertoire and allogeneic bone marrow transplantation. Science *295*, 2094-2097.

Wang, S., Gao, J., Lei, Q., Rozengurt, N., Pritchard, C., Jiao, J., Thomas, G.V., Li, G., Roy-Burman, P., Nelson, P.S.*, et al.* (2003). Prostate-specific deletion of the murine Pten tumor suppressor gene leads to metastatic prostate cancer. Cancer Cell *4*, 209-221.

Wang, X., and Seed, B. (2003). A PCR primer bank for quantitative gene expression analysis. Nucleic Acids Res *31*, e154.

Wang, X., Spandidos, A., Wang, H., and Seed, B. (2012). PrimerBank: a PCR primer database for quantitative gene expression analysis, 2012 update. Nucleic Acids Res *40*, D1144-1149.

Wang, Y., Kreisberg, J.I., and Ghosh, P.M. (2007). Cross-talk between the androgen receptor and the phosphatidylinositol 3-kinase/Akt pathway in prostate cancer. Curr Cancer Drug Targets *7*, 591-604.

Watson, A.J., Sabharwal, A., Thorncroft, M., McGown, G., Kerr, R., Bojanic, S., Soonawalla, Z., King, A., Miller, A., Waller, S.*, et al.* (2010). Tumor O(6)-methylguanine-DNA methyltransferase inactivation by oral lomeguatrib. Clin Cancer Res *16*, 743-749.

Weberpals, J.I., Clark-Knowles, K.V., and Vanderhyden, B.C. (2008). Sporadic epithelial ovarian cancer: clinical relevance of BRCA1 inhibition in the DNA damage and repair pathway. J Clin Oncol *26*, 3259-3267.

Wei, W., Jin, J., Schlisio, S., Harper, J.W., and Kaelin, W.G., Jr. (2005). The v-Jun point mutation allows c-Jun to escape GSK3-dependent recognition and destruction by the Fbw7 ubiquitin ligase. Cancer Cell *8*, 25-33.

Weigman, V.J., Chao, H.H., Shabalin, A.A., He, X., Parker, J.S., Nordgard, S.H., Grushko, T., Huo, D., Nwachukwu, C., Nobel, A.*, et al.* (2011). Basal-like Breast cancer DNA copy number losses identify genes involved in genomic instability, response to therapy, and patient survival. Breast cancer research and treatment.

Welcker, M., Singer, J., Loeb, K.R., Grim, J., Bloecher, A., Gurien-West, M., Clurman, B.E., and Roberts, J.M. (2003). Multisite phosphorylation by Cdk2 and GSK3 controls cyclin E degradation. Mol Cell *12*, 381-392.

Wenk, M.R., Lucast, L., Di Paolo, G., Romanelli, A.J., Suchy, S.F., Nussbaum, R.L., Cline, G.W., Shulman, G.I., McMurray, W., and De Camilli, P. (2003). Phosphoinositide profiling in complex lipid mixtures using electrospray ionization mass spectrometry. Nat Biotechnol *21*, 813-817.

Westbrook, T.F., Martin, E.S., Schlabach, M.R., Leng, Y., Liang, A.C., Feng, B., Zhao, J.J., Roberts, T.M., Mandel, G., Hannon, G.J., *et al.* (2005). A genetic screen for candidate tumor suppressors identifies REST. Cell *121*, 837-848.

Weston, V.J., Oldreive, C.E., Skowronska, A., Oscier, D.G., Pratt, G., Dyer, M.J., Smith, G., Powell, J.E., Rudzki, Z., Kearns, P., *et al.* (2010). The PARP inhibitor olaparib induces significant killing of ATM-deficient lymphoid tumor cells in vitro and in vivo. Blood *116*, 4578-4587.

Weterings, E., and Chen, D.J. (2008). The endless tale of non-homologous end-joining. Cell Res *18*, 114-124.

Williamson, C.T., Muzik, H., Turhan, A.G., Zamo, A., O'Connor, M.J., Bebb, D.G., and Lees-Miller, S.P. (2010). ATM deficiency sensitizes mantle cell lymphoma cells to poly(ADP-ribose) polymerase-1 inhibitors. Mol Cancer Ther *9*, 347-357.

Willmore, E., de Caux, S., Sunter, N.J., Tilby, M.J., Jackson, G.H., Austin, C.A., and Durkacz, B.W. (2004). A novel DNA-dependent protein kinase inhibitor, NU7026, potentiates the cytotoxicity of topoisomerase II poisons used in the treatment of leukemia. Blood *103*, 4659-4665.

Willner, J., Wurz, K., Allison, K.H., Galic, V., Garcia, R.L., Goff, B.A., and Swisher, E.M. (2007). Alternate molecular genetic pathways in ovarian carcinomas of common histological types. Human pathology *38*, 607-613.

Wipf, P., and Halter, R.J. (2005). Chemistry and biology of wortmannin. Org Biomol Chem *3*, 2053-2061.

Wogan, G.N., Hecht, S.S., Felton, J.S., Conney, A.H., and Loeb, L.A. (2004). Environmental and chemical carcinogenesis. Semin Cancer Biol *14*, 473-486.

Wold, M.S. (1997). Replication protein A: a heterotrimeric, single-stranded DNA-binding protein required for eukaryotic DNA metabolism. Annu Rev Biochem *66*, 61-92.

Wu, C.C., Li, T.K., Farh, L., Lin, L.Y., Lin, T.S., Yu, Y.J., Yen, T.J., Chiang, C.W., and Chan, N.L. (2011). Structural basis of type II topoisomerase inhibition by the anticancer drug etoposide. Science *333*, 459-462.

Wu, R., Baker, S.J., Hu, T.C., Norman, K.M., Fearon, E.R., and Cho, K.R. (2013). Type I to type II ovarian carcinoma progression: mutant Trp53 or Pik3ca confers a more aggressive tumor phenotype in a mouse model of ovarian cancer. Am J Pathol *182*, 1391-1399.

Wu, R., Hendrix-Lucas, N., Kuick, R., Zhai, Y., Schwartz, D.R., Akyol, A., Hanash, S., Misek, D.E., Katabuchi, H., Williams, B.O., *et al.* (2007). Mouse model of human ovarian endometrioid adenocarcinoma based on somatic defects in the Wnt/beta-catenin and PI3K/Pten signaling pathways. Cancer Cell *11*, 321-333.

Wullschleger, S., Loewith, R., and Hall, M.N. (2006). TOR signaling in growth and metabolism. Cell *124*, 471-484.

Wurmser, A.E., and Emr, S.D. (2002). Novel PtdIns(3)P-binding protein Etf1 functions as an effector of the Vps34 PtdIns 3-kinase in autophagy. J Cell Biol *158*, 761-772.

Xu, B., Kim, S., and Kastan, M.B. (2001). Involvement of Brca1 in S-phase and G(2)-phase checkpoints after ionizing irradiation. Mol Cell Biol *21*, 3445-3450.

Xu, Y., and Baltimore, D. (1996). Dual roles of ATM in the cellular response to radiation and in cell growth control. Genes Dev *10*, 2401-2410.

Yamanaka, Y., Tagawa, H., Takahashi, N., Watanabe, A., Guo, Y.M., Iwamoto, K., Yamashita, J., Saitoh, H., Kameoka, Y., Shimizu, N.*, et al.* (2009). Aberrant overexpression of microRNAs activate AKT signaling via down-regulation of tumor suppressors in natural killer-cell lymphoma/leukemia. Blood *114*, 3265-3275.

Yang, Z.Z., Tschopp, O., Baudry, A., Dummler, B., Hynx, D., and Hemmings, B.A. (2004). Physiological functions of protein kinase B/Akt. Biochem Soc Trans *32*, 350-354.

Yap, T.A., Carden, C.P., and Kaye, S.B. (2009). Beyond chemotherapy: targeted therapies in ovarian cancer. Nat Rev Cancer *9*, 167-181.

Yeh, E., Cunningham, M., Arnold, H., Chasse, D., Monteith, T., Ivaldi, G., Hahn, W.C., Stukenberg, P.T., Shenolikar, S., Uchida, T.*, et al.* (2004). A signalling pathway controlling c-Myc degradation that impacts oncogenic transformation of human cells. Nat Cell Biol *6*, 308-318.

Yoeli-Lerner, M., Yiu, G.K., Rabinovitz, I., Erhardt, P., Jauliac, S., and Toker, A. (2005). Akt blocks breast cancer cell motility and invasion through the transcription factor NFAT. Mol Cell *20*, 539-550.

You, Z., and Bailis, J.M. (2010). DNA damage and decisions: CtIP coordinates DNA repair and cell cycle checkpoints. Trends Cell Biol *20*, 402-409.

Yuen, J.W., Chung, G.T., Lun, S.W., Cheung, C.C., To, K.F., and Lo, K.W. (2014). Epigenetic inactivation of inositol polyphosphate 4-phosphatase B (INPP4B), a regulator of PI3K/AKT signaling pathway in EBV-associated nasopharyngeal carcinoma. PLoS One *9*, e105163.

Yun, M.H., and Hiom, K. (2009). CtIP-BRCA1 modulates the choice of DNA double-strand-break repair pathway throughout the cell cycle. Nature *459*, 460-463.

Zabludoff, S.D., Deng, C., Grondine, M.R., Sheehy, A.M., Ashwell, S., Caleb, B.L., Green, S., Haye, H.R., Horn, C.L., Janetka, J.W.*, et al.* (2008). AZD7762, a novel checkpoint kinase inhibitor, drives checkpoint abrogation and potentiates DNA-targeted therapies. Mol Cancer Ther *7*, 2955-2966.

Zaidi, N.H., Liu, L., and Gerson, S.L. (1996). Quantitative immunohistochemical estimates of O6-alkylguanine-DNA alkyltransferase expression in normal and malignant human colon. Clin Cancer Res *2*, 577-584.

Zelzer, E., Levy, Y., Kahana, C., Shilo, B.Z., Rubinstein, M., and Cohen, B. (1998). Insulin induces transcription of target genes through the hypoxia-inducible factor HIF-1alpha/ARNT. EMBO J *17*, 5085-5094.

Zeng, X., and Kinsella, T.J. (2008). Mammalian target of rapamycin and S6 kinase 1 positively regulate 6-thioguanine-induced autophagy. Cancer Res *68*, 2384-2390.

Zetterberg, A., and Larsson, O. (1985). Kinetic analysis of regulatory events in G1 leading to proliferation or quiescence of Swiss 3T3 cells. Proc Natl Acad Sci U S A *82*, 5365-5369.

Zhang, F., Fan, Q., Ren, K., and Andreassen, P.R. (2009a). PALB2 functionally connects the breast cancer susceptibility proteins BRCA1 and BRCA2. Mol Cancer Res *7*, 1110-1118.

Zhang, F., Ma, J., Wu, J., Ye, L., Cai, H., Xia, B., and Yu, X. (2009b). PALB2 links BRCA1 and BRCA2 in the DNA-damage response. Curr Biol *19*, 524-529.

Zhang, H.Y., Zhang, P.N., and Sun, H. (2009c). Aberration of the PI3K/AKT/mTOR signaling in epithelial ovarian cancer and its implication in cisplatin-based chemotherapy. European journal of obstetrics, gynecology, and reproductive biology *146*, 81-86.

Zhang, S., Royer, R., Li, S., McLaughlin, J.R., Rosen, B., Risch, H.A., Fan, I., Bradley, L., Shaw, P.A., and Narod, S.A. (2011). Frequencies of BRCA1 and BRCA2 mutations among 1,342 unselected patients with invasive ovarian cancer. Gynecologic oncology *121*, 353-357.

Zhang, X., Succi, J., Feng, Z., Prithivirajsingh, S., Story, M.D., and Legerski, R.J. (2004). Artemis is a phosphorylation target of ATM and ATR and is involved in the G2/M DNA damage checkpoint response. Mol Cell Biol *24*, 9207-9220.

Zhao, Y., Thomas, H.D., Batey, M.A., Cowell, I.G., Richardson, C.J., Griffin, R.J., Calvert, A.H., Newell, D.R., Smith, G.C., and Curtin, N.J. (2006). Preclinical evaluation of a potent novel DNA-dependent protein kinase inhibitor NU7441. Cancer Res *66*, 5354-5362.

Zhou, G.L., Tucker, D.F., Bae, S.S., Bhatheja, K., Birnbaum, M.J., and Field, J. (2006). Opposing roles for Akt1 and Akt2 in Rac/Pak signaling and cell migration. J Biol Chem *281*, 36443-36453.